



**GRIGORE T. POPA** UNIVERSITY OF  
MEDICINE AND PHARMACY IASI

## **HABILITATION THESIS**

**From microscopical to molecular profiling  
in tumor and non-tumor pathology**

**Mihai Danciu, MD, PhD**  
Associate Professor

**2020**



## Contents

<b>Abstract</b> .....	<b>1</b>
<b>Rezumat</b> .....	<b>3</b>
<b>Section I – Professional, academic and scientific achievements</b> .....	<b>5</b>
<b>Chapter 1: Morphological assessing of new prognostic and predictive factors in colorectal cancer</b> .....	<b>9</b>
<b>1.1. State of art</b> .....	<b>9</b>
<b>1.2. Immunoscore. The immune infiltrate quantification and characterization in rectal adenoma-carcinoma sequence</b> .....	<b>11</b>
1.2.1. Introduction.....	11
1.2.2. Aim.....	11
1.2.3. Material and methods.....	12
1.2.4. Results.....	14
1.2.5. Discussions.....	16
<b>1.3. CDX1 and EphB tumor suppression genes expression in colorectal normal mucosa-adenoma-invasive carcinoma sequence</b> .....	<b>19</b>
1.3.1. Introduction.....	19
1.3.2. Aim.....	20
1.3.3. Material and methods.....	20
1.3.4. Results.....	21
1.3.5. Discussions.....	24
<b>1.4. Centrosome-associated serine/threonine kinase 15 oncogene expression in genetic instable colorectal carcinoma</b> .....	<b>27</b>
1.4.1. Introduction.....	27
1.4.2. Aims.....	28
1.4.3. Material and methods.....	28
1.4.4. Results.....	34
1.4.5. Discussions.....	38
<b>1.5. Targeting early detection of premalignant lesions of digestive tract using novel non-invasive techniques – THz imaging and spectroscopy</b> .....	<b>43</b>
1.5.1. Introduction.....	43
1.5.2. Applications of THz imaging and THz spectroscopy in digestive cancers.....	45
1.5.3. Personal preliminary results in THz field.....	48
<b>Chapter 2: New concepts in diagnosing celiac disease</b> .....	<b>50</b>
<b>2.1. State of art</b> .....	<b>50</b>
<b>2.2. Quantitative assessment of intraepithelial lymphocytes and morphology interpretation in determining the cut-off between normal and celiac disease</b> .....	<b>52</b>
2.2.1. Introduction.....	52
2.2.2. Aim.....	53
2.2.3. Material and methods.....	53
2.2.4. Results.....	54
2.2.5. Discussions.....	58
<b>2.3. “Microscopic enteritis” – global consensus on a new entity</b> .....	<b>61</b>
2.3.1. Introduction.....	61
2.3.2. Aim.....	69
2.3.3. Material and methods.....	69
2.3.4. Results .....	71
2.3.5. Discussion.....	73

<b>Chapter 3: HPV-related squamous cell carcinomas of the head and neck assessment by HPV genotyping and immunohistochemistry.....</b>	<b>76</b>
<b>3.1. State of art.....</b>	<b>76</b>
<b>3.2. HPV detection and characterization in head and neck squamous cell carcinomas from North-Eastern Romania area.....</b>	<b>77</b>
3.2.1. Introduction.....	77
3.2.2. Aims.....	78
3.2.3. Material and methods.....	78
3.2.4. Results.....	81
3.2.5. Discussions.....	85
<b>Chapter 4: Histopathological insights over lipids metabolism in obesity, atherosclerosis and wound healing.....</b>	<b>91</b>
<b>4.1. State of art.....</b>	<b>91</b>
<b>4.2. Semiquantitative evaluation of Ghrelin-producing cells and <i>H. pylori</i> in patients with sleeve gastrectomy.....</b>	<b>93</b>
4.2.1. Introduction.....	93
4.2.2. Aims.....	94
4.2.3. Material and methods.....	94
4.2.4. Results.....	97
4.2.5. Discussions.....	102
<b>4.3. The role of adipose-derived stem cells in an experimental rat model wound healing....</b>	<b>108</b>
4.3.1. Introduction.....	108
4.3.2. Aims.....	109
4.3.3. Materials and methods.....	109
4.3.4. Results.....	111
4.3.5. Discussions.....	114
<b>4.4. Different effects of fish oil on serum lipids and hepatic morphology show that a balanced diet is preferable to dietary supplements.....</b>	<b>118</b>
4.4.1. Introduction.....	118
4.4.2. Aim.....	119
4.4.3. Materials and methods.....	120
4.4.4. Results.....	122
4.4.5. Discussion.....	126
<b>Section II – Future projects in professional, academic and scientific fields.....</b>	<b>132</b>
<b>II.1. Projects regarding professional and academic activity.....</b>	<b>132</b>
<b>II.2. Projects regarding scientific activity.....</b>	<b>132</b>
II.2.1. The predictive role of correlation between serology and histopathological stage in celiac disease.....	133
II.2.2. PD-1 and PDL-1 expression in colorectal cancer and in head and neck cancers.....	134
<b>II.3. Final remarks.....</b>	<b>136</b>
<b>Section III – References.....</b>	<b>137</b>

## Abbreviations list

aCGH: array-based Comparative Genomic Hybridization  
ADSC: adipose-derived stem cells  
APC: adenomatosis polyposis coli  
ATR: attenuated total reflection  
BMI: body mass index  
BW: Body weight;  
CA1: Combined alternative 1;  
CA2: Combined alternative 2;  
CCT: Standardized suspension containing 4% cholesterol, 1% cholic acid and 0.5% 2-thiouracil;  
CD: Celiac disease  
CEP: chromosome enumeration probe  
ChIP, chromatin immunoprecipitation;  
ChREBP: Carbohydrate responsive element-binding protein;  
CIN: chromosomal instability  
CoT: core of the tumor  
CRC, colorectal cancer;  
CT: computer tomography  
CVD: Cardiovascular diseases;  
CWTI: continuous wave THz imaging  
DAB: 3,3'- Diaminobenzidine  
DFS: disease free survival  
DHA: Docosahexaenoic acid;  
DMEM: Dulbecco's modified Eagle's medium  
DNMT: DNA methyltransferase  
DW: Distilled water;  
ELISA: enzyme-linked immunosorbent assay  
EMA: endomysial antibody  
EPA: Eicosapentaenoic acid;  
FA: Fatty acids;  
FBS: fetal bovine serum  
FFPE: formalin fixed paraffin embedded  
FISH: fluorescence in situ hybridization  
FO: Fish oil;  
GFD: gluten free diet  
GOAT: ghrelin O-acyltransferase  
GPC: ghrelin producing cells  
HDAC: histone deacetylases  
HDL: High density lipoprotein cholesterol;  
HNSCC: head and neck squamous cell carcinomas  
HFD: High-fat diet;  
Hp: *H. pylori*  
HPF: high power fields  
HPV: human papilloma virus  
I: Immunoscore  
IBD: inflammatory bowel disease  
IBMX: 3-isobutyl-1-methylxanthine  
IEL: intraepithelial lymphocytes  
IL-6: Interleukin 6;  
ILC: innate lymphoid cells  
IM: invasion margin  
LDL: Low-density lipoprotein cholesterol;  
LNR: lymph node ratio  
MALT: mucosa-associated lymphoid tissue  
MBD: methylated DNA-binding domain  
mCGH: metaphase comparative genomic hybridization  
ME: microscopic enteritis  
MRI: magnetic resonance imaging  
MSI, microsatellite-instability

NCGS: Non-celiac gluten sensitivity  
NSAID: non-steroidal anti-inflammatory drugs  
OCT: optical coherence tomography  
OS: overall survival  
pCRT: preoperative chemoradiation therapy  
PD-1: Programmed death-1  
PD-L1: Programmed death-ligand 1  
PDE: phosphodiesterase  
PET: positron emission tomography  
PPAR $\gamma$ : Peroxisome proliferator activated receptor  $\gamma$ ;  
pRb: retinoblastoma protein  
PRC: Polycomb repressive complexes  
PUFAs: Polyunsaturated fatty acids;  
RUT: rapid urease test  
qRT-PCR: quantitative reverse transcriptase PCR  
sCRC: Sporadic colorectal cancer  
SD: Standard diet;  
SREBP-1c: Sterol regulatory element binding protein 1c;  
STK: serine threonine kinase  
TC: Total cholesterol;  
TG: Triglyceride;  
THz-TDS: Terahertz time domain spectroscopy  
TIL: tumor infiltrating lymphocytes  
TMA: tissue microarray  
TNF- $\alpha$ : Tumor necrosis factor  $\alpha$ ;  
TRG: Tumor regression grade  
UBT: urea breath test  
UDE: upper digestive endoscopy  
UGI: upper gastrointestinal  
VEGF: vascular endothelial growth factor  
VLDL: Very low-density lipoprotein cholesterol;  
WC: waist circumference  
WG: Weight gain

## Abstract

The present habilitation thesis summarizes my professional, academic and, especially, scientific activity during the postdoctoral period (2007-2020). Based on these achievements and according to the international trends I included in the end of the thesis some thoughts on future research directions that I intend to follow.

According to the criteria recommended and approved by the National Council for Attestation of Titles, Diplomas and Certificates (CNATDCU), the thesis is structured on three sections, subdivided as follows:

**Section I** presents a summary of my professional, academic and scientific achievements after obtaining the PhD title.

*Chapter 1* details one of the most important part of my postdoctoral research activities focused on colorectal adenocarcinoma. As promised in the end of my doctoral thesis, I continued the collaboration started with the researchers from Freiburg University, Germany, by studying the expression of serine/threonine kinase 15 (STK15, Aurora A) at proteic and genetic level in chromosomal instable and microsatellite instable sporadic carcinomas. I also studied the expression of adhesion molecules CDX1 and ephrin B receptor genes in case-matched colorectal normal mucosa, adenomas and adenocarcinomas.

When worldwide scientists started to focus on the role of the immune system in antitumor defense and its influence on the evolution of the colorectal cancers, I joined the French research team from Paris who coined the term “Immunoscore”. The project we started aimed to assess the prognostic value of Immunoscore on patients with rectal cancer, to compare it with TNM and to evaluate the predictive value of immune reaction about the response of the tumor to preoperative neoadjuvant chemoradiation therapy.

The interest for developing new, non-invasive diagnostic tools encouraged the collaboration between engineers in electromagnetic wave fields and medical scientists/doctors. Terahertz spectroscopy became a promising diagnostic tool for early detection of pre-malignant lesions of digestive tract (including colon and rectum). Therefore, a review of the literature on this topic could be of real interest for scientists.

My personal contributions resulted in research grants and published articles in: J Mol Med (IF 4.820), Modern Pathology (IF 4.406), Epigenetics (IF 4.318), Clin Cancer Res (IF 8.722) and Materials (IF 3.057).

*Chapter 2* presents the studies regarding celiac diseases, as part of an international multicenter study group (19 centers from 8 countries on 3 continents). A first study aimed to improve the diagnostic accuracy of celiac disease by determining the optimal cut-off of intraepithelial lymphocytes count between normal and celiac disease.

The same international team which included gastroenterologists and pathologists, elaborated the Bucharest Consensus on microscopic enteritis, a new entity characterized by symptomatic malabsorption and subtle deficiency of micronutrients and minimal morphological changes of the duodenal mucosa, corresponding to Marsh I-II stages.

The most important results were published in: Gut (IF 17.016), Endoscopy (IF 4.166), World Journal of Gastroenterology (IF 2.787).

*Chapter 3* presents studies designed to investigate the role of HPV infection in head and neck squamous cell carcinomas using immunohistochemical and biomolecular techniques.

The most important was accomplished in collaboration with researchers from Germany, France, Italy and USA, and aimed to determine the proportion of HPV-associated head and neck squamous cell carcinomas by analyzing HPV DNA and RNA status, in

correlation with p16 expression. The study group included patients diagnosed with HNSCC (oropharynx and outside the oropharynx). The study revealed a low concordance between HPV DNA status and HPV ARN or p16 status, meaning that in Northeastern Romania a small proportion of HNSCC cases appears to be HPV-driven.

The results of these studies were published in national and international journals: PLoS ONE (IF 2.766), Rom J Morphol Embryol (IF 1.411).

*Chapter 4* includes studies regarding the correlation Ghrelin-*H. pylori*-metabolic surgery in obesity, an experimental study on diets and lipid metabolism and an experimental study on the role of adipose-derived stem cells (ADSC) in wound healing.

In the first projects, we immunohistochemically quantified the distribution of ghrelin-producing cells in relation with *H. pylori* infection in stomach from obese patients after sleeve surgery.

The first experimental studies on animal models revealed that differentiated adipocytes achieve similar wound healing results as ADSC and fat injection, but differentiated adipocytes and fat grafting accelerate early healing process. In the second experimental study, we demonstrated that omega3-rich fish-oil confers more protection against cardiovascular risk factors and liver lipid accumulation when given to rats consuming regular diets than when given to rats consuming a high-fat diet. This argues for consumption of a healthy diet rather than to the use of fish-oil supplements.

The results of these studies were published in: Lipids in Health and Disease (IF 2.906), J Burn Care Res (IF 1.923) and Rom J Morphol Embryol (IF 1.411).

**Section II** presents the projects for my future development on professional, academic/teaching and scientific fields.

The first two are strongly interconnected, dedication, excellence and professionalism being the mandatory characteristics of my future activity.

The scientific projects will include research on the correlation between serology and histopathological changes for an accurate diagnosis of celiac disease and differentiate it from other gluten sensitivity entities. Also, I intend to develop studies regarding the PD1 and PD-L1 expression in different types of carcinomas (colo-rectal, head and neck, etc.).

**Section III** includes a list of selected bibliographic references cited in the present habilitation thesis.

## Rezumat

Teza de abilitare printă pe scurt, cele mai importante realizări profesionale, academice și, în special, pe cele științifice obținute după finalizarea studiilor doctorale (2007-2020). Pornind de la aceste realizări și în concordanță cu actualele trenduri în cercetarea științifică, am inclus în finalul tezei de abilitare, câteva direcții de cercetare pe care ma voi axa în viitor.

Conform criteriilor recomandate și aprobate de CNATDCU, teze de abilitare este structurată în 3 secțiuni, după cum urmează:

**Secțiunea I** prezintă realizările profesionale, academice și științifice obținute postdoctoral.

*Capitolul 1* detaliază una dintre mai constante activități de cercetare avute în perioada imediat următoare obținerii titlului de doctor în științe medicale: cancerul colo-rectal. După cum am promis la finalul prezentării tezei de doctorat, am continuat colaborarea cu colectivul Departamentului de Patologie din cadrul Universității din Freiburg, Germania, studiind expresia serine/threonine kinazei 15 (STK15/Aurora A) nu numai la nivel proteic, dar și genetic prin studii de biologie moleculară pe un lot de pacienți cu cancer colo-rectal sporadic, cu instabilitate cromozomială sau a sateliților. De asemenea, am studiat expresia molecule de adeziune CDX1 și mutațiile genei receptorului Ephrin B într-un lot de cazuri ce cuprindeau atât mucoasă normală, adenom și carcinom colorectal.

Atunci când oamenii de știință au început să se axeze pe rolul sistemului imun în apărarea antitumorală și pe influența sa în evoluția cancerului colorectal, am avut șansa de a începe o colaborare cu puternicul centru european de cercetări INSERM, Paris, cei care au introdus noțiunea de Imunoscor pentru cancerul de colon. Proiectul a vizat evaluarea Imunoscorului ca factor de prognostic la pacienții cu cancer de rect prin comparație cu sistemul TNM, dar și evaluarea rolului predictiv al inflamației în conexiune cu răspunsul tumorilor la terapia neoadjuvantă preoperatorie.

Interesul crescut pentru identificarea și dezvoltarea de noi tehnici și instrumente de diagnostic non-invaziv a dus la o mai strânsă colaborare între inginerii din domeniul imagisticii și medici. Astfel, spectroscopia cu raze din spectrul terahertzilor pare să fie un instrument cu potențial diagnostic pentru leziunile premaligne ale tractului digestiv. În consecință, un review ce trece în revistă cele mai recente aspecte ale cercetărilor din domeniul medical efectuate cu instrumente ce folosesc unde electromagnetice din spectrul terahertzilor poate fi în interesul cercetătorilor.

Contribuțiile personale în urma acestor cercetări au fost publicate în revistele: J Mol Med (IF 4.820), Modern Pathology (IF 4.406), Epigenetics (IF 4.318), Clin Cancer Res (IF 8.722) și Materials (IF 3.057).

*Capitolul 2* prezintă studiile asupra bolii celiace și enteropatiilor înrudite, studii efectuate ca parte a unei echipe internaționale multicentrice ce a reunit 19 institutii din 8 țări de pe 3 continente. Un prim studiu a vizat creșterea acurateții diagnosticului bolii celiace prin stabilirea de comun acord a unei valori de cut-off pentru numărul de limfocite intraepiteliale cu valoare de graniță între normal și boala celiacă. Același nucleu de cercetători, ce a inclus medici anatomo-patologi și gastroenterologi, a emis Consensul de la București asupra enteritei microscopice, o nouă entitate caracterizată clinic prin sindrom de malabsorbție iar morfologic prin modificări duodenale minime, similare bolii celiace din stadiile March I și II.

Cele mai importante rezultate au fost publicate în Gut (IF 17.016), Endoscopy (IF 4.166) și World Journal of Gastroenterology (IF 2.787).

*Capitolul 3* prezintă o serie de studii în care a fost investigat rolul infecției cu HPV în carcinoamele scuamocelulare din regiunea capului și gâtului, prin metode de imunohistochimie și tehnici de biologie moleculară.

Cel mai important studiu a fost realizat printr-o colaborare cu centre de cercetare din Germania, Franța, Italia și Statele Unite; scopul a fost de a se determina proporția de cazuri cu implicare HPV din totalul tumorilor din sfera cap-gât, prin analiza ADN-ului și ARN-ului HPV, în corelație cu expresia imunohistochimică a p16. Lotul de studiu a inclus pacienți din Iași, diagnosticați cu carcinom scuamocelular orofaringian sau extra-orofaringian. Am constatat că în regiunea noastră, carcinoamele asociate cu infecție cu HPV au o pondere redusă.

Rezultatele au fost publicate în revistele: PLoS ONE (IF 2.766) și Rom J Morphol Embryol (IF 1.411).

*Capitolul 4* include studii cu privire la relația dintre celulele secretoare de Ghrelin, infecția cu *H. pylori* și chirurgia bariatrică a obezității, și studii experimentale pe model animal privind rolul acizilor grași polinesaturați din dietă asupra metabolismului lipidic și privind rolul celulelor stem derivate din adipocite în vindecarea plăgilor.

În privința studiului obezității, am cuantificat imunohistochimic distribuția celulelor secretoare de ghrelin corelată cu prezența infecției cu *H. pylori* la pacienții obezi tratați prin chirurgie bariatrică.

Studiile experimentale pe model animal au demonstrat că adipocitele diferențiate contribuie la vindecarea plăgilor induce experimental similar celulelor stem derivate din adipocite sau țesutului adipos injectat, iar adipocitele diferențiate și grefele cu țesut adipos accelerează procesul de vindecare. Al doilea studiu experimental a demonstrat că uleiul de pește bogat în omega3 are rol protectiv împotriva factorilor de risc cardio-vasculari și a steatozei hepatice dacă este administrat simultan unei diete echilibrate și nu ca supliment la o dietă bogată în grăsimi.

Rezultatele au fost publicate în: Lipids in Health and Disease (IF 2.906), J Burn Care Res (IF 1.923) and Rom J Morphol Embryol (IF 1.411).

În **secțiunea II** sunt prezentate proiectele de viitor în plan profesional, academic și de cercetare.

Primele două sunt puternic interconectate, câteva trăsături fiind comune: dedicarea, excelența și profesionalismul.

Viitoarele proiecte științifice vor include cercetări asupra corelației dintre determinările serologice și modificările histopatologice în scopul unui diagnostic cât mai precis al bolii celiace și diferențierea de alte entități caracterizate prin sensibilitate la gluten. O altă direcție de cercetare va fi legată de expresia PD1 și PD-L1 în diferite tipuri de carcinoame (colo-rectal, cap-gât, și altele).

**Secțiunea III** include o selecție a referințelor bibliografice citate în această teză de abilitare.

## **Section I – Professional, academic and scientific achievements**

### **Introduction**

Career is the professional ascending evolution of a person in his field of activity. The success of this evolution depends, mainly, on internal factors and then on external influences and conditions. I consider that, lacking a personal plan for its own development and a vision, one is exposed to stagnation or random evolution. Therefore, when I visualized my academic future, I took into consideration the fulfillments and the fails, I identified my priorities, my objectives (short, medium and long term), I decided regarding the methods and the steps to be made, but not neglecting the opportunities and the difficulties. From time to time, progress analysis is necessary, in order to evaluate the present stage and, if necessary, to adapt to the changing realities.

To achieve a fruitful evolution, no matter it is about teaching or research activities, I permanently relied on teamwork and honesty, interdisciplinary collaboration, networking and continuous personal training.

### **Professional achievements**

My professional career started after graduating the "Grigore T. Popa" University of Medicine and Pharmacy of Iasi, Faculty Medicine in 1993. For one year (15.01.1994-14.01.1995) I completed 4 internships (Internal medicine and Surgery – Clinic Hospital of Pneumology, Iasi; Obstetrics-gynecology – “Dr. CI Parhon” Clinical Hospital, Iasi; Pediatrics – “Sf. Maria” Clinical Hospital, Iasi).

After the 1994 Residency Competition, I opted for a postgraduate training in Pathology in Colentina Infectious Diseases Hospital, Bucharest. I obtained the transfer to “Sf. Spiridon” Clinical Emergency Hospital, Iasi, based on the approval from Ministry of Health, Public Health District Authority from Bucharest and Iasi, and Universities of Medicine and Pharmacy from Bucharest and Iasi. During the 4 years of residency, I received a strong education following the courses and the seminars in Pathology, Immunopathology, Human Genetics and Laboratory Medicine. I’ve also participated to national conferences in Iasi, Cluj-Napoca and Bucharest. I graduated as Pathologist in October 1998. In 2003 I became primary pathologist doctor.

Since 2000 I worked as pathologist (part time) in Pathology Department of “Sf. Spiridon” Clinical Emergency Hospital, Iasi.

I continuously improved my practice by documentation and participation in postgraduate training courses, national and international scientific meetings.

In 2006, sustained by the Pathology Institute, University of Freiburg, Freiburg im Breisgau, Germany, I introduced the ink staining of surgical excision specimens, in order to better and complete evaluation of resection margins from rectal, pancreatic, breast cancers and other types of resections.

The experience gained from medical practice contributed in the improvement of the teaching process by translating the clinical cases in lectures, enriching them.

### **Academic activity**

Starting with 1999 I became professor’s assistant in Pathology Department, Faculty of Medicine, “Grigore T. Popa” University of Medicine and Pharmacy, Iasi. In the first years

I've learned the teaching abilities during the workshops and seminars and the examination process during exams sessions, when I assisted my professors. I was involved in the teaching process with students from Faculty of Medicine, 3<sup>rd</sup> year, Romanian and English series, Nursing specialization, 2<sup>nd</sup> year. I contributed in the modernization of the teaching process by replacing the slide projector with the PowerPoint system. In 2004, as internet entered more and more in students' life, I created a website, Atlas of Pathology ([www.pathologyatlas.ro](http://www.pathologyatlas.ro)) in Romanian and English, where our students could find explained microscopical images of the slides they had in the Curricula. As a consequence, our students had free access from home to all the slides during the academic year, also during exams sessions.

In 2006, together with Prof. dr. Maria-Sultana Mihailovici, Head of Pathology Department, I developed the "Laboratory for morphological sciences" which included a microscope equipped with video camera and projector for live microscopical images during workshops and seminars. Also, the above-mentioned Laboratory was completely equipped to perform immunohistochemical techniques for the first time.

In 2007, I became Assistant Professor/Lecturer in Pathology Department, therefore I started lectures and final examination for students in 3<sup>rd</sup> year, General Medicine, Romanian language, also lectures for residents in Pathology. In 2008, I launched the second edition of the website Atlas of Pathology, with a new interface, more friendly and modern, and in 2014, the third edition which included explained macroscopy images for most of the pathological entity in the student Curricula.

As a result of the continuous efforts in developing collaborative networks and research teams with academic fellows from other universities, in 2008, I was invited to become co-author for a book-chapter in a monography regarding celiac disease (Rostami K, Allen C, Danciu M: Histogenesis and Histo-morphological Aspects of Coeliac Disease. în Selimoglu A (editor.) Colyak Hastaligi. Istanbul: Logos, 2008, 28-36. ISBN: 978-975-349-058-0).

In 2014, together with a group of students (now residents or specialists in various specialties) and young teaches, I launched Archive of Clinical Cases ([www.clinicalcases.eu](http://www.clinicalcases.eu)), an English language online journal which appears quarterly, continuously since then. The journal is edited by "UMF Gr. T. Popa Iasi Publishing House" and is indexed in over 15 International Databases (Gale Cengage Learning, Index Copernicus, EBSCOhost, etc.). The journal has an international Advisory Board, about half of the published authors being from outside of our University.

As Lecturer I was invited to be part of the Jury of Congressis (International Congress for Medical Students and Young Doctors), Fundamental Sciences Section, held in Iasi every year.

During 2010-2013, I was member of management team of a Human Resources Project (POSDRU/81/3.2/S/58942 „ Pathology Laboratory – Professional and organizational training through the implementation of quality management" ANATOMOPAT. The project targeted a group of over 200 pathologists and technicians working in Pathology Laboratories.

In 2014, I contributed in the modernization of the workshop room in our Department, by acquisition of 30 new modern microscopes for students use, and a research microscope with motorized revolver and video camera for transmission of live HD images and acquisition of digital images of computer.

In 2015, I gained through contest the position of Associate Professor in Pathology Department.

Starting with 2015, I was elected member of the University Senate, and between 2016 and 2018 I was Vice-rector for Postgraduate Studies - cycle of fundamental sciences. During this mandate I coordinated the Admission process for all categories of students, I contributed in the elaboration of Methodologies and Procedures for all the activities regarding the students in the first three years.

The experience gained by the daily professional activity in the field of Nose and

Throat pathology, especially the salivary glands tumors, was essential when writing a book chapter (Danciu M, Ferariu D: Pathological Variety of Extended Parotid Tumors. In Costan VV (ed.) Management of Extended Parotid Tumors. Switzerland: Springer International Publishing, 2016, 77-89. ISBN 978-3-319-26545-2) dedicated to residents and young doctors specialized in Pathology, oto-rhino-laryngology or oncology.

In 2018, I was invited by Prof. dr. Gabriel Becheanu from “Carol Davila” University of Medicine and Pharmacy, Bucharest, to be founder and member of the Board of “Digestive Pathology Association”, a professional association of pathologists, gastroenterologists, oncologists dedicated to diagnosis and treatment of digestive diseases. One of the main activities of the Association regards the continuous medical education, especially of the young doctors, by organizing at least two major Courses per year with international speakers.

### **Scientific activities**

The research activity started once I became member of the teaching staff of the Pathology Department, in 1999.

Right from the beginning, I was included in the research projects run by my colleagues and fellows. I started to communicate the results at the 27<sup>th</sup> European Congress of Cytology (Lillehammer, Norway, 2000).

In 2002, I was admitted as PhD fellow, under the guidance of Prof. dr. Lorica Gavrilita and Prof. dr. Maria-Sultana Mihailovici, the subject of my thesis being “Contributions to the study of colorectal adenoma-carcinoma sequence”. Eager to apply new techniques and methods for my research projects, I looked for collaboration with important European research centers. As results, I obtained a Study Bursary from the British Division of International Academy of Pathology which allowed me to participate at the 24<sup>th</sup> International Congress of the International Academy of Pathology (Amsterdam, Netherlands, 2002). In addition, I could spend two weeks at Academic Medical Center of Amsterdam – Digestive Pathology Department (Course on DNA technology – PCR, under Prof. dr. GJA Offerhaus supervision) and Free University of Amsterdam – Digestive Pathology Department (learning Microarrays - Comparative Genomic Hybridization, under Prof. dr. G. Meijer supervision). I consider it was my initiation in the advanced techniques of medical research, opening new horizons.

More important, between September 2005 and February 2006, I was a DAAD Fellow (Deutsche Akademische Austausch Dienst) at Pathologisches Institut, “Albert Ludwigs” Universitäts Klinikum, Freiburg in Breisgau, Germany. There, under the supervision of Prof. dr. M. Werner and Prof. dr. S. Lassmann, I fulfilled my research project using immunohistochemistry and immunofluorescence in tridimensional microscopy on tissue microarray blocks. The research I accomplished contributed in finalizing the PhD thesis (OMEC nr. 5764/28.11.2006) and, also, publishing articles in important scientific journals.

Starting with 2007, I became member of many multidisciplinary research teams running national grant projects. Among others, noteworthy are two of them: Romanian Academy Grant nr. 162/2007, entitled “Optimization of protocol for detection of families with hereditary non-polyposis colorectal cancer, in order to early detect premalignant lesions in asymptomatic persons”, 2007-2008, and CNMP Project nr. 32168/2008 entitled “Respirable superhydrophobic nanostructures”, 2008-2011, as Responsible on behalf of “Grigore T. Popa” University of Medicine and Pharmacy Iasi. All these research projects were successfully finalized and the results were published in scientific journals as in extensor articles, or presented at national and international meetings. Also, these projects contributed in developing a network with scientists from diverse domains, and improved the research infrastructure of Pathology Department, Microbiology Department and Surgery Simulation

and Training Center.

2016 ROBERT B. LINDBERG AWARD for The Effects of Adipose-Derived Stem Cell-Differentiated Adipocytes on Skin Burn Wound Healing in Rats

As a consequence, my international visibility is reflected in the following indexes:

- Web of Science Clarivate Analytics H-index: 11
- Total number of citations without self-citations: 618
- In extenso ISI papers: 33
- In extenso ISI papers (main author): 13
- In extenso IDB papers: 25

### **Projects, research grants**

#### **1. National research grants as Partner responsible**

1.1. CNMP 32168/2008: „Respirable superhydrophobic nanostructures”; 2008-2011; Partner responsible

#### **2. National research grants**

2.1. CNCS-UEFISCDI PN-III-P2-2.1-PED-2016-1598: "Nanoparticle-enabled Terahertz Molecular Imaging as Advanced Early-stage Diagnostic Method of Gastric Neoplasia", - team member

2.2. UMF Iași Internal Grant, 1644/2013: “Standardization on animal model of skin burn by contact grade 2 (partial dermic burn) and grade 3 (total skin burn) on rat, using an automated system”, 2013-2015; team member

2.3. CNMP 41.030/2007: “Cellular and molecular mechanisms implicated in regression of high-grade cervical dysplasia”, 2007-2010; (399,660 RON); team member.

2.4. CNMP 71.146/2007: “Advanced biomaterials based on nanostructured bioactive protein structures doped with metal nanoparticles”, 2007-2010, 113,903 RON – team member

2.5. Romanian Academy Grants 162/2007: „Optimization of the protocol for detection of the families with Hereditary Non-Polyposis Colorectal Cancer (HNPCC), for an early detection of premalignant lesions in asymptomatic subjects”; 2007-2008; team member

2.6. CNCSIS 29/2006: „Interdisciplinary platform for molecular medicine”, 2006-2008; team member

#### **3. Educational projects**

3.1. Academic Projects Through Sectorial Operational Program for the Development of Human Resource - POSDRU/81/3.2/S/58942, “Pathology Laboratory – Professional and organizational training through the implementation of quality management”; 2010-2013. Long-term expert

Between 2011 and 2015, I was member of five multicenter, randomized, phase 3 studies for drugs used in oncology, mainly for gastric and breast cancers.

## **Chapter 1: Morphological assessing of new prognostic and predictive factors in colorectal cancer**

### **1.1. State of art**

Colorectal cancer is one of the most common cause of cancer-related death in the world (the second in United States, considering the data from the American Cancer Society [Siegel et al., 2019]. The risk to develop a colorectal cancer is 4.6% for men and 4.2% for women [Siegel et al., 2016], while the five-year survival rate for metastatic disease is 14.2% and 71.3% for regional disease [Milano et al., 2017; Siegel et al., 2020].

Sporadic colorectal cancer (sCRC) development includes some specific genetic alterations, and present macroscopic and histologic patterns, all these influencing the individual tumor progression [Jass et al., 2002; Fearon and Vogelstein, 1990]. As methods to investigate and analyze the genetic mutations at DNA level, different techniques were used: metaphase comparative genomic hybridization (mCGH) and fluorescence in situ hybridization (FISH). This way, DNA losses at 5q, 8p, 17p, and 18q and DNA gains at 7, 8q, 13q, and 20q were identified [Diep et al., 2006]. In these chromosomal regions were pointed out oncogenes and tumor suppressor genes, which were thought to have an important role in colorectal adenoma-carcinoma sequence: APC at 5q, DCC at 18q, MYC at 8q. Although, with time, more and more gene mutations and alterations are identified, the profile of gene-specific changes involved in tumorigenesis and tumor progression is far from being completely known. More than this, the development of sCRC has multiple molecular pathways, some of them overlapping [Diep et al., 2006]. Considering the genetic alterations, sCRC can belong to one of the following two types: chromosomal instability (CIN, 85% of cases) or microsatellite instability (MIN, 15% of cases). CIN-type carcinomas are characterized by numerous genomic changes (gene amplifications, deletions), being aneuploid; MIN-type carcinomas present a reduced number of genomic changes (defects of the DNA mismatch repair genes), generally these tumors being diploid [Sugai et al., 2003]. While it has been clearly stated that the mismatch repair genes mutations are the cause of MIN-type tumors, the fundamental mechanism and its pathways are, yet, not completely elucidated. So far, it is known that CIN-type carcinomas may be produced by chromosome non-disjunction and/or telomere-related alterations, or defects in chromosome segregation during cell division [Klein et al., 2006].

Alterations of chromosomal passenger proteins (proteins implicated in chromosomal segregation) and of those responsible for the formation of mitotic spindle are supposed to generate aneuploidy in tumor cells [Ruchaud et al., 2007; Vader et al., 2008]. Also, in the control of chromosome segregation during mitosis might be implicated the adenomatous polyposis coli (APC) protein, a gene frequently mutated in colorectal carcinoma [Aoki and Taketo, 2007]. As a consequence, with or without the direct implication of APC gene, the malfunction of chromosomal segregation induces aneuploidy or polyploidy in tumor cells, through a large genomic alteration. On the other hand, of major importance in chromosomal segregation are the centrosomes [Fukasawa, 2007]. Their deregulation, as supernumerary centrosomes (induced by overexpression of centrosome complex proteins, might induce an abnormal chromosomal segregation, generating aneuploid, tetraploid, or polyploid daughter cells. Such proteins of the centrosome complex are the proteins belonging to the family of Aurora kinases (A, B, and C). Aurora A is implicated in centrosomal complex, while Aurora B is implicated in chromosomal passenger complex [Giet et al., 2005]. Using Southern and Northern blotting of tissue extracts, quantitative PCR and immunohistochemistry, Aurora A was identified to be amplified and overexpressed in colorectal carcinomas [Lam et al., 2008].

American Joint Committee on Cancer (AJCC) or Unio Internationale Contra Cancrum (UICC) - Tumor, lymph Node, Metastasis (TNM) system is used for staging and therapy

management of colorectal tumors in correlation with other prognostic and predictive factors and markers. Assessing the microsatellite instability is an important prognostic marker, but it regards less than 15% of colorectal cancers. Therefore, it is important to find new, reliable prognostic markers, not only in the tumor cell, by characterizing it and its genetic and chromosomal alterations, but also maybe by investigating the microenvironment in the vicinity of the tumor cells. More and more new published data on retrospective cohorts of solid tumors proves that the inflammatory infiltrate has a major role in the outcome of the patients [Fridman et al., 2012]. Gallon et al. 2006 analyzed the intratumoral immune infiltrate (type, density, location) in patients with colorectal cancer and observed that it is correlated with the evolution of the tumor and my influence it. In fact, the T lymphocytes CD3+ (cytotoxic CD8+ and memory CD45RO+ phenotype) from the intratumoral and peritumoral inflammatory infiltrate are an important predictive marker for recurrence and survival. Trusting the importance of the immune reaction assessment, they coined “Immunoscore” as a method to provide a score by counting the CD3+ and CD8+ T lymphocytes in the core of the tumor, but also at the invasion margin of the tumor. Also, they advocate the routinely use of Immunoscore for cancer classification as it seems to be more precise in anticipation of the outcome than the TNM classification [Mlecnik et al., 2011; Galon et al., 2012]. In the following years, other international multicenter projects focused on the reliability of Immunoscore and its utility in routine clinical settings. Rectal cancers should be separately analyzed from colonic carcinomas, as sometimes the epidemiology, the clinic, the pathology, the tumor markers and the therapy are different. Therefore, separate studies should be designed to evaluate the impact of immune reaction on tumor progression and effect of preoperative neoadjuvant therapy.

The terahertz waves are located in the electromagnetic spectrum between high frequency microwaves and long wavelength far infrared, a region defined as 0.1-10THz. Also know as T-rays, T-lux, THz light or THz radiation, 1THz equals  $10^{12}$  Hz having a wavelength of 300  $\mu\text{m}$ , 4.14 meV,  $33.3\text{cm}^{-1}$ . Although they were identified in 1975, the interest of the researchers on THz grew, covering almost all sciences, including medicine and biomedical sciences.

#### Digestive cancers and Terahertz imaging and spectroscopy

As cancer is the second most frequent cause of death worldwide, efforts have been made in the past decades not only in finding a treatment, but also in early detection of premalignant lesions as secondary prevention method, which is safer and cheaper than treating the cancer. Depending on the organ and on the type of the tumor, progresses were made for developing new techniques and imaging methods used in non-invasive early diagnosis. For the investigation of the digestive tract, there are already in use, but none of these new diagnosis methods brings only advantages, as one has to balance between costs, specificity, sensibility, invasiveness, radiation side-effects for patients and doctors. Less investigated, THz waves might bring new benefits in the early diagnosis of carcinomas in preinvasive or early stages. Because the energy transfer with THz depends on the tissue structure, it can produce information about the structure, with almost no invasiveness, especially on those tumors with a greater content of water that strongly absorb the THz waves [Ahi K. 2019]. On the other hand, THz radiation can be used in detecting the presence of the tumor at the resection margins [Joseph et al., 2014].

**This research direction has been realized by publishing the following articles:**

Anitei MG, Zeitoun G, Mlecnik B, Marliot F, Haicheur N, Todosi AM, Kirilovsky A, Lagorce C, Bindea G, Ferariu D, **Danciu M**, Bruneval P, Scripcariu V, Chevallier JM, Zinzindohoué F, Berger A, Galon J, Pagès F: Prognostic and predictive values of the immunoscore in patients with rectal cancer. Clin Cancer Res. 2014; 20(7):1891-1899

<https://clincancerres.aacrjournals.org/content/20/7/1891.full>

Rönsch K, Jäger M, Schöpflin A, **Danciu M**, Lassmann S, Hecht A: Class I and III HDACs and loss of active chromatin features contribute to epigenetic silencing of CDX1 and EPHB tumor suppressor genes in colorectal cancer. *Epigenetics*. 2011; 6(5):610-22. <http://www.tandfonline.com/doi/abs/10.4161/epi.6.5.15300>

Lassmann S, **Danciu M**, Müller M, Weis R, Makowiec F, Schulte-Mönting J, Hopt UT, Werner M.: Aurora A is differentially expressed and regulated in chromosomal and microsatellite instable sporadic colorectal cancers. *Mod Pathol*. 2009; **22(10)**:1385-97; <http://www.nature.com/modpathol/journal/v22/n10/full/modpathol2009111a.html>

Lassmann S, Weis R, Makowiec F, Roth J, **Danciu M**, Hopt U, Werner M. Array CGH identifies distinct DNA copy number profiles of oncogenes and tumor suppressor genes in chromosomal- and microsatellite-unstable sporadic colorectal carcinomas. *J Mol Med*. 2007; **85(3)**:293-304. <http://link.springer.com/article/10.1007/s00109-006-0126-5>

Danciu M, Alexa-Stratulat T, Stefanescu C, Dodi G, Tamba BI, Mihai CT, Stanciu GD, Luca A, Spiridon IA, Ungureanu LB, Ianole V, Ciortescu I, Mihai C, Stefanescu G, Chirilă I, Ciobanu R, Drug VL: Terahertz spectroscopy and imaging: a cutting-edge method for diagnosing digestive cancers. *Materials (Basel)* 2019; 12(9). pii: E1519. doi: 10.3390/ma12091519. <https://www.mdpi.com/1996-1944/12/9/1519>

## **1.2. Immunoscore. The immune infiltrate quantification and characterization in rectal adenoma-carcinoma sequence**

### **1.2.1. Introduction**

Among colorectal cancers, rectal localization represents about 60%, being a major issue for public health with over 75,000 new cases every year in Europe. The therapy for rectal cancer is different comparing to colon cancer, and has a strong impact on patient's comfort [Nagtegaal and Glynne-Jones, 2020]. It relies on clinico-pathological stage which doesn't take into account all biologic features of the neoplasm. Therefore, new prognostic and predictive markers are needed in order to better decide and adjust which neoadjuvant treatment fits better to each patient and induces a better tumor response.

An important biologic feature is the inflammatory infiltrate represented mainly by lymphocytes, which strongly influence the evolution of colorectal tumors. An "Immunoscore" was created to assess the role of the immune infiltrate. As mentioned above, after coining, Immunoscore was tested by an international multicenter study, which included 22 laboratories and over 9000 patients with colon carcinoma, aiming to sustain its utility in routine oncological practice. At that time, due to the differences (clinico-pathological pattern, markers, therapeutic strategies) between rectal and colonic cancer, scientists decided to exclude the rectal tumors from the study. Then the necessity of a dedicated project for studying the role and the impact of the immune reaction on the tumor evolution, prognosis and response to preoperative therapy came ahead. These are the reasons for which a multicenter international team designed a study to assess the intratumor immune response in rectal neoplasms.

### **1.2.2. Aim**

There were 3 purposes of this study: to evaluate reliability of the Immunoscore when assessing the prognostic on patients with localized rectal cancers, treated by primary surgical resection; to compare the Immunoscore prognostic with the TNM one; and to evaluate the

predictive value of the immune reaction about the response of the tumor to preoperative neoadjuvant chemoradiation therapy.

### 1.2.3. Material and methods

#### Patients and database

*Surgery cohort.* In the surgery cohort were included 111 prospectively registered patients with a rectal cancer who underwent radical surgery with mesorectum excision as a primary treatment at the Laennec/HEGP hospitals, Paris, France between 1987 and 2004. Clinical findings and conventional histopathologic parameters were scored according to TNM. Tumor locations and staging were as follows: stage I–IV, high rectum (n=79); stage I (T1–T2, N0, and M0), middle and low rectum (n=32). Postoperative cares were in accord with the general practice for patients with rectal cancer. The mean duration of follow-up was 74 months. The extreme values until progression/death or last follow-up were 0 and 244 months, respectively. A secured database, the Tumoral MicroEnvironment DB (TME.db), was constructed for the management of patient's data. Ethical, legal, and social implications were approved by an ethical review board.

*Neoadjuvant therapy cohort.* In the neoadjuvant therapy cohort were included 55 patients with TNM stage II and III middle or low rectal cancer registered between 2007 and 2012 from the Sf. Spiridon Hospital and the Regional Oncologic Institute (Iasi, Romania), two international expert centers where the Immunoscore is prospectively evaluated and where preoperative biopsies are available. The neoadjuvant therapy was applied following the guidelines of the European Society for Medical Oncology. The Research Ethics Committee of the Grigore T. Popa University of Medicine and Pharmacy, Iasi approved the study.

#### Histopathologic analysis

All the hematoxylin and eosin (H&E) sections of the rectal cancers were examined by pathologists for evaluation of TNM stage, tumor differentiation, lymph node ratio (LNR) defined as the number of positive lymph nodes divided by the total number of lymph nodes examined, presence of tumor emboli in vascular, lymphatic, or perineural structures (VELIPI status), and the quality of resection (R status). "Downstaging" was defined as any pathologic stage (ypTNM) less than pretreatment imagistic stage. Tumor regression grade (TRG) based on tumor: fibrosis ratio was determined as recommended.

#### Tissue microarray construction, staining, and analysis

For tissue samples harvested on surgical specimens, two cores were taken from core of the tumor (CoT) and two cores from the invasion margin (IM) (Fig. 1A) for tissue microarray (TMA) construction as previously described. Slides immunostained for CD3 and CD8 (clones SP7 and 4B11, respectively; Neomarkers) were quantified using an image analysis workstation (Spot Browser; ALPHELYS). The "minimum P value" approach was applied to obtain the cutoff providing the best separation between the groups of patients (high vs. low) related to their disease-free survival (DFS) outcome. Accordingly, the cutoff values determined for CD3+ and CD8+ cell densities were 256 (Fig. 1B) and 202 cells/mm<sup>2</sup> in the CT and 144 and 50 cells/mm<sup>2</sup> in the IM, respectively.

#### Determination of the Immunoscore

Patients were stratified according to the "Immunoscore" ("I") ranging from I0 to I4, depending on the total number of high densities observed (CD3+ cells and CD8+ cells in the tumor regions) (Galon et al., 2012). For example, I4 refers to a tumor with high densities of

CD3+ and CD8+ cells in CT and IM regions of the tumor (4-Hi); I0 refers to tumors with low densities of CD3 and CD8 in both tumor regions (0-Hi; Fig. 1C).

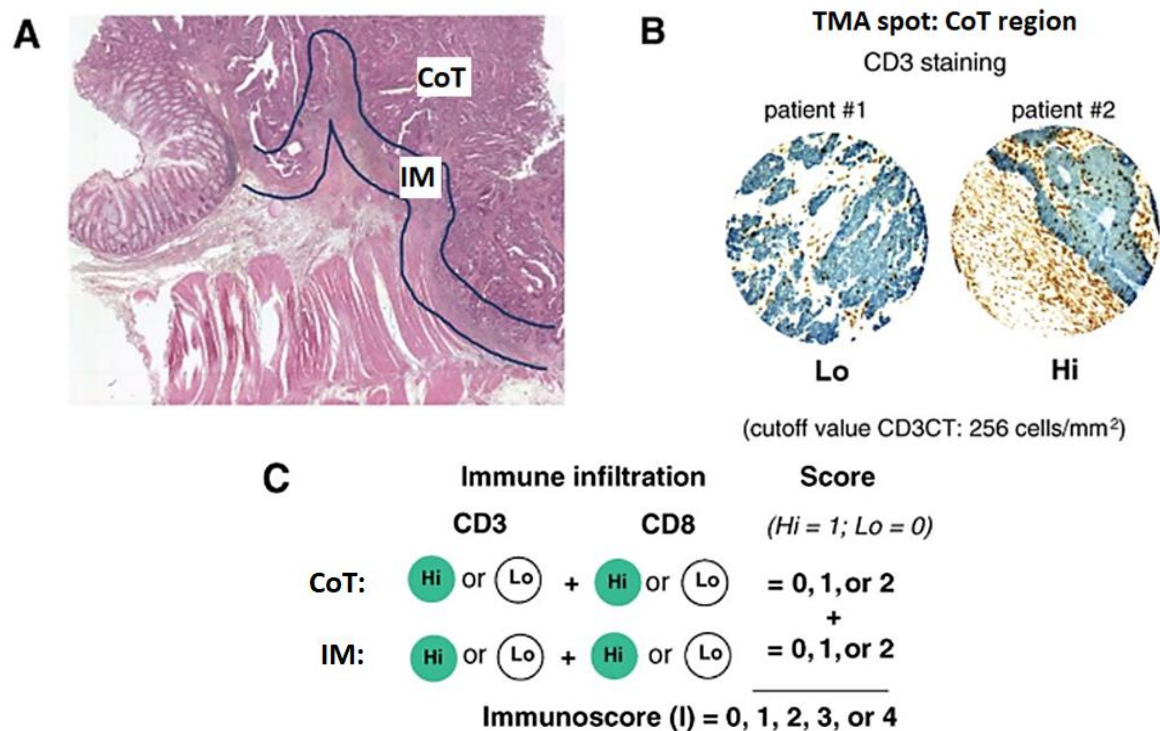


Figure 1. A, H&E section of rectal cancer (original magnification, x200) showing the tumor regions of interest; CoT and IM. B, two spots immunostained for CD3 showing the heterogeneity of CD3+ cell infiltration within tumors among patients. C, establishment of an Immunoscore, based on the numeration of two lymphocyte populations (CD3 and CD8) in CoT and in IM. The density of CD3+ cells and CD8+ cells is determined using an image analysis workstation. Each tumor is categorized into Hi or Lo density for each marker in each tumor region, according to a predetermined cutoff value (CD3 CT, 256 cells/mm<sup>2</sup>; CD3 IM, 144 cells/mm<sup>2</sup>; CD8 CT, 202 cells/mm<sup>2</sup>; CD8 IM, 50 cells/mm<sup>2</sup>) determined using the minimum P value approach. Patients are stratified according to a score ranging from I0 to I4, depending on the total number of high densities observed (two markers assessed in CoT, two markers assessed in IM). For example, I4 refers to a tumor with high densities of CD3+ and CD8+ cells in CoT and IM regions of the tumor (4-Hi). I3 refers to tumors with three high densities. Patients with low densities of CD3 and CD8 in both tumor regions (0 Hi density) is classified I0. CoT, core of the tumor; IM, invasive margin.

### Biopsy samples and staining

Biopsy samples were incubated for 32 minutes at 37°C with mouse monoclonal antibodies against CD8 (C8/144B; Dako; 1:50 dilution) and 20 minutes at 37°C with rabbit monoclonal antibodies against CD3 (2GV6; Ventana). The ultraView Universal DAB IHC Detection Kit (Ventana) was applied for detecting primary antibodies. High-resolution digital slides were obtained with a NanoZoomer scanner (Hamamatsu). The density of stained cells in the tumor areas was determined using the computerized image analysis system Developer XD (Definiens). Each tumor area was divided into tiles of 0.8 mm sides. The density of the immune cells stained in each biopsy was expressed as the mean density of the three most infiltrated tiles.

### Statistical analysis

Parametric (Student t test) and nonparametric (Wilcoxon–Mann–Whitney test) tests were used to identify markers with a significantly different expression among patient groups. Kaplan–Meier curves were used to visualize differences between DFS and overall survival

(OS). Significance among patient groups was calculated by using the log-rank test. DFS log-rank P values were corrected using the formula proposed by Altman and colleagues. We used a multivariate Cox proportional hazards model to determine HRs. HRs were corrected as suggested by Hollander and colleagues. All tests were two-sided, and a  $P < 0.05$  was considered statistically significant. All analyses were done using the statistical software R (survival package) implemented as a statistical module in TME.db.

#### 1.2.4. Results

##### **Prognostic factors in patients with rectal cancer treated by primary surgery**

*Clinicopathologic data.* The prospectively registered cohort of 111 patients with rectal cancer who underwent a primary resection of the tumor with mesorectum excision was investigated. Univariate analysis showed that TNM staging, T stage, and LNR significantly influenced DFS and OS ( $P \leq 0.05$  for all comparisons). In addition, the OS was also influenced by the age of the patients, N stage, and the presence of tumor emboli.

*Impact of the immune infiltration.* The densities of CD3+ and CD8+ immune infiltrates were assessed in CT and IM regions (Fig. 1A) by immunohistochemical-based TMA analyses (Fig. 1B) with image analysis software. Positive significant associations were observed between densities of CD3+ and CD8+ cells in tumor regions and clinical outcomes for DFS and OS. A combined analysis of tumor regions was performed. Patients with high density of a marker in both CoT and IM regions were classified "HiHi"; patients with low density of such marker in both tumor regions were classified "LoLo"; patients with a high density of such marker in a single tumor region (CoT or IM) were classified "Het." HRs were 4.57 and 5.18 for CD3 and 5.88 and 6 for CD8 between patient groups (HiHi vs. LoLo) for DFS and OS, respectively (all  $P = 0.004$  by the log-rank tests). This combined analysis of CoT plus IM regions was more efficient to discriminate patient's outcome when compared with single region analysis. Kaplan–Meier curves illustrate the significant longer DFS and OS times for patients with tumors highly infiltrated in combined tumor regions for CD3 and CD8. Thus, the assessment of the natural immune infiltration of CD3+ and CD8+ T lymphocytes in tumor regions (CoT/IM) classified patients treated by primary surgery in subgroups with statistically different clinical outcomes.

*Impact of the Immunoscore.* The "Immunoscore" uses the numeration of CD3+ and CD8+ cells in the CT and the IM regions to provide a score (from I0 to I4) depending on the total number of high densities observed (two markers assessed in CoT, two markers assessed in IM; Fig. 1C). According to the Immunoscore, repartitions of the cohort were as follows: 35% I4, 28% I3, 25% I2, 7% I1, and 5% I0, with an increasing risk of relapse from I4 to I0, with the associated HRs: 1, 1.69, 2.69, 3.1, and  $\infty$  respectively, for the DFS (log-rank test corrected  $P \approx 0.0038$ ) and HRs of 1, 2.63, 4.45, 4 and  $\infty$  respectively, for the OS (log-rank test  $P \approx 0.0003$ ; Supplementary Table S3). Kaplan–Meier curves illustrating the DFS and OS times according to the Immunoscore are shown in Fig. 2. Significant differences between patient groups for survival times were also observed after grouping the patients I0 and I1, which experienced the poorest postoperative outcome.

When combining the Immunoscore with the clinicopathologic markers, only the Immunoscore and the lymph node ratio (LNR) remained significant for DFS and OS in the model after stepwise-based Cox multivariate analysis (Immunoscore:  $P=0.007$  and  $P=0.002$ ; LNR:  $P=0.04$  and  $P=0.0007$ , for DFS and OS respectively). We then performed a Cox multivariate regression analysis by adding TNM staging to the Immunoscore into the model. Strikingly, the Immunoscore remained highly significantly associated with DFS, whereas the TNM staging did not reach significance. A strong impact of the Immunoscore on the OS was

also evidenced (HR of 0.62  $P=0.0004$ ). As a result, the Immunoscore seems to be a highly significant prognostic factor in the group of patients treated by primary surgery.

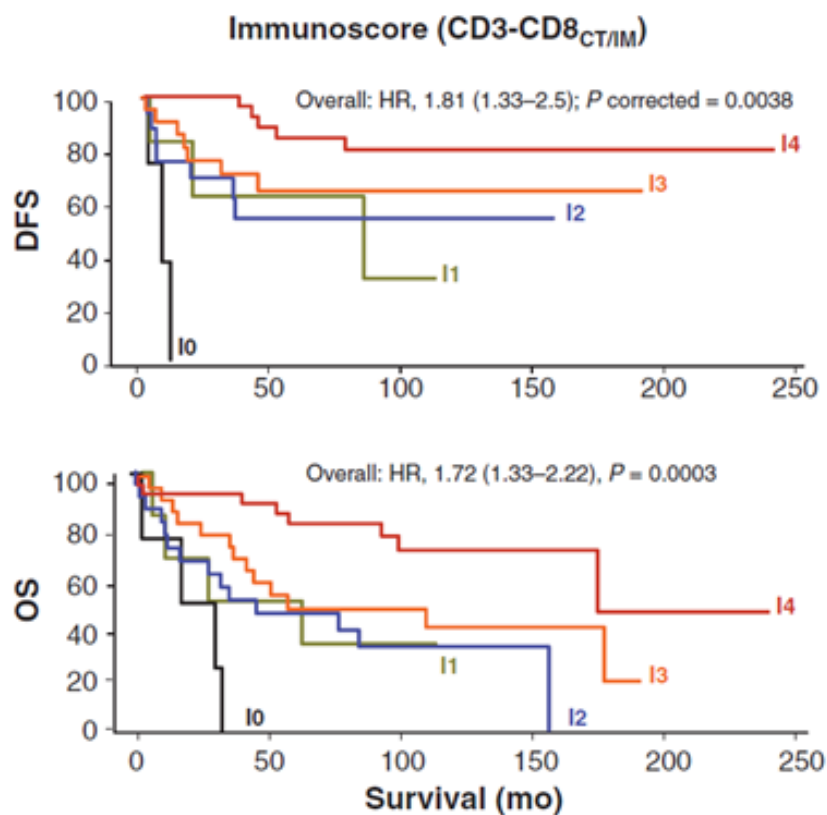


Figure 2. Kaplan–Meier curves for the duration of DFS and OS according to the Immunoscore in patients with rectal cancer eligible for a primary surgery (log-rank statistical test  $P < 0.005$  for all comparisons). Patients with an Immunoscore of 0 or 1 experienced a very poor postoperative outcome and thus could be grouped together.

### Is the natural immune infiltration, in patients treated by pCRT before surgery, a prognostic factor?

To question this issue, we first investigated a historic series of 33 patients that would be nowadays eligible for pCRT, to evaluate whether the natural immune infiltration could influence the clinical outcome. Significant higher densities of CD3+ (Fig. 3A) and CD8+ cells were observed in tumor regions (CoT and IM) of patients who did not experience recurrence (all  $P < 0.05$ ).

pCRT induces histologic reactions precluding the realization of an Immunoscore as the architecture of a treated tumor is deeply modified and the delineation of the analyzed tumor regions (CoT and IM) is often no longer practicable.

To circumvent this issue, biopsies performed before pCRT for diagnosis were investigated for the immune infiltrate in a recent cohort of 55 patients (Fig. 3B). We asked whether the immune infiltration could predict the response to pCRT, as pCRT induces cell death forms with immunogenic potential in rectal tumors. The ypTNM downstaging and TRG were used as endpoints to evaluate response to pCRT. High infiltration of CD3+ cells in tumor biopsies predominated (72% of the cases) in the subgroup of responders (complete or partial response) to pCRT (Fig. 3B), whereas 63% of the biopsies with a low infiltration of CD3+ cells belong to the group of non-responders to pCRT (for CD3, Fisher exact test  $P=0.015$ ). The same pattern was observed for CD8+ cells. The TRG4, 3, 2, 1, 0 evaluated on

surgical specimens from patients treated by pCRT were found in 7.3%, 45.4%, 32.7%, 7.3%, and 7.3% of the cohort, respectively. The lowest infiltration of CD3 and CD8 was observed in patients TRG0, without any sign of tumor regression. Thus, the assessment of the immune infiltrate in biopsies could help to anticipate the patient’s response to pCRT.

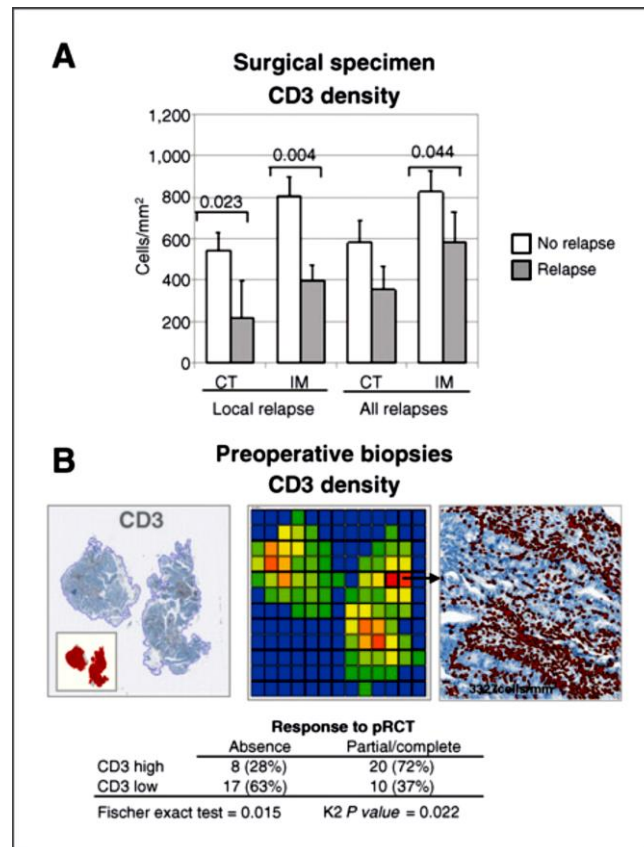


Figure 3. A, comparison of the mean (SEM) densities of CD3+ cells in the CoT and IM regions of tumor from patients eligible for a pCRT, without (white bars) or with (gray bars) tumor recurrence. B, biopsies immunostained were analyzed for the densities of CD3+ cells in tumor areas (in red in the small square) using a computerized image analysis system. The tumor area is divided into tiles for the analysis. A heat map view shows the densities of the stained cells in all tiles, from the minimum (green) to the maximum density (red). Right, illustration of the detection of CD3+ cells (in red) in a tile (magnification x20). Bottom, distribution of high and low densities of CD3+ cells in biopsies of patients that will experience a complete/partial response or an absence of response to pCRT according to the ypTNM downstaging of the tumor. The categorization of the patient's densities for CD3+ cells (high vs. low) was performed at the median of the cohort. The Fisher exact test comparing the distribution of Hi and Lo infiltration in each group,  $P < 0.05$  was considered significant.

### 1.2.5. Discussions

Although, many decades ago, the immune infiltration was suspected and then considered a positive factor for the evolution of cancer, it didn't have implications on tumor classification or clinical decisions. To date, there are over 250 published articles regarding the role of cytotoxic T cells, memory T cells, and T-helper cell subpopulations on prognosis of cancer. The majority of these studies were on colorectal cancer, and almost all of them consider CD8+ T cells to be associated with a good prognosis, while the role of T-helper cells depends on the type of cancer.

The therapeutic strategies for rectal carcinomas are anatomy-based, on the TNM staging systems resulted from the assessment of clinical and pathological features (relying mainly on tumor cell differentiation), and less on other biological characteristics of the tumor.

This generates the interest in finding new prognostic and predictive markers useful in adapting the therapy for each patient. The current study aimed to answer these questions, by including in the study cohort patients with meso-rectal excision of a rectal adenocarcinoma, performed between 1987 and 2003, and followed-up for 10 years. This setup was concordant with other studies already published, regarding the surgical solution and the evolution of the patients.

The Immunoscore relies on the quantification of the CD3+ and CD8+ T lymphocytes, in two areas, at the tumor center and at the margin of invasion. This score ranges from low T cell densities found at both the CT and the IM, named Immunoscore 0 (I0), to high densities classified as Immunoscore 4 (I4), which is associated with a longer patient survival. The slides with tissues immunostained for CD3 and CD8 are scanned and the two corresponding digital images are validated by the human operator. Digital image analysis is performed by a specifically designed software (Immunoscore Analyzer, HaliDx) which automatically detects the tissue histologic structures, followed by an operator-guided definition of the tumor (adenocarcinoma), healthy tissue (submucosa, muscularis propria, serosa), and the epithelium (mucosa). The operator also excludes all areas of tumor necrosis, suppurative inflammation, and artifacts to avoid false positives.

In our study, we demonstrated that the densities of CD3+ and CD8+ lymphocytes and the associated Immunoscore (from I0 to I4) significantly correlated with DFS and OS times. Our results are similar with data from other studies which show a beneficial impact of cytotoxic T lymphocytes and the associated Th1 immune orientation in tumors of diverse origins: melanoma, head and neck, breast, bladder, urothelial, ovarian, renal, prostatic, lung, colorectal [Fridman et al., 2012; Nosho et al., 2010] and few series of rectal cancer. These data advocate the idea that tumor behavior is the result of the continuous interaction between the tumor cells invasive process and the inflammatory reaction of the host, represented mainly by its immune system [Hanahan and Weinberg, 2011; Fridman et al., 2012]

The current study also shows the beneficial impact of a coordinated immune reaction in specific tumor regions (i.e., the core of the tumor and the invasive margin) to prevent recurrence and increase survival, as we observed in colon cancers [Galon et al., 2006]. As a result, we demonstrate the prognostic power of the Immunoscore, which summarizes the information of the immune-cell densities in these tumor regions [Mlecnik et al., 2011]. The Immunoscore classified nearly 50% of the patients with very distinct behaviors: 35% with very a good outcome (I4) as opposed to 12% with a poor outcome (for I0 and I1). This study confirms that there is an inverse relationship between tumor invasion and the extent of immune cell infiltration [Mlecnik et al., 2011]; 90% of the patients with the highest Immunoscore I4 presented with a localized cancer (stage I–II). But importantly, 34% of the patients with a localized cancer (stage I–II) presented with an Immunoscore associated with a very poor outcome (I0–I2); conversely, 16% of the patients with an advanced rectal cancer (stage III–IV) presented with an Immunoscore associated with a very good outcome. These data illustrate how the Immunoscore overcomes the TNM scoring system in multivariate analyses, as we observed in colon cancer [Mlecnik et al., 2011]. To reinforce the confidence on the statistical association observed, patients with poor postoperative outcome (I0 and I1) were pooled; again, the multivariate analysis showed the prognostic power of the Immunoscore.

Secondary, we demonstrated that the lymph node ratio is the only parameter adding information to the Immunoscore to better predict the DFS and the OS. Loco-regional LNR, which evaluates the proportion between the positive *vs.* the total number of surgically excised and analyzed lymph nodes, has been shown to be a more accurate and valuable prognostic marker than the absolute number of positive lymph nodes that is currently used in the TNM staging system. The information provided by the lymph node ratio rather reflects

complementary aspects of the antitumor immune response not depicted by the Immunoscore than mechanistic filtering activities attributed to lymph nodes.

Regarding the patients who received preoperative chemoradiation therapy, assessment of inflammatory immune reaction against the tumor by the Immunoscore is inappropriate as preoperative chemoradiation therapy induces profound changes (carcinoma regression, fibrosis, or mucous lakes) that make difficult a precise delimitation of the tumor and the invasive margin. To prevent this inconvenient, biopsies performed preoperatively for diagnosis purpose are the only material free of radiation or chemotherapy effects. We highlighted a significant correlation between densities of CD3+ cells (and of CD8+ cells, data not shown) and the response to preoperative chemoradiation therapy, as another study reported in a series of 48 patients [Yasuda et al., 2011]. One hypothesis explaining this correlation could be that preoperative chemoradiation therapy is an immune adjuvant acting through both the innate and adaptive immune responses. Future accurate tools predicting response to preoperative chemoradiation therapy should probably take into account both the immune components and the genetic features of the tumor. Our study is evaluating, on a large cohort of rectal carcinomas with a 10-year follow-up, whether the immune infiltrate in preoperative endoscopic biopsies could predict DFS and OS times, as suggested by the immune investigation performed on surgical specimens of our historic cohort of 33 patients. A positive result could provide a rationale to assess the immune infiltrate in biopsies to predict responders to preoperative chemoradiation therapy and to select patients achieving complete clinical tumor regression for their inclusion in prospective studies evaluating new strategies with minimal or even no surgery.

After the study was published in 2014, Pages and the international multicenter team, extended and supported by the Society for Immunotherapy of Cancer, continued to investigate the role of the Immunoscore in order to confirm and consolidate its role as prognostic factor for time to recurrence, defined as time from surgery to disease recurrence.

The consortium aimed to find a strategy to demonstrate the viability and reproducibility of the Immunoscore, confirmed its major prognostic value in CRC stages I-III, and proved the utility of the Immunoscore in predicting recurrences in patients with stage II [Galon et al., 2012]. The primary study endpoint was time-to-recurrence for Immunoscore (high/low), which was reached in the three cohorts of patients tested. Secondary endpoints were also validated, such as significance in DFS and OS, significance with Immunoscore tiered in 3 vs. 5 groups, significance in patients with stage II CRC, and significance in multivariate analysis, adjusted for Immunoscore such as, age, sex, T-stage, N-stage, and microsatellite instability. Immunoscore was proved to have the highest relative contribution to the risk among all clinical parameters, including the AJCC/UICC-TNM staging [Pages et al., 2018]. The Consortium strongly advocated for implementation of Immunoscore in clinical settings and the introduction of an “immune” component (I) to the TNM staging system (which would become TNM-I). Multiple benefits would run from this approach, for instance: a better prognosis of patients with CRC; a higher rate of identification of patients at high risk of tumor recurrence; and a better stratification of patients in what concerns the benefit from immunotherapies and specific combined adjuvant therapies [Galon and Bruni, 2019]. The results confirmed that Immunoscore provides a reliable estimate of the risk of recurrence in patients with colon cancer and, therefore, it should be implemented in association with the TNM classification system as a new component in the classification of cancer, designated TNM-Immune [Pages et al., 2018].

Lately, a new concept, “hot” and “cold” tumors have been used to differentiate tumors depending on their degree (high and low, respectively) of immune infiltration. Still, there is no consensus on the definition and use of these categories. In order to find a more standardized and univocal definition of these tumors based on the consensus Immunoscore, two intermediate categories (altered-immunosuppressed and altered-excluded) were proposed

[Galon and Bruni, 2019; Granier et al., 2017]. By stratifying these major groups based on T-cell infiltration, the Immunoscore might be used as a tool to identify phenotypes responding to distinct classes of mono- or combinational therapies. Furthermore, understanding how the immune landscape changes in subsets of molecular segments of disease is of great importance [Angell et al., 2020].

### **Final remark**

We can conclude that our study demonstrated the performance of the immune inflammatory reaction and the Immunoscore to predict the clinical behavior of the patients. This opens new perspectives for an international multicenter project designed to further evaluate the immune markers. These results were confirmed by further studies which were developed thereafter.

## **1.3. CDX1 and EphB tumor suppression genes expression in colorectal normal mucosa-adenoma-invasive carcinoma sequence**

### **1.3.1. Introduction**

The initial phases of carcinogenesis the majority of colorectal carcinomas, is characterized by aberrant activation of the Wnt/ $\beta$ -catenin pathway, which is consistent with its role in control of stem and progenitor cell proliferation [Clevers, 2006]. Alterations in Wnt/ $\beta$ -catenin pathway components lead, initially, to tissue proliferation generating adenomas which exhibit spatially restricted growth. Major effectors of cell positioning and compartmentalization within the intestinal crypts are the Wnt/ $\beta$ -catenin target genes EPHB2-4 [Merlos-Suarez and Batlle, 2008]. The interaction between EphB receptor tyrosine kinases and membrane-bound ligands of the ephrin family modulate the adhesive and repulsive cell properties, supporting an epithelial phenotype in many tissues [Merlos-Suarez and Batlle, 2008]. At early phases of carcinogenesis (for instance, the sequence of normal to dysplastic epithelial cells), functional EphB-ephrinB signaling effectively confines dysplastic epithelial cells to ephrinB-negative domains. Then after, at the adenoma-carcinoma transition, dysplastic cells breach this barrier and acquire tumor cell invasiveness [Chiu et al., 2009]. Inactivation of the EphB-ephrin system can occur by mutational crippling or transcriptional silencing of EphB receptor genes. In fact, EPHB2 and EPHB3 are transcriptionally inactive in a sizeable fraction of colorectal cancers [Fu et al., 2009]. Similar findings exist for EPHB4 and CDX1, another Wnt/ $\beta$ -catenin target important for cellular differentiation and with potential tumor-suppressor functions [Crissey et al., 2008]. However, the molecular mechanisms responsible for downregulation of CDX1 and EPHB2-4 in tumorigenesis despite continuous Wnt/ $\beta$ -catenin pathway activity are a matter of debate [Kumar et al., 2009].

Alterations of epigenetic features at regulatory regions is implicated in transcriptional inactivation of tumor-relevant genes. Hypermethylation of promoter DNA is often found in transformed cells and can silence tumor suppressor genes. Additional features of tumor cells are the loss of active histone marks and/or gain of repressive histone marks [Cedar and Bergman, 2009]. Consistent with changes in DNA and histone modification patterns, genes which encode the corresponding DNA- or histone-modifying proteins, are often deregulated in tumor cells. This includes histone deacetylases (HDACs), components of Polycomb repressive complexes (PRC) and de novo DNA methyltransferase (DNMT). Notably, epigenetic regulators appear to act in a coordinated fashion based on complex molecular

interactions [Cedar and Bergman, 2009]. Thus, to fully understand epigenetic deregulation of tumor-relevant genes, a comprehensive knowledge of the associated changes in DNA methylation and histone modifications as well as the underlying enzymatic machinery is required. Currently, however, epigenetic landscapes characterizing different expression states of CDX1 and EPHB2-4 in CRC cells are only ill-defined. Silencing by DNA hypermethylation has consistently been described only for CDX1 [Davalos et al., 2006; Wong et al., 2004]. Patterns of histone modifications associated with different expression states have been determined neither for CDX1 nor for the EphB receptor genes.

### 1.3.2. Aim

The purpose of the current project was to investigate the expression dynamics of a particular subset of Wnt/ $\beta$ -catenin target genes in colorectal carcinogenesis and to explore how epigenetic mechanisms contribute to their downregulation in carcinomas.

### 1.3.3. Material and methods

#### *Cell culture and inhibitor treatment*

The human cell lines HT29 and U2OS were obtained from the American Type Culture Collection. SW480, HCT116 and HEK293 cell lines were obtained from the Max Planck Institute of Immunobiology, Freiburg. The cell line LS174T was a gift from T. Brabletz (Freiburg). All cell lines were authenticated by expression and sequence analyses of indicative genes. Cells were cultured in Dulbecco's modified Eagle's medium (PAN-Biotech) supplemented with 10% fetal calf serum (Invitrogen), 100 units/ml penicillin streptomycin (Invitrogen), 10 mM HEPES buffer (PAN-Biotech) and 1% MEM non-essential amino acids (Invitrogen). For the inhibition of the DNMTs,  $2 \times 10^5$  cells were seeded per well of 6-well plates. After 16 h the cells were treated with 2  $\mu$ M, 10  $\mu$ M or 50  $\mu$ M 5-Aza-2'-deoxycytidine (Aza) (Sigma-Aldrich) which was replenished every 24 h. For HDAC inhibition,  $1 \times 10^6$  cells were seeded per well of six-well plates. The next day, cells were treated with either 15 mM or 30 mM nicotinamide (NIA), 300  $\mu$ M or 600  $\mu$ M splitomicin (SPT), 2 mM valproic acid (VPA), 2 mM sodium butyrate (NaBut) (Sigma- Aldrich), or 3  $\mu$ M MS-275 (Enzo), respectively. Treatment with 75 nM or 150 nM trichostatin A (TSA) (Sigma-Aldrich) was initiated 3.5 h before harvest. For time courses, cells were treated with either 3  $\mu$ M or 9  $\mu$ M MS-275, respectively, as indicated.

#### *Tissues*

Cells of normal colorectal mucosa (n = 21), low- (n = 14) and high-grade (n = 6) dysplasia/intraepithelial neoplasia and invasive colorectal adenocarcinomas (n = 21) were obtained by microdissection from FFPE tissue specimens of 21 patients resected for sporadic colorectal adenocarcinoma, also harboring sporadic adenomas [Lassmann S, et al. 2009]. Since there was no statistical difference among adenomas showing low-grade versus high-grade dysplasia, both groups were combined and are presented as "adenoma". The use of tissues had been approved by the local ethics committee.

#### *RNA isolation and reverse transcriptase PCR*

Isolation of total RNA from cell lines, cDNA synthesis and reverse transcriptase PCR (RT-PCR) analysis were performed as before using the NucleoSpin RNA II kit (Macherey and Nagel) and Superscript II reverse transcriptase (Invitrogen) according to the manufacturer's protocol. RNA from human tissue specimens in sufficient yield and quality was isolated and transcribed into cDNA, using the MMLV reverse transcriptase (Invitrogen). Quantitative RT-PCR (qRT-PCR) was performed in an iQ5 multicolor real-time PCR detection system (Bio-Rad) using SYBR green reaction mix (Peqlab), and an equivalent of 50

ng RNA per sample in case of cell lines. The expression data were normalized to  $\alpha$ -TUBULIN or GAPDH expression as indicated in figure legends. Expression data from human tissue specimens were normalized to  $\beta$ 2-MICROGLOBULIN.

#### *Western blotting*

Preparation of whole cell lysates and nuclear extracts, western blotting and signal detection was performed. CDX1 was detected using rabbit polyclonal antibodies (1:1,000) kindly provided by R. Kemler, Freiburg. Additional antibodies used were: mouse monoclonal anti-EPHB2 (1:1,000) (Santa Cruz; sc-100298), mouse monoclonal anti-EPHB3 (1:1,000) (Abnova; H00002049-M01), mouse monoclonal anti-EPHB4 (1:1,000) (Invitrogen 35-2900), mouse monoclonal anti- $\alpha$ -TUBULIN (1:10,000) (Sigma- Aldrich; T9026) and mouse monoclonal anti-GSK3 $\beta$  (1:1,000) (BD Biosciences; 610201).

#### *Analysis of DNA methylation*

Genomic DNA from  $5 \times 10^6$  cells was isolated using the DNeasy Blood & Tissue Kit (Qiagen) according to the manufacturer's protocol and sonicated on ice 10 times for 10 s each at amplitude setting 15 using a Branson sonifier model W-450D. Average DNA fragment size was 200 to 500 bp. Analysis of DNA methylation was done with 100 ng fragmented DNA and the MethylCollector<sup>TM</sup>-kit (Active Motif) following the manufacturer's protocol. Quantitative PCR (qPCR) was performed using 4  $\mu$ l of the precipitated DNA. 50 ng of fragmented genomic DNA not subjected to the MethylCollector<sup>TM</sup> served as reference material and were used for normalization.

#### *Chromatin immunoprecipitation*

ChIP assays were performed as previously described. Antibodies used were rabbit anti-trimethyl histone H3K4 (Abcam; ab8580), rabbit anti-acetyl histone H3K9/14 (Upstate; 06-599), rabbit anti-histone H3 (Abcam; ab1791) and isotype control immunoglobulin (IgGs) (Santa Cruz; sc-2027). DNA was analyzed by qPCR. One microliter of precipitated DNA and 2% of the input material were used as templates. Results from experiments with modification-specific antibodies are presented as % of input DNA after normalization using data from ChIPs with pan-H3 antibodies to correct for variations in nucleosome density.

### **1.3.4. Results**

Expression changes of CDX1 and EphB receptor genes in case-matched colorectal tissue specimens. To acquire expression profiles for CDX1 and the EphB receptor genes EPHB2, EPHB3 and EPHB4 during CRC tumorigenesis, we measured their expression in microdissected cells of a previously characterized group of human case-matched tissue specimens of colorectal normal mucosa, adenoma and invasive carcinoma using qRT-PCR. A more than two-fold change between case-matched samples was defined as increase or decrease. For CDX1, transcript levels vary between normal mucosa, adenoma and carcinoma only in few cases. In contrast, expression of EPHB2-4 was increased in the majority of both adenomas and carcinomas when compared to normal mucosa. This was most pronounced for EPHB3 where 85% of the adenomas and 81% of the carcinomas, respectively, showed elevated expression compared to normal mucosa. Although EphB receptor gene expression was largely maintained from adenomas to carcinomas, there was a noticeable downregulation of EPHB2 and EPHB3 in 33% and 35% of cases, respectively. Expression of EPHB4 increased, decreased or remained unchanged with equal frequencies in carcinomas. Importantly, by comparing changes in CDX1 and EphB receptor expression and the occurrence of nuclear  $\beta$ -catenin in the tissue specimens, we find that their expression can be decreased in carcinomas despite the presence of nuclear  $\beta$ -catenin-positive tumor cells. Thus, it appears that certain Wnt/ $\beta$ -catenin target genes can be subject to secondary downregulation in carcinomas which is not simply the result of diminished Wnt pathway activity.

Furthermore, comparison of expression changes in the case-matched tissue specimens provided no evidence for a coordinated regulation of CDX1 and EphB receptor genes during CRC tumorigenesis. Within carcinomas, there was a trend towards reduced EPHB2 levels in CRCs with lymph node metastasis and poorer differentiation, which is in agreement with previous findings and confirms its clinical relevance. An association of CDX1 or EphB receptor gene expression with Microsatellite- Instability (MSI) status or T category, respectively, was not determined because the majority of the investigated carcinomas was MSI negative and T3.

Differential expression of CDX1 and EphB receptor genes in human colorectal cancer cell lines. To further probe the divergent expression observed in carcinoma samples we investigated mRNA amounts and protein levels of CDX1 and EPHB2-4 in the CRC cell lines LS174T, SW480, HCT116 and HT29, and the non-CRC cell lines HEK293 and U2OS by qRT-PCR and western blotting. The CRC cell lines carry activating pathway mutations, and show high expression of the Wnt/ $\beta$ -catenin target AXIN2, except for HCT116 in which the AXIN2 promoter is silenced by DNA hypermethylation. Importantly, as seen with the different cases of invasive carcinoma tissue specimens, the distinct CRC cell lines differ with respect to expression of CDX1 and EPHB2-4. The highest expression levels of all four genes are found in LS174T, whereas in the other CRC and non-CRC cell lines these genes are expressed at much lower levels or not at all. Taken together, this identifies a set of CRC cell lines which reflect heterogeneous expression of CDX1 and EPHB2-4 in human tissue specimens of CRC and which can serve as a model for mechanistic investigations.

Differential methylation of CDX1 and the EphB receptor genes. To analyze whether differential expression of CDX1 and EPHB2-4 is due to epigenetic modifications, we first tested whether differences in the DNA methylation status correlate with alterations in their expression. CpG islands were identified at the promoter regions and the first introns of the genes under investigation, and DNA methylation patterns in these regions were examined by affinity precipitation using recombinant methylated DNA-binding domain (MBD) protein. PCR amplification of precipitated material revealed differential methylation at the distal promoter, the transcriptional start site (TSS) and the first intron of CDX1 which are unmethylated in LS174T, but are highly methylated in SW480, HCT116, HT29 and HEK293. In contrast, the EPHB2 and EPHB4 loci appear to be unmethylated in the CRC cell lines at all positions investigated. Similarly, with the sole exception of an intronic site, EPHB3 is neither methylated in the region upstream of the TSS, nor in the region spanning the TSS in any of the CRC cell lines tested. Preliminary results from bisulfite sequencing of genomic DNA also indicate that the EPHB3 promoter is not methylated. We additionally confirmed these results using the methylationsensitive enzyme HpaII and its methylation-insensitive isoschizomere MspI. Genomic DNA was digested by HpaII and MspI and used as template for PCR. Untreated genomic DNA was used as amplification control. The results of the analyses also indicate that the EPHB3 intronic site is methylated in SW480, HCT116, HT29 and HEK293 but not in LS174T, whereas the TSS appears to be unmethylated in all CRC cell lines. Taken together, despite similar patterns of transcriptional activity, CDX1 and EPHB2-4 exhibit differences with respect to DNA methylation.

The observed differences in methylation of promoter DNA correlate with differential sensitivity of CDX1 and EPHB2-4 expression towards the DNMT inhibitor Aza. Consistent with the absence of DNA methylation at the promoter regions of EPHB2-4, their expression was not or only marginally affected by treatment with Aza regardless of cellular background. In contrast, Aza-treatment resulted in a concentration-dependent increase in CDX1 expression of up to 30-fold in SW480 and HCT116. Yet, no increase in CDX1 expression was observed in HT29 despite similar levels of DNA methylation. As expected from the lack of DNA methylation at CDX1 in LS174T cells, Aza-treatment did not result in expression changes in these cells. Thus, as seen in previous studies, aberrant DNA methylation is able to

silence CDX1 gene expression, but additional factors which seemingly vary depending upon cellular background, can play a role. Furthermore, repressive mechanisms other than DNA methylation are engaged in EphB receptor downregulation and CDX1 and EPHB2-4 are silenced by distinct mechanisms.

Decreased promoter occupancy by RNA polymerase II and loss of active histone modifications accompany reduced expression of CDX1, EPHB2 and EPHB3. Next, we performed chromatin immunoprecipitations (ChIP) to investigate if posttranslational histone modifications could provide mechanistic explanations for reduced transcription of CDX1 and EPHB2-4. Active histone marks [trimethylated histone H3 lysine 4 (H3K4me3), acetylated histone H3 lysines 9 and 14 (H3K9/14ac), monomethylated histone H3 lysine 27 (H3K27me1), monomethylated histone H3 lysine 9 (H3K9me1), monomethylated histone H4 lysine 20 (H4K20me1)], as well as repressive histone marks [trimethylated histone H3 lysine 27 (H3K27me3), di- and trimethylated histone H3 lysine 9 (H3K9me2; H3K9me3)], were analyzed. In addition, promoter occupancy by RNA polymerase II (RNAPII) was monitored. In strongly expressing LS174T cells, CDX1 and the EphB receptor genes are associated with RNAPII and active histone modifications. Loss of CDX1 expression correlates with the disappearance of RNAPII and active histone marks. Similarly, at EPHB3 RNAPII levels and active histone marks decrease concomitant with reduced transcription. At EPHB2 and EPHB4, we observe a similar regression of some active marks (H3K27me1, H3K9me1 and H4K20me1) in SW480, HCT116 and HT29 cells. However, promoter occupancy by RNAPII and levels of H3K4me3 and H3K9/K14ac are maintained despite a decline in expression. As an exception, H3K4me3 and H3K9/K14ac are reduced at EPHB2 in HT29 cells. Unexpectedly, repressive histone marks are not associated with any of the investigated genes in SW480 and HCT116 cells. Only HT29 cells show a modest enrichment of H3K27me3 and H3K9me3 at several positions of the CDX1 locus, at the TSS and intronic regions of EPHB3 and EPHB4, as well as at a promoter-distal and an intronic site of EPHB2. Nonetheless, the CRC cell lines express components of the Polycomb repressive complexes 1 and 2 including the H3K27 methylase EZH2 as well as several methyltransferases which target H3K9. Also, bulk histone preparations from the CRC cell lines contain H3K9me2, H3K9me3 and H3K27me3. Therefore, absence of repressive histone marks appears to be a specific feature of the inactive CDX1 and EPHB2-4 loci rather than the result of a general deficiency in repression systems based on H3K9 and H3K27 methylation in certain CRC cell lines. Taken together, these findings reveal further variability in the epigenetic landscapes of the genes under investigation and suggest that a decrease of active chromatin characteristics underlies the differential expression of certain Wnt/ $\beta$ -catenin target genes in CRC cell lines.

Involvement of class I and class III HDACs in the repression of CDX1, EPHB2 and EPHB3. Functional relevance of reduced histone acetylation levels for CDX1 and EphB expression was tested by use of three different HDAC inhibitors: TSA, acting on class I and class II HDACs; SPT and NIA, acting predominantly on the NAD<sup>+</sup>-dependent sirtuins (class III HDACs). CRC cell lines were treated with increasing concentrations of each of these inhibitors. Additionally, treatment with TSA was combined with either SPT or NIA. Subsequent expression analyses using qRT-PCR revealed stable expression levels in LS174T cells. Similarly, HDAC inhibition had no effect on CDX1 and EPHB4 expression. However, TSA-, NIA- and SPT-treatment led to reactivation of EPHB2 specifically in HT29 cells. Combined treatment, especially of TSA and NIA, almost doubled the effect. The results for EPHB3 were even more striking. In all of the CRC cell lines with low EPHB3 gene expression, HDAC inhibition by TSA or NIA restored EPHB3 expression.

To narrow down the HDACs involved in the regulation of EPHB2 and EPHB3, we used VPA and NaBut, specifically acting on class I and class IIa HDACs, as well as MS-275, acting on class I HDACs only. Expression levels of CDX1 and the EphB receptor genes were compared to those in TSA-treated cells. In case of EPHB2 and EPHB3, the class I specific

inhibitor MS-275 restored expression to levels similar to or even exceeding those seen with TSA and the other reagents. MS-275 and NaBut also affected CDX1 expression in SW480 and HT29 revealing a contribution of class I HDACs to the repression of CDX1 as well. No change in expression of EPHB4 was observed. Taken together, these results suggest that class I HDACs in addition to class III HDACs are important to subdue expression of CDX1, EPHB2 and EPHB3 in certain CRC cells.

To obtain evidence that CDX1, EPHB2 and EPHB3 are immediate targets of HDACs we established temporal profiles for changes in their expression upon treatment of CRC cell lines with MS-275 and NIA over time courses from 3 to 24 h. In parallel, we analyzed the behavior of the CDKN1A/p21CIP1 gene which is an accepted and well characterized direct target of class I HDACs.<sup>33-35</sup> Furthermore, we performed ChIP analyses to monitor changes in H3K9/14 acetylation at these loci. Increases in CDX1, EPHB2 and EPHB3 transcript levels were seen in SW480 cells as early as three hours after addition of either 3  $\mu$ M or 9  $\mu$ M MS-275, respectively. A more delayed response of CDX1, EPHB2 and EPHB3 was observed in HT29 cells. In HCT116 cells, CDX1 and EPHB2 levels remained unchanged upon MS-275 treatment as before, while upregulation of EPHB3 resembled that in HT29 cells. NIA elicited responses of EPHB3 in SW480 and HT29 cells and of EPHB2 in HT29 cells with temporal profiles similar to MS-275. Of note, the observed time courses of MS-275-induced reactivation of CDX1, EPHB2 and EPHB3 are in complete accordance with the behavior of CDKN1A/p21CIP1 both in SW480 and HT29 cells. Moreover, ChIP analyses detected significantly elevated levels of H3K9/14ac at the CDX1, EPHB2 and EPHB3 and CDKN1A/p21CIP1 loci in the presence of MS-275. Taken together, these observations strongly suggest that HDACs are directly involved in the downregulation of CDX1, EPHB2 and EPHB3 promoter activity.

Upregulation of HDACs has been linked to colorectal tumorigenesis. Therefore, we investigated whether differences in expression of the class I enzymes HDAC1, HDAC2, HDAC3 and HDAC8 and the class III members SIRT1 and SIRT2 might underlie the formation of distinct epigenetic landscapes at the CDX1, EPHB2, EPHB3 and EPHB4 loci. Expression analyses were performed by RT-PCR. However, we did not detect differential expression of any of these enzymes which could explain the differential occurrence of H3K9/K14ac. Therefore, despite the functional importance of HDACs, these findings rule out that solely altered expression levels of these enzymes are responsible for decreased histone H3 acetylation at regulatory regions of CDX1 and EPHB2-4.

### 1.3.5. Discussions

Published data regarding the deregulation of CDX1 and EphB receptor genes based on separate analyses in different collections of cell lines and patient-derived samples raised the possibility that certain Wnt/ $\beta$ -catenin targets might be coordinately repressed in colorectal cancer carcinogenesis and progression [Merlos-Suarez and Batlle, 2008]. A rationale for synchronized silencing could be highly redundant functions of the genes affected or cumulative effects [Kumar et al., 2009]. To this end, we performed comparative quantitative expression analyses for CDX1 and EPHB2-4 in human tissue specimens of case-matched colorectal normal mucosa, adenoma and carcinoma. Furthermore, we employed a model of CRC cell lines to systematically analyze DNA methylation and histone modification patterns in relation to the expression status of CDX1 and the EphB receptor genes. Our findings suggest biphasic, albeit not strictly coordinated, expression patterns with a surge in activity in adenomas followed by downregulation in the corresponding invasive carcinomas. In the CRC cell line model, reduced expression of CDX1 and the EphB receptor genes is accompanied by massive changes of epigenetic features. Considerable heterogeneity among epigenetic

landscapes and differential responses towards inhibition of DNMTs and HDACs reveal that the mechanisms of repression differ among CDX1 and EphB receptors in a gene-specific manner and depending upon cellular background although class I and III HDACs generally appear to play critical roles in the silencing process.

The current study demonstrates that transcript levels of EphB receptor genes, especially EPHB3, markedly increase in adenomas and are subsequently downregulated at the transition from adenoma to carcinoma in up to 35% of cases, supporting the view that their repression confers growth advantages and invasiveness to tumor cells. However, our parallel qRT-PCR analyses in case-matched tissue specimens of normal mucosa, adenoma and carcinoma revealed divergent expression profiles of CDX1 and EPHB2-4 and thus clearly refute the hypothesis of coordinate misregulation. On the other hand, variable downregulation in carcinomas fits our findings that distinct mechanisms operate in the inactivation of CDX1 and EPHB2-4. It is also consistent with their non-overlapping expression in vivo [Wong et al., 2004]. Overall, this suggests that the various EphB receptors affect different aspects of tumor cell physiology, such as the ability of CRC tumor cells to metastasize which seems to be linked more strongly to EPHB2.

The highly variable CDX1 and EPHB2-4 expression in CRC tissue specimens and their strongly reduced expression in carcinomas and in carcinoma cell lines with an active Wnt/ $\beta$ -catenin pathway are remarkable. A general defect in pathway activity is unlikely to underlie this downregulation. This would be difficult to reconcile with the observed divergent behavior of CDX1 and EPHB2-4. Furthermore, active Wnt/ $\beta$ -catenin signaling is essential at all stages of tumor formation [Clevers, 2006]. On the other hand, epigenetic mechanisms would be ideally suited to impinge on the control of individual Wnt/ $\beta$ -catenin target genes. Indeed, hypermethylation of promoter DNA and repressive histone marks can render genes refractory to Wnt induction during embryogenesis [Wohrle et al., 2007]. Interestingly, one of the models proposed to explain epigenetic silencing of tumor relevant genes is based on the observation that transformed cells increasingly acquire features of embryonic stem cells (ESCs) [Cedar and Bergman, 2009]. Thus, genes under control of polycomb repressive complexes in ESCs are predisposed to epigenetic silencing in tumor cells. BMI1 and EZH2, components of PRCs, are upregulated in cancer cells and this may contribute to the reconstitution of gene expression patterns similar to ESCs [Cedar and Bergman, 2009]. Known physical interactions between DNMTs and PRCs in cancer cells could account for the additional recruitment of DNMTs to PRC targets and explain aberrant promoter hypermethylation of tumor-relevant genes. This model is consistent with chromatin features at the inactive CDX1 locus in HT29 cells. The dual action of DNMTs and PRCs could also explain why Aza treatment in HT29 cells failed to restore CDX1 expression. However, H3K27me<sub>3</sub>, the mark laid down by the EZH2 lysine methylase, is absent from CDX1 in SW480 and HCT116 cells while promoter hypermethylation nonetheless occurs. Clearly, variable mechanisms of repression can operate at a single locus and embryonic modes of gene regulation need not necessarily be recapitulated in CRC tumorigenesis.

In SW480 and HCT116 cells, reduced expression of EPHB2-4 occurs in the absence of repressive histone marks and hypermethylation of promoter DNA. For EPHB2 and EPHB4 there are conflicting results as to the contribution of DNA methylation to their inactivation in tumor cells [Fu et al., 2009; Davalos et al., 2006]. DNA methylation at EPHB3 had not been systematically analyzed in the past. We believe that the observed hypomethylation of all three EphB receptor genes in our cellular model reflects genuine properties of these loci since we could show hypermethylation of CDX1 and SFRP2 under the same experimental conditions. However, our observations of pronounced heterogeneity and divergence concerning expression patterns and epigenetic features of CDX1 and EPHB2-4 in different tissue specimens and cellular backgrounds provide a potential explanation for the discordant literature data. Nonetheless, our findings support previous reports showing that diminished

expression of EPHB2-4 is based on mechanisms other than DNA methylation [Fu et al., 2009]. Since it remains unclear what brings about reduced expression of EPHB4, a striking finding of our study is that the CDX1 and EPHB3 loci show reduced levels of the active histone marks in non-expressing CRC cell lines. This holds true also for EPHB2 in HT29 cells. Generally, a decrease in H3K4 trimethylation and H3 acetylation is paralleled by a strong decline in gene expression [Wang et al., 2009]. Histone methylation and acetylation are regulated by the precise interplay between antagonistic groups of lysine methylases/demethylases and HATs/HDACs, respectively [Wohrle et al., 2007]. Changes in HAT activity due to mutations are known to play a role in certain forms of leukemia, whereas in epithelial cancers, HDACs feature more prominently [Ropero and Esteller, 2007; Cedar and Bergman, 2009]. The results of our inhibitor studies clearly reveal the repressive influence of class I and class III HDACs on CDX1, EPHB2 and EPHB3.

How could HDACs be targeted to CDX1, EPHB2 and EPHB3 in a context-dependent manner? Overexpression seemingly suffices to grant epigenetic modifiers access to their targets. However, our results did not reveal differences in expression levels of the HDACs investigated. HDACs can be recruited to promoters as part of co-repressor complexes through interactions with DNA-binding transcriptional repressors. Recently, the NF $\kappa$ B family member c-Rel was described as a negative regulator of EPHB2 in the CRC cell line SW620 [Fu et al., 2009]. NF $\kappa$ B proteins are known to interact with HDACs raising the possibility that the HDAC inhibitor-sensitive repression of EPHB2 which we detect in HT29 cells, involves a c-Rel/HDAC complex. However, we do not think that this mechanism is generally involved in the regulation of EphB receptor genes because repression of EPHB2 is refractory to HDAC inhibition in SW480 and HCT116 cells. Also, bioinformatic analyses of the EPHB3 and EPHB4 promoter sequences did not identify c-Rel binding sites. Yet, this does not exclude the possibility that other transcriptional repressors bind to these promoters and recruit epigenetic modifiers including HDACs.

New data were published in the years after, revealing the nature of complex pathways that influence the tumorigenesis in human, but also, in murine models (which partially recapitulate the human colorectal cancer). Some of these pathways are the activating mutations of K-Ras and lesions in the TGF- $\beta$  and Eph-Ephrin signaling pathways. The CDX family of transcription factors are also potential contributors to the colorectal carcinoma phenotype. Both, CDX1 and CDX2 are mandatory for the normal development of the gastrointestinal tract and its homeostasis during life [Hryniuk et al., 2012; 363]. Nowadays, it is thought that, in murine models, CDX function in intestinal tumorigenesis is restricted by the peri-implantation lethality of CDX2 null mutants. Moreover, although CDX1 null mice do not display any overt intestinal phenotype, CDX members probably play interfering roles in the intestinal tract, and the impact of concomitant loss of CDX1 and CDX2 on intestinal tumorigenesis has not been reported yet [Hryniuk et al., 2014].

Recent studies showed that loss of CDX2 expression was identified in about 30% of human CRC and is associated with higher tumor grade, proving that CDX2 suppresses colorectal cancer (Hryniuk et al., 2014). Although the observations in murine models support a tumor-suppressive function for CDX2 as a member of the CDX family, it is uncertain if its increase in polyposis is reflective of neoplastic-related CDX2 functions or of Cdx2-dependent developmental events. Moreover, the potential functional partial superposition between CDX1 and CDX2 has confounded a clearer understanding of a role for CDX in colorectal carcinoma [Hasson et al., 2014].

The role of EphB in carcinogenesis was recently showed also in lung carcinomas, proving that the effect of EphB1 on the tumor cells migration and invasion is context-related and depends on EphB1 phosphorylation [Wang et al., 2020]. Also, it was demonstrated that overexpression of Ephrin-B2 is correlated with poor overall survival and disease-free survival

in HNSCC, pancreatic adenocarcinoma and bladder urothelial carcinoma [Oweida et al., 2017].

### **Final remarks**

In conclusion, expression profiling of CDX1 and EphB receptor genes in colorectal cancers tissue specimens and a set of colorectal cancer cell lines as well as the comprehensive study of DNA methylation and histone modifications at these four Wnt/ $\beta$ -catenin target genes shows that mechanisms which lead to their transcriptional repression are highly divergent and, moreover, can vary for a given locus depending upon cellular background. The observed mechanistic heterogeneity underlying gene-specific and context-dependent deregulation of tumor suppressors may reflect the multi-faceted nature of genetic and epigenetic changes found in colorectal carcinomas. In view of therapeutic applications this may necessitate careful investigations of epigenetic features in individual tumor samples, yet, our data further support the notion that HDAC and DNMT inhibitors are promising agents for the treatment of solid cancers.

## **1.4. Centrosome-associated serine/threonine kinase 15 oncogene expression in genetic instable colorectal carcinoma**

### **1.4.1. Introduction**

According to the genetic alterations which affects the sporadic colorectal cancers during tumorigenesis, cancers can be with chromosomal instability (CIN-type), representing 85% of cancers, and with microsatellite instability (MIN-type), representing the rest of 15%. Due to the multiple abnormalities in chromosomal number, CIN-type are aneuploid; MIN-type carcinomas harbor fewer alterations and are considered, mainly, diploid [Sugai et al., 2003]. Genetic differences between CIN-type and MIN-type cancers regarding tumor-associated candidate genes were revealed using techniques as mCGH and FISH for DNA analysis and cDNA microarray for mRNA expression profiling. Still, little is known about the genome-wide differences of DNA copy number changes, when comparing CIN-type and MIN-type colorectal carcinomas at a gene-specific level. More than this, it is unclear if a gene specific profile of DNA copy number change can induce the differential mRNA expression profile and each CIN- or MIN- specific clinico-pathological phenotypes. There are some studies aiming to screen the DNA copy number changes using the technique of array-based Comparative Genomic Hybridization (aCGH) in colorectal carcinoma [Camps et al., 2006; Jones et al., 2005; Nakao et al., 2004]. The weakness of those studies resides in the fact that they used fresh frozen tissue samples with no prior microdissection of tumor cells, the quantity and the quality of aCGH data to be biased. More than this, there was no distinction between the sporadic and familial character of colorectal carcinomas. Only one of the above-mentioned studies [Nakao et al., 2004] investigated by comparing 125 cases of CIN- and MIN-type colorectal carcinomas and found distinct chromosomal regions altered in each type. Affected chromosomal regions were identified also by the other two studies [Camps et al., 2006; Jones et al., 2005], but the studied cohort was unbalanced in what concerns the CIN- and MIN-type carcinomas ratio (32 vs. 2) or too few (4 vs. 6) to obtain a valid conclusion on DNA copy number differences between CIN- and MIN-type carcinomas. Therefore, although previous studies identified candidate chromosomal regions in CIN- and MIN-type colorectal carcinomas, there is still need for studies to detect gene-specific targets specifically characteristic for CIN- or MIN-type carcinomas of colon and rectum.

In CIN-type colorectal carcinomas, step-wise aurora A mRNA upregulation was identified by quantitative RT-PCR [Gerlach et al., 2006] and amplification of the aurora A gene locus at 20q13 was proved by aCGH [Lassmann et al., 2007]. In another study [Lassmann et al., 2009] detected overexpression of aurora A gene in CIN-type colorectal carcinomas using mRNA expression profiling on micro-dissected invasive tumor cells from tissue blocks fixed in formalin and embedded in paraffin. On the other hand, MIN-type colorectal carcinomas rarely present aurora A gene amplification detected by PCR [Nishida et al., 2007]. Interestingly, in vitro, ectopic aurora A overexpression in tumor cells generate aneuploidy, converting a MIN-type tumor into an aneuploid (CIN-like) colorectal tumor cell [Lentini et al., 2007]. All these studies suggest that aurora A is differentially regulated and expressed in CIN- vs. MIN-type colorectal carcinomas, numerous tumor cells being positive for aurora A (overexpression of aurora A). The variable amount of aurora A detected during cell cycle, especially in colorectal carcinomas with aurora A gene amplification, might be explained by the variable fraction of proliferating cells, reflected in the mitotic rate of the tumor [Nishida et al., 2007; Burum-Auensen et al., 2008].

### 1.4.2. Aims

The research I was involved in had two directions grouped in two studies. The first one aimed to evaluate if the genomic DNA mutations occur differently in CIN- than in MIN-type colorectal cancers and to identify the specific oncogenes and/or tumor suppressor genes, by analyzing using aCGH DNA of tumor cells micro-dissected from sporadic chromosomal instable and microsatellite instable colorectal carcinomas. A panel of 287 target sequences (most of them being oncogenes and tumor suppressor genes) was designed for aCGH screening and validation of candidate genes by FISH using serial sections obtained from FFPE tissue blocks.

In the second study of the same research team, the purpose was to analyze the aurora A expression and regulation in the normal mucosa-adenoma-carcinoma sequence in patients diagnosed and treated for sporadic colorectal carcinoma. The study aimed to identify whether aurora A is differently regulated and expressed in CIN-type vs. MIN-type carcinomas and if it is linked to CIN- and MIN-associated (aneu-)ploidy.

### 1.4.3. Material and methods

#### Study 1

##### *Tissue samples*

The 22 cases of sporadic colorectal carcinomas, already characterized as CIN- (11 cases) or MIN-type (11 cases), were analyzed in this study. The majority (19 cases) were located in colon, and the rest (3 cases) were rectal. No neoadjuvant therapy was administrated to these patients prior to surgery which was an R0 resection for 21 patients and R1 for one patient with rectal tumor, palliative surgery. The samples were routinely processed by formalin fixation and paraffin embedding. thin sections (4-5 microns) were obtained and stained Hematoxylin and Eosin for histopathological diagnosis, grading and staging according to WHO classification. Table 1 presents the clinicopathological data of all cases. Specific areas of interest representing normal mucosa adjacent to carcinoma or from the resection margins (at least 10 cm away from the tumor, and invasive carcinoma were marked on the HE sections from case-matched FFPE tissue blocks in order to microdissect them and prepare the genomic DNA.

Table 1 Clinicopathological data of the study cases

Case ID	Age	Sex	pT	pN	Hist. type	G	Genetic instability
1	71	Male	3	0	Tubular	2	CIN
2	86	Male	3	0	Tubular	2	CIN
3	88	Male	3	0	Tubular	2	CIN
4	67	Male	3	0	Mucinous	3	MIN
5	74	Male	3	0	Tubular	3	CIN
6	64	Female	2	0	Tubular	2	CIN
7	70	Male	3	0	Tubular	2	CIN
8	83	Female	3	2	Tubular	3	MIN
9	90	Female	3	1	Tubular	2	MIN
10	77	Female	3	0	Tubular	2	CIN
11	75	Male	3	0	Tubular	2	CIN
12	80	Female	3	0	Tubular	2	MIN
13	90	Female	3	0	Mucinous	2	MIN
14	76	Male	3	0	Tubular	2	CIN
15	82	Male	3	0	Mucinous	3	MIN
16	66	Female	3	0	Undiff.	3	MIN
17	69	Female	3	0	Tubular	2	MIN
18	86	Female	2	0	Mucinous	2	MIN
19	72	Male	2	0	Undiff.	3	MIN
20	64	Male	3	1	Tubular	3	CIN
21	79	Female	3	0	Tubular	2	MIN
22	77	Male	3	0	Tubular	2	CIN

#### *Microdissection and DNA isolation*

To obtain normal epithelium of colorectal mucosa and tumor cells from invasive carcinoma, sections of 10 microns were used for microdissection with fine needles. The harvested cells were then immediately placed into tissue lysis buffer (QIAamp DNA Kit, Qiagen, Hilden, Germany) and incubated overnight at 55°C. DNA was purified the next day according to the manufacture's protocol, eluted in 20 µl of water, and measured in a spectrophotometer (ND1000, Peqlab, Erlangen, Germany). In addition, DNA fragment length was assessed by agarose gel electrophoresis and showed good quality for aCGH analysis.

#### *aCGH experiments and statistical data analysis*

For aCGH, commercially available arrays, including 287 target clones of oncogenes and tumor suppressor genes spotted in triplicate ("GenoSensor™ Array 300" Abbott, Wiesbaden, Germany), were used according to the manufacturer's protocols with some modifications: A pool of all 22 normal DNAs was used as "reference DNA" for the aCGH experiments. This approach had been successful before in our laboratory, but was additionally assessed in the present study by aCGH analysis of individual normal DNA against the pooled normal reference DNA. From this, the threshold for significant DNA copy number changes above normal variation was defined for DNA losses and gains at <0.8 and >1.2, respectively. For each aCGH experiment, 300 ng of pooled reference DNA and 300 ng of one tumor DNA were subjected to random priming with Cy3- and Cy5-labeled deoxycytidine 5'-triphosphates, respectively ("Microarray Random Priming Kit," Abbott). This was followed by a DNase digestion step, probe purification using microspin columns (S-200 HR, Amersham), and checking the reaction on an agarose gel, with all processed samples having an acceptable size range of 50–200 bp. For sample, hybridization, Cy3-labeled pooled reference DNA, and Cy5-labeled tumor DNA were incubated together at equal amounts with hybridization buffer containing Cot-1 DNA, denatured, and incubated on the aCGH at 37°C for 72 h. Microarrays were washed three times in 2×SSC/50% formamide at 40°C for 10 min each, three times in 1×SSC at room temperature for 5 min each, and rinsed in distilled water

before embedding in diamidino-2-phenylindole (DAPI)-mounting medium. Microarrays were left for 45 min before scanning in the “GenoSensor Reader System” (Abbott, Wiesbaden, Germany). DNA copy number changes from scanned microarrays were identified by the software and analysis program supplied (Abbott, Wiesbaden, Germany). This, first, segments and identifies target spots on the captured image and rejects debris, then measures the intensity and ratios of tumor to reference DNA signals hybridized to triplicate target clones, performs normalization, and finally statistically evaluates significant copy number changes. The thresholds for significant DNA copy number changes were for DNA losses of  $<0.8$  and for DNA gains of  $>1.2$ . Differences of copy number changes between CIN and MIN tumors were evaluated by calculating the frequencies of aberration per target gene.

#### *Validation of aCGH results by FISH analysis*

To validate individual genes detected by aCGH, serial sections (5  $\mu\text{m}$ ) of a tissue microarray containing representative invasive carcinoma areas of all 22 sCRC cases were hybridized with gene-specific and centromere-specific (chromosome enumeration probe, CEP) fluorescent hybridization probes. A dual color probe for EGFR/CEP7 (Spectrum Orange™, Spectrum Green™) and a single-color probe for ZNF217 (Spectrum Orange™) were commercially available (Abbott/Vysis, Wiesbaden, Germany). A STK15-specific single-color probe (Cy3™, red) and a single color CEP20-specific probe [fluorescein isothiocyanate (FITC), green] were custom made (Chrombios, Raubling, Germany). The single-color probes for ZNF217 and STK15 were each cohybridized with the single color CEP20 probe, so as to allow assessment of gene-specific (red) and centromere-specific (green) signals in the same cells. Before probe hybridization, tissue sections were subjected to deparaffination (2 $\times$  xylene and 100, 95, 70, and 50% ethanol) and pretreatment in citrate buffer (pH 6.0) in a microwave oven (180 W) for 20 min followed by Pronase E (0.05%) digestion for 3 min at 37°C. Subsequently, tissue sections were denatured in 50% formamide at room temperature for 15 min and in 70% formamide at 75°C for 5 min. Slides were immediately immersed in ice cold ethanol (70, 95, and 100%, 5 min each) and dried at 37°C. In the meantime, fluorescent hybridization probes had been denatured at 75°C for 5 min and were pipetted onto dried slides, followed by incubation for 16 h at 37°C. Slides were then washed in 2 $\times$ SSC at room temperature and in 2 $\times$ SSC at 37°C for each 2 min and finally counterstained with DAPI for 3 min. Cover-glassed (Vecta-Shield, Molecular Probes) slides were stored at  $-20^{\circ}\text{C}$  until analysis.

Microscopic analysis of FISH sections was performed using a fluorescence microscope with ApoTome imaging system for 3D visualization (“Zeiss AxioPlan2 imaging microscope” equipped with a PlanApochromat  $\times 63/\text{NA}1.4$  oil objective, Carl Zeiss MicroImaging GmbH, Göttingen, Germany). A total of 5–10 image stacks were taken with a pixel size of  $1,388 \times 1,040$  at 0.925- to 0.945- $\mu\text{m}$  intervals from representative tumor areas. The AxioVision software converted the image stacks into a 3D view, which was then assessed for the number of gene and centromere signals. Evaluation of FISH was done by an investigator who did not know the results of the aCGH. Signals of gene- and CEP-specific probes were counted in at least 50 cells and the mean ratio of gene/CEP signals was calculated for each case.

## **Study 2**

### *Patients*

The study included 71 patients with surgical resection for sCRC (median age of patients = 72 years; Table 2). We used FFPE tissue blocks representing samples of normal mucosa obtained from resection margins (71 cases), adenomas with low-grade dysplasia (36 cases) and high-grade dysplasia (13 cases) and invasive adenocarcinoma (71 cases). Case-

matched samples of normal mucosal epithelium, dysplastic epithelium and adenocarcinoma were obtained from surgical resection specimens. As a rule, the normal epithelium should have been from at least 150 mm away from the adenocarcinoma (resection margin). Adenomas should have been from the same resection specimen but in separate location, or from a previous colonoscopic polypectomy, and not from the immediately adjacent dysplastic mucosa, in order to rule out a bias due to carcinoma-associated dysplastic lesion. For easier statistical inclusion, data for low- and high-grade dysplasia/intraepithelial neoplasia were merged and designated as “dysplastic epithelium” or adenoma. Table 1 presents the histopathological features of all 71 cases included in the study, and separately for CIN- and MIN-type tumors. For classification of microsatellite instable carcinomas, microsatellite analysis was performed by analysis of five microsatellite loci in DNA derived from microdissected tumor cells and normal epithelial cells.

Three of 71 cases yielded uninformative data and were excluded from statistical analyses addressing differences between chromosomal and microsatellite instability. Appropriate tissues samples were selected after re-classification of hematoxylin and eosin-stained sections by an experienced pathologist, as described before for 41 of the cases [Gerlach et al., 2006; Lassmann et al., 2007]. The study had been approved by the local Ethics Committees (#251/04 Ethik-Kommission, Albert-Ludwigs-Universitat, Freiburg, Germany; and the Grigore T. Popa University Medicine and Pharmacy, Department of Pathology, Iasi, Romania).

Table 2: Clinico-pathological parameters of sporadic colorectal cancer patients investigated (\* For 3 cases, no MSI-data could be obtained. \*\* no neoadjuvant RCTx.)

	All CRC	CIN-type CRC*	MIN-type CRC*
<b>Number of cases (N)</b>	71	54	14
<b>Sex</b>			
male	44	35	6
female	27	19	8
<b>Age (median, range)</b>	72 (46-90)	72 (46-88)	76 (67-90)
<b>Location</b>			
Colon	63	46	14
Rectum**	8	8	0
<b>Tissue samples (N)</b>			
Normal epithelium	71	54	14
Adenoma (LGIN, HGIN)	49 (36, 13)	40 (30,10)	6 (4,2)
Invasive carcinoma	71	54	14
<b>Tumor classification</b>			
T1	3	3	0
T2	9	7	2
T3	53	38	12
T4	6	6	0
N0	46	34	10
N1	11	10	1
N2	11	8	2
Nx	3	2	1
<b>Grading</b>			
G1	5	5	0
G2	48	37	8
G3	18	12	6

#### *Analysis of Aurora A mRNA Expression*

We had previously determined aurora A mRNA levels in 41 cases [Gerlach et al., 2006] and in this study examined aurora A mRNA levels of the additional 30 new cases. For this, and as before [Gerlach et al., 2006], RNA extracts of microdissected cell populations (normal or dysplastic epithelial cells, invasive tumor cells) of formalin-fixed and paraffin-embedded tissue specimens were prepared and subjected to quantitative RT-PCR (qRT-PCR) analysis using established protocols and the comparative Ct-method for final calculation of

aurora A mRNA expression levels. Of all tissue samples analyzed, 183/191 (96%) yielded sufficient RNA of appropriate quality for qRT-PCR analysis (acceptable signals for both reference gene/ TATA box binding protein, target gene/aurora A). Failures to obtain sufficient mRNA and/or appropriate signals in qRT-PCR analysis (reference gene/TATA box binding protein, target gene/aurora A) were observed in 1/71 (1%) normal epithelium samples, 3/49 (6%) dysplastic samples and 5/71 (7%) invasive carcinoma samples.

#### *Analysis of Aurora A Protein Expression and Tumor Cell Proliferation*

For analysis of aurora A protein expression and tumor cell proliferation, tissue microarrays were constructed from representative tissue areas (normal and dysplastic epithelium, invasive carcinoma) by punching 2 mm cores per tissue sample. Comparative analyses of entire tissue sections and 2 mm cores demonstrated that staining patterns were homogeneous throughout the selected tissue blocks. Serial tissue microarray sections of 4 microns thickness were subjected to immunohistochemistry with aurora A and Ki67 specific antibodies [Gerlach et al., 2006; Lassmann et al., 2007]. In brief, sections were cut, dried and deparaffinized. Antigen retrieval was done by boiling sections in Tris-EDTA buffer pH9 (aurora A) or citrate buffer pH6 (Ki67), followed by incubation with primary antibodies for aurora A (1:50, aurora kinase 2, clone JLM28, Loxo/Novocastra, Dossenheim, Germany) and Ki67 (clone MIB-1, 1:500; DakoCytomation) for 60 min. Secondary antibodies were incubated for 30 min and detection was with the LSAB-Fast red System (DakoCytomation). Positive controls for aurora A and Ki67 protein stainings were routinely processed formalin-fixed and paraffin-embedded tonsils and negative controls sections were stained by omission of the primary antibody. All stainings were performed on a DAKO Autostainer (DakoCytomation) and evaluated semi-quantitatively in tumor cells with scores for cytoplasmic and nuclear aurora A staining as before (Figure 4) and scores for nuclear Ki67 staining: score 0=all tumor cells negative, score 1<10% tumor cells positive, score 2=10–50% tumor cells positive and score 3>50% positive.

#### *Analysis of Aurora A Gene Copy Numbers and Aneuploidy by Fluorescence In Situ Hybridisation*

Aurora A gene copy numbers and tumor cell aneuploidy were assessed as follows: Serial tissue microarray sections of 5 mm thickness were subjected to deparaffination, pre-treatment in pH6 citrate buffer in a microwave oven (180 W) for 20 min and Pronase E (0.05%) digestion for 3 min at 37°C. Subsequently, sections were denatured in 2xSSC/50% Formamide (room temperature), and 2xSSC/70% Formamide (75°C, 15 min), immersed in ice cold ethanols (70, 95 and 100%, 5 min each) and dried at 37°C. In the meantime, the fluorescence in situ hybridization (FISH) probes had been denatured (75°C, 5 min) and were hybridized to the dried sections (16 h, 37°C) as follows: Section (i) probe specific for the aurora A gene and centromere 20 (chromosome enumeration probe, CEP20; Chrombios, Raubling, Germany) and section (ii) to (v) probes specific for CEP7, CEP8, CEP11 (Abbott Vysis) and CEP13 (QBiogen). After hybridization, sections were washed in 2xSSC (room temperature) and in 2xSSC (73°C, for 2 min), cover-glassed with DAPI-containing mounting medium (Vector) and stored at minus 20°C until analysis. Stained sections were evaluated on a fluorescence microscope (AxioPlan 2 imaging with ApoTome system, Carl Zeiss MicroImaging GmbH, Gottingen, Germany) by taking image stacks at 0.5–1.0 mm intervals for each three representative areas per case (x63 magnification). Image stacks were converted into 3D view by AxioVision software and then assessed for Aurora A- (section i) and centromere- (sections i–v) specific signals. For aurora A gene copy numbers, FISH data are presented as the mean number of aurora A gene- and CEP-specific signals per tumor cell per case. A mean of  $67 \pm 21$  tumor cells (range, 13–100) were counted per case. The ratio of the mean aurora A gene- to CEP20-specific signals per cell was calculated to assess aurora A gene amplification for each case. For determination of tumor cell aneuploidy by FISH, 57 first

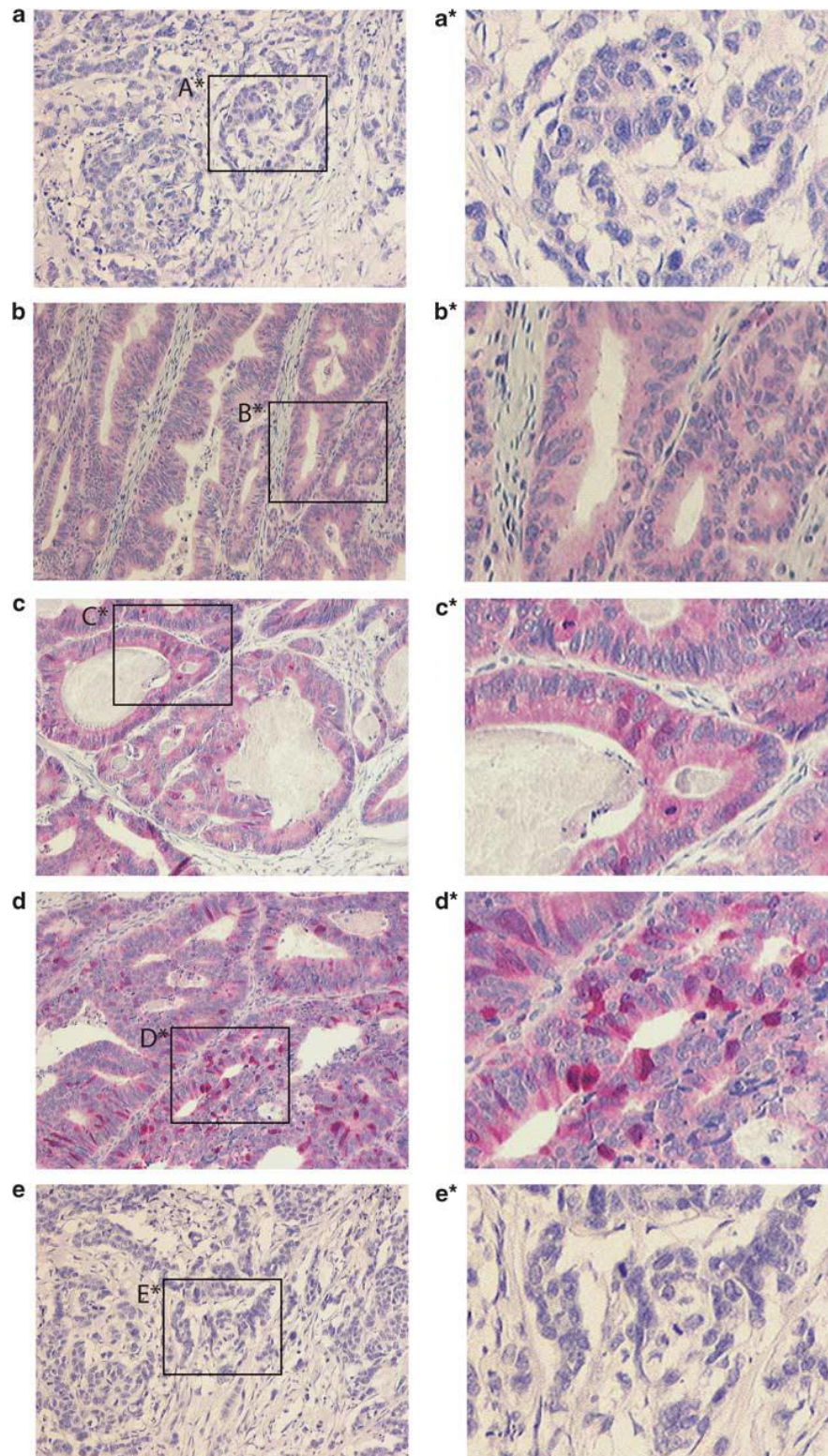


Figure 4: Representative immunohistochemical stainings of aurora A protein expression in sporadic colorectal cancers. The figure shows representative photographs of sections stained with an aurora A specific antibody. (a–d) (magnification x100): Four examples of invasive carcinomas with immunohistochemistry score 0 (a; case #23; chromosomal instable), 1 (b; case #13; microsatellite instable), 2 (c; case #16; chromosomal instable) and 3 (d; case #5; chromosomal instable). (e) Negative control staining (no primary antibody; case #23). A\*–E\* (magnification x200): enlarged inserts from a–e.

20 samples of normal colonic epithelium were analyzed with FISH probes specific for CEP7, CEP8, CEP11, CEP13, CEP20. The mean CEP-specific signals per normal epithelial cell were (number of cells counted in brackets): CEP7:  $2.13 \pm 0.2$  (n=131); CEP8:  $2.17 \pm 0.12$  (n=140); CEP11:  $2.23 \pm 0.07$  (n=140); CEP13:  $2.1 \pm 0.18$  (n=130) and CEP20:  $2.01 \pm 0.11$  (n=98). The mean ( $2.15$ )  $\pm 3$  standard deviations ( $3 \times 0.15$ ) of all five CEP-signals per normal epithelial cell was 2.6 and this was set as cut-off for classification of aneuploidy in invasive tumor cells. In invasive carcinomas, a mean of  $88 \pm 25$  tumor cells per case (range, 2–105) were evaluated for the five CEP-signals and the corresponding mean calculated.

### *Statistics*

Statistical evaluation included experimental data of aurora A mRNA (qRT-PCR: dCT values) and protein (immunohistochemistry: scores 0–3) expression, aurora A gene- and CEP20-specific FISH signals, tumor cell proliferation (Ki67-specific immunohistochemistry: scores 0–2), ploidy (diploid or aneuploid) and microsatellite status as well as clinicopathological parameters of tumor T and N category and tumor grading. Samples of low- and high-grade intraepithelial neoplasia were combined as ‘dysplastic epithelium’ for these analyses and three cases were excluded from comparisons of chromosomal and microsatellite instable cases, due to lacking microsatellite status. Correlations between parameters were performed using the Spearman correlation coefficient. Wilcoxon signed rank test was applied to compare continuous parameters of paired samples. Frequency tables were tested by Fisher’s exact test for comparison of binary parameters. A *P*-value of  $<0.05$  was considered significant.

## **1.4.4. Results**

### **Study 1**

#### *Validation of aCGH approach*

To validate sample preparation and aCGH analysis of the formalin-fixed and paraffin-embedded tissue samples, normal colonic epithelium DNA samples from a female were hybridized against those from a male case. No copy number changes were detected, except for losses at the X chromosome. The mean copy number change for the 287 targets was  $1.0034 \pm 0.06$  (coefficient of variation= $2.53 \pm 2.06\%$ ). In addition, aCGH analysis of a single normal DNA against the pooled normal reference DNA revealed no significant copy number changes (Fig. 1b). However, a slightly higher variation of signals (mean copy number change for 287 targets= $1.0156 \pm 0.17$ , coefficient of variation= $2.02 \pm 1.45\%$ ) was detected and the threshold for significant DNA losses and gains was adapted accordingly to  $<0.8$  and  $>1.2$ , respectively.

#### *Evaluation of aCGH profiles of sCRC*

All 22 cases with sCRC (Table 1) were analyzed as described in the “Materials and methods”. Purified DNA from microdissected, formalin-fixed, and paraffin-embedded invasive colorectal tumor cells did exhibit an acceptable fragment size of  $>200$  bp. After fluorescence labeling and DNase digestion, both tumor DNAs and simultaneously processed reference DNAs had comparable fragment sizes between 50 and 200 bp, and these resulted in high quality aCGH data (coefficient of variation= $2.05 \pm 2.7\%$  for all 22 tumors). Analysis of all DNA copy number changes from the 22 tumor DNAs showed that chromosomal regions known to be affected in colorectal cancers (metaphase CGH) were also identified in the present aCGH approach. Thus, aCGH revealed frequent DNA gains at 20q, 13q, 8q, and 7p

and losses at 18q, 17p, and 8p and specifically pinpointed oncogenes and tumor suppressor genes located within these chromosomal regions.

#### *Comparison of aCGH profiles between CIN- and MIN-type colorectal cancers*

Upon separate evaluation of the CIN- and MIN-type tumor aCGH profiles, differences were observed between the two groups for the frequency of DNA gains and losses at specific chromosomal regions and for gene-specific amplifications and deletions. With respect to the frequency of specific chromosomal regions, those previously associated with colorectal tumors by mCGH, i.e., DNA gains at 20q, 13q, 8q, and 7p and losses at 18q, 17p, and 8p, were more often observed in CIN-type, but less in MIN-type tumors. In particular, DNA gains at 20q were detected at a frequency of 36–64% in CIN-type, but only 9–27% in MIN-type tumors; DNA gains at 13q were identified at a frequency of 45–54% in CIN- and only 18–36% in MIN-type tumors; DNA amplifications at 7pq were seen at a frequency of 9–72% in CIN- and only 9–27% in MIN-type tumors and DNA losses at 17p occurred at 18–55% in CIN- and only 9–18% in MIN-type tumors. Moreover, aCGH allowed the identification of specific target sequences within these differentially altered chromosomal regions. Thus, genes preferentially altered within the identified CIN-tumor-associated chromosomal regions (20q, 13q, 7pq, and 17p) included DNA amplifications of eight genes on chromosome 20q (TOP1, AIB1, MYBL2, CAS, PTPN1, STK15, ZNF217, and CYP24), two genes on chromosome 13q (BRCA2 and D13S25), and three genes on chromosome 7 (IL6, CYLN2, and MET) as well as DNA deletions of two genes on chromosome 17p (HIC1 and LLGL1). Finally, additional differences of gene-specific DNA amplifications and deletions between CIN- and MIN-type tumors were observed at other chromosomal regions than 20q, 13q, 7pq, and 17p: CIN-tumor associated DNA amplifications were identified for EXT1 (8q24.11) and MYC (8q24.12) as well as DNA deletions for MAP2K5 (15q23) and LAMA3 (18q11.2). In contrast, distinct MIN-tumor-associated DNA amplifications were detected for E2F5 (8p22–q21.3), GARP (11q13.5–q14), ATM (11q22.3), KAL (Xp22.3), XIST (Xq13.2), and DNA deletions for RAF1 (3p25), DCC (18q21.3), and KEN (21q tel).

#### *Validation of aCGH findings by FISH*

To validate aCGH findings, FISH analysis of three selected genes was performed on serial tissues as those used for aCGH, including one gene showing normal DNA copy numbers in CIN- and MIN-type tumors (EGFR on chromosome 7p) and two genes (STK15 and ZNF217) on chromosome 20q, which were differentially altered in CIN- and MIN-type tumors. Normal DNA copy numbers of EGFR as determined by aCGH in both CIN- and MIN-type tumors corresponded to normal EGFR copy numbers or polyploidy of chromosome 7 by FISH. Preferential amplification of STK15 and ZNF217 in CIN-type tumors as determined by aCGH was confirmed by FISH analysis. Note that aCGH data and FISH ratios are different parameters, as aCGH is based on a comparative analysis of DNA extracted from normal colorectal epithelium and microdissected tumor cells, whereas FISH is a direct cell-specific analysis and quantification is different for the two methods (“Materials and methods”).

## **Study 2**

### *Aurora A Expression in the Adenoma-Carcinoma Sequence of Sporadic Colorectal Cancer*

Aurora A mRNA and protein expression was determined in case-matched normal and dysplastic epithelium and invasive carcinomas of 71 cases with sporadic colorectal cancer [Gerlach et al., 2006; Lassmann et al., 2007]. As shown in Figure 5a and Table 3, significant upregulation of aurora A mRNA expression occurred between normal and dysplastic

epithelium ( $P=0.0008$ ) as well as between dysplastic epithelium and invasive carcinoma ( $P=0.0001$ ). Aurora A mRNA expression was significantly higher in invasive carcinomas than normal epithelium ( $P<0.0001$ ). Similarly, the frequency of aurora A protein expressing (hereafter referred to as ‘aurora A positive’) cells increased significantly from dysplastic epithelium to invasive carcinoma ( $P=0.0027$ ) and was markedly higher in invasive carcinomas as compared with normal epithelium ( $P=0.001$ ) (Figures 4 and 5b; Table 3). There were, however, no significant differences in the number of aurora A positive cells in normal and dysplastic epithelium ( $P=1.000$ ). In invasive carcinomas, aurora A mRNA expression and aurora A positive tumor cells were significantly correlated between each other ( $P=0.0151$ ). High numbers of aurora A positive tumor cells were preferentially found in node-negative cases (pN0 category;  $P=0.0419$ ) but were not associated with pT category ( $P=0.9316$ ) or tumor grading ( $P=0.5864$ ).

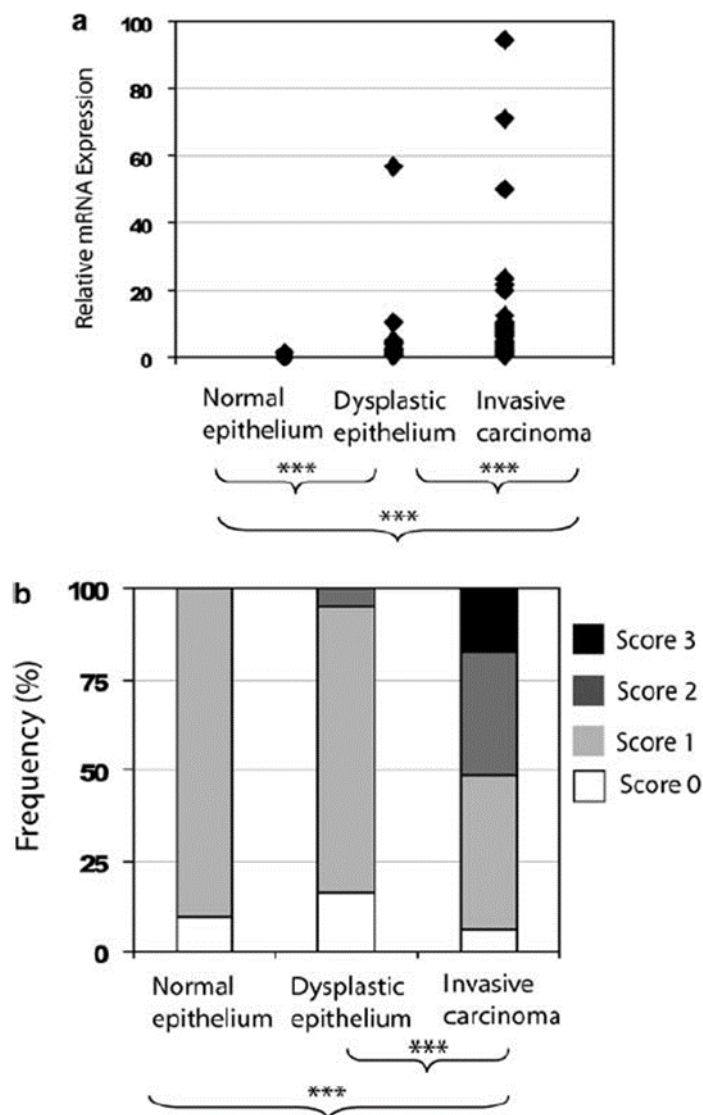


Figure 5 Aurora A mRNA and protein expression in the carcinogenesis of sporadic colorectal cancers. The graphs summarize findings of relative aurora A mRNA levels determined by qRT-PCR (a) and aurora A protein expression determined by semiquantitative immunohistochemistry (b). Note the significant increase of aurora A mRNA expression from normal to dysplastic to invasive epithelial cells (a). The increase of aurora A mRNA expression is paralleled by a significant increase of the frequency of aurora A positive cells from dysplastic epithelia to invasive carcinoma (b). Significant correlations are marked by brackets with \*\*\* (P-values are given in the main text).

Table 3: Summary of AURKA mRNA and protein expression. The numbers of successfully analyzed cases (n) are given for all investigated cases (N). Data on AURKA protein expression (AUKRA IHC) is presented as the percent (number) of cases for each IHC score, which are defined in Materials and Methods. Relative AURKA mRNA expression (with standard deviation in brackets) are given for low (LGIN) and high (HGIN) grade dysplasia and invasive carcinomas (CA) as compared to those observed in normal epithelium (No, set to "1").

	Normal epithelium	Dysplastic epithelium		Invasive carcinoma
		(LGIN)	(HGIN)	
<i>Aurora A mRNA</i>				
n/N (%)	70/71 (99%)	34/36 (94%)	12/13 (92%)	66/71 (93%)
Mean $\pm$ s.d.	1	1.59 ( $\pm$ 1.1)	7.41 ( $\pm$ 15.8)	8.08 ( $\pm$ 15.2)
<i>Aurora A protein</i>				
Score 0	6/64 (9%)	6/31 (19.4%)	1/12 (8%)	4/68 (6%)
Score 1	58/64 (91%)	25/31 (80.6%)	9/12 (75%)	29/68 (43%)
Score 2	—	—	2/12 (17%)	23/68 (34%)
Score 3	—	—	—	12/68 (17%)

#### *Analysis of Aurora A Gene Copy Numbers and Tumor Cell (Aneu)ploidy*

To examine aurora A gene copy numbers and tumor cell ploidy, serial sections of 39/71 invasive carcinomas in which aurora A expression had been measured, were subjected to established FISH-based analyses [Lassmann et al., 2007]. FISH revealed a wide range of aurora A gene- (2.18–14.40) and CEP20- (2.00–14.62) specific signals, generally elevated above the normal copies of 2. Low level of aurora A gene amplification (defined as aurora A/CEP20 signal ratio  $>1.25$ ) was detected in 15/39 (38.5%) invasive carcinomas. Having defined a cut-off for aneuploidy by analysis of the five CEP probes in normal epithelial cells (cut-off=2.6, Materials and methods), 20/39 (51.3%) of invasive carcinomas showed marked aneuploidy. Elevated aurora A gene- ( $P=0.0001$ ) and CEP20- ( $P=0.0002$ ) specific FISH signals were significantly linked to tumor cell aneuploidy.

#### *Comparison of Chromosomal- and Microsatellite Instable Sporadic Colorectal Carcinomas*

Alterations of chromosome 20q13 and/or the aurora A gene appear to occur preferentially in (aneuploid) chromosomal instable colorectal cancers. We therefore compared ploidy and aurora A specific DNA, mRNA and protein levels in chromosomal (n=30) versus microsatellite (n=10) instable sporadic colorectal carcinomas. Aneuploidy was exclusively seen in invasive carcinomas with chromosomal (20/30; 67%), but not microsatellite (0/10; 0%) instability ( $P=0.0004$ ). In addition, chromosomal instable invasive carcinomas exhibited significantly higher aurora A specific FISH signals (range, 2.18–14.40) as compared with microsatellite instable invasive carcinomas (range, 2.70–4.30) ( $P=0.0206$ ). CEP20-specific FISH signals also tended to be elevated in chromosomal instable invasive carcinomas, but this did not reach significance ( $P=0.0853$ ). Whereas we did not detect a significant difference between sporadic chromosomal and microsatellite instable invasive carcinomas at the aurora A mRNA level ( $P=0.8427$ ), surprisingly microsatellite instable invasive carcinomas displayed significantly higher numbers of aurora A positive tumor cells ( $P=0.0043$ ; Figure 6a).

#### *Correlation of Aurora A Expression to Tumor Cell Proliferation*

Since aurora A function is tightly associated with the cell cycle, we next examined whether the high number of aurora A positive tumor cells in microsatellite instable invasive carcinomas is simply reflecting a high rate of tumor cell proliferation. Indeed, by semi-quantitative evaluation of tumor cell proliferation using Ki67-specific immunohistochemistry, microsatellite instable invasive carcinomas exhibited significantly

higher tumor cell proliferation as chromosomal instable invasive carcinomas ( $P=0.0335$ , Figure 6b), an observation previously reported by others. Moreover, aurora A mRNA ( $P=0.0259$ ) and protein ( $P<0.0001$ ) expression was closely linked to tumor cell proliferation.

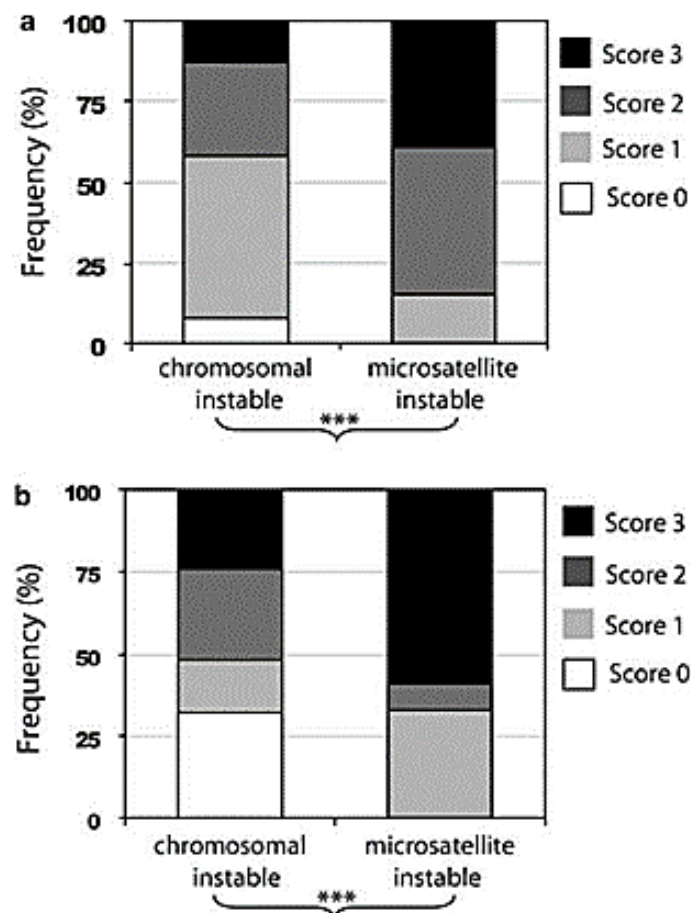


Figure 6 Comparison of aurora A protein expression and tumor cell proliferation in chromosomal and microsatellite instable sporadic colorectal cancers. The figure summarizes results of aurora A- (a) and Ki-67- (b) specific immunohistochemistry in chromosomal and microsatellite instable invasive carcinomas. Note that high aurora A- and Ki67-scores were significantly more frequent in microsatellite instable as compared with chromosomal instable invasive carcinomas (marked by brackets and \*\*\*; P values are given in the main text).

### 1.4.5. Discussions

#### Study 1

For the time being, the study was the first that analyzed DNA copy number changes of a large series of mostly known oncogenes and tumor suppressor genes in CIN and MIN unstable sCRC. Several other studies have investigated CIN- and MIN-type colorectal cancers with respect to their mRNA expression profiles using cDNA microarrays or to genome-wide DNA copy number changes using array Comparative Genomic Hybridization (aCGH) [Champs et al., 2006] or the relationship between aCGH and cDNA profiles. Not only by their contribution to the understanding of colorectal tumorigenesis and progression, these studies became significant for dissection of the differential clinical responses of CIN- and MIN-type colorectal carcinomas to particular chemotherapeutic drugs, such as 5-FU. An important weakness of these studies is the use of inhomogeneous patient cohorts (for instance, sporadic and familial cases) and DNA extracted from tissue samples without prior

microdissection. However, the latter is especially decisive for the detection of tumor-cell-specific DNA alterations because carcinoma resection specimens contain a highly variable number of tumor cells and associated intra- and peritumoral stromal components. Our study purpose was to provide a genome-wide profile of tumor-cell-specific DNA copy number changes in sporadic colorectal cancers and to define CIN- and MIN-type-specific oncogenes and tumor suppressor genes, which most likely contribute to the deregulation of functional pathways as those seen on the mRNA level by cDNA microarrays. To obtain this, we included an equal number of previously well characterized CIN- and MIN-type sCRC. Second, we used an aCGH approach with a small number (287) of target sequences to avoid a potential bias introduced by large-scale screening of DNA alterations in small sample series. Besides telomeric sequences and microsatellite markers, these target sequences included mostly known oncogenes and tumor suppressor genes, which readily allowed candidate-specific validation. Third, aCGH was applied to microdissected matched normal colorectal epithelium and invasive tumor cells from 22 surgically resected, FFPE tissue samples. Fourth, we used reference DNA extracted from normal colorectal mucosal epithelium of the same resection specimens and hence tissues that had been equally processed as microdissected tumor cells. This way we avoided potential false positive or false negative results due to differential quality of test and reference DNAs. Finally, FISH validation of three genes was performed on serial tissues as those used for aCGH. By doing this, aCGH profiles obtained from the 22 sCRC, irrespective of their CIN or MIN status, confirmed DNA gains at 20q, 13q, 8q, and 7p and losses at 18q, 17p, and 8p chromosomal regions also previously reported by metaphase CGH and recent aCGH studies [Nakao et al., 2004; Champs et al., 2006]. However, chromosomal regions 20q, 13q, 7, and 17p were preferentially altered in CIN-type tumors. Novel candidate oncogenes and tumor suppressor genes located within these CIN-type tumor associated chromosomal regions were identified and included the amplified genes TOP1, AIB1, MYBL2, CAS, PTPN1, STK15, ZNF217, and CYP24 on chromosome 20q, BRCA2 and D13S25 on chromosome 13q and IL6, CYLN2, and MET on chromosome 7 as well as the deleted genes HIC1 and LLGL1 on chromosome 17p. Furthermore, additional CIN-tumor-associated gene amplifications were identified for EXT1 (8q24.11) and MYC (8q24.12) and gene deletions for MAP2K5 (15q23) and LAMA3 (18q11.2). In contrast, distinct MIN-tumor-associated DNA amplifications were detected for E2F5 (8p22–q21.3), GARP (11q13.5–q14), ATM (11q22.3), KAL (Xp22.3), and XIST (Xq13.2) and DNA deletions for RAF1 (3p25), DCC (18q21.3), and KEN (21q tel). The preferential amplification of 8/11 investigated target sequences on 20q in CIN tumors is of particular interest, especially as the relevance of this amplicon in CRC is supported by other studies of early dysplastic lesions and colorectal liver metastasis. Of these eight amplified candidate genes, three (STK15, ZNF217, and CYP24) had also been detected in colorectal carcinomas in an independent aCGH study [Nakao et al., 2004], but without showing differences between CIN- and MIN-type tumors. Whereas little is known about the functional role of ZNF217 and CYP24 in colorectal cancer, STK15 (20q13.2, Aurora-A) is a known oncogene and overexpression of this centrosome-associated kinase was detected in genetic instable solid tumors, including colorectal cancer. Moreover, our own studies [Gerlach et al., 2006] showed higher STK15-specific mRNA expression in CIN- than MIN-type colorectal tumors. Together, it is therefore likely that the preferential overexpression of STK15 mRNA in sporadic CIN-type tumors is the result of STK15-specific DNA amplification. Further investigations of the mechanisms of STK15 gene alterations and associated STK15 mRNA and protein expression in CIN- and MIN-type colorectal tumors and dysplastic precursor lesions will also be of high clinical relevance in view of the novel therapeutic strategies of Aurora kinase inhibition. Another highly relevant finding of the present aCGH study relates to the 17p chromosomal region. The involvement of this chromosomal region in colorectal cancer, in particular the p53 gene (17p13.1), was extensively studied. The present study has

now shown the preferential loss of this region in CIN-type colorectal tumors and has pinpointed two novel candidate genes, HIC1 (17p13.3) and LLGL1 (17p12), preferentially deleted in CIN-type tumors. It is interesting to note that HIC1 encodes for a transcription factor that can interact with p53-induced cellular functions and mice with a heterogeneous disruption of HIC1 that spontaneously develop epithelial tumors (male) and soft tissue tumors and lymphomas (female). In contrast, LLGL1 encodes for a structural protein, which contributes to cellular polarity and which was shown to interact with the WNT pathway in model system. In fact, Schimanski et al. [Schimanski et al., 2005] showed that downregulation of LLGL1 appears to contribute to progression of human colorectal cancer. However, the detailed functional effect of the differential DNA copy number changes of HIC1 and LLGL1 in CIN- and MIN-type colorectal tumors and their potential cross-talk to the p53 and WNT pathways remain to be resolved.

## Study 2

About 85% of all sporadic colorectal carcinomas are CIN-type that manifest with alterations in genome and number of gene-specific copies, being aneuploid [Sugai et al., 2003]. The full elucidation of the mechanism on which is based the chromosomal instability is not yet complete. Still, it is known that alterations in chromosomal segregation are induced by defects in proteins of the chromosomal passenger complex and/or of the proteins responsible for the function of mitotic spindle, thus resulting in aneuploidy of the tumor cells [Ruchaud et al., 2007; Vader et al., 2008]. Also, cellular ploidy is regulated by proteins from the centrosomal complex [Fukasawa, 2007]. One of these proteins is aurora A, a centrosomal kinase whose gene amplification and overexpression can be associated supernumerary centrosomes and, consequently, aneuploidy, in some gastro-intestinal (esophagus, stomach, colon and rectum) and gynecological tumors [Giet et al., 2005; Lam et al., 2008]. Apart from colorectal carcinomas, overexpression of aurora A was identified also in cell lines from colorectal cancer, linked to aneuploidy. The current study was the first to investigate the expression of aurora A at both, RNA and protein level, focusing on the normal mucosa-adenoma-adenocarcinoma sequence, in distinct CIN- and MIN-type sporadic colorectal cancers. It was still uncertain if overexpression of aurora A is a result of tumor cell hyperproliferation with no implications in chromosomal instability and aneuploidy. The answer to this question might bring a therapeutic solution by using inhibitors of aurora kinases [Gautschi et al., 2008]. It is conceivable that differential aurora A regulation and expression may affect the efficacy of aurora inhibitors: e.g., colorectal carcinomas with numerous tumor cells only seemingly overexpressing aurora A due to active proliferation, may respond differently to aurora inhibitors as compared with colorectal carcinomas with a low number of aurora A positive tumor cells, but in which aurora A expression is associated with gene amplification, abnormal centrosome function and/or CIN.

The current study aimed to respond to these questions, investigating 71 patients with CIN- and MIN-type sCRC and confirmed previous results in that aurora A is overexpressed at mRNA and protein level in sporadic invasive colorectal carcinomas. The first, mild change of aurora A mRNA expression was identified with transition from normal to dysplastic epithelium. A significant overexpression was observed at the transition from dysplasia to invasive carcinoma. There were no statistically significant differences in aurora A expression at mRNA or protein level between low- and high-grade dysplasia in adenomas; as a consequence, these samples could have been analyzed together as “dysplasia”. Missing to observe a close association of aurora A mRNA and proteins levels in dysplasia could be explained by potential post-transcriptional modifications as is, aurora A protein dynamics. All these results may be the consequence of an increased proliferation of dysplastic and/or invasive tumor cells. However, as low level of aurora A gene amplification (aurora A /CEP20

ratio  $>1.25$ ) was evident in 40% of invasive tumors, additional levels of aurora A regulation appear to be involved in sCRC. Indeed, comparative analyses between CIN- and MIN-type invasive CRC strengthened the hypothesis that (de)regulation of aurora A expression occurs (uncoupled from proliferation) also at the level of aurora A gene copy numbers. Our detailed FISH analysis of serial tissue specimens of invasive carcinomas revealed that this occurs exclusively in those with CIN and correlates with aneuploidy. Surprisingly, our analyses revealed that, despite aneuploidy and increased aurora A gene copy numbers in chromosomal instable invasive carcinomas, the microsatellite instable invasive carcinomas had significantly more aurora A positive tumor cells, whilst there were no significant differences between CIN- and MIN-type invasive carcinomas at the aurora A mRNA level. Aurora A expression and associated regulatory mechanisms of post-transcriptional modifications and/or protein stability may be distinct in chromosomal and microsatellite instable invasive carcinomas, especially in view of aurora A gene amplification in chromosomal instable invasive carcinomas. More important seems to be to find out if aurora A overexpression is regulated by proliferation of tumor cells, because aurora A is essential in cell cycle and MIN-type carcinomas of colon and rectum are characterized by an increased rate of cell proliferation. Since only aurora A protein expression (and not also mRNA levels) was different between CIN- and MIN-type colorectal carcinomas, one may consider that the increased cell proliferation is linked to an increased activity and/or stability of aurora A. Indeed, also in our series of sporadic colorectal cancers microsatellite instable invasive carcinomas exhibited a higher frequency of Ki67 positive tumor cells, respective increased tumor cell proliferation on comparison to chromosomal instable invasive carcinomas. The number of aurora A positive tumor cells was statistically significant correlated with the proliferation rate of the tumor cells. Taken together, we reason that aurora A overexpression is tightly associated and regulated by tumor cell proliferation in MIN sCRC, whereas an additional level of (de)regulation of aurora A overexpression occurs at the DNA level in CIN sCRC. In fact, aurora A overexpression can be seen in both MIN- and CIN-type invasive carcinomas, only in a different frequency of tumor cells. This might introduce a measurements bias of aurora A levels obtained from whole populations of colorectal cancer cell lines and/or entire tumor extracts. Further to the difference of aurora A expression and regulation at the level of specific molecular subtypes of colorectal cancer cells, the heterogeneity of aurora A within individual colorectal cancers requires further attention. In particular, it has been recently shown that aurora A is functionally linked with signaling mechanisms of cell polarity [Wirtz-Peitz et al., 2008], suggesting that aurora A may also play a role at the invasive tumor edge. Thus, further studies, for example, clinical phase trials of aurora inhibitors, should also include early/prospective in situ analyses of individual tumor cells in tissue specimens. Clearly, as suggested by other studies, strong aurora A expression alone does not suffice to induce chromosomal instability and/or aneuploidy, as observed in this study for diploid microsatellite instable sporadic colorectal cancers. In contrast, the close association of, and rather moderate, aurora A expression with aneuploidy in chromosomal instable sporadic colorectal cancers points to the involvement of e.g. additional defects of checkpoint controls. Thus, within the chromosomal instable invasive carcinomas it might be those with defective p53 signaling or other checkpoint controls, in which also marginally elevated aurora A expression is able to trigger overt aneuploidy. In this case, the effect of aurora (-A) inhibitors may be less efficient than in aurora A expressing tumor cells without additional defective checkpoint controls. In addition, it is reasonable that the activation status of aurora A, controlled by phosphorylation as well as protein stability [Lim and Gopalan, 2007], may introduce a further functional level affecting successful aurora (-A) inhibition and tumor cell death. In this context, functional investigations of inactive/active aurora A protein levels as well as other centrosomal and chromosomal passenger complex proteins in chromosomal and microsatellite instable colorectal tumor cell lines with specific reference to their interaction

with the p53 and adenomatosis polyposis coli pathways [Aoki and Taketo, 2007], will certainly be a worthwhile effort and are subject of our ongoing in vitro investigations. Irrespective of the potential differential therapeutic response of chromosomal and microsatellite instable colorectal cancers to aurora A inhibitors, this study shows that between 42 and 85% of sporadic colorectal cancer cases may be considered for novel, aurora-targeted therapies. Whereas previous studies have analyzed the antitumoral effect of aurora inhibitors, targeting both aurora A and aurora B, in a study, Manfredi [Manfredi et al., 2007] have evaluated the antitumor activity of an aurora A specific inhibitor, which has also entered phase I clinical trials for solid tumors. Specifically, the authors had included three colorectal cancer cell lines in their study, two of which are microsatellite instable (HCT-116, DLD-1) and one of which is chromosomal instable (SW480). In HCT116 cells, the mechanism of action of the tested compound was a reduction of aurora A activity, but not aurora A degradation or down-regulation. The reduced phosphorylation of aurora A led to cell cycle progression delay and tumor cell growth inhibition in vitro as well as to a high efficacy for growth inhibition of in vivo HCT116 xenografts. This is in accordance with our data on aurora A expression and deregulation in microsatellite instable sporadic colorectal cancers. A detailed comparison of the effects of this aurora A inhibitor in chromosomal and microsatellite instable colorectal cancer cell lines, potentially also showing differences in mitotic checkpoint controls, will be a valuable experimental setup before further clinical testing. Besides, aurora A expression in colorectal cancers may also be a valuable predictive marker for current therapeutic strategies, as shown for other epithelial tumors or in the neoadjuvant setting of rectal cancer [Guan et al., 2007]. In fact, we found a weak association of high aurora A protein expression with node-negative colorectal cancer cases. One explanation may be that during migration (tumor) cells downregulate their proliferative activity and hence aurora A expression. Therefore, the high proliferation rate and/or presence of high numbers of aurora A positive cells may reflect a non-migratory phenotype of colorectal cancer, i.e. the node-negative cases. Clearly, further studies need to address the prognostic and predictive impact of aurora A expression in view of clinical UICC stages.

Recent studies aimed to evaluate the association between the two STK15 polymorphisms and susceptibility to digestive system cancers. There are at least two non-synonymous polymorphisms, 91T>A (rs2273535) and 169G>A (rs1047972), in the STK15 gene [Goos et al., 2013; Koh et al., 2017]. Recent data demonstrates that the A allele of the 91T>A (31Ile>Phe) polymorphism is amplified and stronger than the T allele concerning the evolution to aneuploidy and transformation, leading to an inhibition of p53 binding and the decreased degradation of STK15 [Cervantes et al., 2012]. The other type of polymorphism [169G>A (57Val>Ile)] interacts with the kinase activity of aurora kinase A increasing the risk of digestive system cancers [Casorzo et al., 2015].

STK15, also known as Aurora A or AURKA is overexpressed in 45-48.5% of CRC using immunohistochemistry, but in metastatic samples, the range of positivity is larger, from 33% to 82.5% [Koh et al., 2017]. The STK15 expression is correlated with gender, tumor location, histology, tumor grade and other clinicopathological parameters. Other study proved a significant relationship between STK15 expression and the histologic grade of the tumor tissue [Goktas et al., 2014]. Regarding the prognostic impact of STK15 expression in CRC patients, its overexpression was significantly associated with recurrence in stage II or III colon cancer [Goos et al., 2013; Goktas et al., 2014]. The results concerning the correlation between Aurora A overexpression and survival of patients with metastatic CRC are divergent, some authors finding a positive effect on survival [Goktas et al., 2014], while others associating it with a poor overall survival in CRC patients with liver metastasis [Goos et al., 2013]. Also, STK15 overexpression in CRC patients is associated with poor PFS [Koh et al., 2017].

Another recent study has shown that Aurora A inhibitors have anticancer activity in various preclinical cancer models, and some inhibitors have entered clinical trials [D'Assoro et al., 2015]. Such studies have underlined the incremental therapeutic efficacy of combining AURKA inhibitors with conventional anti-cancer drugs to inhibit tumor progression and restore chemosensitivity. It looks like targeted treatment with AURKA inhibitors can improve progression-free survival and assist in planning the treatment of colorectal cancer patients.

Therefore, AURKA expression is an independent molecular prognostic factor for poor outcome in CRC patients. Thus, AURKA expression may serve as a valuable prognostic marker for CRC.

### **Final remarks**

The first conclusion is that aCGH revealed distinct DNA copy number changes between sporadic CIN- and MIN-associated CRC. A differential role of these candidate oncogenes and tumor suppressor genes in tumor development and progression of sporadic chromosomal-unstable and microsatellite-unstable colorectal carcinomas is likely and may also be involved in the response or resistance to therapeutic interventions, such as shown for MIN and 5-FU.

The research sustains the role played by aurora A in tumorigenesis of sCRC. Moreover, it proves that in a minority of predominantly MIN-type sCRC, the presence of aurora A positive tumor cells is merely reflecting tumor cell proliferation. In contrast, the large majority of CIN-type sCRC harbor supplementary (de)regulation of aurora A by gene amplification and concomitant tumor cell aneuploidy. Thus, sCRC present different mechanism of aurora A regulation and this may be targeted by aurora-inhibitor therapies and/or may influence the associated therapeutic protocols.

## **1.5.Targeting early detection of premalignant lesions of digestive tract using novel non-invasive techniques – THz imaging and spectroscopy**

### **1.5.1. Introduction**

The terahertz waves are located in the electromagnetic spectrum between high frequency microwaves and long wavelength far infrared, a region defined as 0.1-10THz. Also know as T-rays, T-lux, THz light or THz radiation, 1THz equals  $10^{12}$  Hz having a wavelength of 300  $\mu\text{m}$ , 4.14 meV,  $33.3\text{cm}^{-1}$ . Because of the difficulties in generating and detecting them, terahertz are also named THz gap. [Mantsch and Naumann, 2010]. The terahertz region is characterized by many variate molecular vibrations, such as molecular rotational, torsional, crystalline phonon, intra- or intermolecular. In 1975, David Auston from AT&T Bell Laboratories produced and identified for the first-time pulses of THz, using a stable ultrafast femtosecond laser source [Ren et al., 2019]. Then, in 1995, the first THz image was obtained using the newly improved THz time domain spectroscopy and other imaging techniques. Then after, the interest of the researchers on THz grew, covering almost all sciences, including medicine and biomedical sciences. For instance, searching using Web of Knowledge from Clarivate Analytics engine turned up 40200 records for “terahertz” term, continuously increasing from 1 term in 1975 to 3287 in 2019.

#### *Digestive cancers and Terahertz imaging and spectroscopy*

As cancer is the second most frequent cause of death worldwide, efforts have been made in the past decades not only in finding a treatment, but also in early detection of

pre-malignant lesions as secondary prevention method, which is safer and cheaper than treating the cancer. Depending on the organ and on the type of the tumor, progresses were made for developing new techniques and imaging methods used in non-invasive early diagnosis. For digestive tract, for instance, there are already in use: conventional colonoscopy and endoscopy, X-ray CT, magnetic resonance imaging (MRI), optical coherence tomography (OCT), and positron emission tomography (PET). But none of these new diagnosis methods brings only advantages, as one has to balance between costs, specificity, sensibility, invasiveness, radiation side-effects for patients and doctors. Gamma waves are extremely useful in diagnosis and follow-up of cancer, PET-CT and PET-MRI have the advantage of both spatial resolution and molecular functional character of images, which are now considered to be the golden standard when speaking about cancer diagnosis. Less investigated, THz waves might bring new benefits in the early diagnosis of carcinomas in pre-invasive or early stages. Because the energy transfer with THz depends on the tissue structure, it can produce information about the structure, with almost no invasiveness, especially on those tumors with a greater content of water that strongly absorb the THz waves [Ahi K. 2019]. On the other hand, THz radiation can be used in detecting the presence of the tumor at the resection margins [Joseph et al., 2014]. Below I present the main THz-based technologies used as diagnosis techniques.

### 1. THz Spectroscopy

The THz time domain spectroscopy (THz-TDS) uses short pulses of THz radiation in order to identify changes of the molecules, compounds or profound structures, over the frequency range 0.2–4 THz in transmission, reflection, and attenuated total reflection (ATR) modes. The basic principle of the THz-TDS is based on a direct measurement using laser beam technology of both the amplitude and phase information of the THz pulse simultaneously as the function of time that is further Fourier transformed to obtain the spectra [Ren et al., 2019]. It can be used for the detection of nucleic acids of DNA. THz-TDS can make the distinction between all 4 nucleobases which have different coefficients of absorption of THz. Also, it can distinguish between single- and double-strand DNA or between hybridized and denatured DNA, it can detect some proteins or amino acids, peptides and carbohydrates. It is related to THz imaging in defining the optical properties in the frequency domain.

But THz spectroscopy has some limitations, as only small areas can be investigated and it cannot differentiate between substances having the same THz spectrum.

### 2. THz-Tomography

When studying the internal structure of an object, tomography uses reconstruction of an object in bi- or tri-dimensions using slices. THz radiation is used in many tomographic techniques, such as: THz diffraction tomography, THz tomosynthesis, time-of-flight pulsed imaging, 3D THz holography, and THz computed tomography. THz computed tomography (CT) uses pulsed THz radiation to provide sectional images of 3D entities. It functions in the same way with X-ray CT, but it is more expensive, and the acquisition takes longer time and is not as profound as the X-ray CT [Guillet et al., 2014]

### 3. THz-Endoscope

Although not a real endoscope, in vivo THz investigation is limited in practice to the assessing of lesions of the superficial organs, e.g. mammary gland. Efforts have been made to create tools capable to go deeper and examine profound organs.

In 2009, Ji et al. designed a small-sized fiber-coupled THz endoscope able to generate and then detect THz waves using an optical fiber connected to a femtosecond laser close to

the reflective surface of an organ, through the excitation of the detector and generator [Ji et al., 2009]. At that time, when examined with this endoscope the initial and easier to access parts of the digestive tract (as mouth or tongue), the high local moisture generated confusing results of THz reflections. Later on, in 2014, a THz new instrument using single-channel detection based on flexible metal-coated THz waveguides and a polarization specific exposure method was commercially promoted [Doradla et al., 2014].

#### 4. THz Sensors Metamaterial Based

An interesting THz capability based on the high concentration of the electric field is represented by its potential for sensing the complex dielectric properties of small compounds of a different nature, whether it is chemical or biochemical. An approach for ultrasensitive sensing of biomolecules proposes a THz sensor based on a graphene metamaterial layer that boosts the absorption of samples and tunes the sensing domain by changing the Fermi energy [He et al., 2016].

#### 5. Enhancing THz Contrast

Gold nanoparticles of metamaterials with high index of refraction can be used to increase the contrast in THz spectroscopy and to create a characteristic THz fingerprint by measuring the specific absorption coefficient and index of refraction of a tissue [Kashanian et al., 2015].

### 1.5.2. Applications of THz imaging and THz spectroscopy in digestive cancers

This review offers a comprehensive overview of current data published on THz investigation techniques highlighting its utility in medicine, especially in digestive cancers. It summarizes the technical characteristics of THz radiation and its interaction with tissues and subsequently presents available THz-based technologies (THz spectroscopy, THz-tomography, and THz-endoscope) and their strengths and disadvantages for future clinical use. The review highlights the current in vitro and in vivo research progress in the field, for identifying specific digestive malignant tumors (i.e., oral, esophageal, gastric, colonic, hepatic, and pancreatic).

Despite the huge human and material effort allocated by the humanity in its war against cancer, there are still many important issues to be solved in prevention, diagnosis and treatment. Cancer remains the second cause of mortality with over 8 million deaths/year and 14 million new diagnosed cases every year. Digestive cancers can be better diagnosed, staged and sometimes treated by using new imaging techniques such as conventional colonoscopy/endoscopy, X-ray computer tomography, magnetic resonance imaging (MRI), optical coherence tomography (OCT), and positron emission tomography (PET). Obviously, each of them has certain advantages but also disadvantages such as cost, limited specificity or sensitivity, invasiveness, or side effects such as radiation exposure, as shown in Table 4.

New discoveries in the electromagnetic wave spectrum brings great expectations for the development of medical imaging. THz can achieve an energy transfer in relation to tissue structure, providing information that can characterize its structure, with limited side-effects and no invasiveness [Kashanian et al., 2015]. A diversity of types of electromagnetic radiation are used in many imaging methods for tumor diagnosis. Gamma radiation has revolutionized the diagnosis and the follow-up of cancer treatment (e.g., 18F FDG PET). In addition, fused images (PET-CT/PET-MRI) have brought the benefit of both spatial

resolution and a molecular functional character of images and are considered the imaging gold-standard in many types of cancers.

Recent data indicate that THz could become a useful tool in early diagnosis of carcinomas, starting from the fact that some malignant tumors have a greater content of water in its structure that strongly absorbs the THz radiation. Another use for THz imaging is the possibility to detect tumor tissue at the resection margins.

#### 1. Oral Carcinoma

Sim et al. used THz endoscopy to investigate tumors in head and neck region by evaluating tumor specimens from 7 patients diagnosed with carcinoma. They confirmed that the THz endoscope is a valid tool in differentiating between tumor and normal cells and more precise if THz imaging was performed in fresh frozen sections [Sim et al., 2013].

#### 2. Esophageal Carcinoma

A comparative analysis of different segments of rat gastro-intestinal tract was realized by Ji et al. using THz reflection imaging and spectroscopy. He included in his study fragments of esophagus, stomach, small intestine, and colon harvested after perfusion with saline solution, and use as reference the refraction of THz in water. The spectroscopic analysis showed a smaller refraction index and smaller absorption coefficient in esophageal squamous epithelium when compared with glandular epithelium of the colon and stomach, indicating a possible higher accuracy of the technique when diagnosing an esophageal cancer compared to a gastric and intestinal one [Ji et al., 2014].

#### 3. Gastric Carcinoma

Although gastric cancer is one of the most frequent, there are not too many studies that used THz spectroscopy to assess them. Theoretically, the diagnosis might be quite difficult due to its anatomy and structure with different layers thicknesses, because a precise THz spectroscopy characterization depends on the thickness of the examined tissue [Kashanian et al., 2015].

A study performed on six surgical resected specimens of gastric adenocarcinoma preserved four hours in saline solution NaCl 9% demonstrated that gastric cancers have a refraction index of about 2.5, quite similar to water, while normal tissues have a refraction index of  $<2$ . This could be explained by the fact that tumors are edematous and present an increased vascularization. [Goryachuk et al., 2017].

Another study on gastric carcinomas used tumor specimens harvested intraoperatory, routinely processed by formalin fixation and paraffin embedding and then analyzed by THz spectroscopy and compared to normal tissues [Hou et al., 2014]. Two different peaks of absorption were obtained, one in 0.2–0.5 THz wave range and the other in 1–1.5 THz wave range, possibly explained by different tissues physiological changes and composition. These results were confirmed by a study on 21 paraffin tissue blocks with invasive gastric carcinoma analyzed by THz spectroscopy identified an increased refraction index and absorption coefficient [Wahaia et al., 2015].

In 2015, Ji YB et al. investigated human early gastric carcinomas and correlated the THz spectroscopy results of the gastric specimens with their macroscopical aspect. Although both the refraction index and the absorption coefficient were increased in carcinoma, the result might be altered by the injection of saline solution during endoscopy. Another limitation of THz spectroscopy is that it cannot differentiate the signet ring cell carcinoma from normal tissue [Ji et al., 2015].

#### 4. Colorectal Tumors

The transmission of THz-time domain spectroscopy and continuous wave THz imaging (CWTI) were used also for assessing of the absorption coefficient and refractive indices in FFPE human colon tissue samples [Wahaia et al., 2011]. Each set contained 4 samples as follows: one normal mucosa and 3 adenocarcinomas. In carcinomas they found higher absorption coefficient and refractive indices than in normal mucosa. In addition, the

authors concluded that several parameters, such as coefficient of absorption, refractive indices, cell densities, vascular pattern, and abnormal microenvironment (O<sub>2</sub> level, pH value, glucose level, and lipid concentration) have an impact on the results. Later on, the same team studied thirty FFPE blocks of human colon tissue samples (normal and carcinomas - 11 pT3 adenocarcinoma and 10 pT4 adenocarcinoma) [Wahaia et al., 2016] through multipoint transmission THz-TDS. The purpose was to evaluate if the contrast depends on the cell alterations, abnormal density alternations, abnormal vascular patterns, or cell density. They concluded that pT4 adenocarcinoma has a higher absorption coefficient and refractive indices than pT3 adenocarcinoma. The THz absorption and reflection may also be assessed in the absence of water.

In a study on normal mucosa, dysplastic colon epithelium and tumor samples from 30 patients using a conventional THz-TDS system, the sensitivity was 82% and the specificity was 77% useful in distinguishing the normal from the tumor tissue, while a sensitivity of 89% and a specificity of 71% helped differentiating normal from dysplastic epithelium [Reid et al., 2011]. The above-mentioned study of Ji YB et al. (2014), using neural networks, decision trees, and support vector machines re-evaluated the data provided by Reid et al. This method increased the sensitivity to 90–100% and the specificity to 86–90%, which improves the overall precision of the diagnosis [Ji et al., 2014].

Continuous-wave polarization imaging THz method was used to study 14 fresh 0.3–0.5 cm thick human colonic samples from 8 patients. Prior, the tissues were included in a wet compress at 7.4 pH. The results proved good correspondence between THz imaging and histology.

#### 5. Hepatocarcinoma

There are a few studies that have been published about the use of THz imaging on liver, with methods including ex vivo analysis of fresh, formalin-fixed and paraffin-embedded liver tissue. A study on freshly resected human liver tissue with hepatocellular carcinoma found the absorption coefficient at about 9 to 12 mm<sup>-1</sup> for normal liver tissue, while carcinoma had a coefficient higher than 12 mm<sup>-1</sup>. The authors compared the THz near-field images with the corresponding histopathological aspect and concluded that THz permits an accurate identification of normal and tumor tissue [Chen et al., 2013].

Since there is no standardized method for measuring the amplitude and refractive spectra under THz radiation, the evaluation of paraffin embedded human tissue samples can be enhanced by performing the acquisition of data in a mixture of paraffin and water. This method reduces the background noise and accelerates the image acquisition while enhancing the differences between hepatocellular carcinoma cells and normal cells.

Table 4. Comparative performance parameters of imaging diagnostic methods.

Technique	Spatial Resolution, mm	Damage to Healthy Tissue	Limits
Conventional colonoscopy/ endoscopy	Lack of spatial resolution	Invasive	Operator dependent and can have high false-negative rates
X-ray computer tomography	0.5–2	Minimal radiation exposure	Low sensitivity for digestive cancers and cannot be repeated very often-
MRI	0.1–2 (depended on Tesla range)	Non-invasive, uses contrast agents	High cost, time consuming investigation
OCT	0.01	Non-invasive	High cost, subjectivity in image interpretation, research use only
PET	0.54–6 (dependent	Minimized risk tissue damage	High-cost, the lack of anatomic

Technique	Spatial Resolution, mm	Damage to Healthy Tissue	Limits
	on the isotope)	due to radiation	correlation, restricted availability
THz technology	0.1–0.25	Non-invasive and non-ionizing under controlled radiation power density and exposure time	As discussed in a previous section

## 6. Pancreatic Cancer

Due to the profound anatomical location of the pancreas, studies involving normal pancreas and pancreatic tumors are rare. A study performed by Brun et al. (2010) used 10 microns thick tissue sections that were processed in a watery solution. Images were obtained using digital slides processing and THz imaging techniques, and showed that the THz method can accurately differentiate between normal and tumor cells, can assess the degree of invasiveness, and can even identify two distinct tissue subtypes in the tumor area [Brun et al., 2010].

### 1.5.3. Personal preliminary results in THz field

The Iasi team, headquartered in CEMEX research center, targeted two THz domains of interests, as follows:

(A) The initial steps involve the development and assessing of tailored nanoparticle as THz molecular imaging contrast agents for early diagnosis of premalignant gastric lesions. Therefore,  $\text{Fe}_3\text{O}_4$  and  $\text{Gd}_2\text{O}_3$  nanoparticles were functionalized by citric acid and carboxymethylcellulose and then were tested in vitro and in vivo through specific tests in order to evaluate their capability as viable contrast agents. The most adequate formulations for nano-assemblies as contrast agents were established through validation of contrast efficiency, along with successful stealth properties and functional tests. The cell viability tests on standardized human gastric cell line AGS of different nanoparticle concentrations revealed a dose-dependent effect in 24-h determinations [Mihai et al., 2019]. The in vivo studies on mice revealed adequate biocompatibility of the administered nano-assemblies when compared to the control batch. In the next step, the magnetite nanoparticles stabilized in citric acid and carboxymethylcellulose were evaluated as THz imaging contrast agents in gastric cancer cell lines. The preliminary results of THz images obtained at 1.1 THz showed consistent differences between normal and tumor tissue. The influence of the optical effect of the nanoparticles on the frequency domain of 1.1 THz was clearly observed.

(B) The second step consisted in finding solutions for THz imaging limitations. It is well known that THz imaging has a poor signal-to noise ratio, slow processing, and low-brightness. Therefore, the development of advanced image processing software may lead to an important breakthrough in early detection of a gastric cancer application. The development of an image processing software for THz imaging must ensure the following parameters: versatility vs. frequency, adaptability to transmission or reflection measurements, provision of accuracy and selectivity of images with control on image quality, and reduction of the irregularities of received data, the possibility to increase the visibility of fine details in an image by adjusting pixel intensities, and expansion of smaller regions on predefined criteria for cancer detection, along with selective 2D and 3D visualization options of the rendered object [Ciobanu et al., 2018]. Further research is needed to overcome the current limitations in THz imaging and spectroscopy and to find new innovative solutions in clinical applications.

**Final remark**

In conclusion, THz-based imaging technology is a promising and innovative new instrument for medical non-invasive diagnosis. Although remarkable advancement has been made in THz emission, detection and tissue imaging, there are still several problems to be solved before it becomes used on a large-scale: high costs, insufficient discriminative precision, software data analysis, interpretation, and trained staff. However, considering that THz techniques and instruments are not yet completely developed and are continuously improving and that THz is being integrated into miniaturized medical devices, it is safe to assume that these issues will be surpassed in a few years. Due to its unmatched sensing as well as non-invasive and non-destructive features, THz radiation can potentially replace other forms of radiation used for the diagnosis and monitoring of different types of conditions, but having important side-effect on patient.

## Chapter 2: New concepts in diagnosing celiac disease

### 2.1. State of art

Celiac disease (CD) is an autoimmune disorder occurring as a response to gluten intake in genetically predisposed individuals [Green et al., 2015]. CD is an important public health problem which affects about 1% of individuals in most populations, being diagnosed mainly in pediatric patients, although the onset may occur at any age. Due to its autoimmune mechanism, it may have a polymorphic clinical presentation [Chou et al., 2017]. The diagnosis relies on signs and symptoms related to intestinal malabsorption, such as abdominal distension, chronic diarrhea, anorexia, and failure to thrive, but extraintestinal involvement is not uncommon in CD. Patients may develop unexplained chronic hypertransaminasemia, iron deficiency anemia, chronic migraine, peripheral neuropathy, learning disabilities and concentration deficit [Freeman et al., 2012; Rostami et al., 2017]. The long-term outcome of untreated CD is associated with the development of intestinal neoplasia resulting in increased morbidity and mortality [Freeman et al., 2012]. Epidemiological studies have shown that there is a delay in CD diagnosis mostly in oligosymptomatic cases. Silent CD is a serologic and histologic evidence of CD, but without any evident symptoms, signs, or deficiency states. The proportion of CD that is silent is not well known, but it is thought to account for at least 20% of patients [US Preventive Services Task Force et al., 2017]. Lately, the diagnostic rates are increasing, and this seems to be due to a true rise in incidence rather than increased awareness and detection [Garnier-Lengline et al., 2015; Many and Biedermann, 2016]. At this point, instruments helping to identify affected individuals are in demand.

The classical form of CD is rarely diagnosed in western studies, while the atypical presentations are more frequent [Rostami and Villanacci, 2009]. There are few data on severe malabsorption in CD. Often, serological tests are used with success for CD diagnosis, having a superior value in severe disease compared to milder forms. Still, due to limited access to duodenal biopsy and serology, in developing countries a big proportion of persons with classical CD remain undiagnosed [Rostami et al., 2004; Abu-Zekry et al., 2008]. This financial limitation may explain the overt malabsorption of the patients at presentation. CD develops slowly in a gradual fashion, starting with small bowel mucosa inflammation, to hyperplasia of the crypts and, in some patients, villous atrophy. Microscopic enteritis, as a new entity [Rostami and Villanacci, 2009], is a milder enteropathy which seems to be the first stage of CD at presentation. Non-celiac gluten sensitivity (NCGS) is another new entity, characterized by intolerance to gluten, but without morphological features of CD [Bizzaro et al., 2012]. The CD/GS ratio is estimated to 1/6.5. It is estimated that about 10% of the population are affected by wheat allergy, CD or NCGS. Milder enteropathy is underdiagnosed by pathologists, be it CD or NCGS. In less developed countries, where infectious diseases, parasitosis and malnutrition are more frequent, CD is underdiagnosed, especially if it has a borderline pattern. Due to its non-specific nature, mild enteropathy is still difficult to be diagnosed even after excluding the other etiologies. Lately, CD turned to be considered a treatable disease only when it was associated with important mucosal alterations, although most CD present as microscopic enteritis (Marsh I-II) [Kurppa et al., 2009]. But new strategies were adopted for atypical CD and NCGS. Some symptoms, such as diarrhea, might be present in some patients but absent in others, and the histopathological changes on the duodenal biopsies range from microscopic enteritis (corresponding to stages Marsh 0-II) to macroscopic enteritis (stages Marsh IIIa-c), without any correlations with symptomatology [Rostami and Villanacci, 2009]. Since microscopic enteritis refers to enteropathies with unchanged aspect of the mucosa under the endoscopically examination, macroscopic enteritis could be easily visualized and correlated to Marsh III lesions. Therefore, a better understanding of milder enteropathy regarding the pathology and

symptoms, will ease the diagnosis, reducing the unnecessary biopsies and opening new treatment strategies [Rostami et al., 2010].

Mucosa of the gastro-intestinal tract can present mild inflammatory infiltrate – microscopic inflammation which include: eosinophilic esophagitis/gastritis/enteritis, lymphocytic or collagenous colitis and autoimmune inflammation [Aziz et al., 2010]. Described for the first time in 2009, microscopic enteritis is a new entity characterized by symptomatic malabsorption and subtle deficiency of micronutrients [Rostami and Villanacci, 2009]. Histologically, the villous architecture is generally preserved, but the epithelium has an increased number of intraepithelial lymphocytes and the crypts may present hyperplasia. These aspects can extend resulting in microvillous changes, plasmacytosis and increased eosinophils in lamina propria, which can represent the morphological support for malabsorption or other symptoms [Zanini et al., 2014]. Relevant etiologies include coeliac disease, non-coeliac gluten sensitivity with microscopic or sub-microscopic changes, microvillous inclusion disease, common variable immunodeficiency, tufting enteropathy, parasitic infestations or infections like *Helicobacter pylori* (*H. pylori*), drugs including non-steroidal anti-inflammatory drugs (NSAIDs) and inflammatory bowel disease (IBD) [Catassi et al., 2013; Thoeni et al., 2014; Ranganathan et al., 2014]. Microscopic enteritis was proposed in order to explain how the histological aspect (even if there are only submicroscopic changes) can explain and sustain the malabsorption. It arisen after Marsh described the morphological changes of CD, in 1992 (to remember that Marsh IV doesn't exist anymore today). Although worldwide recognized, Marsh classification is used with changes by some laboratories, considering it as nonspecific with reference to multiple etiologies, besides the gluten sensitivity. All these particular cases of malabsorption, non-gluten related, but with morphological changes similar to Marsh classification, were referred to as microscopic enteritis. Normally, there are between 11 and 25 IELs per 100 enterocytes. Historically, after long debates, Marsh admitted that IEL population is abnormal distributed and increased in CD, compared to normal tissue. Although difficult, it is important to quantify the intraepithelial lymphocytes in ME and determine the clinical significance of ME. At that time, there was little information to help clinicians interpreting the pathology reports. Therefore, a consensus regarding the entities with microscopic and submicroscopic changes (the so-known “non-specific” or “functional”), in order to help clinicians to find a therapy against specific symptoms was needed.

An important issue when following-up the patients with CD regards the indication for endoscopy [Cammarota et al., 2007]. Many centers are not performing endoscopy by routine to evaluate or monitor the histological recovery, considering the method is not recommended for patients with clinical improvement and/or who respond to gluten-free diet (GFD) [UEG, 2001]. Still, if the patient is not recovering or is not responding to GFD endoscopy with biopsy is recommended to rule out other diagnosis or complications. Endoscopy alone is not enough, because the histological examination of the biopsied intestinal sample is more effective and specific for diagnosis and prognosis. Taking into account the advantages and the side-effects of an invasive follow-up procedure (endoscopy with biopsy), one can conclude that diagnostic endoscopy can be avoided only in patients presenting with classic symptoms and positive serology. In fact, this kind of patients represent a small group of patients, as the majority present with milder mucosal lesions with non-specific symptoms and signs, mimicking other conditions, a real challenge for the clinician and for the pathologist.

**This research direction has been realized by publishing the following articles:**

Rostami K, Marsh MN, Johnson MW, Mohaghegh H, Heal C, Holmes G, Ensari A, Aldulaimi D, Bancel B, Bassotti G, Bateman A, Becheanu G, Bozzola A, Carroccio A,
-------------------------------------------------------------------------------------------------------------------------------------------------------------

Catassi C, Ciacci C, Ciobanu A, **Danciu M**, et al. ROC-king onwards: intraepithelial lymphocyte counts, distribution & role in coeliac disease mucosal interpretation. *Gut*. 2017; 66(12):2080-2086. doi:10.1136/gutjnl-2017-314297. <http://gut.bmj.com/content/early/2017/09/16/gutjnl-2017-314297>

Rostami K, **Danciu M**: Endoscopy and small-bowel biopsy in celiac disease: indications and implications – Letter to the editor. *Endoscopy* 2007; **39**:1; <https://www.thieme-connect.com/DOI/DOI?10.1055/s-2007-966492>

Rostami K, Aldulaimi D, Holmes G, Johnson MW, Robert M, Srivastava A, Fléjou JF, Sanders DS, Volta U, Derakhshan MH, Going JJ, Becheanu G, Catassi C, **Danciu M**, Materacki L, Ghafarzadegan K, Ishaq S, Rostami-Nejad M, Salvador Peña A, Bassotti G, Marsh MN, Villanacci V: Microscopic enteritis: Bucharest consensus. *World J Gastroenterol*. 2015; 21(9):2593-2604. <http://www.ncbi.nlm.nih.gov/pmc/articles/PMC4351208/>

Shahraki T, Rostami K, Shahraki M, Bold J, **Danciu M**, Al Dulaimi D, Villanacci V, Bassotti G: Microscopic Enteritis; clinical features and correlations with symptoms. *Gastroenterol Hepatol Bed Bench* 2012;5(3):146-154 <http://eds.b.ebscohost.com/eds/pdfviewer/pdfviewer?sid=de18f510-662a-4b66-8894-5b41e6867db5%40sessionmgr111&crlhashurl=login.aspx%253fdirect%253dtrue%2526profile%253dehost%2526scope%253dsite%2526authype%253dcrawler%2526jrnl%253d20082258%2526AN%253d77565227&hid=103&vid=0>

Rostami K, Al Dulaimi D, Rostami Nejad M, Villanacci V, **Danciu M**: Microscopic enteritis and pathomechanism of malabsorption. *Autoimmunity Highlights* 2010; 1, (1):37-38 [http://download-v2.springer.com/static/pdf/681/art%253A10.1007%252Fs13317-010-0006-4.pdf?token2=exp=1432806301~acl=%2Fstatic%2Fpdf%2F681%2Fart%25253A10.1007%25252Fs13317-010-0006-4.pdf\\*~hmac=113ce52cb41db0548a7dc74555164670e4c88a32628b0d6a5c67bd45f73982a3](http://download.v2.springer.com/static/pdf/681/art%253A10.1007%252Fs13317-010-0006-4.pdf?token2=exp=1432806301~acl=%2Fstatic%2Fpdf%2F681%2Fart%25253A10.1007%25252Fs13317-010-0006-4.pdf*~hmac=113ce52cb41db0548a7dc74555164670e4c88a32628b0d6a5c67bd45f73982a3)

## 2.2. Quantitative assessment of intraepithelial lymphocytes and morphology interpretation in determining the cut-off between normal and celiac disease

### 2.2.1. Introduction

Celiac disease can present in a large range of clinicopathological aspects. The structural changes of the duodenum range from nearly-normal to severe abnormalities when villi are completely atrophied and the mucosal surface is flat [Marsh and Rostami, 2016]. T lymphocytes from the lamina propria are responsible for the flattening of the villi and the hypertrophy of the crypts. There is a correlation between the increasing number of intraepithelial lymphocytes (IEL) and villi damage, but their function and role are incompletely known. Although the IEL increase is considered characteristic for CD, it is non-specific, as it can be found in other, non-CD, lesions – coined as microscopic enteritis by the Bucharest Consensus [Rostami et al., 2015]. Although, the international experts involved in the Bucharest Consensus were first of all looking for clarifying the subtle microscopical changes and the IEL increase in CD and normal mucosa, they observed a lack of data regarding the cut-off point for a positive diagnosis. It was necessary to define the “normal” value for IEL. As mentioned before, Ferguson and Marsh tried to agree on the methodology used then counting the IEL: thickness of the section, type of distribution, use of immunohistochemistry in routine practice. Variate cut-offs were proposed, ranging from 20IEL/100 enterocytes to 40 IEL/100 enterocytes [Ferguson and Murray, 1971]. There are different opinions regarding the compulsoriness of using immunohistochemistry when

assessing the IEL in CD, because for some laboratories this is a time-, human resource- and financial-consuming technique, and did not increase the precision of the diagnosis.

Nonetheless, it is known that increased IEL represents a sensitive marker for CD diagnosis, as T lymphocytes survey the lumen and the lamina propria and are implicated in the CD pathogenesis.

### **2.2.2. Aim**

The purpose of this study was to improve the diagnostic accuracy by re-examining the current procedures used in different laboratories. The IEL count would have been made on more than 400 hematoxylin-eosin stained sections from duodenal mucosa biopsies from patients with CD and non-celiac, in order to establish what “normal” IEL means. The optimal cut-off between normal and CD (Marsh III) would be calculated using receiver operating characteristic (ROC) curve analysis, in an international multicenter project.

### **2.2.3. Material and methods**

This case-control study was designed during the International Meeting on Digestive Pathology held in Bucharest, November 2015. It was a multicenter international study involving eight countries, comprising 19 laboratories, each of which provided histological reviews of 10 patients with CD and 10 disease control (DC) patients. The 19 participating centers provided their data from Europe, Middle East and America, which included Ancona, Bologna, Brescia, Salerno, Perugia, Milan and Sciacca (Italy); Dudley, Glasgow, Luton and Milton Keynes (UK); Mashhad and Tehran (Iran); Amsterdam (The Netherlands); Ankara (Turkey); Bucharest and Iasi (Romania); Lyon (France) and Boston (USA). In total, this provided assessments on 401 biopsy specimens and IEL counts on 198 patients with CD (142 (71.7%) women and 56 (28.3%) men) and 203 DC patients (120 (59.1%) women and 83 (40.9%) men). The CD and DC biopsies were selected if they had 4–6 well-oriented tissue samples to allow evaluation of villous/crypt ratio and the number and distribution of the lymphocytes. The number of IEL/100 epithelial cell nuclei was counted in a continuous manner, leaving out the crypt openings. Each laboratory reanalyzed the quality of cases before sending the results centrally for consolidation and review. The inclusion criteria for recruitment were positive coeliac serology and typical histological abnormalities consistent with Marsh III changes. The subjects with DC were selected from patients with iron deficiency and a negative coeliac serology. Exclusion criteria for DC included active infections, for example, *Helicobacter pylori* or bacterial overgrowth, non-steroidal anti-inflammatory drugs use, food allergy or any other small bowel disorders. In this retrospective study, H&E-stained 4–5  $\mu\text{m}$  thick sections cut from formalin-fixed paraffin-embedded archival material were used in 162 cases. Some centers additionally employed CD3 immunohistochemistry, involving 36 patients, using commercially available anti-CD3 antibodies. The CD3 antibody clone and vendor and dilutions were different in each center. The project aimed to measure the number of IEL/100 enterocytes in well-oriented duodenal biopsies from patients with untreated CD compared with a corresponding number of DC subjects. A definitive diagnosis of CD was defined as those patients demonstrating Marsh III histological abnormalities with positive serology in line with the current and previous guidelines, whereas those with seronegative Marsh III lesions were excluded.

*Ethical considerations.* This study involved re-scoring of archived histology slides, and all identifiable medical information was removed and all analyses were performed using anonymized data. The data collection was in line with good clinical practice policies with

approval by research and development/audit departments of countries involved. The study was also fully approved by the ethical committee of Research Institute for Gastroenterology and Liver Disease, Shahid Beheshti University of Medical Science, Tehran under the following ethical number: IR.SBMU.RIGLD.REC.1395.87.

*Statistical analysis.* Data are reported as mean ( $\pm$ SD) for continuous variables and as proportion for categorical variables. Comparisons were performed using the Student's t-test or  $\chi^2$  test, as appropriate. Receiver operating characteristic (ROC) curves were used to evaluate sensitivity and specificity for different cut-off levels of IEL/100 in detecting CD. Statistical significance was set at  $\alpha=0.05$ .

#### 2.2.4. Results

The mean ages of DC and CD groups were 38.3 (range: 2–88) and 45.5 years (range: newborn to 82), respectively, of which 59% and 71% were women. The mean IEL count was  $54\pm 18/100$  enterocytes for CD compared with  $13\pm 8$  for DC ( $p=0.0001$ ). We present data (Figure 7) from IEL counts based on the largest series of intestinal biopsies analyzed to date, obtained from eight countries across three continents (North America, Europe and Middle East).

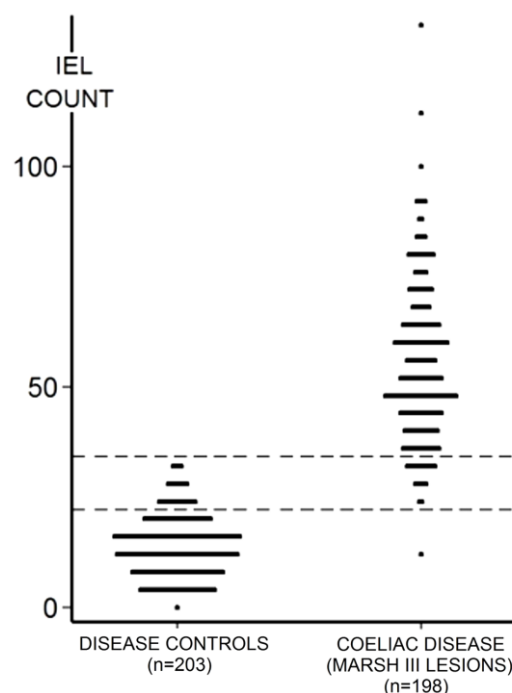


Figure 7: The numerical IEL counts (non-transformed) for the entire series of 401 specimens are shown for coeliac and disease control intestinal mucosae. The overlap of 56 between IEL counts for each population is stressed. Although when the same data are accumulated, biopsy-on-biopsy, a perfectly shaped dose–response curve is obtained.

In total, 401 specimens were studied, of which 198 came from well-defined patients with CD who were either endomysial antibodies (EMA) or tissue transglutaminase antibodies (tTG) antibody positive. Of the 198 patients with CD with Marsh III, 27% had iron deficiency anemia, 13% abdominal pain, 34% diarrhea and 6% weight loss. The mean $\pm$ SD for the DC was  $13\pm 7$  IEL/100 enterocyte nuclei (95% CIs 1–27). The normality of the variable was assessed visually using a histogram/assessed using a Shapiro-Wilk test which confirmed that the data are skewed to the right and distinctly non-normal. The mean IEL count for CD was  $54\pm 18$  (95% confidence limits 19–54), differing significantly from DC

( $p < 0.0001$ ). The ‘normalized’ CD mean was  $51 \pm 14$  (95% confidence limits 24–78). Overall, using numerical data, CD and DC biopsies showed an overlap of 56 biopsies comprising 14% of the total specimens analyzed. More interestingly with log-transformation, the distributions were ‘tightened’, so that the gross overlap was then reduced to 1%, or 38 biopsies. The literature presents a variety of optimum cut-off points ranging between 20 and 40 IEL/100 enterocyte nuclei, as criteria in the diagnosis of CD. However, these levels were, surprisingly, determined from means and SD originating from some extremely small groups. In this study, we had the advantage of large numbers of CD and DC biopsies which were further evaluated through ROC curve analysis (Figure 8). This offered an optimal cut-off point of 25 IEL/100 enterocytes, with a sensitivity of 0.990 and specificity of 0.931, respectively; the area under the curve was 99.5%. Here, each point on the ROC curve represents a sensitivity/specificity pair for any threshold value chosen. With perfect discrimination (no overlap in the two distributions), the ROC curve should pass through the upper left-hand corner, indicating a sensitivity and specificity of 100%. Our curve does not fulfil that criterion exactly, pointing to the inevitable overlap of IEL populations between both groups.

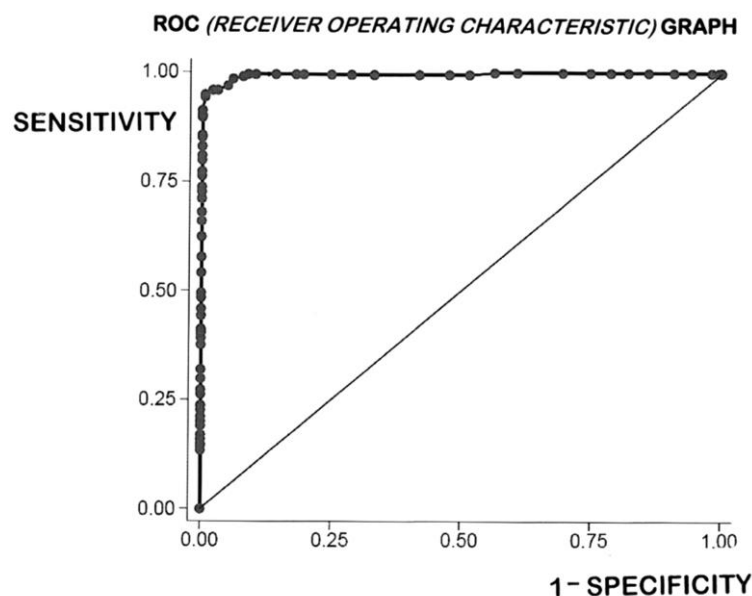


Figure 8: The receiver operating characteristic (ROC) curve for all 401 biopsies employed in this study is shown here. If there had been no relationship between the two samples, the curve would have followed the diagonal line. Our ROC graph shows considerable between-group homogeneity, the area under the curve being 99.5%. However, the sensitivity axis does not pass through the upper-left corner, indicative of the overlap which is further examined in detail elsewhere.

Using our derived ROC curve, we were able to further evaluate the currently existing published extremes (20–40 IEL) in the literature (Table 5). Thus, for a high cut-off of 40 IEL, the sensitivity was reduced to 0.80 with a specificity of 1.000. At this level, the false-negative rate was 19.7%, representing a total of 31 patients with CD who would have been missed. Conversely, with the lower cut-off of 20 IEL, the sensitivity was increased to 0.995, although the specificity was now reduced to 0.081. This led to an 18.2% false-positive result, which would have represented 37 DC biopsies being incorrectly labelled as ‘possible CD’. Since the actual numbers of cases misdiagnosed at these outer IEL counts are very high, their accuracy as histopathological guidelines is clearly evident. Both the numerical overlapping (Figure 7) and the shape of the ROC curve (Figure 8) confirmed our previously published assertion [Marsh and Rostami, 2016] that IEL do not represent bimodally distributed populations. This was further confirmed by our cumulative IEL count, biopsy-on-biopsy (Figure 9), indicative of a graded dose–response by IEL to environmental (gluten) antigenic influence.

Table 5: Summary of literature on IEL counts

Study	Methods	Number of biopsies	Upper range	Comments
Ferguson and Murray, 1971	H&E staining, IEL/100 enterocytes, 7 µm sections	40	40	Used controls, coeliac & autoimmune conditions, incorrect about normally distributed IEL, highest IEL count recorded: 155
Batman et al., 1989	H&E staining, 5 µm sections	8	33	Study of HIV enteropathy
Hayat et al., 2002	H&E staining, 4 µm sections	20	25	Counts made on uninterrupted length of epithelium >500 EC, controls defined only by a 'normal' sugar permeability
Mahadeva et al., 2002	H&E staining, 3 µm sections	29	22	Major interest in normal villi with IEL infiltrate. Really difficult to infer group numbers here
Kakar et al., 2003	H&E staining	12	39	Interest in normal villi with IEL infiltrates
Veress et al., 2004	H&E staining, 3 µm CD3+	64	HE: 20 CD3+: 5-9	In H&E sections, if IEL to EC ratio >5:1, do CD3 count
Biagi et al., 2004	H&E staining	17	45	Major interest in promoting villous tip counts
Lähdeaho et al., 2005	H&E staining	76	26	No reasons given for this cut-off value: referred to Ferguson and Murray (1971) and Kuitunen et al (1982) who give no reference range
Nasseri-Moghaddam et al., 2008	H&E staining, CD45+ cells	46	H&E: 46 CD45+: 47	Establishing normal criteria by histology and immunocytology
Siriweera et al., 2015	H&E staining	75	8	Retrospective study on 38 control and 37 coeliac specimens. Inexplicably small upper ranges for both groups

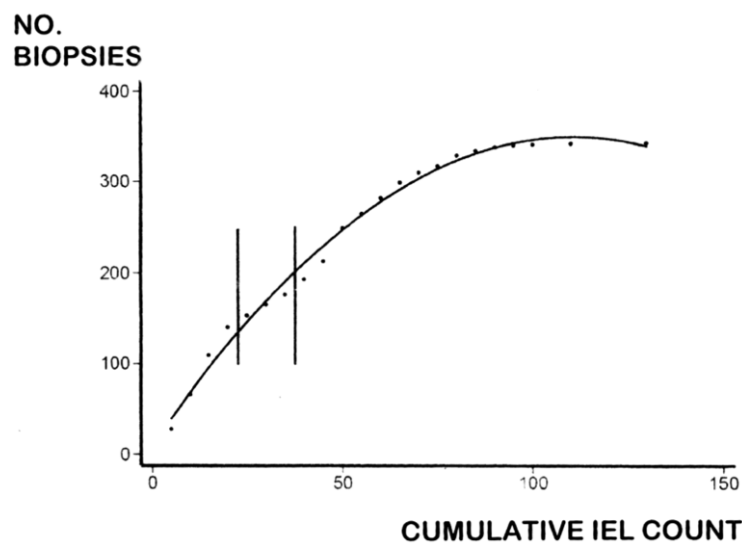


Figure 9: The cumulative IEL count, biopsy-on-biopsy, is illustrated in this diagram. The curve does not reach 401 on account of the overlapping counts between CD and DC mucosae, the overlap between biopsies being indicated by the two vertical parallel lines. The shape of the curve resembles a dose-response (to luminal antigen) and clearly demonstrates the absence of any bimodality between the two IEL populations.

By taking 25 IEL/100 enterocytes as the optimal distinguishing value, a significant reduction was seen in the numerical overlap between patients with CD and DC patients (Figure 7). In most previously published series, this overlap has not previously received much in-depth analysis. Given that the IEL are not bimodally distributed, any proposed cut-off between DC and CD biopsies should be seen as arbitrary. In this series, the ROC-based overlap consisted of 3 CD women as false negatives and 12 DC as false positives. Although

we had expected to have seen an increase in IEL counts in eastern biopsies, this impression was not borne out in practice (Figure 10). There were significant differences in the results between the UK and Romania ( $p=0.011$ ) and between Italy and Romania ( $p<0.0001$ ). We did not pursue these correlations since the numbers of biopsies per group were too small to deduce any insightful conclusions that could be safely drawn.

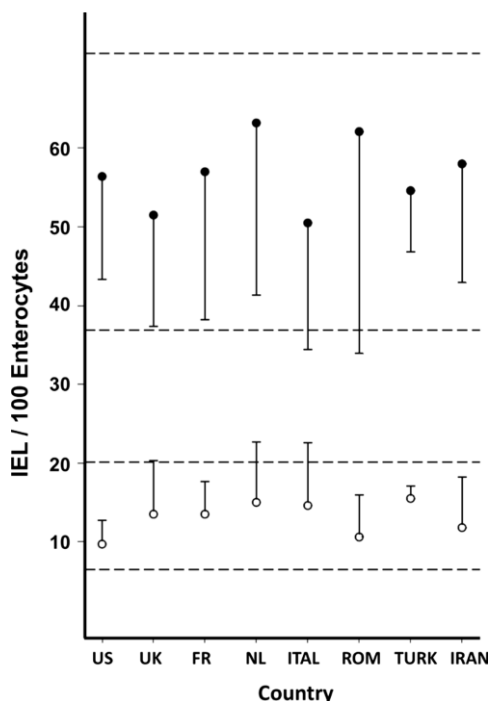


Figure 10: This diagram illustrates the individual measurements from biopsies sampled across the Western hemisphere (USA, UK, France (FR), Netherlands (NL), Italy (ITAL), Romania (ROM), Turkey (TURK) and Iran). Bars reflect mean±SD for disease control (open circles) and coeliac disease (closed circles). The two sets of horizontal dotted lines indicate the overall mean±SD for the two groups of biopsies studied.

All 198 specimens analyzed in this study fulfilled Marsh III criteria, of which 132 (66.7%) specimens were graded as IIIa, IIIb or IIIc. In graded specimens, a high proportion (60; 45%) were graded as Marsh IIIc. Conversely, 34 Marsh IIIa specimens comprised only 26%, whereas the 38 remaining specimens (29%) were classified as Marsh IIIb. The grading report was not reportable for 66 of 198 specimens, because six pathologists had already ceased grading this lesion and two others graded biopsies as a+b or b+c or even a+b+c. The IEL populations between these three groupings, however, were not significantly different (Table 6). Six groups submitted their counts as CD3+ totals, allowing the possibility of determining percentage counts for each Marsh III subdivision. Again, no differences were found (Table 6) with the arithmetic mean, being 63 immunolabelled cells/100 enterocyte nuclei.

Table 6: Breakdown of Marsh III mucosal lesions

Subgroup	Biopsies (n)	H&E IEL (mean±SD)	Biopsies (n)	CD3+ IEL (mean±SD)
IIIa	36	54±14	10	60±11
IIIb	38	52±17	12	67±19
IIIc	63	55±21	14	62±31
<b>Total</b>	137	54±18	36	63±23

Statistics: H&E: IIIa vs IIIb,  $p=0.91$ ; IIIa vs IIIc,  $p=0.96$  IIIb vs IIIc,  $p=0.96$ . CD3+: IIIa vs IIIb,  $p=0.84$ ; IIIa vs IIIc,  $p=0.92$ ; IIIb vs IIIc,  $p=0.98$ . Note: The subclassification of the Marsh III lesion has, to our knowledge, never been subject to critical analysis despite its widespread adoption, as almost a ‘matter of faith’. Here we show that the IEL counts across each of these subdivisions reveal no statistical differences. This is most worrying, since the subdivisions were supposed to represent specific, detectable and progressively deteriorating

pathologies during the terminal phases of mucosal flattening. Moreover, despite smaller numbers, no detectable differences in CD3+ IEL were detected between the IIIa, b and c subdivisions of the specimens analysed, in parallel with other findings.

### 2.2.5. Discussions

The most significant results of the current study which included centers from 3 continents are: (1) the optimal cut-off point between CD and DC duodenal mucosa was 25 IEL/100 enterocytes, (2) there was no significant difference in IEL counts from different countries across the Western hemisphere, (3) CD IEL counts are not normally distributed, although correction by log-transformation did not materially affect outcomes, (4) the cumulative IEL population, biopsy-on-biopsy, is indicative of a graded dose-response and thus does not represent a bimodal response between CD and DC IEL, and that any proposed cut-off value is arbitrary and (5) the total number of IEL in graded Marsh III lesions (a, b and c) was identical throughout, as was also demonstrated with the (smaller) number of CD3+ labelled IEL.

The increased number of IEL has, since the '70s, been used in the histological diagnosis of CD. The original study which highlighted this advance by Ferguson and Murray [Ferguson and Murray, 1971] contains several misconceptions. First, the false conclusion that IEL are normally distributed. The data from our study reveal that error, together with the skewing in the CD distribution. It should be noted that there was a marked difference between the overlap as expressed by the numerically bulked data (Figure 7), compared with our log-transformed results. Log-transformation does 'tighten up' the distributions, reducing overlapping from 47 to 38. However, irrespective of the theoretical importance of this observation, from a practical point of view, the question arises whether, in routine practice, all suspected CD counts need to be log-transformed to provide the most critically based diagnostic information. Our analyses confirm that this is unnecessary, since log-transformation does not afford any materially different result. For example, the difference for DC distribution was only 2 IEL/100 enterocytes (Figure 7), and for CD was 3 IEL/100 enterocytes. This is an important outcome of our study, and certainly an important message for histopathologists.

Second, Ferguson and Murray took 40 IEL as their upper limit of normal which is one of the highest results published (Table 6). Based on our ROC curve analysis, a count of 40 IEL/100 enterocytes has a markedly reduced sensitivity of 0.790, compared with 0.995, when using a 25 IEL/100 enterocytes cut-off. Our established value corresponds to that of Hayat et al's [Hayat M, et al. 2002] study but whose outcome was based on an exceptionally low mean count of 11 IEL/100 enterocytes. Indeed, their range was 2–26 IEL, so that with a SD of 7, their upper calculated limit of normal was 25 (11+14). It is interesting to note that they studied only 20 biopsies obtained from apparently 'healthy' subjects, defined by a 'normal' sugar permeability test. Their counts were also based on enumerating IEL along an uninterrupted length of 500 enterocytes, which to us seems a technical impossibility. Nor were there any comparisons with CD biopsies, so on these three grounds, their study cannot be regarded as a critical evaluation.

Third, Ferguson and Murray introduced the methodology of counting IEL against epithelial cells, the inaccuracy of which was demonstrated by a point-counting technique. These revelations were subsequently confirmed by computerized morphometric analysis which showed that IEL counts were likely to be overestimated twofold.

By calculating both the number of enterocytes and IEL present in a controlled unit of villous volume, the numerical discrepancy of the earlier counting technique was exposed. The flaw is in trying to obtain a meaningful result when both parameters (epithelial cell and IEL populations) are independently changing. The absolute IEL count in untreated CD mucosae is not increased, although it appears elevated since the number of enterocytes on the surface of a

Marsh stage III lesion is, comparatively, markedly reduced. Conversely, with Marsh I and Marsh II stage lesions, the increase in IEL is absolute, representing a truly elevated population. Several groups have tried to establish definitive cut-off points.

However, these papers exemplify the precarious background on which current practice rests, and which is clearly in need of revision. The question of a cut-off, and how to locate it, is of both theoretical and practical importance. As evident from the published data, a range of values lying between the extremes of 20 and 40 IEL has been proposed. Beyond that, there have been no further attempts to obtain a more reliable answer. Using our ROC curve (Figure 8), we were able to investigate IEL values published in the literature. At the highest notional cut-off value of 40 IEL, we predicted that there would have been 31 false negatives (coeliac cases undiagnosed), but without any false positives. On the other hand, at the lower 20 IEL level, there would have been 37 false positives and 1 (coeliac) false negative. In comparison with our results (with 12 disease controls and 3 coeliac misdiagnosed), the values given in the literature fare badly. The important point to remember is that any cut-off is an arbitrarily fixed point.

Nevertheless, given the large numbers of specimens examined in this study, together with their respective IEL populations, the results of our analysis probably represent the best result achievable and hence the most effective cut-off level of 25 IEL on H&E-stained sections for working practice. However, in another recent publication, IEL counts were accumulated from the preceding 40-year literature, yielding 607 separate data points. In combining H&E-derived IEL counts from both studies (giving a total of 255 CD and 271 DC biopsies), ROC curve analysis provided an optimal cut-off of 26 IEL with 95.81% of the combined sample correctly identified. Marsh and Heal [Marsh and Heal, 2017] also found that separate ROC curve analyses for CD3+, and  $\gamma\delta$ +, IEL counts yielded less satisfactory cut-off points. Therefore, their results are consistent with the current Bucharest conclusion that H&E-derived IEL counts are adequate for its purpose. These are extremely interesting new insights and of great help to routine histopathologists in being reassured that immunohistochemistry does not offer improved diagnostic certainty.

IEL populations represent graded intestinal responses to antigenic challenge. This has been experimentally demonstrated in treated patients after gluten challenge. Here we have again confirmed and revealed the dose–response curve to gluten across all the specimens studied (Figure 9). On inspecting our data, we were a little surprised that IEL counts did not increase across the globe from America to the near Middle East (Figure 10), which we had suspected. The statistical differences that were demonstrable are probably of little significance and were not evaluated further. It is, however, noteworthy that the IEL count is dependent on a surprisingly large number of internal and external factors including age, genetic background, ethnicity, geo-cultural factors, diet, food sensitivities, parasites, chronic liver disease, infections, drugs, the maternal and local intestinal microbiomes, and recent travel. The large numbers of biopsies employed in this work helped to reveal the extent to which false-negative and false-positive misdiagnoses are incurred.

A histologically negative result for CD appears to have less impact, since the clinician can employ additional assessments including Human Leucocyte Antigen (HLA) typing, EMA, increased anti-tTG titers or even deamidated gliadin assays [Mooney et al., 2015] to aid the diagnosis. A more difficult issue occurs when a normal biopsy is misclassified as CD, since there may be no additional pointers to avoid imposition of a lifelong gluten-free diet.

Finally, our study has cast more light on the subclassification of the Marsh stage III coeliac lesion that originated from Dutch studies. The subdivision of Marsh III was introduced to demonstrate a correlation between serology and degrees of mucosal abnormalities that led to first description of seronegative CD concept. Within our total sample, 132 biopsies were contributory, but we were surprised that nearly one-half (60, or 46%) were classified as Marsh IIIc, whereas only 38 (29%) were considered Marsh IIIb, and

even less, 34 (25%), as Marsh IIIa. It should also be observed that we found no significant differences between the IEL populations within any of these subgroups (Table 6). Although this subclassification was supposed to provide a ‘standardized procedure for mucosal classification’, no empirical measurements accompanied the modifications suggested, thus leaving this to subjective interpretation. A subsequent set of ‘guidelines for pathologists’, written by pathologists [Dickson et al., 2006], offered micrographs of biopsies which did not correspond to those originally given. In a separate study of CD IEL and their immunohistological subtypes [De Andrés et al., 2015], no differences in the ‘lymphogram’ in terms of the subclassification of Marsh stage III mucosae could be found. That would be inconsistent with the original proposal that each subdivision supposedly represents a progressively greater degree of mucosal involvement and damage. Previous detailed morphological studies with transmission and scanning electronic microscopy have further degraded this subclassification by demonstrating their lack of relevance to mucosal architecture interpretation. A recent study from Australia which employed principal component and discriminant analyses [Charlesworth et al., 2017] found that defined algorithms could accurately distinguish the major Marsh grades, but were unable to discriminate between any of the so-called Marsh IIIa, b and c sublesions. Together, this growing body of information seems to indicate that attempted subclassifications of Marsh stage III lesions have no intrinsic status or value, and therefore would best be abandoned.

In that regard, six contributory groups within this study had already abandoned this subclassification, whereas two other groups classified their biopsies with multiple combinations of a+b+c, indicating the impossibility, if not gross frustration, of forcing one subclassification to fit into one or the other category.

This might be an explanation for the anomalous finding that almost 50% of biopsies were classified as Marsh IIIc, with far less weight put on the other two subcategories. Clearly, if morphological, immunohistochemical or mathematically based analyses fail to reveal any major differences in the progressive degrees of tissue damage implied by this subclassification, then what value can emerge from its continued use? Equally strained is the growing habit of equating Marsh IIIa with so-called ‘partial villous atrophy’, Marsh IIIb with ‘subtotal villous atrophy’ and Marsh IIIc with ‘total villous atrophy’. Interestingly, in flat lesions, there is no evidence of an atrophic process, but only hypertrophic mucosal responses, and a striking absence of villi.

Regarding the intestinal mucosal interpretation, IEL counts, comparisons between lamina propria cells composition, and villus vs. crypt ratios are still imperfect procedures because of no agreement on numerical foundation, relative to an invariant index within the mucosa. Over the past decade, there has been a strong predisposition to ignore the necessity for mucosal biopsies and its role in diagnosis, because the interest turned to more noninvasive genetic or serologic tests for coeliac disease.

Besides the IEL count, it should be mandatory to establish what “normal” mucosa means, as no criteria are still set. All researchers compare the duodenal mucosa from patients with celiac disease to a “normal” mucosa, without stating which are the criteria. Also, the ratio between the length of the villi compared to the depth of the crypt is subject to disagreements, as in bi-dimensional microscopy, it is very difficult to correctly and completely assess the full length of a such pliant structure, especially in pathological conditions. Therefore, assessing the villi/crypt ratio would be better realized in a 3D computerized system [Charlesworth and Marsh, 2019].

New morphological concepts state the upper and lower compartments, represented by the villi and the crypts, respectively. In fact, there is very difficult to precisely point out the origin of the villi. More information is needed for this issue, such as mRNA locations of the origin of villous cell membrane hydrolases (esterase, alkaline phosphatase).

In what concerns the lamina propria, it is now clear that the subepithelial stroma, including all basement membranes, has major influences on the differentiation and maintenance of duodenal epithelial structures [Charlesworth et al., 2019]. The interrelations between mesenchyme and epithelium needs to be detailed, as well as the microvasculature is re-shaped as the mucosa itself is progressively re-modelling into a flat mucosa [De Gregorio et al., 2018]. Furthermore, it might be interesting to identify pathways in which the microvasculature begins to regenerate with new capillaries in order to sustain mucosal regeneration (after a gluten-free diet is initiated) leading to the villous regrowth.

### **Final remarks**

In conclusion, the international multicenter team studied the IEL in more than 400 biopsies established a cut-off point of 25 IEL/100 enterocyte, which can be a reliable criterion when differentiating CD Marsh III from non-celiac biopsies. No differences were observed in IEL counts on biopsies obtained from countries from different continents. Although the IEL count in CD patients is not normally distributed, this does not make any substantial difference to laboratory counting in the routine work of histopathologists. The current study found no differences in IEL count over the 3 subtypes of Marsh III (a, b or c), suggesting that subdividing Marsh III stage in 3 sub-stages is useless, as long it doesn't offer diagnostic or prognostic help to the gastroenterologist. Still, as a follow-up of this study, a similar project involving a multi-institutional collaborative team is needed to identify optimal cut-offs points to diagnose celiac disease in patients with milder mucosal lesions (Marsh I and II).

## **2.3. “Microscopic enteritis” – global consensus on a new entity**

### **2.3.1. Introduction**

Celiac disease in its earlier stages (Marsh 0-II) is the most common form at presentation. It is called atypical gluten sensitivity or microscopic enteritis. Advanced stages (Marsh IIIa-c) is rarely diagnosed at first presentation, but the symptomatology, the serology and the microscopical changes strongly sustain the diagnosis, while in microenteropathy, the symptomatology and the morphological changes seem not to be correlated. Sometimes, important epithelial lesions of the duodenal mucosa are not reflected in aggravated symptomatology [Ciclitira, 2007]. As nutritional deficiencies can be present in patients with ME, it is questionable if the villous atrophy is the only cause of malabsorption, but maybe the systemic inflammation who explains the nutritional deficiency. Inflammation and cytokine stimulation produce malabsorption, because gluten-sensitized lymphocytes and Tumor Necrosis Factor-alpha (a pro-inflammatory cytokine) inhibits the uptake of micronutrients (i.e. iron, phosphates) by acting on enterocytes before destroying them and producing villi atrophy [Chen et al., 2009]. Perhaps this is why the symptomatology in patients with mild lesions is severe, similar to those with Marsh III lesions, or, in other words, the malabsorption in patients with villous atrophy is not worse than in patients with mild lesions [Ciclitira, 2007]. Sustaining this theory, in some patients, although the villous atrophy persists for years even after successful treatment, clinically, the disease is silent, asymptomatic. For patients with CD and mild lesions (microscopic enteropathy), the quality of life is very important. Since they have positive serology for CD antibodies, they should adopt a gluten-free diet. Serology, therefore, is more important than histological changes in ME [Guandalini, 2006], despite the fact that, in early stages of CD, the clinical diagnosis is often quite difficult.

Within this general context, during the 5<sup>th</sup> and 6<sup>th</sup> International Courses of Digestive Pathology organized by the Carol Davila University of Medicine and Pharmacy, Bucharest, held in Bucharest in 2012 and 2013, a group of expert pathologists and gastroenterologists from different countries around the world specialized in small bowel diseases formed a working group to formulate a consensus statement on ME. The 21 experts reviewed 20 statements on a five-step agreement score (from strongly agree to strongly disagree) (Table 7) in order to find an algorithm for investigation and treatment of microscopic enteropathy, according to its etiology, symptomatology and diagnosis criteria.

Each member of the group filled-in a pre-determined statement form relating to the definition, etiology, diagnosis and treatment of microscopic enteritis. Statements were considered unanimously endorsed if more than 75% of the panel members shared a similar opinion (agree and strongly agree or disagree and strongly disagree).

Table 7: Results consensus agreement

	<b>Total responses</b>	<b>Agreement</b>
Definition	21/21	95%
Clinical	21/21	95%
Aetiology	21/21	95%
Histological	21/21	100%
Immunogenetic	21/21	90%
Pathogenesis 1-2	21/21	80%-90%
Diagnosis 1-3	21/21	85%-100%
Investigation	21/21	95%
Management	21/21	60%-100%

The consensus statements agreed upon supporting evidence are described as follows:

#### Definition

Microscopic enteritis is a histopathological condition affecting the small bowel, being characterized by microscopic and submicroscopic lesions that may result in micronutrient deficiencies (agreement: 95%). It is an early stage of mucosal abnormalities in many inflammatory diseases, representing a common finding in patients with intestinal inflammation induced by different causes. Advances in IHC techniques proved submicroscopic changes and enhanced detection of other microscopic abnormalities described by Marsh and others [Sbarbati et al., 2003]. The ill-defined mucosal lesions consistent with ME previously known as functional and non-specific may affect the duodenum, jejunum and/or ileum with associated micronutrient malabsorption. It is well known that celiac disease with mild enteropathy is not necessarily a mild disease, as there is no correlation between mucosal lesion and clinical presentation of CD. Pathological changes can range from mild enteropathy with sub-microscopic abnormalities [which means: alteration of enterocytes, shortening of microvilli and increased  $\alpha/\beta/ \gamma/\delta$  T cell receptors (Marsh 0)] to microscopic changes [meaning: increased number of IEL (> 20 IEL/100 enterocytes) and/or crypt hyperplasia (Marsh I-II)] (agreement: 100%). Marsh described a spectrum of small intestinal mucosal changes associated with CD but these are not specific and may be also seen in other inflammatory disorders of the small intestine. True normal mucosal architecture and IEL count (Marsh stage 0) was considered possible but extremely rare for CD. The mucosal aspect then progressed to an “infiltrative type”, which is characterized by normal architecture with increased IEL count infiltration (Marsh stage I), “hyperplastic type”, characterized by hyperplasia of the crypts and increased mitotically active epithelial lymphocytes (Marsh stage II) and “destructive type”, characterized by partial, subtotal or complete villous atrophy (Marsh stage III). The latter classification was modified to describe the degree of villous destruction in Marsh stage III lesions: mild,

marked and complete (IIIa, IIIb and IIIc, respectively) [Corazza et al., 2007]. However, recent evaluations suggest that destructive lesions are not usefully subdivided into A, B, C subgroups with the routine tools available to most pathologists, and therefore are best abandoned. Nevertheless, the original worldwide used Marsh classification seems to be the most reliable way of evaluating intestinal lesions not necessarily limited to CD. Inflammation associated with ME is better understood if the original Marsh classification is used as originally described. Several studies have observed that normal IEL counts are less than that initially defined by Marsh and may range between 11 and 25 IELs/100 enterocytes. Before the development of the “infiltrative type” lesion of Marsh stage I has occurred, many other submicroscopic abnormalities may occur, including subtle alteration to enterocytes, shortening of microvilli and altered ratio of T cell receptor  $\alpha\beta$  and  $\gamma\delta$  subsets of IELs [Han et al., 2013]. Interleukin (IL)-2 receptor upregulation may also be detected in conjunction with IEL T cell activation. These cases, with sub-microscopic changes but normal mucosal architecture and IEL counts, currently fall into Marsh stage 0. ME is characterized by mucosal changes of Marsh stages 0 to II and additional inflammatory changes not described in the current Marsh classification. From these critical studies, important conclusions arise: (1) A histologically “normal” mucosa doesn’t exclude an underlying intestinal disease process; and (2) the term “non-specific” should never be used diagnostically since every biopsy reflects the physiologic or pathological state of the small intestinal mucosa at the time of biopsy.

#### Etiology

Microscopic enteritis is a multifactorial inflammatory entity that may be caused by gluten intolerance, infections (for instance, *H. pylori*), drug therapies and other systemic inflammatory processes (agreement: 100%).

ME results from an inflammatory process with several etiological triggers. Recruitment and activation of IELs is pivotal and it is likely this is etiology-specific with unique pro-inflammatory cytokine profile and triggering antigens. Established causes of ME include gluten exposure, infection, drug therapy, systemic inflammatory conditions and autoimmune diseases. In most cases an etiology can be identified. Aziz et al [Aziz et al., 2010] found a definite cause for lymphocytic duodenitis (LD) in 66% of their patients. Multiple etiologies may co-exist and a detailed diagnostic workup is imperative. Rosinach et al. [Rosinach et al., 2012] found more than one initial potential etiology in 44% of patients with LD.

#### *Gluten related disorders*

The gluten related disorders associated with microscopic enteritis are celiac disease with minimal macroscopic lesions, gluten/wheat allergy and non-coeliac gluten sensitivity (NCGS) (agreement: 83%).

Gluten related disorders are a major cause for ME affecting the small intestine and other organs in different ways. The triggering factor is exposure to the protein component of wheat and associated species of barley, rye and oats. Oats are safe in most CD patients. Innate and adaptive immune reactions lead to various abnormalities and symptoms in and out of the gastrointestinal tract in genetically susceptible individuals [Peña, 2014]. Subtypes of gluten intolerance have distinct mechanisms. In CD, ingestion of gluten and related prolamins stimulates adaptive immunity by tissue transglutaminase-mediated deamidation, human leucocyte antigen (HLA)-DQ2 complex formation and T-cell activation [Gujral et al., 2012]. In comparison, enteropathic gluten/wheat allergy results from an IgE-mediated or cell-mediated reaction to allergenic intra-luminal gluten and wheat-proteins. The nature and timing of reactions following oral or epicutaneous gluten challenge is crucial for diagnosis. NCGS is a re-discovered condition applicable to patients who fail to satisfy diagnostic criteria for CD or gluten/wheat allergy but benefit from GFD [Sapone et al., 2012]. The

pathogenesis of NCGS is currently poorly understood but an enhanced innate immune response has been [Peña, 2014]. Further research should clarify the differences between NCGS and CD. ME is a common presenting histological finding in CD. Symptom severity may not correlate with the degree of enteropathy in patients with CD. Therefore, recognition of subtle villous abnormalities is extremely important so that symptoms are not attributed inappropriately to a functional disorder. It should be noted that villous atrophy may be present in asymptomatic CD or persist despite treatment and clinical improvement. Similarly, deterioration of mild enteropathy into frank villous atrophy might not be associated with deterioration in symptoms or micronutrient deficiency.

#### *Infection*

Although most of the cases is associated with peptic ulceration, non-autoimmune chronic gastritis, primary gastric mucosa-associated lymphoid tissue (MALT) and gastric cancer infection with *Helicobacter pylori* was identified also in patients with microscopic duodenitis and functional dyspepsia [Lebwohl et al., 2013]. In studies on patients with lymphocytic duodenitis and abdominal pain, *H. pylori* infection was considered the single or the most frequent cause in about a quarter of cases [Rosinach et al., 2012; Santolaria et al., 2013]. Also, other small bowel bacterial overgrowth caused lymphocytic duodenitis in 22% of patients [Santolaria et al., 2013]. The mechanism might be the depletion of essential nutrients which are needed for the normal function of mucosal epithelium or by the effects of the toxins produced by bacteria. Tropical sprue, post-infections malabsorption or parasites (such as: giardia and threadworm) might sometimes represent an infectious cause of ME.

#### *Drug therapy*

Nonsteroidal anti-inflammatory drugs and aspirin therapy are unanimously considered as causes of ME with a prevalence of about 15% in patients with lymphocytic duodenitis [Santolaria et al., 2013]. Exposure to drugs may, directly or after being entero-hepatic circulated, damage the intestinal epithelium. In vitro mechanisms of NSAID-induced intestinal lesion need more studies, still villous ischemia induced by focal sludging of blood flow in villi capillaries and damage to surface small vessels, were identified in animal model. Firstly, villous shortening and endothelial swelling were observed, followed by mucosal ulceration, and this may represent an early NSAID-induced lesion. Also, Olmesartan was identified in a severe form of sprue like enteropathy [Fiorucci et al., 2014].

#### *Systemic inflammatory conditions*

Microscopic lesions could be the presenting or at least the early stage of chronic inflammatory conditions including inflammatory bowel disease and microscopic colitis (MC) (agreement 93%).

Systemic inflammations implicated in ME include sarcoidosis and IBD. Microscopic duodenitis was identified in about a quarter of patients with ulcerative colitis and significantly increased CD3+ and CD8+ IELs and lamina propria mononuclear cells compared with disease free controls. Sometimes, ME may be the initial non-specific finding that leads to diagnosis of a chronic inflammatory condition.

#### *Autoimmune disease*

Several autoimmune entities, such as, rheumatoid arthritis, Hashimoto's thyroiditis, Graves' disease, psoriasis and multiple sclerosis, might be associated with ME. Mucosal changes may result from an associated autoimmune enteropathy characterized by elevated gut epithelial cell antibodies. The incidence of CD is higher in patients with autoimmune disease, therefore careful diagnostic workup is needed [Gentile et al., 2012].

#### ME and malabsorption

The malabsorption is due to activation of local and systemic cytokines leading to inhibition of the uptake of micronutrients (agreement: 80%).

The clinical presentation in CD does not correlate with the degree of mucosal damage. Instead the underlying inflammatory process, common to each stage of enteropathy, may impair micronutrient uptake contributing to symptoms. Tumor necrosis factor  $\alpha$  and IL-1, key pro-inflammatory cytokines, may act directly on the intestinal mucosa to cause malabsorption. This has been observed in non-gastrointestinal malignancies in which systemic cytokines are increased. Similarly, IL-6 may impair iron transport in enterocytes by direct action at the local level or indirectly via hepcidin induction. Impaired iron absorption and elevated IL-6 levels were demonstrated in patients with active CD compared with inactive disease controls [Semrin et al., 2006]. Future studies should further characterize the effects of cytokines on mucosal cells, specifically their absorptive function.

Malabsorption does not correlate with the length of small bowel micro/macrosopically affected (agreement: 80%).

Despite a macroscopically normal small bowel, microscopic and sub-microscopic mucosal abnormalities consistent with ME may exist with associated malabsorption. Clinical presentation does not correlate with the degree of villous atrophy. However, patients with partial villous atrophy had greater hemoglobin and bone mineral density (measured at lumbar spine, hip and distal radius) than patients with subtotal and total villous atrophy. This may be explained by ongoing inflammation, causing progressive bowel damage and cumulative systemic micronutrient deficiency. Instead, gastrointestinal symptoms may be the acute manifestation of micronutrient malabsorption that correlates with the severity of inflammation at that time. Therefore, micronutrient absorption rate may not correlate with the degree of villous atrophy since it is not reflective of the duration of inflammation. Further studies are needed to test this theory and confirm that micronutrient absorption capacity does not relate to the degree of macroscopic small bowel damage.

### Diagnosis

The term ME can be proposed in cases of Marsh 0-II mucosal changes with clinical, serological, genetic and histological data supportive or unsupportive for a specific etiology (agreement: 100%).

ME is confined to microscopic or sub-microscopic small intestinal enteropathy (Marsh 0-II) even if the etiology is undetermined despite extensive clinical, serological, genetic and histological investigation. An underlying etiology may not be detected on initial screening so further investigations become necessary to cover particular suspected diagnoses. Investigations may cover clinical suspicions according to the algorithm below.

A diagnosis of underlying etiology of ME is dependent upon taking a careful history and detailed examination in suspected cases (agreement: 93%).

An accurate evaluation of ME requires a careful history and detailed clinical examination in the first instance. The findings elicited will help to select further investigations so that an accurate underlying diagnosis can be arrived at.

The history should pay particular attention to any chronic inflammatory conditions, drug therapies and symptoms affected by dietary changes (agreement: 100%).

Chronic inflammatory disease, drug therapies and gluten intolerance are common causes of ME and hence should be evaluated with particular attention to the history. Occasionally an underlying occult chronic inflammatory disease may exist and therefore the practitioner should explore potential extra-intestinal features including arthritis, inflammatory ocular disease and dermatological peculiarities. Current and recently ceased medications should be reviewed, including NSAIDs, angiotensin II inhibitors and “over the counter” medications. Time required for complete mucosal recovery following the cessation of medications is unclear. Many patients may have trialed particular diets in an attempt to alleviate symptoms following formal medical advice or, increasingly, attempted self-diagnosis. Others modify diet for weight loss. The effect of current or previous dietary

modifications may provide useful diagnostic information. Symptomatic improvement with gluten or lactose free diet suggests underlying gluten intolerance. Furthermore, a current GFD may influence coeliac antibody serology results. The clinical presentation of cases with ME with different etiology may include gastrointestinal symptoms of abdominal discomfort, bloating, steatorrhea, chronic diarrhea and constipation; and systemic symptoms of lethargy and fatigue. Abnormal liver transaminases, specific micronutrient deficiency or weight loss may be present. Some studies suggest irritable bowel syndrome (IBS) may present with mild enteropathy and demonstrate exposing the food intolerant cases labelled as IBS to food antigens may cause immediate breaks, increased intervillous spaces and IEL in the intestinal mucosa [Catanzaro et al., 2014; Fritscher-Ravens et al., 2014]. The symptoms are clearly similar in both cases with milder enteropathy (ME) compared to severe mucosal damages despite the form of underlying conditions.

Investigations should include routine blood tests including a renal, liver and bone profile, serum B12, folate, ferritin and thyroid function tests, serum immunoglobulins, coeliac serology, *H. pylori* assessments (fecal antigen or blood serology) and HLA typing (agreement: 100%).

Initial investigations may help to establish the etiology of ME and should evaluate micronutrient deficiency. Full blood count, renal and bone profile including vitamin D (25-OH-D3). Vitamin B12, folate and ferritin may reveal anemia, electrolyte imbalance or specific micronutrient deficiency. Liver function tests may demonstrate elevated transaminases and cholestasis suggesting a chronic inflammatory disease such as primary biliary cirrhosis or sclerosing cholangitis potentially with concomitant IBD. Thyroid function tests are important. These investigations are useful in assessing systemic conditions that may affect any organs. Coeliac serology should include anti-tissue transglutaminase (anti-tTg) and endomysial antibodies (EMA), immunoglobulin titres and HLA typing. The sensitivity of coeliac antibody serology is poor in CD with mild enteropathy. Detection of HLA DQ2 and to lesser extent DQ8 genotypes (both strongly associated with CD) may be more useful when investigating patients with ME for underlying CD. HLA DQ2 and DQ8 genotype is however present in 25%-40% of the general population, so their absence is more useful in tending to exclude CD. Evaluation for concomitant CD is particularly important in patients with pre-existing autoimmune disease given its increased prevalence and since multiple potential ME etiologies may co-exist [Rosinach et al., 2012]. In ME with negative coeliac serology and no clear alternative etiology the authors recommend a trial of GFD for potential underlying non-coeliac gluten sensitivity as 38% of patients with LD and non-HLA DQ2 or DQ8 genotype improved with initiation of GFD. In contrast, patients with Marsh I or II intestinal lesions should only commence GFD if coeliac antibody serology becomes positive. Further investigations should be guided by clinical suspicion based on the history, examination and initial serological screen.

Other investigations include colonoscopy, ideally with intubation of the terminal ileum, and multiple colonic biopsies to look for MC (agreement: 80%).

MC may rarely be a precursor of IBD. Therefore colonoscopy, ideally with intubation of the terminal ileum and multiple biopsies from right and left colon, may be a useful additional investigation when an etiology for ME cannot be identified or in patients with other potential etiology who do not respond to treatment. Microscopic colitis may cause a similar spectrum of clinical symptoms as ME including abdominal pain, cramping, bloating and diarrhea. Early detection and treatment of IBD will minimize long term complications.

For ME upper gastrointestinal endoscopy with multiple duodenal biopsies (at least four) from the second part of the duodenum, 2 from first part of duodenum in cases with high risk for coeliac disease is required and additional biopsies should be taken to investigate for *Helicobacter* infection and lymphocytic gastritis (agreement: 100%).

To detect ME, the authors advocate for upper GI endoscopy with at least four duodenal biopsies from D2. In a retrospective study of 132352 patients without known CD, a minimum of four biopsies was significantly more effective at achieving a pathological diagnosis of CD, defined as Marsh stage IIIA/B/C, compared with less than four biopsies (1.8% vs 0.7%,  $P < 0.0001$ ) [Lebwohl et al., 2011]. Marsh stages I and II lesions were found in 4.5% of patients although the cause was not reported. There may be additional diagnostic yield from including a duodenal bulb biopsy particularly in patients with patchy villous atrophy. In children with patchy villous atrophy and positive coeliac serology (EMA, anti-tTg antibodies and HLA-DQ2/DQ8 heterodimers), villous atrophy was detected at the duodenal bulb. Another study advised at least three duodenal biopsies including one from the duodenal bulb to detect villous atrophy in patients with serology suggestive of CD [Hopper et al., 2008]. Concurrent antral gastric biopsies are recommended to assess for lymphocytic gastritis and *H. pylori* infection (rapid urease test “RUT”, biopsies from antrum and corpus), a common treatable cause of ME. C13 breath test should be considered as sensitivity of RUT is low. Biopsies from esophagus and stomach might also be indicated in dyspeptic patients.

Microscopic enteritis can progress to overt coeliac disease in genetically susceptible patients (agreement: 93%).

Following a diagnosis of ME, regular follow up is vital to detect initially silent but potentially treatable etiology and to evaluate for evolving micronutrient deficiency. This includes CD which may not be detected on initial investigations. It is well documented that initially negative serology for CD may subsequently become positive. Duodenal abnormalities may progress from ME to Marsh stage III with continued ingestion of a gluten containing diet in genetically susceptible patients.

#### Treatment

Treatment of ME is dependent on the etiology (agreement: 100%).

In celiac and non-celiac gluten sensitivity, dietetic review and initiation of gluten free diet is the cardinal intervention (agreement: 100%).

The cardinal intervention for gluten related disorders is dietetic review and initiation of GFD. This supersedes advice that a GFD should only be recommended in CD patients with severe enteropathy. A GFD should be trialed to assess possible non-coeliac gluten sensitivity in patients with ME and no clear alternative etiology. In the absence of clinical improvement, repeat celiac serology and follow-up duodenal biopsies may be required to assess for histopathological improvement before the patient is considered gluten tolerant. The optimal interval of GFD trial prior to repeat biopsy is poorly established but anecdotally at least six weeks seems to be appropriate.

For treatment of ME, any enteric infections including *H. pylori* should be eradicated (agreement: 93%).

Eradicating existing enteric infections is important both in the management of ME and to reduce potentially overlapping morbidity from alternative sources. *H. pylori* infection is also associated with peptic ulcer disease, non-ulcer dyspepsia, gastric cancer and gastric MALT lymphoma. Standard triple therapy eradication regimen is recommended for *H. pylori* infection in the first instance. Some enteric infections may cause concomitant microscopic colitis. Giardiasis is empirically treated with metronidazole. Other parasitic infections such as threadworm may require mebendazole or piperazine therapy.

Wherever possible any drugs associated with ME should be stopped (NSAIDs, aspirin or angiotensin II inhibitors) (agreement: 93%).

Currently a small group of medications, specifically NSAIDs, are known to cause ME however this will expand as clinical experience and understanding of the condition grows. Olmesartan has been described associated with severe enteropathy. But mild enteropathy might also be associated with this drug and so far, this association has not been excluded. A

thorough clinical assessment of drugs and their indication is essential when looking for the etiology of enteropathy with different severity and contributory medications should be stopped where possible. In cases of ME where offending medication like NSAIDs or angiotensin II inhibitors cannot initially be ceased regular review is recommended to assess the ongoing need for the medication and to detect micronutrient deficiencies amenable to treatment.

Appropriate diet associated to medical therapy is required for eosinophilic enteritis (agreement: 93%).

Eosinophilic enteritis, characterized by unexplained intestinal mucosal eosinophilia, is often associated with atopy and food allergies. Elimination of allergenic foods or initiation of an amino-acid based elemental diet may provide symptomatic benefit however some patients may need concomitant treatment with anti-inflammatory medications (e.g., oral corticosteroids). Other causes of ME including systemic inflammatory conditions and autoimmune disease should be managed with targeted medical therapy guided by the appropriate specialist.

It is important to review progress and a repeat upper GI endoscopy should be considered to confirm response to therapy (agreement: 87%).

Following initiation of etiology-targeted treatment it is important to assess clinical and/or histological improvement particularly in patients with multiple potential etiologies, where a stepwise approach to treatment with regular review to determine response is recommended. If there is no improvement despite treatment the perceived etiology should be reevaluated. The duration of an ineffective treatment should be minimized since dietary modifications may be socially inhibiting and expensive and medical therapies may cause unpleasant side effects.

Patients should be considered for repeat assessments including an endoscopy and duodenal biopsies if symptoms persist (agreement: 87%).

In patients who fail to clinically improve despite treatment directed at the presumed etiology, reassessments including endoscopy and gastroduodenal biopsies are indicated to evaluate for concomitant etiology and to re-evaluate mucosal integrity. There is no known treatment for idiopathic ME. Regular assessments are keys to detecting initially undetected etiologies and correcting micronutrient deficiencies, particularly in patients with persistent or worsening symptoms. The increased IEL in so called idiopathic cases may normalize in the majority of cases at six weeks, although it is unclear whether this improvement correlates with symptom resolution. This suggests idiopathic ME may be self-limiting in a proportion of cases. Further work is needed to better define the natural history and long-term clinical significance of ME, particularly whether it represents a precursor for more sinister pathology such as lymphoma which has a wellrecognised association with CD. Whilst this remains unclear the authors advocate that all patients with ME including those who improve with treatment are monitored and considered for repeat upper GI endoscopy if clinically indicated.

#### Summary and recommendations

The number of pathology reports identifying ME has increased markedly in recent years alongside advances in immunohistochemical techniques and an increasing caseload of patients undergoing endoscopic investigation. This has created uncertainty amongst some clinicians faced with interpreting a finding of ME in the clinical setting. This expert consensus opinion provides evidence-based recommendations to aid clinical practice, particularly regarding the diagnosis, investigation and management of ME.

Concluding, microscopic enteritis is a relatively new histopathological entity affecting the small bowel and featuring microscopic and submicroscopic lesions (which are similar to Marsh stage 0-II stages of celiac disease). Micronutrient deficiencies and clinical symptoms are a consequence of the submicroscopical changes. The etiology of microscopic enteritis

may include intolerance to gluten, gastrointestinal infections, allergy, drug therapy, systemic inflammatory disease (i.e., IBD) and autoimmune diseases. The severity of clinical signs and symptoms in CD is not correlated to the degree of mucosal damage or length of bowel lesions. Also, it seems there is no correlation between the degree of mucosal lesions and the severity of malabsorption. A diagnosis of microscopic enteritis is indicated when Marsh I or II mucosal lesions are diagnosed by the pathologist. If the patient presents with gastrointestinal symptoms or signs of malabsorption, then a Marsh 0 lesion should be subjected to further detailed investigations, such as: clinical, serological, genetic, histopathological and imagistic explorations, in order to establish the etiology. Microscopic enteritis should be investigated with a deep history and clinical examination, serological screening and upper gastrointestinal endoscopy with stomach biopsies, *Helicobacter pylori* testing and more than 4 duodenal biopsies from D2 and 2 biopsies from D1, especially from patients at high risk. In some cases, complete colonoscopy with biopsies taken from ascending and descending segments might be useful. Treatment should be according to the etiology. Follow-up and regular monitoring reassessment is essential, especially in those cases in which the symptoms persist and the natural history of microscopic enteritis remains obscure. Evaluation of the clinical significance, etiology-specific pathogenesis, natural history, specific biomarkers and long-term sequelae of microscopic enteritis needs further studies correlated to the main histopathological or immunological mucosal changes of each etiology.

The most specific and strongest biomarker for CD with microenteropathy is serology acting as the gold standard in this group. Villus height and crypt depth would serve as complementary tools in diagnosis of mild CD and NCGS patients. NCGS seem to have a milder morphological change compared to CD even when they present with similar Marsh scores. This study also confirms the cut off of IEL for CD with microenteropathy is similar to CD with severe enteropathy at 25 IEL/100 enterocytes.

### **2.3.2. Aim**

The purpose of this study was to evaluate the clinical characteristics of the patients with celiac disease in correlation with the degree of duodenal mucosa changes.

### **2.3.3. Material and methods**

#### **Study design and inclusion criteria**

The study included 111 patients with malabsorption and typical gastrointestinal symptoms (failure to thrive, chronic diarrhea, abdominal pain, bloating and constipation) or extraintestinal symptoms (anemia caused by iron deficiency, abnormal transaminase level and short stature), diagnosed between 2005 and 2009. To be considered chronic, diarrhea should have persisted for more than two weeks. Iron deficiency anemia and failure to thrive was defined according to CDC criteria and Global Database on Child Growth and Malnutrition [de Onis and Blossner, 2003]. The following clinical parameters were assessed using a questionnaire: age and gender, duration of symptoms, clinical findings, growth parameters (height and weight Z scores) laboratory and intestinal biopsy findings; all these data were recorded in a special database format. Before admission, the majority of the patients were treated by their general physicians with different combinations of anti-parasitic drugs for the treatment of chronic diarrhea or/and failure to thrive. All of children had previously ingested gluten for at least a three-month period.

#### **Exclusion criteria**

The patients with inconstant follow up, bloody diarrhea, incomplete data, or genetic/chromosomal disorder were excluded from study.

#### Investigation

All patients were investigated as follows: blood tests, coeliac serology and gastroscopy with duodenal biopsy for pathological examination. All serum samples were collected at the time of diagnosis when the patients were receiving a normal diet without any restrictions. Routine hematology, biochemical and serology tests [endomysial antibody (EMA)] were performed. In order to exclude selective IgA deficiency, total IgA level by immunodiffusion method was determined in all 111 patients who underwent upper gastrointestinal endoscopy. IgA deficiency was ruled out in all patients.

#### Ethical approval and consent

The study was approved by Ethical and Research Center for Children and Adolescents Health. Informed consent from the parents of all minor subjects who agreed to participate in this study was obtained before any investigation (collecting samples and endoscopy).

#### Intestinal biopsy and pathology

Upper gastrointestinal endoscopy using a pediatric optic fiber endoscope was performed in 111 symptomatic children with negative tests for parasitic illnesses, in order to obtain four biopsies from different parts of duodenum. All tissue samples were examined by expert pathologists who were not aware of clinical findings and evaluated according to Marsh classification (Table 8). Serology was performed after Endoscopy

Table 8: Histological classification for coeliac disease

Classification	Histology	IEL/100 enterocytes	Crypts	Villi	Endoscopy
<b>Normal mucosa</b>	Marsh 0 Normal	<25/100 EC	Normal	N	Normal
<b>Microscopic enteritis</b>	Marsh 0 SME (Microenteropathy)	<25/100 EC	Normal	N	Normal
	Marsh I Lymphocytic enteritis	>25/100 EC	Normal	N	Normal
	Marsh II Hyperplastic stage	>25/100 EC	Hyperplastic	N	Normal
<b>Macroscopic enteritis</b>	Marsh IIIa	>25/100 EC	Hyperplastic	PVA	Abnormal
	Marsh IIIb	>25/100 EC	Hyperplastic	STVA	Abnormal
	Marsh IIIc	>25/100 EC	Hyperplastic	TVA	Abnormal
	Marsh IV	<25/100 EC	NCD, HP	TVA	Abnormal

SME= sub-microscopic enteritis, N= normal, EC= enterocytes, PVA= Partial villous atrophy, STVA= Subtotal Villous atrophy, TVA= Total villous atrophy, NCD, HP= Normal crypt depth, but hypoplasia

**Diagnosis and treatment:** The diagnosis was made based on clinical symptoms, serology including total serum IgA, IgA EMA and duodenal biopsy. All patients were given a dietary chart form including written information about foods to be avoided (wheat, barley, rye, oat) and received iron and multivitamin as a supplementation. The importance of compliance with a GFD was repeatedly explained to the parents and the child. Gluten-free diet was recommended for all children with Macroscopic enteritis (Marsh IIIa-c) and those with Microscopic enteritis (Marsh I-II) with positive serology (Figure 11). All serum samples were collected at the time of diagnosis when the patients were receiving a normal diet without any restrictions. Routine hematology, biochemical and serology tests endomysial antibody (EMA) were performed. In order to exclude selective IgA deficiency, total IgA level by immunodiffusion method was determined in all 111 patients who underwent UGIE.

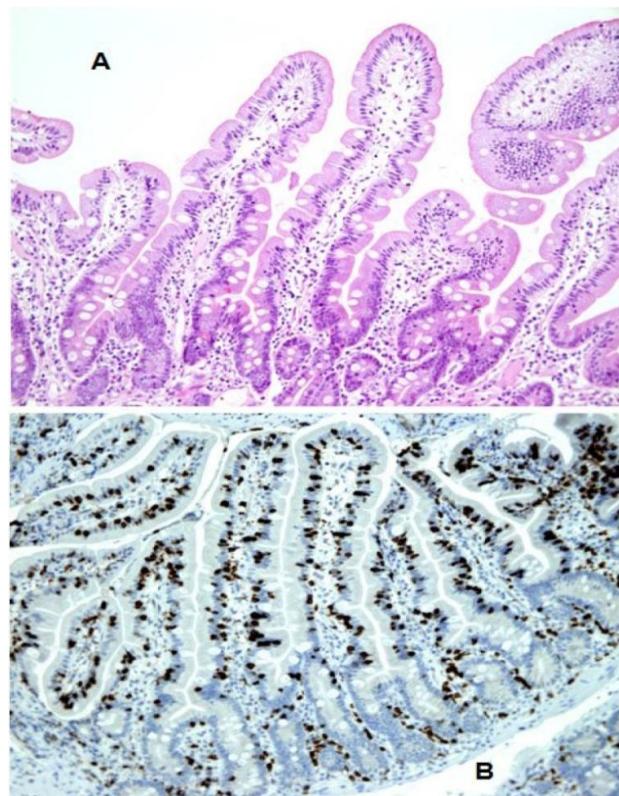


Figure 11. Microscopic Enteritis (Marsh I and Marsh II); Normal villi with pathological increase of T Lymphocytes (A) with crypt hyperplasia (B); A H&E x 10 B CD3 x10. This form of mucosal abnormality is overlooked by many pathologists.

**Statistical analysis**

We calculated frequencies and percentages for qualitative variables and means, medians and standards deviations for quantitative variables. The links between qualitative variables were assessed using Chi square test. P value <0.05 were considered significant. Data are expressed as mean ± SD.

**2.3.4. Results**

**Data analysis**

From 111 symptomatic children with negative tests for parasites, 84 patients fulfilled the diagnostic criteria for celiac disease, meaning all symptomatic patients with enteropathy (stage Marsh I-IIIc) and positive serology. All patients with macroscopic enteritis (Marsh IIIa) and negative serology were considered as CD, while children with microscopic enteritis (Marsh 0-II) and negative serology were not diagnosed as having celiac disease. Those patients with milder enteropathy (27/111) and negative serology could have been non-celiac gluten sensitivity. Summary of data analysis is shown in Table 9 and Fig. 12.

Table 9: Histology and serology in 111 patients with enteropathy according to Modified Marsh classification

Histology	Marsh 0	Marsh I	Marsh II	Marsh IIIa	Marsh IIIb	Marsh IIIc	Total
	N = 13(11.7%)	n = 11 (9.9%)	n = 27 (24.3%)	n = 44 (39.6%)	n = 10 (9%)	n = 6 (5.4%)	
EMA +ve	10/13(76.9%)	2/11 (18%)	12/27 (44.4%)	36/44 (81.8%)	10/10 (100%)	6/6 (100%)	76/111 (68.5%)
EMA -ve	3/13(23)	9/11 (82%)	15/27(55.5%)	8/44(18%)	0	0	35/111 (31.5%)
	Mic.E*	Mic.E	Mic.E	Mac.E**	Mac.E	Mac.E	

\*Microscopic Enteritis

\*\*Macroscopic Enteritis

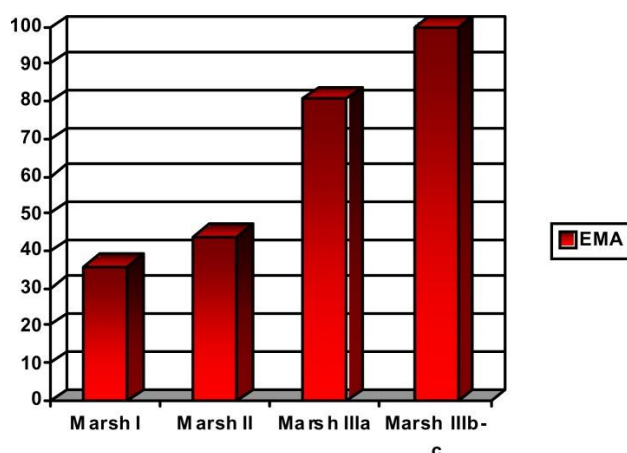


Figure 12: Sensitivity of serology (%) in patients with different degrees of mucosal abnormalities

General characteristics

The mean ± SD age of children with CD was 4.9 ± 3.5 years (range, 6 month - 16 years) and the mean duration of symptoms was 8 ± 20.5 months. Regarding the gender, 50/111 cases (45%) were girls and 61/111 cases (55%) were boys. The most common clinical signs were failure to thrive in 80/111(72%) cases, chronic diarrhea in 73/111(65.8%) and iron deficiency anemia in 66/111(59.5%) cases followed by abdominal pain in 62/111(55.9%), fatty stool and abdominal distension in 54/111(48.6%) (Table 10). An association with a family history of diabetes, hypothyroidism and CD was found in 4, 7 and 13 cases, respectively. Among subjects with coeliac disease, 2 cases of hypothyroidism, 1 case of cirrhosis and diabetes were found. Chronic diarrhea, constipation failure to thrive, and short stature were significantly more prevalent in patients with Marsh I compared to those with Marsh III.

Laboratory and Histopathology findings

IgA EMA was positive in 68/98 of subjects. Histology revealed Marsh 0 in 13 cases (11.7%), Marsh I in 11 cases (9.9%), Marsh II in 27 cases (24.3%), Marsh IIIa in 44 cases (39.6 %), Marsh IIIb in 10 cases (9 %) and Marsh IIIc in 6 cases (5.4 %) of patients, respectively. Positive EMA were found in 10/13(76.9%) of patients with Marsh 0, 2/11 (18%) of patients with Marsh I, 12/27 (44.4%) in Marsh II and 36/44 (81.8%) with Marsh IIIa. Sensitivity of EMA was 100% in patients with Marsh IIIb and Marsh IIIc (Table 9). Chronic diarrhea, constipation failure to thrive, and short stature were significantly more prevalent in patients with Marsh I compared to those with Marsh III (Table 10).

Table 10: Comparing clinical findings between Marsh I-II and Marsh IIIa-c in 111 patients with malabsorption syndrome and abnormal histology

Variable	Marsh 0 N = 13/111	Marsh I N = 11/111	Marsh II N = 27/111	Marsh IIIa-c N = 60/111	p-value
Chronic diarrhea	3 (23%)	9(82%)	18(66.6%)	43 (71.7%)	0.005
Failure to thrive	7(53.8%)	9(81.8%)	20(74%)	44(73.3%)	0.43
Short stature	7(53.8%)	7(63.6%)	15 (70.3%)	33(55%)	0.96
Abdominal pain	5(38.5%)	4(36.4%)	17(63%)	36(60%)	0.24
Abdominal distension	4(30.8%)	5(45.5%)	15(55.5%)	30(50%)	0.52
Fatty stool	1(7.7%)	4(36.4%)	10(37%)	39(65%)	0.001
Decreased appetite	4(30.8%)	4(36.4%)	10(37%)	30(50%)	0.56
Constipation	3(23%)	4(36.4%)	6(22.2%)	3 (5%)	0.01
Vomiting	2(15.4%)	4(36.4%)	5(22.7%)	21(35%)	0.27
Rickets	0	0	3(11.1%)	11(18.3%)	0.16
Tibial edema	0	0	1(3.7%)	6(10%)	0.54
Anemia	3(23%)	4(36.4%)	13(48.1%)	46(76.7%)	0.001
EMA	10(79.9%)	2(18.2%)	12(44.4%)	52(86.7%)	0.001

### 2.3.5. Discussions

The present study demonstrates that microscopic enteritis is the most common histological presentation of CD. A high percentage of patients with Marsh I had diarrhea and other clinical symptoms of overt malabsorption but without evidence of mucosal atrophy. This may suggest that histology doesn't reflect the severity of disease and the degree of damages in intestinal mucosa might not be a reliable prognostic factor. This study also highlights that sensitivity of EMA may be increased by grade of histopathology. Despite the limitation of sensitivity of serology, EMA was positive in a significant number of patients with ME. This may suggest that serology is a far more reliable marker for CD compared to histology with milder enteropathy. Conflicting reports exist on the distribution of lesions in CD along the small bowel mucosa and the relationship between symptoms and the length of lesions. However, despite the previously belief, symptomatology in CD does not seem to be related to the degree or length of affected bowel [Koskinen et al., 2008]. Same study has attempted to correlate the degree of villous atrophy with the mode of clinical presentation and suggests patients with mild enteropathy of any kind with positive antibodies may experience clear gluten-induced symptoms, and the severity of CD doesn't reflect in the depth or the length of mucosal abnormalities. The lack of relationship between pathology and symptoms was impressively supported by our data. We show that the percentage of patients with diarrhea, constipation and failure to thrive was even higher in Marsh I patients compared to Marsh III. Anemia and positivity for autoantibodies were the only parameters that significantly correlated with the macroscopic lesions (Marsh III) in this study. Although we are not quite sure why sensitivity of serology is co-relating so closely with the degrees of mucosal abnormalities (Fig. 12) small bowel inflammation is not reported only as severe (Marsh III) in anemic patients in other studies [Zamani et al., 2008]. Interestingly 10/13 symptomatic patients with Marsh 0 had positive EMA. It is very unlikely that these symptomatic cases with malabsorption who were extensively investigated for other conditions to be false positive. As the depth, length or degrees of the mucosal abnormality do not seem to correlate with the severity of symptoms, should there be a different explanation for malabsorption syndrome in all cases with normal, mild and severe enteropathy? Accumulated evidence suggests that the gluten-sensitized lymphocytes in the mucosa have the crucial role in the pathogenesis and they give real aspect of what CD means, irrespective of mucosal damages. In other words, it seems that the sensitized mucosal lymphocytes even when within normal range or something that correlates closely with that state of sensitivity are the key factors not only in pathogenesis but also in the genesis of the symptoms. This hypothesis was proved with the range of severe symptoms of our patients presenting with ME. Low specificity would be other explanation but not for EMA as this auto-antibody are extremely specific for CD. Even in absence of mucosal abnormalities subtle systemic and local inflammatory factors are implicated in the genesis of anemia and suggest that pro-inflammatory cytokine TNF $\alpha$  inhibits at the level of the enterocytes affects the uptake of the micronutrients like iron [Harper et al., 2007] or phosphate [Chen et al., 2009] in patients with microenteropathy. It seems that malabsorption in CD is secondary to inflammation and cytokines stimulation. This theory would perhaps explain why our Marsh 0-II patients with non-celiac gluten sensitivity may behave like full blown CD. Focusing on symptomatology in choosing the candidate for therapy seems to be a better strategy than concentrating on the degrees of the mucosal abnormalities. The lack of significant severity of disease in patients with Marsh III compared to Marsh I in our study would be in favor of such a strategy. Similar to other studies [Murray et al., 2008] children in both groups presented with classical picture of coeliac disease and the extent of visible enteropathy did not explain differences in clinical presentation. Our patients had typical symptoms like growth impairment with positive or negative antibodies and anemia. We clearly experienced that the degrees of intestinal

mucosal abnormalities alone are not reliable predictors of disease behavior. The quality of life of the symptomatic cases with Marsh I and II with CD or NCGS could be dramatically improved by introducing a gluten-free diet. The overall aim should be treating the symptoms whether full blown CD or NCGS rather than treating the medical terms like villous atrophy. The question for the future agenda would be how far symptomatic, NCGS with Marsh 0-II would benefit from a gluten free diet after exclusion of other causes for their microenteropathy. Although the size of our study was small but nonetheless our results are adding solid evidence to the existing literature to emphasize the superiority of serology compared to milder histology like ME in diagnosing CD. The other limitation of our study was the lack of possibility of follow up of our patients and implementing a GFD in NCGS as the study was performed before description of this new entity. But again, this would not prevent us to suggest that treatment of gluten sensitive cases should not be based on villous atrophy as histology does not always reflect the severity of CD. The lack of awareness between clinicians is one of the main reasons for delaying the diagnosis and treatment of NCGS and CD cases with microenteropathy.

In the past decade, many pathologists have called the early stages of celiac disease (Marsh 0, I and II) as lesions “non-specific”. Still, it would be wise to consider that no tissue could be “non-specifically” damaged, since it must reflect the patho-physiological state of its place of origin within the patient’s body. Within context, however, infiltrated villi indicate gluten sensitivity, especially when appears in a family with a genetic background, and associated with ingestion of gluten-containing products. Therefore, the early lesions can be grouped under the umbrella of microscopic enteritis.

When the celiac disease initially presents with extra-intestinal manifestations (gluten-induced and/or gluten-dependent), these manifestations can be diagnosed before the duodenal mucosa is damaged or when it shows only minor or non-specific changes. In susceptible persons, after they ingest gluten, CD develops gradually from normal mucosal morphology through mucosal inflammation, crypt hyperplasia, and villous atrophy to the “flat” mucosal lesions [Popp and Mäki, 2019]. For instance, when the mucosa is morphologically preserved but fractures appear caused by gluten ingestion, it is not recommended to include it in potential celiac disease. Moreover, the clinician should not wait for the manifest mucosal lesion to develop instead of receiving early adapted treatment. The benefit of treating these patients may be due to correction of micronutrient deficiencies having an impact on extra-intestinal manifestations [Rostami et al., 2015] and the term celiac trait be used in these cases [Popp and Mäki, 2019].

Another recent study confirmed our results and proved that non-celiac gluten sensitivity may have a cohort of autoimmune signs that can precede the diagnosis and may have a predictive value [Losurdo et al., 2018]. Since, so far there is no biological marker for NCGS and autoimmunity investigations could support the diagnosis in some cases, this concept might be useful. Considering that the most common causes of microscopic enteritis are irritable bowel syndrome, drugs and bacterial/viral infections (including *H. pylori*), the presence of such autoimmune stigmata is anything but representative of these conditions, helping the differential diagnosis. The above-mentioned study suggests that ANA and AGA positivity, headache and autoimmune thyroiditis, are positively associated with a diagnosis of NCGS in a setting of patients with microscopic enteritis. Still, it is impossible to conclude that they are real predictors of NCGS development. Therefore, it would be appropriate to suspect NCGS and propose a diagnostic protocol according to Salerno criteria in patients with microscopic enteritis showing the above reported stigmata of autoimmunity [Losurdo et al., 2018]. Moreover, a recent study demonstrated that a gluten-free diet may bring clinical benefits to women with autoimmune thyroid disease by reducing anti-thyroid antibody titers [Krysiak et al., 2019].

### **Final remarks**

In conclusion, atrophy of the villi is not the only change presented in patients with CD and NCGS, and this might be reflected in the quality of life of patients with symptoms and mild enteropathy. Therefore, it is necessary for the pathologists to rethink the minor lesions as precocious forms, and the cut-off point of 25 IEL/100 enterocytes in correlation with the number and quality of the biopsy samples. Also, the pathological aspect of the tissue under the microscope represents a single moment in the history of the disease. It is very likely that ME starts with T cell inflammation in the lamina propria, advancing upwards to affect the villi epithelium. This is the natural history of premacroscopic lesions implicated in malabsorption related symptoms with no management place in the current guidelines. A larger scale study would be required to assess further the pathological modalities, the clinical characteristics/implications and long-term complications.

## **Chapter 3: HPV-related squamous cell carcinomas of the head and neck assessment by HPV genotyping and immunohistochemistry**

### **3.1. State of art**

Mortality from cancers of oral cavity, lip, naso-pharynx and larynx affecting males ranks Romania on the second place in European Union, according to Globocan 2012, with 32.4 cases per 100,000 people [Ferlay et al., 2015]. Infection with human papilloma virus (HPV) is now considered a trigger factor for squamous cell carcinomas of the head and neck region (HNSCC), with an important prognostic and predictive role. There is no concluding data on the prevalence of HPV DNA in these carcinomas; still, the most consistent identified HPV DNA in 35-50% of oropharynx compared to 5-15% for the rest of the oral cavity [Bosch et al., 2012]. After molecular techniques were introduced to test for HPV infection in cervix cancer, scientists focused on HNSCC and HPV in order to study its sensitivity, specificity, clinical impact and therapeutic management. Although in cervical carcinomas HPV is strongly linked to carcinogenesis, its clinical relevance is limited, while in head and neck carcinomas HPV detection is important for the prognosis, even in advanced tumors [Venuti and Paolini, 2012]. Identification of high-risk HPV DNA, viral E6 oncogene and wildtype p53 gene in HNSCC tumor tissues and lymph nodes carcinoma metastasis proves the carcinogenetic role of HPV [van Houten et al., 2001]. In a single center study between 2010 and 2014, 226 cases of head and neck keratinizing and non-keratinizing SCC were diagnosed, classified as follows: 119 oral cavity – lips and tongue (age range 39-80 years), 1.68% (12/119) women; 56 larynx (age range 47-58 years), 3.57% (2/56) women; 15 hypopharynx (age range 54-67 years), 26.66% (4/15) women; 36 oropharynx (age range 41-71 years), 5.55% (2/36) women [Ursu et al., 2015].

Carcinomas developed at the junction between oro-pharynx and the retromolar trigone present special features regarding the clinical symptomatology and local invasion with consequences on the surgical treatment and prognosis. Usually, these carcinomas are asymptomatic in early stages, therefore are diagnosed in locally advanced stages and need complex surgical procedures in order to obtain a good surgical access, oncological safety and proper closure of the jaw joint. On the other hand, increased survival depends not only on surgical skills and techniques, but also on the molecular profiling of the tumors for a better individualized oncological management of the case. HPV-induced carcinomas are diagnosed more often in recent decades, especially in young patients. Research progresses in carcinogenesis not only help the diagnosis accuracy, treatment management and prognosis, but also offer new resources for prophylaxis by the development of new vaccines. The molecular profiling of these carcinomas, for instance, regarding the p53 and p16 markers, can also explain the evolution, treatment response and suggest the prognosis. p16, a cyclin-dependent kinase inhibitor molecule, blocks the cell cycle progression, arresting the cells in G0/G1 phase by inhibiting the retinoblastoma protein (pRb) phosphorylation [Chung et al., 2014]. Also, Rb can be inactivated by E7, which is an HPV viral oncogene product. As a result, in HPV-related cancers, p16 should be upregulated, thus overexpressed on immunohistochemistry test [Roman and Munger, 2013]. Therefore, immunohistochemical testing of p16 in HNSCC can be a useful and also cheaper tool to identify the HPV-related cancers, compared to molecular biology tests [Lewis et al., 2018; Ursu et al., 2018]. The transcription factor p53, regulates the DNA damage and repair them. It induces apoptosis if the DNA damage is too important and its repair mechanisms fail. Normally, p53 is implicated in cell cycle checkpoints, except when it is mutated or inactivated by various pathways and factors. For instance, in HPV infection, E6 inhibits the wild-type p53 and the tumor cells proliferate by deregulating cycle checkpoints [Psyrrri and DiMaio, 2008]. Being activated by

radiations, the levels of p53 increase, explaining why HPV-related HNSCC responds better to radiotherapy [Liu et al., 2018].

**This research direction has been realized by publishing the following articles:**

Ursu RG, **Danciu M**, Spiridon IA, et al: Role of mucosal high-risk human papillomavirus types in head and neck cancers in Romania. PLoS ONE 2018; 13(6): e0199663. <https://doi.org/10.1371/journal.pone.0199663>

<https://journals.plos.org/plosone/article?id=10.1371/journal.pone.0199663>

Cobzeanu MB, Costan VV, **Danciu M**, et al: Environmental factors involved in genesis of retromolar - oropharynx junction cancer. Environmental Engineering & Management Journal (EEMJ) 2017; 16(5). <http://eemj.eu/index.php/EEMJ/article/view/3264>

Cobzeanu BM, Popescu E, **Danciu M**, et al. Correlations between HPV, p53 and p16 in malignancies involving the retromolar trigone-oropharynx junction. Rom J Morphol Embryol 2019; 60(3):853-859.

### **3.2. HPV detection and characterization in head and neck squamous cell carcinomas from North-Eastern Romania area**

#### **3.2.1. Introduction**

According to GLOBOCAN 2012, HNSCC is considered the sixth most common cancer in the world, with more than 630,000 cases and 350,000 deaths each year and situates Romania on the second place in Europe in mortality from HNSCC [Ferlay et al., 2015]. Its incidence is significantly increased between 1980 and 2000. Among the numerous and variate etiologies (tobacco or some other chemical ab(use), alcoholism, poor oral hygiene, genetic features, viral infection was recently recognized as an important one, especially some high-risk human papilloma virus subtypes [Marur et al., 2010; Gillison et al., 2015]. Subtype 16 of HPV is the most common having a high-risk for malignancy, affecting more than 80% of all head and neck carcinomas [Bratman et al., 2016]. Due to the decline of tobacco use in the past 2 decades, the HNSCC incidence decreased in developed countries. Still, the proportion of HPV-related oro-pharyngeal carcinomas among total HNSCC increased in USA, Sweden, Australia and New Zealand, and this might be explained by an increase of HPV infection rate. Also, oral and laryngeal carcinomas were associated with HPV infection, but to a lower rate. For instance, a study from India revealed a 2% proportion of HPV-related carcinomas [Gheit et al., 2017]. There is a high variability in data reported on HPV DNA prevalence in HNSCC when referring to country and tumor localization. For instance, the prevalence is high in USA (71%), Denmark (62%), Czech Republic (57%), low to intermediate in Brazil (15%) or Germany (35%), and declared to be absent in China or Mozambique. In these studies, HPV was detected using the DNA detection tools, although other studies advocate for increasing the accuracy by using of complementary methods such as: viral RNA and p16INK4a (p16) expression as a surrogate for HPV-induced transformation in order to better classify these carcinomas [Chernock et al., 2013]. The HPV-attributable fraction after being positive for HPV DNA and for either HPV E6\*I mRNA or p16, was 20-25.7%, 4.4%, and 3.5% for cancers of the oropharynx, oral cavity, and larynx, respectively [Castellsague et al., 2016; Adilbay et al., 2018; Baboci et al., 2016]. In central India, HPV DNA/RNA double positivity was found in only 9.4% of oropharyngeal cancer cases [Gheit et al., 2017], while in Philippines was tested double negative. An international multicenter study [Castellsague et al., 2016] which included 3680 HNSCCs from Europe,

Africa, Asia, North and South America, found that 22.4% of the oropharyngeal cancers were positive for HPV DNA and for either HPV RNA or p16, while 18.5% were positive for all these markers. Regarding the HPV-associated oropharyngeal carcinomas, the highest incidence is in South America (53.6%), Northern, Central and Eastern Europe (50%), Asia (22.4%), Central America and Western Europe (19.4-19.7%), and Southern Europe (9.4%).

### 3.2.2. Aims

My research regarding the HPV-positive HNSCC followed two directions. The first one aimed to determine the HPV-attributable fraction in HNSCC by analyzing HPV DNA and HPV RNA status, as well as by determining the p16 expression level, within a large retrospective cohort of HNSCC cases from Northeastern Romania. The second study aimed to assess the p16 and p53 immunohistochemical expression in carcinomas located in the retromolar trigone and oropharynx and to establish a correlation with treatment and prognosis, that could better orientate the individual therapeutic management.

### 3.2.3. Material and methods

#### Study 1

##### *Patients and samples*

The study included 203 patients diagnosed with HNSCC in the Departments of Oral and Maxillofacial Surgery, Otorhinolaryngology, and Plastic Surgery at the Grigore T. Popa University of Medicine and Pharmacy (Iași, Romania), between January 2010 and September 2014. All specimens were fixed for 18-24 hours in 10% neutral formalin, at room temperature. The formalin-fixed, paraffin-embedded tissue blocks included squamous cell carcinoma of the oropharynx (International Classification of Diseases for Oncology [ICD-O] C01 - base of tongue, C02.4 - lingual tonsil, C09 - tonsil, C10 - oropharynx), pharynx (ICD-O C14 - other and ill-defined sites in the lip, oral cavity and pharynx, C14.8 - overlapping lesion of lip, oral cavity and pharynx), oral cavity (ICD-O: C00.0-C00.9, C01, C02.0-C02.9, C03.0-C03.9, C04.0-C04.9, C05.1-C05.9, C06.0-C06.9, C09.1-C09.9, C10), and hypopharynx and larynx (ICD-O: C13, C32). The FFPE tissue samples were retrieved from the hospital archives and comprised 34 HNSCC cases from the oropharynx and 169 HNSCC cases outside the oropharynx (16 larynx/hypopharynx, 51 pharynx, and 102 oral cavity cancer samples). All patients were diagnosed with keratinizing or non-keratinizing squamous cell carcinomas. Histological analyses on hematoxylin and eosin stained slides were performed in order to confirm that all FFPE blocks contain cancer tissues. Clinical and epidemiological information was collected from the hospital databases using a form and questionnaire developed in the context of a European and Indian case study (HPV-AHEAD; <http://hpv-ahead.iarc.fr>). Ethical clearance for the investigations reported in this study was obtained from the Institutional Ethical Committee of the Grigore T. Popa University of Medicine and Pharmacy, Iași, Romania (reference number 7150). The study implied the use of archival material only, and it did not envisage any contact with the patients. Adequate measures to ensure data protection, confidentiality, patients' privacy, and anonymization were taken into account. No informed consent was available, due to the retrospective design of the study and the large proportion of deceased and untraceable patients. All data were fully anonymized before access.

##### *Preparation of paraffin sections and DNA extraction*

FFPE tissue blocks were sectioned according to the HPV-AHEAD protocol, which includes the preparation of 31 sections from each FFPE tissue block. Sections 1, 10, and 31

(S1, S10, and S31) were used for histology, S2 and S9 were used for p16 immunohistochemistry, and S11-S30 were stored for future IHC analyses in independent studies. In addition, S3-S5 and S6-S8 were collected in two different vials and subsequently used for DNA and RNA analysis [Mena et al., 2017]. To minimize the risk of cross-contamination during sectioning, a new blade was used for each FFPE block and the microtome was extensively cleaned after each block with ethanol 70% and DNA Away (Dutscher, Brumath, France). In addition, to monitor possible cross-contamination during the sectioning, empty paraffin blocks were processed every 10<sup>th</sup> cancer specimen. DNA was extracted by an overnight incubation of the paraffin tissue sections in a digestion buffer (10 mM Tris/HCl pH 7.4, 0.5 mg/ml proteinase K, and 0.4% Tween 20). The percentage of tumor cells (0%, <10%, 10-50%, 50-90%, >90%) was estimated by two pathologists on H&E-stained slides (S1 and S10).

#### *HPV DNA genotyping*

HPV DNA positivity was determined by using a type-specific multiplex genotyping (TS-MPG) assay, which combines multiplex PCR and bead-based Luminex technology (Luminex Corporation, Austin, TX) as previously described. This assay detects 19 HR or probable high-risk (pHR) HPV types (HPV16, 18, 26, 31, 33, 35, 39, 45, 51, 52, 53, 56, 58, 59, 66, 68a and b, 70, 73, and 82) and two low-risk (LR) HPV types (HPV6 and 11), as well as cellular beta-globin gene, which is used to control for DNA quality. After PCR amplification, 10 $\mu$ l of each reaction mixture was analyzed by multiplex HPV genotyping (MPG) using Luminex technology (Luminex Corporation, Austin, TX) as described previously [Gheit et al., 2014]. All HPV DNA-positive FFPE specimens and a randomly selected subgroup of approximately 10% of HPV DNA-negative specimens were further analyzed for the presence of HPV E6\*I mRNA and for overexpression of the cell-cycle inhibitor p16, which is considered a surrogate marker for HPV infection. The 10% of HPV DNA-negative cases were selected randomly and blindly, while the study was still anonymized.

#### *HPV RNA analysis*

Total RNA was purified from three pooled sections of the same tissue block using the Pure Link FFPE Total RNA Isolation Kit (Invitrogen, Carlsbad, CA). RT-PCR was carried out using the QuantiTect Virus Kit (Qiagen, Hilden, Germany), in a total volume of 25 $\mu$ l containing 5 $\mu$ l of 5xQuantiTect Virus Mastermix, 0.25  $\mu$ l of 100xQuantiTect Virus RT Mix, 0.4 $\mu$ M of each oligonucleotide, and 1 $\mu$ l RNA. The HPV type-specific E6\*I mRNA assay developed for 20 HR- or pHR-HPV types was applied for the detection of viral transcripts. The assay amplifies a 65 $\pm$ 75 base pair amplicon of HPV and an 81 base pair amplicon of ubiquitin C (ubC) cDNA. Biotinylated amplification products are hybridized to ubC and HPV type-specific probes representing splice junction sequences on Luminex beads, followed by staining with streptavidin-phycoerythrin, and quantified in a Luminex analyzer. The use of a splice product sequence as detection probe makes this assay absolutely specific for RNA and avoids false positivity from residual viral DNA in the RNA preparation, which is a risk in RNA assays assessing unspliced RNA sequences. The analytical sensitivity of the respective assays per reaction is 10,000 copies for HPV70, 1,000 copies for HPV67, and 10-100 copies for the remaining 19 HPV types and for ubC. The HPV RNA assay has been widely applied and validated as a marker for HPV transformation in carcinoma of the anogenital region, such as the cervix, vulva, penis, lung, and scrotum, as well as carcinoma of the head and neck, and specifically oropharynx, unknown primary of the neck, larynx, and esophagus. All HPV DNA-positive specimens and the randomly selected 10% of HPV DNA-negative specimens were analyzed for the presence of (i) HPV16 E6\*I mRNA and (ii) ubC mRNA as a cellular mRNA positive control. Tissues positive for DNA of a non-HPV16 type were, in addition, analyzed for E6\*I mRNA of the respective type. Specimens that were HPV E6\*I and/or ubC mRNA-positive (RNA+) in RNA analysis were considered HPV RNA valid.

### *p16 immunohistochemistry*

Expression of p16 was evaluated manually by IHC in FFPE sections using the CINtec p16 Histology kit (Roche mtm laboratories AG, Mannheim, Germany) according to the instructions of the manufacturer. Briefly, slides were de-paraffinized in xylene and rehydrated in graded alcohol. The antigens were retrieved for 10 minutes using a pH 9.0 epitope retrieval solution (95-99°C), followed by a 20-minute cool-down period at room temperature. Different from the instructions of the manufacturer, specimens were then microwaved in preheated Vector H-3300 unmasking solution (Vector Laboratories, Burlingame, CA) for 15 minutes. This step was followed by incubation of the p16 primary mouse anti-human antibody (clone E6H4) for 60 minutes. The samples were subsequently incubated with the goat anti-mouse IgG secondary antibody/peroxidase conjugate reagent, followed by signal generation using DAB. Finally, slides were counterstained with hematoxylin, dehydrated, mounted with permanent mounting medium, and cover-slipped. Immunoreactivity was visualized by light microscopy. Expression of p16 was evaluated by IHC in all HPV DNA-positive FFPE specimens and in a randomly selected subgroup of approximately 10% of HPV DNA-negative specimens. A continuous, diffuse staining for p16 within the cancer area of the tissue sections was considered as positive, and a focal staining or no staining was considered negative. Positive p16 expression was defined as diffuse nuclear and cytoplasmic staining in 70% or more of the tumor cells. The validity of the p16 IHC staining result was assessed by evaluating the presence of p16 internal control staining. IHC slides were evaluated by three pathologists blinded to any other clinical information or HPV DNA or RNA status, as specified in the HPV-AHEAD protocol. Discrepant cases were re-checked by a pathologist, and the final classification of the staining was based on the majority consensus of the working group.

### **Study 2**

The study population consisted of 46 men and four women, aged between 39 and 78 years old, admitted in the Departments of Oral and Maxillo-Facial (OMF) Surgery and Ear, Nose and Throat (ENT – Otorhinolaryngology), in between 2011–2015. The written informed consent was obtained from all participants. The inclusion criteria were the presence of histological confirmed oropharyngeal cancer or cancer located at the junction between the retromolar trigone and the oropharynx. Patients not able to provide informed consent due to medical comorbidities, and other types of oral and pharyngeal cancers were excluded from the study.

The diagnosis and staging were established by a multidisciplinary team, including ENT, OMF surgery, pathology, radiology and oncology, on the basis of the clinical features, performed biopsy, presence of HPV and tumor markers, and the highlighting of the local spread assessed on computed tomography (CT) scanner. Each case was discussed in the Oncological Board and the treatment protocol was advised in accordance with the National Comprehensive Cancer Network (NCCN) Clinical Practice Guidelines in Oncology, Head and Neck Cancers. HPV detection, p16 and p53 evaluation were performed in all patients.

#### *HPV detection*

The samples were collected using the HPV Screening kit from AID Diagnostika GmbH (Germany), by collecting in special tubes samples of epithelial cells from the oral cavity. For genotyping, we used the IVD kit (Opegen by Operon, Spain), allowing the genotyping of 19 HPV strains of medium and high risk. We isolated the genomic DNA from the cytology product, which was then amplified by the multiplex polymerase chain reaction (PCR) technique, according to the Seeplex® HPV4A ACE Screening kit, or subsequently hybridized on strips from the High Papilloma Strip kit (Operon®), and the obtained product was migrated in agarose gel (2%). The HPV genotyping was performed by the qualitative (reverse blot) method and by the multiplex PCR qualitative method.

### *p53 and p16 immunostaining*

The biopsy tissues were routinely processed by fixation in 10% buffered formalin and then embedded in paraffin. Four  $\mu\text{m}$  thin sections from paraffin blocks were stained with Hematoxylin–Eosin for histopathological diagnosis. p53 and p16 were immunohistochemically quantified using primary antibodies: anti-p53 monoclonal antibody (clone DO-7, Novocastra, Leica Biosystems, Newcastle upon Tyne, UK, 1:800 dilution, 30 minutes, at 25°C) and anti-p16 monoclonal antibody (clone G175-405, BD Pharmingen, 1:25 dilution, 60 minutes, at 25°C). The IHC technique included the following steps: deparaffinization, hydrating, exposing the antigenic sites, neutralizing the endogenous peroxidase, incubation with the primary antibody, visualization with Novolink™ Polymer Detection System, 3,3'- Diaminobenzidine (DAB) and chromogen counterstaining with Mayer's Hematoxylin. Positive controls (p53- and p16-positive squamous cell carcinomas, previously diagnosed) and negative (tonsil) controls were used. Cases were independently evaluated by three pathologists. For p16, positivity was considered when both nuclear and cytoplasmic staining was present. This study was performed on the basis of obtained informed consent from each participant. It was approved by the Ethics Committee of Sf. Spiridon Hospital, Iași, Romania and of the Grigore T. Popa University of Medicine and Pharmacy, Iași.

### *Statistical analysis*

All data were analyzed with Statistical Package for the Social Sciences (SPSS) software version 24.0 for Windows (SPSS Inc., Chicago, IL, USA). Statistical tests specific to the type of categories were applied. The association of the variables was assessed on the basis of the Pearson's  $\chi^2$  (chi-square) or Yates chi-square test and the correlation between the studied aspects was based on the Spearman's rank R. The involvement of HPV, p53 and p16 tumor markers in retromolar trigone–oropharynx junction malignancies has been highlighted based on the results of multivariate analysis (logistic regression). The significance level for the final hypothesis decision was 0.05 (95% confidence interval).

## **3.2.4. Results**

### **Study 1**

Of the 203 HNSCC cases, 2 cases (1 oral cavity and 1 pharyngeal) were excluded due to insufficient DNA quality as evidenced by negative beta-globin results, and 11 cases were excluded due to invalid RNA and/or p16 data. One case was excluded as the tissue block did not contain cancer tissue. The final study therefore comprised 189 HNSCC patients, with a median age of 62.5 years (range, 35-89 years). The vast majority of the patients were male:  $n = 171$  (90.5%) (Table 11). Only FFPE blocks where the first and last H&E sections reflected tumor tissue were included in the study. More than 36% of the samples showed >50% of invasive carcinoma in the section, while 47.6% and 15.9% of the samples showed respectively 10-50%, and <10% of tumor cells. Table 12 shows the HPV DNA, RNA, and p16 detection in HNSCC cases. HPV DNA was detected in 23 of the 189 (12.2%) HNSCC cases. HPV16 was the most prevalent type, being present in 20 of the 23 HPV DNA-positive tumors (86.9%), followed by HPV18 (5/23, 21.7%) and HPV39 (1/23, 4.3%). The oropharynx cases showed higher HPV DNA prevalence (14/28, 50.0%), followed by cancers of the larynx (5/14, 35.7%) and of the oral cavity (4/99, 4.0%). Multiple HPV type infections were detected in 3 HNSCC cases; 2 cases were positive for both HPV16 and HPV18 (1 larynx case and oropharynx case), and 1 oral cancer was positive for both HPV18 and HPV39 (Tables 11 and 12). One larynx case was positive for a low-risk HPV type (HPV6). HPV RNA and p16 expression was examined in all HPV DNA-positive cases ( $n = 23$ ) and a randomly selected subset of HPV DNA-negative cases ( $n = 13$ ). The percentage of HPV-

related HNSCCs was 1.1% (2/189) for both HPV DNA and RNA positivity. The highest percentage of combined HPV DNA and RNA positivity was found in the oropharynx (1 of the 28 HPV DNA-positive cases, 3.6%). The corresponding tonsil case tested positive for HPV18. Only one non-oropharyngeal case (1/161, 0.6%) was positive for both HPV DNA and RNA. The corresponding posterior hypopharyngeal wall case tested positive for HPV16 (Table 12). The p16 IHC data were stratified per HR-HPV DNA and RNA status (Table 13). Only one HPV DNA-positive case (1/23; 4.3%) was p16-positive, and 7.7% (1/13) of HPV DNA- and RNA-negative cases were p16-positive, regardless of the anatomical sub-localization. In addition, none of the HNSCC cases that were HPV DNA- and RNA-positive tested positive by p16 IHC. Moreover, 2 of the 34 HPV RNA-negative cases (5.9%) were p16-positive (Table 13). Among the cases that tested positive for HPV DNA, the smoking status was available for only 10 patients, among whom 8 were current smokers and 2 were former smokers. Most importantly, the clinical information was available for the HPV-driven HNSCCs (n = 2). Both tumors (1 tonsil case and posterior hypopharyngeal wall case) were late-stage (III and IV) and were from current smokers: patients aged 54 years (female) and 55 years (male), respectively.

Table 11: Description of cases by HPV DNA status

CHARACTERISTIC	n total	HPV DNA- n (%)	HPV DNA+ n (%)
No. of cases	201	171 (85)	30 (15)
Median age, years (range)	62 (37-89)	63 (37 – 89)	56 (41 – 86)
<b>Gender</b>			
Female	15	11 (6)	4 (13)
Male	186	160 (94)	26 (87)
<b>Cancer site</b>			
hypopharynx	16	8 (5)	8 (27)
oropharynx	34	16 (9)	18 (60)
oral cavity	101	97 (57)	4 (13)
pharynx	50	50 (29)	0 (0)
<b>HPV RNA</b>			
positive		0 (0)	2 (7)
negative		10 (100)	28 (93)
<b>p16 Staining pattern</b>			
p16 high		0 (0)	3 (10)
p16 low		18 (100)	27 (90)

Table 12: HPV DNA, RNA and p16<sup>INK4a</sup> positivity in different subsites of HNSCC

Test positivity	Any HPV types DNA+	HPV16			Non-HPV16 HR types		
		DNA+	DNA + RNA	DNA + RNA + p16 <sup>INK4a</sup>	DNA+	DNA + RNA	DNA + RNA + p16 <sup>INK4a</sup>
	N(%)	N (%)	N (%)	N (%)	N (%)	N (%)	N (%)
HNSCC (n=201)	30 (15)	26 (13)	1 (0.5)	0 (0)	5 (2.5)	1 (0.5)	0 (0)
By sub-site							

Oropharynx (n=34)	18 (53)	16 (47)	0 (0)	0 (0)	3 (9)*	1 (3) <sup>†</sup>	0 (0)
Hypopharynx(n=16)	7 (44)	7(44)	1 (6) <sup>§</sup>	0 (0)	1 (6)**	0 (0)	0 (0)
Oral cavity (n=101)	4 (4)	3 (3)	0 (0)	0 (0)	1 (1)***	0 (0)	0 (0)
Pharynx(n=50)	0	0 (0)	0 (0)	0 (0)	0 (0)	0 (0)	0 (0)

<sup>§</sup>ICD-O code: C09; <sup>†</sup> positive for HPV 18 (ICD-O code: C13.2); \* positive for HPV18 (n=2) and one positive for HPV 16 and 18 (ICD-O code: two of C09, C10.9); \*\* positive for HPV 16 and 18 (ICD-O code: C10.1); \*\*\*positive for HPV 18 and 39 (ICD-O code: C02.1)

Table 13: HPV RNA, and p16<sup>INK4a</sup>positivity among HPV DNA positives cases (n = 24) (Table 3A) and among randomly-selected HPV DNA negative cases (n = 12) (Table 13B).

Table 13A

HPV DNA*	HPV RNA	p16 <sup>INK4a</sup>	HPV DNA + (N=24)	%	OPX	HPX	OC	PX
+	+	+	0	0	0	0	0	0
+	+	-	2	8.3	1 <sup>†</sup>	1 <sup>Φ</sup>	0	0
+	-	+	1	4.1	1 <sup>§</sup>	0	0	0
+	-	-	21	87.5	12	5	4	0

Table 13B

HPV DNA*	HPV RNA	p16 <sup>INK4a</sup>	HPV DNA - (N=12)	%	OPX	HPX	OC	PX
-	+	+	0	0.0	0	0	0	0
-	+	-	0	0.0	0	0	0	0
-	-	+	1	8.3	0	0	1	0
-	-	-	11	91.6	1	1	6	3

\*Any HPV DNA and HPV RNA; <sup>†</sup> positive for HPV 18; <sup>Φ</sup> positive for HPV 16; <sup>§</sup>positive for HPV16

### Study 2

Upon testing 50 patients (46 men and 4 women), 16 (32%) were detected with HPV infection (14 men and 2 women). In the positive patients, the subtypes were: HPV 16 (2 cases), HPV 18 (1 case), HPV 31 (1 case), HPV 33 (2 cases), HPV 51 (4 cases), HPV 66 (6 cases). Also, 32 (64%) carcinomas were p53 positive (28 men and 4 women) and 18 were negative. p16 immunostaining was positive in 43 (86%) cases (39 men and 4 women) and negative in 7 cases. All HPV-positive patients had p16-positive status, yet only 11 were p53 positive. Most squamous carcinomas (35, representing 70% of the study group) were moderately differentiated, 9 were well differentiated and 6 poorly differentiated (Figures 13–16). Nine of the investigated patients underwent surgical treatment without prior adjuvant therapy, 7 of them being HPV-positive. All 50 patients underwent radiotherapy; in 16 of them, radiotherapy was associated with chemotherapy. A good result was noticed in 28 cases, of which 15 were HPV-positive patients. From the whole cohort, 16 (32%) cases relapsed (1 HPV-positive) and 6 (12%) patients died (HPV-negative) during the study interval. Best results were obtained in patients undergoing surgical treatment followed by radiotherapy or radio-chemotherapy. Patients who underwent surgical treatment had a better survival rate compared to those who did not. Chemotherapy alone provided a lower survival rates compared to adjuvant associated chemo- and radiotherapy. Moderately differentiated carcinomas who received either radiotherapy or chemo-radiotherapy had a better evolution. Recurrences and deaths were recorded in patients who underwent radiotherapy, but no surgical resection and/or chemotherapy. Results following treatment were overall superior for the HPV-positive group, including postoperative outcomes. Most HPV-positive patients had good results following treatment and increased survival.

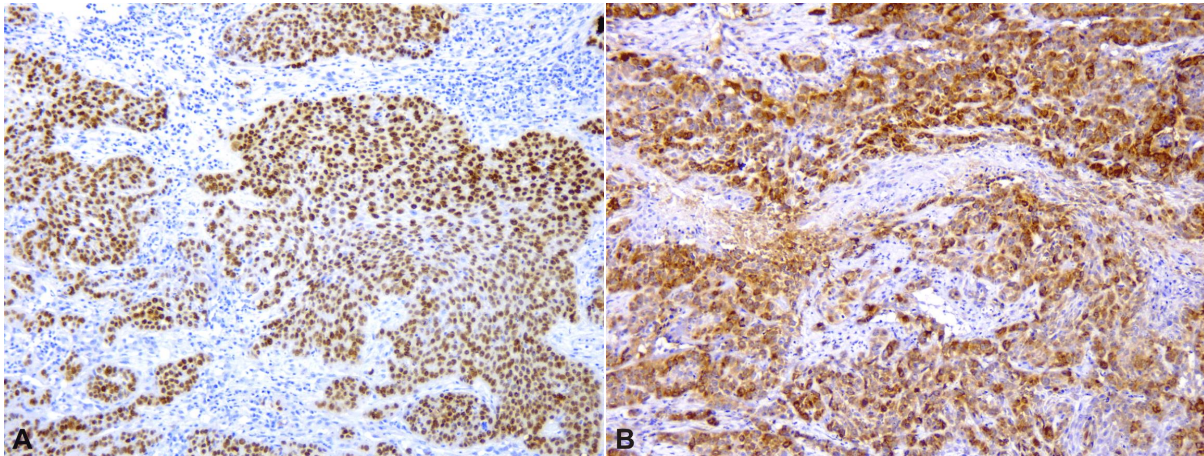


Figure 13: HPV-positive moderately differentiated, invasive oral squamous cell carcinoma: (A) p53 intense and diffuse positivity in tumor cells (Anti-p53 antibody immunomarking,  $\times 100$ ); (B) p16 intense and diffuse positivity in tumor cells (Anti-p16 antibody immunomarking,  $\times 100$ ). HPV: Human papilloma virus.

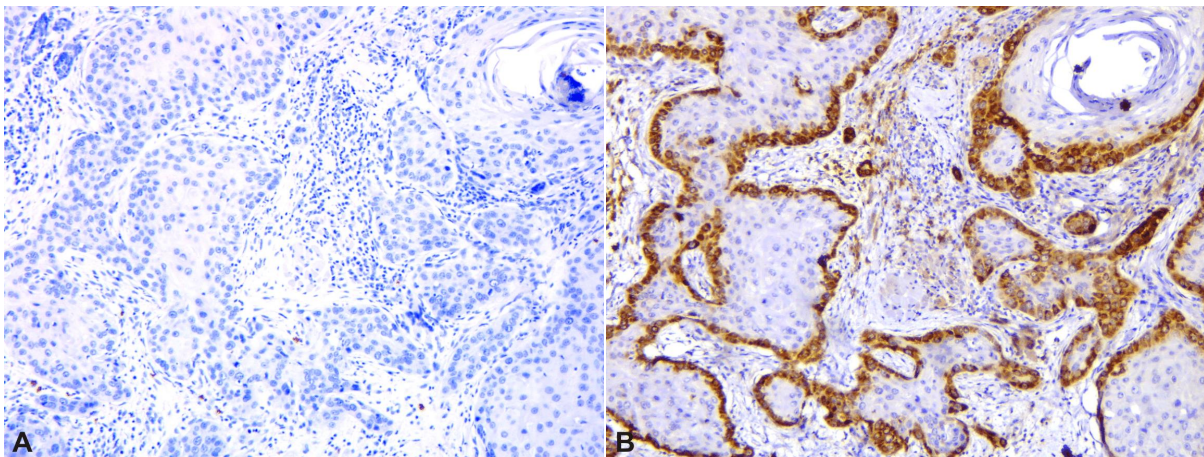


Figure 14: HPV-negative well-differentiated, invasive oral squamous cell carcinoma: (A) p53 negative in tumor cells (Anti-p53 antibody immunomarking,  $\times 100$ ); (B) p16 intense positivity in tumor cells (Anti-p16 antibody immunomarking,  $\times 100$ ). HPV: Human papilloma virus.

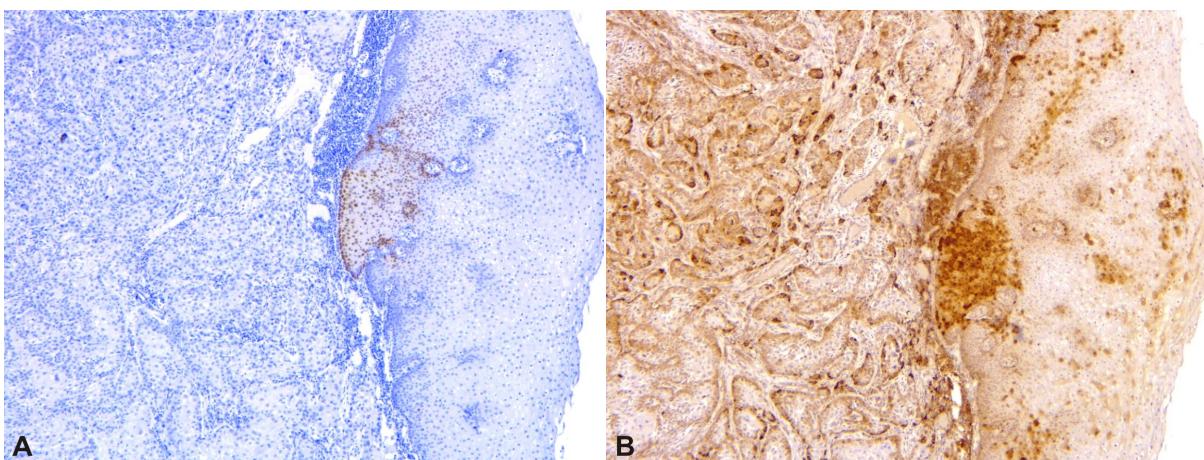


Figure 15: HPV-positive well-differentiated, invasive oral squamous cell carcinoma: (A) p53 negative in tumor cells, focal positivity in basal layer of surface epithelium (Anti-p53 antibody immunomarking,  $\times 50$ ); (B) p16 diffuse positivity in tumor cells and basal layer of mucosa (Anti-p16 antibody immunomarking,  $\times 50$ ). HPV: Human papilloma virus.

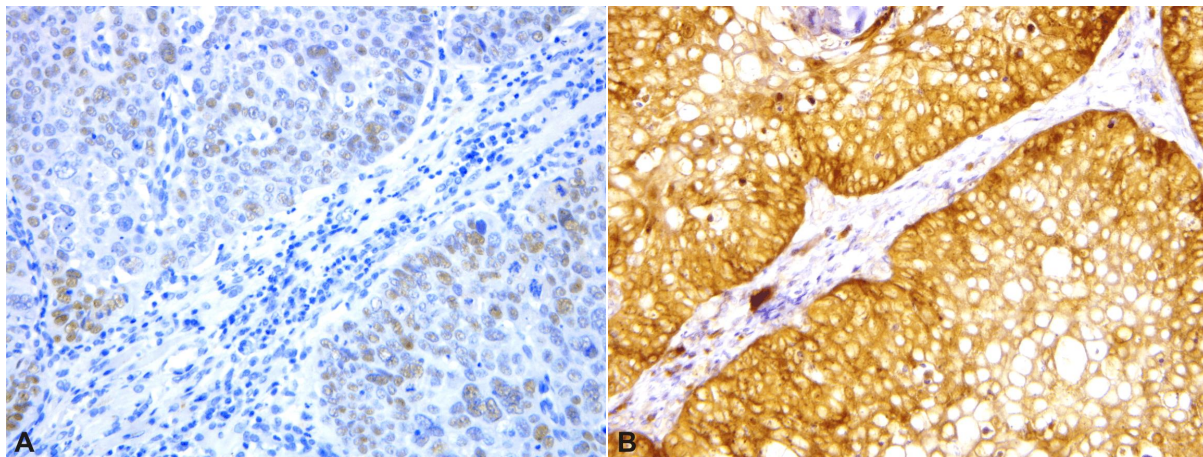


Figure 16: HPV-positive moderately differentiated, invasive oral squamous cell carcinoma: (A) p53 weak and diffuse positivity in tumor cells (Anti-p53 antibody immunomarking,  $\times 200$ ); (B) p16 intense and diffuse positivity in tumor cells (Anti-p16 antibody immunomarking,  $\times 200$ ). HPV: Human papilloma virus.

By contrary, HPV-negative cases had the highest frequency of recurrences and deaths. The best outcome was observed in p53-positive and p16-positive patients ( $r=0.452$ ,  $p=0.03539$ ). Most p53 cases (46%) that had good results, underwent either surgery associated with radiotherapy or surgery followed by radiotherapy and chemotherapy ( $r=0.617$ ,  $p=0.01411$ ).

### 3.2.5. Discussions

#### Study 1

Squamous cell carcinoma located in oropharynx (OPSCC) tends to become the most frequent type of head and neck carcinomas in well developed countries. Among different etiologies, infection with HPV exceeds tobacco smoking, which is decreasing in the past decades [Gillison et al., 2015]. Not only due to its different etiology, but mostly because of the different prognosis after neoadjuvant therapy, according to WHO, oropharyngeal HPV-positive carcinomas should be considered separately from HPV-negative ones or from squamous cell carcinomas located elsewhere in the head and neck. Patients with HPV-related SCC have a better prognosis after radio- or chemo-radiotherapy [Lassen et al., 2018]. Still, a history of tobacco smoking worsening the prognosis, even for patients with HPV-associated disease. Targeting the personalization of the treatment for each patient and the reduction of the side-effects of neoadjuvant therapy, scientists showed an interest towards the study of the immune system role in cancer biology and finding new treatment methods. According to the ability of tumor cells to avoid the immune protective system, different immune subclasses of cancer types were described [Thorsson et al., 2018]. Multiple gene expression subtypes were described in head and neck carcinomas, correlated with HPV infection and immune response [Lilja-Fischer et al., 2020].

In our geographical area, the research on HPV-associated HNSCC is relatively new and sometimes it is difficult to get fresh samples from surgical rooms. Similar to the cervical cancer testing, many HPV testing methods are available for HNSCC (PCR/Real Time PCR/Reverse Transcriptase from fresh/frozen/FFPE samples/oral cavity brushing, in situ hybridization for HR HPV types, p16 immunostaining, DNA/RNA microarray). Also, a standardized assay is needed to assess the full clinical relevance of the obtained results. There are data suggesting that detection of E6 and E7 mRNA expression in carcinomas is a reason to assume that the virus has been etiologically involved [Braakhuis et al., 2009]. Improved survival in patients with an HPV-positive carcinoma may be related to the type of treatment.

Preliminary data from small studies indicate that HPV-positive tumors are more likely to respond to induction chemotherapy and radiation therapy [Westra, 2014]. Recent studies found increased survival in HPV/p16-positive oro-pharyngeal cancer patients treated with postoperative radiation therapy [Masterson et al., 2014]. It is now well demonstrated that mucosal HR-HPV types, mainly HPV16, are causally involved in a significant proportion of oropharyngeal cancers and to a much lesser extent in a subset of other HNSCCs [Castellsague et al., 2016]. However, the contribution of HR-HPV to the carcinogenesis of HNSCC appears to be subject to major geographical variability.

Compared with other European countries, cervical cancer rates are highest in Romania (28.6/100,000), highlighting the importance of HPV infections in this population. However, limited information is available about HPV-associated HNSCC in Romania. Here, we have evaluated the contribution of HPV to HNSCC development in a study in Northeastern Romania by analyzing HPV DNA and HPV RNA status within a large retrospective cohort of HNSCC cases, as well as by determining the p16 expression status. The most frequent HR-HPV type was HPV16, followed by HPV18 and HPV39. The high HPV16 DNA prevalence in this study was similar to other findings published in the literature [Michaud et al., 2014].

Approximately 12% of HNSCCs tested positive for HPV DNA, but only 1.1% of all cases ( $n = 2$ ) were positive for both HPV DNA and RNA and thus considered as being HPV-driven [Rietbergen et al., 2013; Boscolo-Rizzo et al., 2016]. According to a recent review [Rietbergen et al., 2013], the term HPV-positive oropharyngeal squamous cell carcinoma refers to carcinomas of the oropharynx presumed to be associated with HPV, on the basis of positivity to HPV DNA and p16 IHC. In this study, only one case tested positive for both markers: HPV DNA and p16. Thus, the fraction of HNSCCs attributable to transforming HPV infections in this Romanian region appeared to be considerably lower compared with various other geographical regions. However, the low HPV prevalence in the FFPE samples is in line with the analysis of fresh tumor tissues from Romania, all being HPV-negative.

Both HPV DNA- and RNA-positive cases tested negative for p16. In addition, the great majority (95.6%) of HPV DNA-positive cases were p16-negative. The lack of expression of p16 in HPV DNA- and RNA-positive cases has been reported in other studies. These data contrast with the scenario observed in the Netherlands, where a double positivity for p16 and HPV DNA was shown to be valid to identify HPV RNA-positive cases [Rietbergen et al., 2013], and in Italy, where a fair agreement between HPV16 RNA-positivity and p16 overexpression in oropharyngeal cancer has been reported. The absence of p16 expression in HPV DNA-positive HNSCC could be due to the fact that HPV, despite its presence in the tumor, is biologically inactive and is present in the tumor as a passenger virus or viral contaminant. Loss of p16 expression is a frequent event in cancer, and it occurs by deletion, point mutation, or hypermethylation. The inactivation of p16 by hypermethylation of its promotor is common in HNSCC. Hypermethylation of p16 promotor has been reported to be an early event in the development of oral cancer. Exposure to certain carcinogens, such as tobacco, may lead to alterations of p16 expression. Indeed, hypermethylation of the p16 promoters was observed in several smoking-related human cancers, for example in non-small cell lung carcinoma and cervical squamous cell carcinoma. In addition, increased methylation of p16 was observed in laryngeal squamous cell carcinoma, and in normal oral mucosa, in smokers. Therefore, loss of p16 expression by hypermethylation in HNSCC, due to smoking or to other exposure factors, could precede HPV infection, which would not induce p16 accumulation in this specific circumstance.

Increasing chromosomal instability induced by HPV oncoproteins may lead to the loss of p16 in these cancers. Moreover, one HPV DNA- and RNA-negative case tested positive for p16. A similar result was reported in a recent worldwide HNSCC study, thus suggesting that p16-positivity is not a perfect surrogate for HPV [Castellsague et al., 2016]. A limitation of our study is that information on other HNSCC risk factors (e.g. alcohol consumption,

smoking) was available for only a few patients. This limitation was mainly due to the fact that the study implied the retrieval of archived HNSCC specimens, which were often not associated with detailed clinical information. From the available data in clinical questionnaires, 75.6% of the patients declared that they were smokers and 81.3% that they were users of alcohol.

According to the latest WHO Report on the Global Tobacco Epidemic, 2015, the smoking prevalence in Romanian male adults was 37.4% [WHO, 2017]. This high percentage supports the idea that smoking can be an important risk factor for HNSCC in our study. Tobacco smoking and alcohol consumption are important risk factors for HNSCC. More than 70% of HNSCCs are attributable to tobacco use and alcohol consumption. Cigarette smoking is a strong risk factor for HNSCC independent of alcohol consumption. The risk of developing laryngeal cancer was 10-20-fold higher in current smokers compared with non-smokers, and a 4-5-fold increased risk was observed for cancers of the oral cavity, oropharynx, and hypopharynx.

Alcohol consumption alone plays an independent role in approximately 4% of HNSCCs only. However, pooled data from 17 case-control studies in Europe and the USA highlighted a multiplicative joint effect, rather than an additive effect, of tobacco use and alcohol consumption on HNSCC risk. Another limitation of the study was the limited number of oropharyngeal cancers analyzed. This was mainly due to the fact that the majority of archival HNSCCs were from the oral cavity. The results of this study warrant additional analyses, to describe the risk factors, the natural history and the clinical role of oral HPV infections in Romania.

## Study 2

HPV-positive carcinoma cells diffusely overexpress the p16 protein, which is directly related to the molecular process involved in the carcinogenesis induced by the major HPV oncogenes (E6 and E7). The p16 protein is an essential factor of the negative feedback mechanism of mitosis, which is mainly aimed at promoting the inhibition by Rb of the transition to the cell cycle, but also a regulator of cell growth factor [Sathyamurthy A, et al. 2016]. Genetic or epigenetic alterations through inactivating p16, cause cancer cell growth in HPV-negative oropharyngeal cancers. There are significant correlations between the involvement of HPV in oropharyngeal carcinogenesis, epidemiology of HPV and specificity with tumor localization, HPV genome expression and p16 protein expression. For this reason, the immunohistochemical testing of p16 may be a satisfying surrogate marker for the detection of the HPV genome.

Our study confirmed this since we found that all HPV-positive cases were also p16 positive, while not all HPV-positive cases were also p53 positive. Given the high rate of false negative results of PCR and the low sensitivity of in situ hybridization techniques, it is important to perform HPV testing in oropharyngeal cancers by using at least two different techniques. Therefore, it is recommended to use both the viral genome detection techniques, and techniques that show the overexpression of the p16 protein [Schache AG, et al. 2011]. Considering the worldwide increasing number of HPV-positive head and neck carcinomas, which can be considered “epidemic”, HPV testing should be routinely performed correlated with screening programs aiming the high-risk patients.

The inactivation, degradation or mutation of the p53 gene can result in the its disfunction, resulting in cellular proliferation, accumulation of DNA mutations and survival of abnormal cells. The loss of p53 function alone is not sufficient to initiate the carcinogenesis, other mutations being necessary [zur Hausen H. 2009]. p53 mutations with high molecular expression are involved in malignancies found in chronic smokers.

Molecular profiling can be a useful tool in determining elements related to treatment response and prognosis with implications in treatment decision. Consistent with the outcomes

of our study, HPV-positive cancer patients with overexpression of p16 and p53 negative status are associated with a better response to treatment and an improved prognosis. Contrary to the results obtained by our study, the most common subtype of HPV detected according to the literature is HPV 16, consisting about 90% of all HPV-positive SCCs of the head and neck [Marur et al., 2010]. In our study, out of the 16 HPV-positive tumors, only 2 were HPV16 subtype. This could be explained by a geographical distribution of some HPV subtypes. In this regard, prophylaxis can be adapted accordingly using geographically specific vaccines. Further studies could be useful for rendering a more relevant statistical analysis regarding all factors. In oropharyngeal SCC, determination of baseline HPV status, upon IHC expression of p16INK4a, and detection of HPV DNA by PCR can have prognostic value. Smoking and chronic alcohol consumption are well known, universally accepted risk factors for HNSCC, that frequently associate to the HPV status. This leads to the loss of p16 and p53 gene mutations. The decrease in smoking coupled with an increase in HPV-positive tumors changed the frequency pattern of oropharyngeal cancers, now appearing more often in nonsmokers.

Additionally, patients with HPV-positive cancers tend to be younger than those with HPV-negative tumors, raising the presumption of dysfunctional sexual habits. Most HPV-positive patients in our study were under the age of 60 at the time of diagnosis with the youngest patient aged 39. HPV-positive cancers are associated with a very good survival, despite an advanced tumor stage at diagnosis. This is particularly important since the posterior location of oropharyngeal–retromolar trigone malignancies can lead to presentation in more advanced stages, the main reason for the reduced number of patients included in our study that underwent initial surgical resection. Best outcomes were obtained by association of surgery, radiotherapy and chemotherapy. Most HPV-positive patients had good results following treatment, including postoperative and increased survival, as opposed to HPV-negative cases in which recurrences and deaths had the highest frequency.

The risk of lymph nodes metastasis increases with the tumor stage. Patients with p16-positive oropharyngeal carcinomas have been detected with persisting lymph node metastases after neoadjuvant therapy and it was hypothesized that a cervical neck dissection can therefore be avoided. During the study, there was only one recurrence in an HPV-positive, p16-positive patient. This sustains the importance of molecular profiling of HNSCC in order to orientate the treatment strategy. The inclusion of high-risk HPV-positive patients in screening programs could help the diagnosis of the disease in an incipient stage with increased chances of achieving prolonged survival. Although the number of patients included in the study was reduced, there was a clear prevalence of improved outcomes of HPV-positive subjects and good results related to the expression of p16 protein.

As mentioned before, the high-risk factors for carcinogenesis of oral carcinomas (OC) are HPV infection, chronic tobacco and alcohol consumption. Usually, premalignant lesions can be identified before or adjacent the malignant invasive lesion. Such oral potentially malignant disorders (OPMD) are: leukoplakia, erythroplakia, oral lichen planus, oral submucous fibrosis, actinic cheilosis, and snuff patch [Tang et al., 2020].

Although it is proved that HPV plays a significant role in oropharyngeal cancers/carcinomas (OPC), it is still unclear to what extent this also applies to OC. Studies published after ours, aimed to determine the HPV16 prevalence in OPMD and OC, by using different sampling methods [Tang et al., 2020]. Interestingly, the study showed a non-significantly higher HPV16 prevalence in OC than in OPMD and a HPV16 positivity significantly associated with heavy tobacco consumption. Moreover, Tang et al. found that only the purely episomal HPV16 form was detected in all HPV16-positive OPMD and OC patients. Also, a high difference in viral load was found between HPV16 positive OPMD and

OC cases. Considering these data, the authors conclude that HPV is unlikely to play an etiological role in oral carcinogenesis [Tang et al., 2020].

Although the Australian study found a lower prevalence of HPV in OPMD cases when compared to other previous studies, the HPV prevalence rate in OC patients was found to be concordant with the findings of studies from other countries (including ours).

Our conclusions regarding a geographical variability of the HPV-associated OPC prevalence were also confirmed by a French team who found a higher prevalence in France compared to Southern and Eastern countries (including Romania), but lower compared to Northern Europe [Mirghani et al., 2019]. Still, there are some differences in the study design, as the Mirghani study included about 10 times more patients with cancers oropharyngeal located, being a multicenter study. However, it is important how HPV-driven cancers are defined. French authors consider those positive for both p16 and HPV-DNA by ISH, as currently, E6/E7 mRNA expression is the gold standard for defining HPV status [Mirghani et al., 2014].

Also, a recent Danish study found a difference between the methods used to investigate HPV-associated HNSCCs. They concluded that examination by both methods, HPV DNA and p16 overexpression, were the most frequently used, although in some studies the authors only used HPV DNA detection. It seems that using only one of them, p16 overexpression or HPV DNA, returned a lower specificity compared to the combination of the two [Stjernstrøm et al., 2019]. In what concerns the prevalence of HPV-associated HNSCC, their data confirms previous published data, including ours, advocating for a geographical-dependent distribution of these cases.

Nowadays, the oropharynx became the leading primary site for HPV-related HNSCC, transforming HPV positive oropharyngeal squamous cell carcinoma (HPV+ OSCC) in an epidemic disease, although with an improved survival, but generating difficulties in diagnosis and management. Thus, HPV status is generally recognized as a stratification factor in clinical trials and a clinically relevant parameter for patient consultation. This resulted in the inclusion as a separate staging manual for HPV+ OSCC in the latest edition of AJCC/TNM staging [Economopoulou et al., 2020].

## **Final remarks**

### **Study 1**

A very small subset of HNSCC cases within the study group from Northeastern Romania appeared to be HPV-driven, as evidenced by a low concordance between HPV DNA status and HPV RNA or p16 status of the analyzed HNSCC cases. Our study provides novel insights into the contribution of mucosal HR-HPV types in the development of head and neck carcinomas from this region of Romania and highlights potential differences in the carcinogenesis of HNSCC in this area compared with other European and non-European countries. We consider that young subjects, with no history of chronic alcohol and tobacco consumption, should be studied. The objective of these investigations is to reduce chemotherapy and radiation therapy applied to HPV-related carcinomas, according to current therapeutic protocols. Sensitive and specific biomarker tests (e.g., E6\*I mRNA, p16INK4a, UBC9, microRNA expression profile) would help to correctly classify the different types of HNSCC.

### **Study 2**

The present study sustains the involvement of HPV carcinogenesis of tumors located at the junction between the retromolar trigone and the oropharynx, at the borderline of two surgical specialties, oro-maxillary surgery and ear, nose and throat surgery. Additionally, we

highlighted the implications of HPV status, p16 and p53 expression in prognosis and treatment. Although our results correlate with those of other studies, further research on larger cohort of patients is needed for translating the information regarding molecular profiling and prognosis into relevant treatment protocols. In conclusion, the involvement of HPV in oropharyngeal carcinomas predict favorable response to treatment and a good overall prognosis by the expression of p16, that can act as a marker for identifying HPV-associated HNSCC.

## Chapter 4: Histopathological insights over lipids metabolism in obesity, atherosclerosis and wound healing

### 4.1. State of art

According to WHO, obesity become an epidemic chronic pathological condition, with major cardiometabolic effects induced by excessive fat accumulation threatening the life [WHO, 2014]. Currently, weight control might be obtained only by the metabolic surgery, in order to obtain significant and sustained weight loss. The beneficial metabolic effects appear prior to weight loss, and this led to the introduction of this method in the international guidelines for the treatment of diabetes mellitus [Rubino et al., 2016]. The mechanisms through which metabolic surgery improves the obesity metabolic changes are incompletely understood. Different hypotheses have been launched: from restrictive mechanism based on the reduced volume of the stomach and of the absorption surface, changes in digestive secretions, or in digestive tract microbiota to food intake changes and energy expenditure by the stomach-gut-brain axis [Batterham and Cummings, 2016]. Laparoscopic sleeve gastrectomy is the surgical method generally used in one step or as an intermediate step in extreme obesity. During sleeve gastrectomy, a longitudinal segment of the stomach (representing by part of fundus and corpus) is removed, together with of a portion of the antrum. Peptides secreted in the resected stomach specimen (such as ghrelin) and involved in the regulation of energy balance can be therefore studied. Firstly, isolated and described by Kojima et al., its expression is mainly located in the gastric cells distinct from other peptide-secreting cell types. Ghrelin immune-positive cells are found in the entire gastrointestinal tract and their density decreases from the stomach to the duodenum, ileum, cecum and colon. It is the peripherally-secreted hormone with central level action to increase appetite [Kojima et al., 1999]. To become active, ghrelin requires acylation under the action of ghrelin O-acyltransferase (GOAT) enzyme, the substrate for acylation being the dietary medium chain fatty acids [Romero et al., 2010].

Regarding the relationship between serum ghrelin level, number of ghrelin-producing cells (GPC) and weight status, a study conducted on a group of patients with Prader–Willi syndrome showed that plasma ghrelin level and density of GPC are 2–3 times higher in these patients compared to normal weight individuals, even at young ages [Choe et al., 2005]. The majority of circulating ghrelin is secreted by endocrine cells located in the gastric glands and, therefore, chronic gastric mucosal lesions (for instance, chronic gastritis) can affect ghrelin production, with possible effects on food intake and body weight change. *Helicobacter pylori* (*H. pylori*) is a Gram-negative bacterium widespread globally, with an estimated prevalence of over 50% of the world population, mainly in developing countries, because the poor socio-economic status is an important risk factor. It produces inflammation in the gastric mucosa, and is involved in the pathogenesis of atrophic or non-atrophic gastritis, gastric and duodenal ulcer, gastric tumors such as adenocarcinoma and lymphoma of mucosa-associated lymphoid tissue (MALT) type (therefore it is considered a group I human carcinogen). Ghrelin production, its acylation and/or secretion may be compromised by the presence of chronic gastritis and atrophy, the consequences being changes in appetite and weight. *H. pylori* infection can produce the endocrine cell damage by inflammation and induce atrophy. In addition, *H. pylori* infection is accompanied by nutrients malabsorption (secondary to hypochlorhydria, vomiting, dyspepsia, increased susceptibility to other enteric pathogens), which gave rise to speculation that modified food dietary intake or even dysregulated absorption of medium-chain fatty acid substrate for GOAT enzyme could influence the acylated/ total ghrelin ratio during *H. pylori* infection. Controversial data exist in the literature regarding the relationship between plasma ghrelin level, number of ghrelin-producing cells and *H. pylori* infection, both in normal-weight and supraponderal individuals.

*H. pylori* infection may influence weight status and metabolic profile of patients. As a consequence, eradication by treatment of *H. pylori* infection induces a subsequent increase in the level of appetite-regulating peptides, such as ghrelin, weight gain and obesity. Often, obese individuals associate numerous nutritional deficiencies, regardless of *H. pylori* infection, partly due to restrictive and/or reiterated diets in an attempt to get a proper weight control. On the other hand, the possible role played by *H. pylori* infection on nutritional absorption was subjected by numerous research teams and some of them found an association between *H. pylori* infection and iron deficiency anemia, which is even more important in children compared to adults [Qu et al., 2010]. Other studies found that *H. pylori* infection can cause malabsorption of some vitamins (fat- or water-soluble), microelements and minerals. For instance, there is an association between *H. pylori* infection and B12 hypovitaminosis,  $\beta$ -caroten and  $\alpha$ -tocopherol deficiency in the gastric secretion, with vitamin C deficit and folic acid decrease. With regards to the relationship between *H. pylori* infection and plasmatic levels of some minerals (Zn or Se), published data are limited and sometimes controversial.

Since *H. pylori* is a proved carcinogenic factor, its eradication reduces the risk of gastric cancer, dependent however on the presence, severity and extension of atrophic and dysplastic lesions at the time of diagnosis and eradication [Sugano et al., 2015]. *H. pylori* infection could also have a pathogenic role in the development of numerous other diseases; studies demonstrate the association between *H. pylori* infection and increased risk of metabolic syndrome, atherosclerosis, cardiovascular disease, hepatic disease, idiopathic thrombocytopenic purpura, and altered neurological and cognitive status [Waluga et al., 2015].

The mechanisms involved are complex and imply metabolic disturbances and endothelial dysfunction, pro-inflammatory and pro-atherogenic status. Obesity is an important risk factor both for digestive pathology and for cardio-metabolic disease, cancer, respiratory, rheumatologic and dermatological pathologies. Superior digestive tract diseases (gastro-esophageal reflux disease, erosive esophagitis, hiatal hernia, esophageal adenocarcinoma and *H. pylori* infection) have been reported as being 2–3 times more frequent in obese persons compared to normal weight. Because *H. pylori* infection can complicate and aggravate the complications and comorbidities associated with obesity per se, by supplementary influencing weight status, it can act as a negative factor in limiting access to bariatric surgery. However, the role of routine endoscopy before bariatric surgery remains controversial. The American guidelines do not give clear indications regarding screening and management of *H. pylori* (screening is recommended to symptomatic patients from high prevalence areas and endoscopy is recommended in selected cases) [Mechanick et al., 2013], while the European guidelines recommend endoscopy prior to surgery in all patients, symptomatic or not, and treatment of any lesion that might lead to postoperative complications, including *H. pylori* [Sauerland et al., 2005].

The lack of correlation between the endoscopic aspect and patients' symptoms was documented by various authors, who even suggested that routine preoperative endoscopy would still be useful in detecting the lesion and inflammation [De Palma and Forestieri, 2014]. Still, the procedure is invasive and the risks associated with sedation are limits that do not justify the routine performance of this procedure in asymptomatic patients. The influence of *H. pylori* infection on the postoperative follow-up of these patients could mean early postoperative complications, like leakage, collections or intraabdominal abscesses, ulcer with or without perforation, longer length of stay in hospital or higher rate of early postoperative readmission, although reported data are contradictory in this field [Brownlee et al., 2015]. Therefore, it is of major importance to detect *H. pylori* infection pre-operatory in these patients. To date, published data is controversial because of uneven inclusion criteria (general population, or patients with dyspeptic symptoms – most frequently, or patients already diagnosed with cardiovascular or metabolic pathology). Another reason for the discrepancies

in results is the different adjustment of results, for various parameters; however, probably the most important reason for the contradictory results is the different means of diagnosis, influencing both the prevalence of *H. pylori* infection, and its association with cardio-metabolic risk.

Dietary n-3 polyunsaturated fatty acids (PUFAs) have a role in preventing cardiovascular and hepatic diseases. However, their effects might be significantly different depending on individual dietary patterns. The role of different schedules of  $\omega$ -3 fatty acids (FA)-administration effects on hepatic and aortic histological structure, lipid profile, and body weight (BW) in male Wistar rats, under standard (SD), high-fat diet (HFD), and mixed-feeding pattern conditions might be of interest. Therefore, designing a study in order to analyze, compare and quantify the  $\omega$ 3-efficacy in conditions of Western, Mediterranean, and heterogeneous diet or simulation of different metabolic profiles would bring new insights on this matter.

**This research direction has been realized by publishing the following articles:**

Mihalache L, Arhire LI, Giușcă SE, Gherasim A, Niță O, Constantinescu D, Constantinescu RN, Pădureanu SS, **Danciu M**: Ghrelin-producing cells distribution in the stomach and the relation with *Helicobacter pylori* in obese patients. Rom J Morphol Embryol. 2019;60(1):219-225. <http://www.rjme.ro/RJME/resources/files/600119219225.pdf>

**Danciu M**, Simion L, Poroch V, Pădureanu SS, Constantinescu RN, Arhire LI, Mihalache L: The role of histological evaluation of *Helicobacter pylori* infection in obese patients referred to laparoscopic sleeve gastrectomy. Rom J Morphol Embryol. 2016; 57(4):1303-1311. <http://www.rjme.ro/RJME/resources/files/57041613031311.pdf>

Chen YW, Scutaru TT, Ghetu N, Carasevici E, Lupascu CD, Ferariu D, Pieptu D, Coman CG, **Danciu M**: The Effects of Adipose-Derived Stem Cell-Differentiated Adipocytes on Skin Burn Wound Healing in Rats. J Burn Care Res. 2017; 38(1):1-10. doi: 10.1097/BCR.0000000000000466

Godea (Lupei) S, Ciubotariu D, **Danciu M\*** et al. Improvement in serum lipids and liver morphology after supplementation of the diet with fish oil is more evident under regular feeding conditions than under high-fat or mixed diets in rats. *Lipids Health Dis* 2020; 19:162 <https://lipidworld.biomedcentral.com/articles/10.1186/s12944-020-01339-y#citeas>

## **4.2. Semiquantitative evaluation of Ghrelin-producing cells and *H. pylori* in patients with sleeve gastrectomy**

### **4.2.1. Introduction**

After GPC were identified and described by Kokima, interest in studying them grew [Kojima et al., 1999] and in 2000, it has been demonstrated that its expression is located mostly within certain gastric cells distinct from other peptide-secreting cell types. Several studies that follow aimed to characterize GPC using various methods, on animal and human models. The distribution of GPC is still debatable. The highest number of GPC was reported in the upper part of the stomach, fundus, or gastric body [Kim et al., 2012]. In a personal study that included obese subjects, the main location of GPC was in the gastric body, with statistically significant differences between the number of the cells present in this region compared to fundus and antrum. To our knowledge, few data are available in the literature on the number of GPC in the stomach of obese patients. A study published in 2009 on 18 morbidly obese patients who underwent metabolic surgery showed hypoactivity of gastric X/A-like cells in the obese group compared to controls [Dadan et al., 2009], the interpretation

of these results suggesting the existence of an adaptive mechanism in obese people, which decreases ghrelin levels and thus food intake in order to restore the body's energy balance. Studies on plasma ghrelin level, distribution of ghrelin messenger ribonucleic acid (mRNA) expression by reverse transcription polymerase chain reaction (RT-PCR) and distribution of GPC by immunohistochemistry in resected stomach specimens from 20 morbidly obese patients who underwent sleeve gastrectomy showed that the expression of ghrelin mRNA decrease gradually from the fundus towards the preantral region. Also, the prevalence of GPC shared the same pattern, with the highest percentage of positive ghrelin cells in the fundus, intermediate in the body, and the lowest in the preantral region ( $p=0.08$ ) [Goitein et al., 2012]. High number of GPC in the gastric fundus were reported compared to the body and antral region in obese patients who underwent metabolic surgery [Abdemur et al., 2014].

There's large variability regarding prevalence of *H. pylori* infection in patients with grade III obesity, ranging from 8.7% to 85.5%. An explanation could be in different diagnostic and/or research methods. Many authors evaluated the correlation between weight and the prevalence of *H. pylori* infection, obtaining controversial conclusions. Thus, a 2014 analysis of 50 studies that included 99,000 subjects showed that the prevalence of overweight and obesity was inversely correlated with the prevalence of *H. pylori* infection, statistically significant ( $r = -0.292$ ,  $p < 0.05$  and  $r = -0.43$ ,  $p < 0.01$ ), respectively [Lender et al., 2014]. By contrary, a national cross-sectional study conducted on a significant and representative sample of the US population, involving over 7000 subjects, did not see any relationship between *H. pylori* infection and weight status assessed by anthropometric parameters (weight and BMI), even after adjusting for demographic variables or for those related to lifestyle [Cho et al., 2005]. The relationship between seric ghrelin levels, number of ghrelin producing cells in stomach and *H. pylori* associated infection, in normal and obese patients, is not fully elucidated. *H. pylori* infection may influence weight status and metabolic profile of patients, and treatment of *H. pylori* infection would induce a subsequent change in the level of appetite-regulating peptides (i.e., ghrelin). The reasons explaining the divergent data and conclusions rely on the different characteristics of included subjects and the different adjustment of results, for various parameters; however, probably the most important reason for the contradictory results is the different means of diagnosis, influencing both the prevalence of *H. pylori* infection, and its association with cardio-metabolic risk.

#### **4.2.2. Aims**

In this actual context, my research was designed to follow two directions. In the first study, the purpose was to quantify the number and distribution of GPC in the stomach and to assess the serum acyl ghrelin level, with further correlations regarding the relationship with the *H. pylori* infection in a group of obese patients who underwent laparoscopic sleeve (subtotal longitudinal) gastrectomy.

In the second study, we aimed to evaluate the concordance between two different methods of detection of *H. pylori* in gastric mucosa in individuals with morbid obesity proposed for sleeve gastrectomy in order to propose a preoperative assessing algorithm of these patients.

#### **4.2.3. Material and methods**

##### **Study 1**

###### *Patients, materials and methods*

In this prospective study, we included consecutive patients, who were evaluated in order to undergo laparoscopic sleeve gastrectomy between September 2014 and November 2015, at the Centre for Obesity of the "Sf. Spiridon" Clinical Emergency Hospital, Iasi,

Romania. All the included patients fulfilled the current guideline criteria for the indication for bariatric surgery and were followed-up using the same algorithm for the complex preoperative multidisciplinary evaluation. Anthropometric parameters were assessed according to the recommendations of the World Health Organization (WHO) and allowed the classification of subjects in two weight categories: stage II obesity [body mass index (BMI) of 35–39.9 kg/m<sup>2</sup>) and stage III obesity (BMI  $\geq$ 40 kg/m<sup>2</sup>). Excess weight was calculated with the difference between real weight of patients and ideal weight, using the Devine formula.

All patients included in the study underwent an upper gastrointestinal endoscopy, performed by the same experienced gastroenterologist, who took gastric mucosa biopsies, which were immediately sent to Department of Pathology for morphological evaluation. The macroscopic aspects observed during the upper gastrointestinal (UGI) endoscopy were divided into four categories: normal, congestion, gastritis, and other lesions (granular aspect, hypertrophic folds, and biliary reflux). The histological examination of the gastric biopsy provided two types of information regarding gastritis: classification and grading the inflammation (which resulted into three categories: normal, superficial chronic gastritis and profound chronic gastritis), and assessment of *H. pylori* infection. All patients with histological diagnosis of *H. pylori* infection received the same eradication treatment regime – the triple therapy and surgery was performed only after completion of the treatment.

The serological diagnosis of *H. pylori* infection was based on the detection of anti-*H. pylori* (Hp) IgG antibodies, for which a 5 mL blood sample was taken from each patient and immediately transported to the immunology laboratory, where the serum was separated and tested right away. IgG antibodies to *H. pylori* were detected in fresh serum using a solid phase chemiluminescent immunometric assay, commercially available IMMULITE® 2000 *H. pylori* IgG EIA (enzyme immunoassay) reagents (Siemens) and an IMMULITE® 2000 immunoassay system (Siemens Healthcare). The presence of IgG antibodies to *H. pylori* is an indication of previous exposure to the organism. Titers higher than or equal to 1.1 U/mL were considered to be “positive” and indicate that *H. pylori* IgG antibodies were detected in the sample. Titers lower than 0.9 U/mL were considered to be “negative” and indicate that *H. pylori* IgG antibodies were not detected in the sample. Negative results do not preclude recent primary infection. Titers higher than or equal to 0.9 U/mL and lower than 1.1 U/mL were considered to be “indeterminate” and were subject to retesting.

All patients underwent laparoscopic sleeve gastrectomy including the greater curvature of fundus and stomach body and the resected gastric sample was subsequently morphologically analyzed. All fresh surgical specimens were measured and the gross appearance was described. Fixation was done for 18–24 hours in 10% neutral buffered formalin, pH 6. From each gastric sample, three fragments were selected from the proximal, middle and distal sites. They were routinely processed for paraffin embedding using a Leica ASP200 tissue processor. To obtain thin 4–6  $\mu$ m sections, we used a Leica RM2135 manual rotary microtome; sections were stained with Hematoxylin–Eosin (HE) and Giemsa. Microscopic examination and image acquisition were done using a Nikon Eclipse E600 light microscope with Nikon Coolpix 4500 camera and LuciaNet software. For the classification and grading of gastritis, we used the updated Sydney System [35]. Hence, the observed modifications were classified into three categories: normal, superficial chronic gastritis and profound chronic gastritis.

Data was analyzed using Microsoft Office Excel and SPSS ver. 17.0. Numerical data were expressed as means and standard deviation (SD), minimum and maximum and significant differences between numerical data were found using Student’s t-test. For the description of categorical variables, we used frequencies and percentage and the significant differences were assessed with the chisquare ( $\chi^2$ ) test (or Fisher’s test for small samples) with a significance value of  $<0.05$ . We also used cross tabulation to determine specificity and sensibility of a diagnosis test, Cohen’ kappa coefficient of agreement and calculated odds

ratio for adequate variables. The Ethics Committee of the University granted approval for the study and all the patients gave their consent to participate.

## Study 2

### *Patients*

The study group included 21 patients with obesity (16 women) who underwent metabolic surgery (September 2014–November 2015) at the Center for Obesity and Bariatric Surgery, “Sf. Spiridon” Clinical Emergency Hospital, Iași, Romania. The Ethics Committee of the “Grigore T. Popa” University of Medicine and Pharmacy, Iași, granted approval for the research and patients gave their consent to participate. Patients included in the study met the current metabolic surgery eligibility criteria and were followed up using the same algorithm for the complex preoperative multidisciplinary assessment. Patients were submitted to an upper digestive endoscopy (UDE), performed by experienced gastroenterologists who evaluated the gastric mucosa appearance and harvested biopsies for the morphological assessment. Patients with histological evidence of *H. pylori* infection received the same eradication treatment regime (the triple therapy) and surgery was performed only after completion of the treatment. All patients underwent laparoscopic sleeve gastrectomy including the greater curvature of fundus and stomach body. Patient’s characteristics (gender, age, weight, and the anthropometric parameters – body mass index (BMI) and waist circumference (WC) assessed according to WHO recommendations) are shown in Table 14.

Table 14: General characteristics of the study group

Characteristics	Unit	Total	Women (16; 76.2%)	Men (5; 23.8%)
<i>Age [years]</i>	mean±SD	43.9±12.522	43.63±12.612	44.8±13.646
	min.; max.	18; 61	18; 58	25; 61
<i>Weight [kg]</i>	mean±SD	120.5±21.74	112.9±16	144.7±21.11
	min.; max.	90; 175	90; 145	117; 175
<i>BMI [kg/m<sup>2</sup>]</i>	mean±SD	43.24±5.51	42.77±6.03	44.74±3.46
	min.; max.	35.05; 53.911	35.05; 53.91	40.48; 48.47
<i>WC [cm]</i>	mean±SD	126.35±13.55	123±13.15	136.4±9.91
	min.; max.	104; 147	104; 144	122; 147

### *Histopathological methods*

All endobiopsies were routinely processed by fixation in 10% neutral buffered formalin, pH 6, for six hours, and paraffin embedding. All fresh surgical specimens were measured and the gross aspect was described. Fixation was done for 18–24 hours in 10% neutral buffered formalin, pH 6. From each gastric sample, three fragments were selected from the proximal, middle and distal sites. They were routinely processed by paraffin embedding, using a Leica ASP200 tissue processor. Five µm thin sections were cut using a Leica RM2135 manual rotary microtome and stained with Hematoxylin–Eosin (HE) and Giemsa. Microscopic examination and image acquisition were done using a Leica DM 3000 motorized light microscope with Leica camera and Leica Application Suite (LAS) image acquisition software. For the classification and grading of gastritis, we used the updated Sydney System.

### *Immunohistochemical methods*

Representative tissue sections placed on slides coated with poly-L-lysine were dewaxed, hydrated, and then immersed in Target Retrieval Solution pH 6 (code S1700, DAKO, Denmark), at 96°C, for 25 minutes, to unmask the antigen [heat-induced epitope retrieval technique (HIER)]. Tissue sections were incubated overnight with the primary anti-ghrelin monoclonal antibody (mouse antihuman, 1:150, IgG2a, ab57222, Abcam, Cambridge,

MA, USA), at 40°C. The detection of the immunoreaction was performed using NovoLink™ Polymer Detection System (Leica Biosystems, Germany). Sections were developed using 3,3'-Diaminobenzidine tetrahydrochloride chromogen (DAB, code K5001, DAKO, Denmark) and counterstained with Lille's Hematoxylin.

#### *Histopathological and immunohistochemical assessments*

The length and width of the resected gastric specimen were measured and based on them its volume was calculated, and then each specimen was subdivided into three regions: proximal (fundus), medium (corpus) and distal (antral region). The histological examination of the gastric samples included the classification and grading of the inflammation (resulting in three categories: normal, superficial chronic gastritis and profound chronic gastritis), and assessment of *H. pylori* infection presence. For each region of the resected specimen, five high power fields (HPFs), randomly chosen, were evaluated by counting the number of GPC with cytoplasmic ghrelin positive immunoreexpression.

#### *Immunological methods. Serological diagnosis of H. pylori infection*

The serological diagnosis of *H. pylori* infection was based on the detection of anti-*H. pylori* immunoglobulin G (IgG) antibodies, in blood samples of each patient. Titers  $\geq 1.1$  U/mL were considered to be "positive", titers  $< 0.9$  U/mL were considered as "negative" and titers values  $\geq 0.9$  U/mL and  $< 1.1$  U/mL were considered to be "indeterminate" and were subject to retesting. Negative results do not preclude recent primary infection.

#### *The dosage of plasma ghrelin*

Acyl ghrelin level was preoperatively determined in all patients. Plasmatic acylated ghrelin was quantified using commercially available enzyme-linked immunosorbent assay (ELISA) kits (BioVendor Laboratory, USA) based on a double-antibody sandwich technique.

#### *Statistical analysis*

Data were analyzed using Microsoft Office Excel and Statistical Package for the Social Sciences (SPSS) version 17.0. Numerical data were expressed as means and standard deviation (SD), minimum and maximum. Significant differences between numerical data were found using Student's t-test. For the description of categorical variables, we used frequencies and percentages and the significant differences were assessed using the chi-square ( $\chi^2$ ) test (or Fisher test for small samples) with a significance value of  $p < 0.05$ .

## **4.2.4. Results**

### **Study 1**

The study cohort included 70 patients, among which 19 (27.1%) were men. Considering the macroscopic aspects observed in gastroscopy, in 30% (21 patients), it was normal, 50.8% (37 patients) had congestion, 7.1% (5 patients) had gastritis and 10% presented other lesions. All macroscopic, serological and histological description of the study group (whole group and separately by gender) is presented in Table 15.

Analyzing the serological titers of anti-*H. pylori* antibodies, we observed that there were no patients with an "indeterminate" titer, meaning that the patients were divided in just two categories: *H. pylori* positive and *H. pylori* negative in serology. As such, 58.6% of patients were *H. pylori* positive by serology. In the histological examination of the biopsy, we found that 51.4% of patients were *H. pylori* positive. Among those patients who were *H. pylori* positive in serology, 82.4% were also positive in the histological exam. Among those who were *H. pylori* negative in serology, 12.5% were *H. pylori* positive in the histological examination. The Cohen's kappa agreement factor between the serological and histological diagnosis was 0.686 ( $p < 0.001$ ) (Table 15). Considering the histological diagnosis as gold standard, we found that the serological diagnosis of *H. pylori* had a sensibility of 90.3% and a specificity of 77.8%. Patients who were positive for *H. pylori* serologically, had an odds ratio

of 32.667 (95% confidence interval – CI 7.311–145.956) of having *H. pylori* infection at the histological examination.

Microscopic examination revealed that 16 (22.8%) cases presented normal morphology, as no neutrophils were observed and mononuclear inflammatory cells were absent or extremely rare (Figure 17). Minimal edema, congestion and lymphoid aggregates without germinal centers basally located above the muscularis mucosae (Figure 18) were considered to be normal. On Giemsa staining, the presence of *H. pylori* was not observed in none of these cases (Figure 19).

In 16 (22.8%) cases, we identified a reduced inflammatory infiltrate with lymphocytes and plasma cells in the upper third of the lamina propria, edema and/or congestion. These cases were classified as chronic superficial gastritis (Figure 20). Six (37.5%) of them were associated with infection with *H. pylori*.

A number of 38 (54.4%) patients were diagnosed with chronic profound gastritis, when the inflammatory infiltrate was present diffusely in the whole thickness of lamina propria. In some cases (11 cases), lymphoid aggregates with germinal center (follicles) were detected (Figure 21). Most of these cases, namely 29 (76.3%) were *H. pylori* – positive on Giemsa staining (Figure 22).

Focally, in a reduced number of cases (two cases) with chronic profound gastritis, we observed intestinal metaplasia, the complete type. Complete type of intestinal metaplasia in stomach was diagnosed on the presence of mucin-producing goblet cells, enterocytes with brush border and Paneth cells, sometimes with a villous architecture in the surface of the mucosa (Figure 23).

No patients presented acute gastritis or chronic gastritis in the active phase. No atrophy and no dysplasia were seen in our cases. When present, the inflammatory infiltrate was limited to mucosa. Muscularis propria and subserosa were normal in all our cases. In the resected gastric specimens, we found *H. pylori* infection in 11.4% of cases (8 cases). Among these, only one patient was also positive for *H. pylori* in the preoperatively histological examination.

The presence of *H. pylori* in the resected stomach was associated with more severe degrees of chronic gastritis in the histological examination of the resected stomach: among those positive for *H. pylori* in the resected stomach, 50% had profound chronic gastritis and 37.5% had superficial chronic gastritis ( $p=0.037$ ). More information regarding the association of histological diagnosis of *H. pylori* infection with the other parameters investigated in the study can be found in Table 16.

Table 15: Serological and histological characteristics of the study population

Characteristic	Total (N=70)	Women (N=51)	Men (N=19)	p
	N (%)	N (%)	N (%)	
<i>Hp</i> (+) serology	41 (58.6)	29 (56.8)	12 (63.1)	>0.05
<i>Hp</i> (+) histology endobiopsy	36 (51.4)	24 (47.1)	12 (63.1)	>0.05
<i>Hp</i> (+) resected stomach	8 (11.4)	6 (11.8)	2 (10.5)	>0.05
Macroscopic aspect in gastroscopy	normal	21 (30)	17 (33.3)	>0.05
	congestion	37 (50.8)	25 (49)	
	gastritis	5 (7.1)	4 (7.8)	
	other	7 (10)	5 (9.8)	
Histological aspect in gastric biopsy	normal	16 (22.8)	13 (25.5)	>0.05
	superficial chronic gastritis	16 (22.8)	12 (23.5)	
	profound chronic gastritis	38 (54.4)	27 (52.9)	
Histological aspect of resected stomach	normal	35 (50)	26 (50.9)	>0.05
	superficial chronic gastritis	10 (14.3)	8 (15.7)	
	profound chronic gastritis	25 (35.7)	17 (33.3)	

*Hp* (+) indicates infection with *H. pylori*.

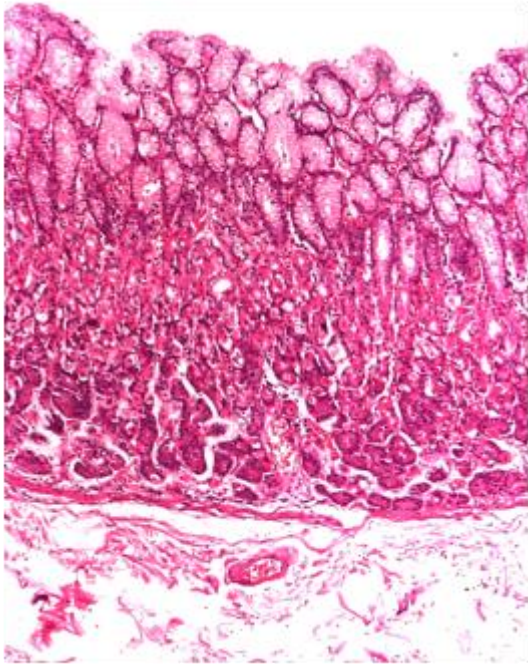


Figure 17: Normal gastric body mucosa with minimal congestion and edema in lamina propria. HE staining,  $\times 40$ .

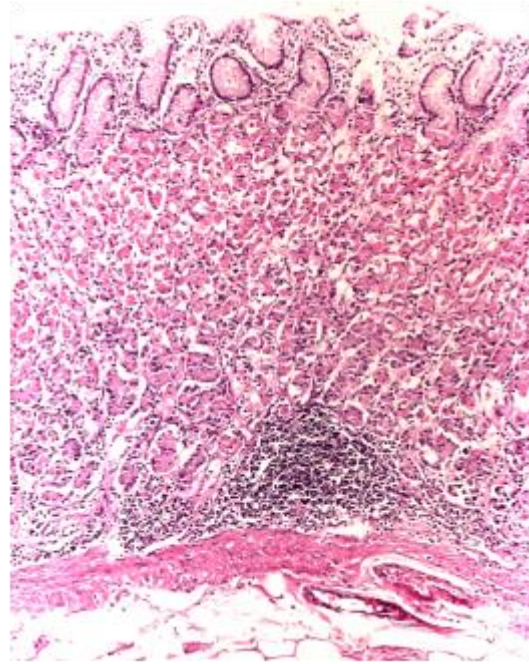


Figure 18: Normal gastric body mucosa with lymphoid aggregates without germinal centers, basally located. HE staining,  $\times 40$ .

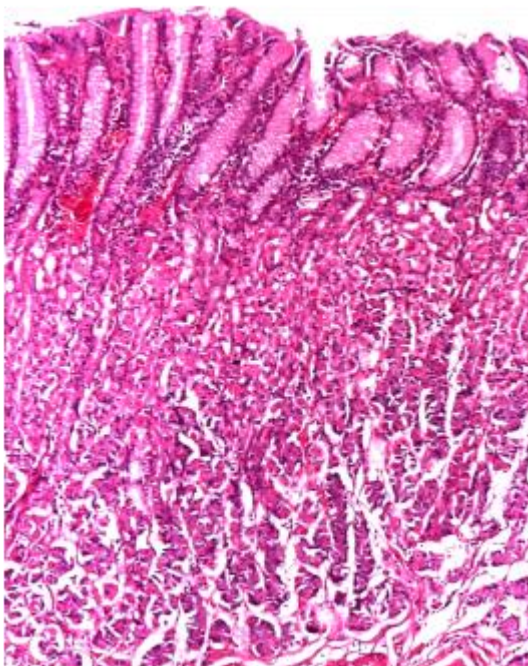


Figure 20: Chronic superficial gastritis: reduced mononuclear inflammatory infiltrate in the upper third of the gastric mucosa. HE staining,  $\times 40$ .

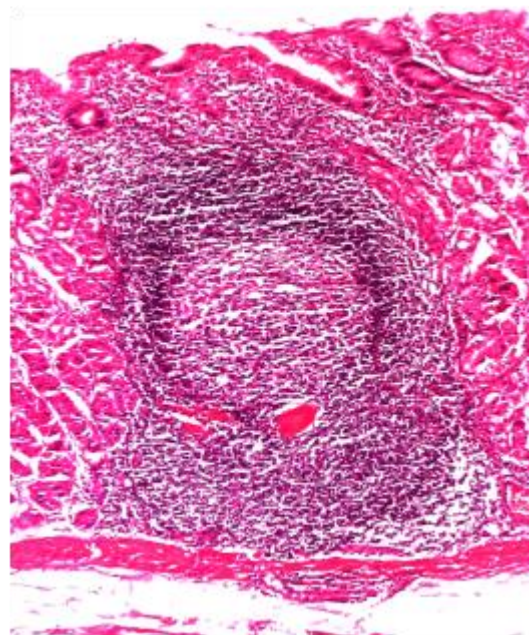


Figure 21: Chronic profound follicular gastritis: abundant mononuclear inflammatory infiltrate with lymphoid follicles. HE staining,  $\times 40$ .

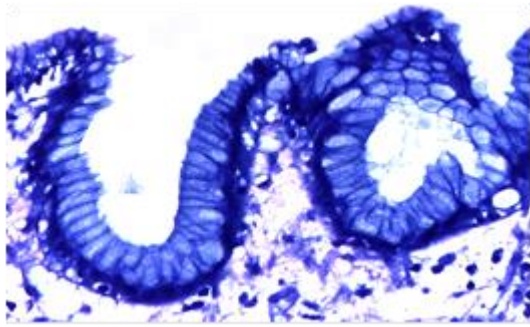


Figure 19: Normal gastric mucosa, no *H. pylori* infection. Giemsa staining,  $\times 200$ .

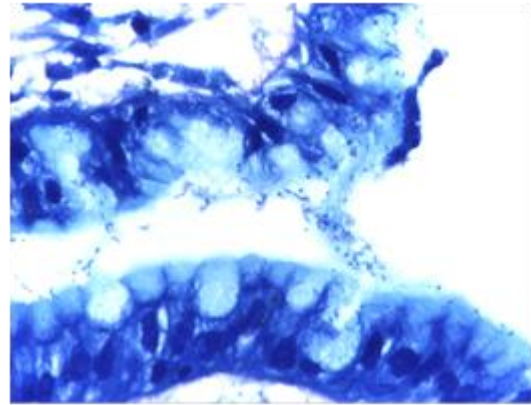


Figure 22: Chronic gastritis associated with *H. pylori* infection. Giemsa staining,  $\times 400$ .

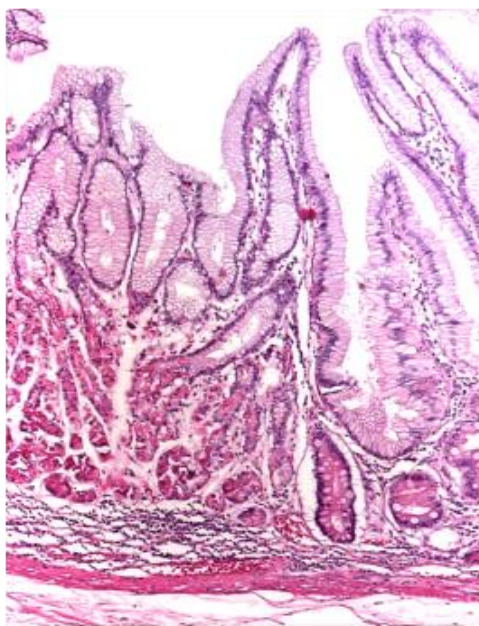


Figure 23: Chronic gastritis with complete type intestinal metaplasia (right). HE staining,  $\times 40$ .

Table 16: Differences in study population according to the histological diagnosis of *H. pylori* infection

Characteristic	<i>H. pylori</i> in endobiospy		$\chi^2; p$	$\kappa; p$	
	+	-			
	<i>N</i> (%)	<i>N</i> (%)			
<i>H. pylori</i> by serology	+	33 (80.5)	8 (19.5)	27.59; <0.001	0.686; <0.001
	-	3 (10.3)	26 (89.6)		
<i>H. pylori</i> in resected stomach	+	1 (12.5)	7 (87.5)	6.343; 0.019	-0.0199; 0.012
	-	37 (59.7)	25 (40.3)		
Histological aspect in gastric biopsy	normal	0	16 (100)	22.439; <0.001	-
	superficial chronic gastritis	6 (37.5)	10 (62.5)		
	profound chronic gastritis	29 (76.3)	9 (23.7)		
Histological aspect in resected stomach	normal	15 (42.9)	20 (57.1)	2.896; >0.05	-
	superficial chronic gastritis	7 (70)	3 (30)		
	profound chronic gastritis	15 (60)	10 (40)		
Macroscopic aspect in gastroscopy	normal	6 (28.6)	15 (71.4)	7.605; 0.055	-
	congestion	21 (56.8)	16 (43.2)		
	gastritis	4 (80)	1 (20)		
	other	5 (71.4)	2 (28.6)		

## Study 2

The macroscopic aspects observed during the UDE were divided into four categories: normal, congestion, gastritis, and other lesions (granular aspect, hypertrophic folds, and biliary reflux). Histopathological examination of the gastric resection specimens showed the presence of gastritis lesions in 14 (66.7%) patients, in 10 patients the lesions being superficial, and normal gastric mucosa in seven (33.3%) patients.

In the entire study group, the *H. pylori* infection was identified only in two (9.5%) patients. Statistical analysis between the anthropometric parameters and size of the resected gastric specimen revealed a positive correlation between patient height and specimen length ( $p=0.023$ ) and specimen volume ( $p=0.051$ ), and between specimen width and patient weight ( $p=0.042$ ) and WC ( $p=0.023$ ).

GPC were mainly identified in the basal half of the gastric mucosa. They were present in all cases, both in those with normal aspect (Figures 24 and 25) as in those with chronic gastritis, superficial (Figure 26) or profound (Figure 27). The total mean number of GPC in the gastric resection specimen of the study group was  $15.06 \pm 5.97$ , the highest number of cells being found in the gastric body ( $16.6 \pm 7.2$ ), followed by fundus ( $14.85 \pm 7.02$ ) and antral region ( $13.75 \pm 8.12$ ) – the differences being statistically significant ( $p < 0.001$ ) (Table 17). The total number of GPC was higher in women compared to men, but the differences both in total number, and by each region (fundus, body and antral region) were not statistically significant (Table 2). The number of GPC in the gastric body correlated inversely with weight ( $p=0.011$ ), BMI ( $p=0.017$ ) and WC ( $p=0.066$ ). The anti-*H. pylori* antibody was detected in 14 (66.7%) patients and these patients had a smaller number of GPC compared to patients with *H. pylori* absent ( $14.78 \pm 6.27$  vs.  $15.64 \pm 5.76$ ,  $p > 0.05$ ). The number of GPC was lower in the patients with *H. pylori* infection and in those with gastritis lesions ( $14.928 \pm 6.38$  vs.  $15.35 \pm 5.53$ ), decreasing with the increase in depth of gastritis lesion ( $p > 0.05$ ).

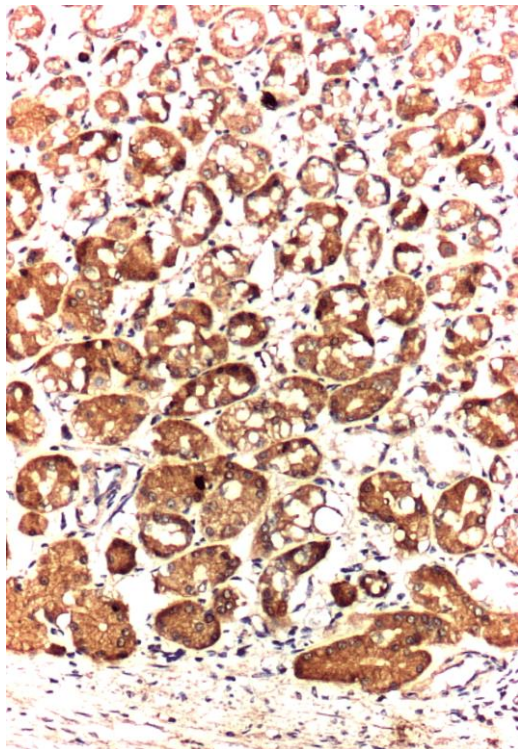


Figure 24: Normal gastric mucosa, fundic region, with low number (2) of GPC (Anti-ghrelin antibody immunomarking,  $\times 100$ ). GPC: Ghrelin-producing cells.

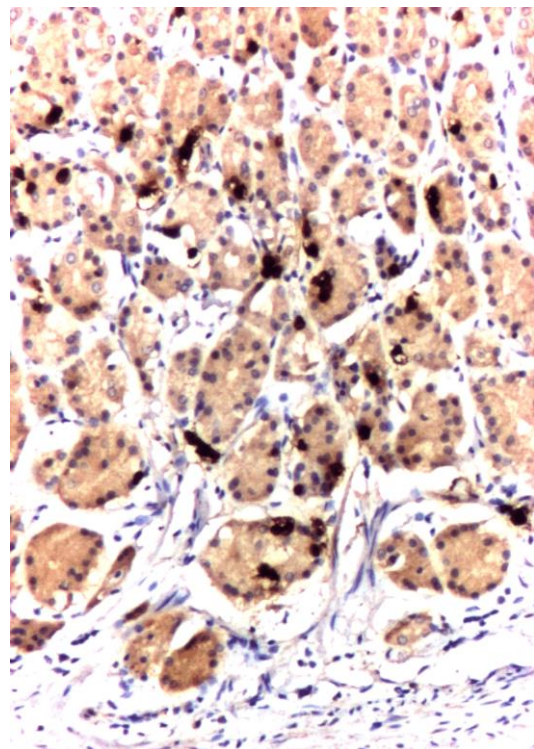


Figure 25: Normal gastric mucosa, fundic region, with high number (37) of GPC (Anti-ghrelin antibody immunomarking,  $\times 100$ ). GPC: Ghrelin-producing cells.

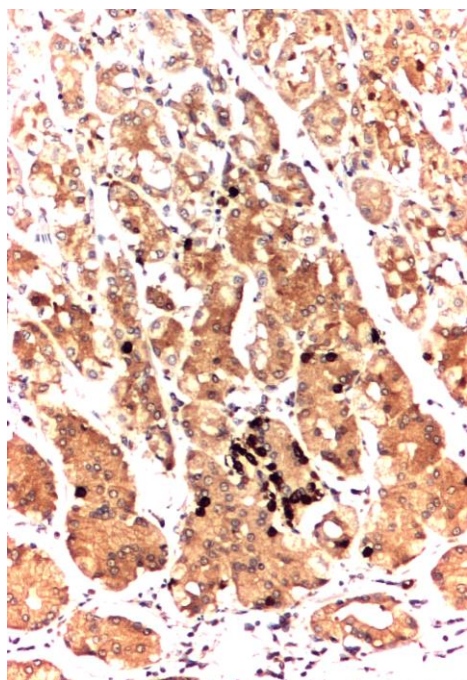


Figure 26: Superficial chronic gastritis, fundic region, with high number (28) of GPC (Anti-ghrelin antibody immunomarking,  $\times 100$ ). GPC: Ghrelin-producing cells.

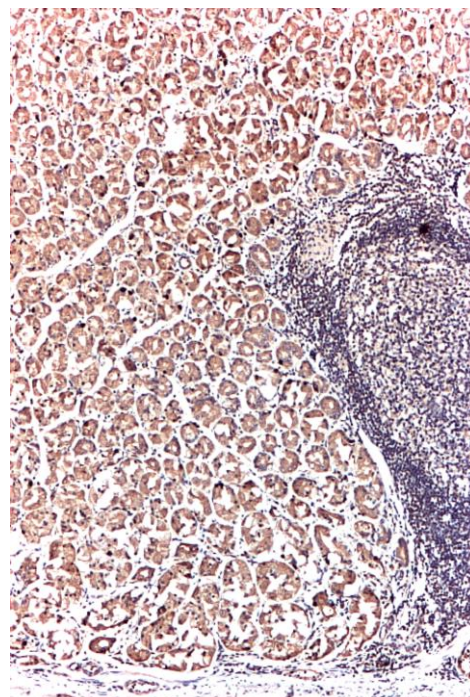


Figure 27: Profound chronic follicular gastritis, body region, with moderate number (12) of GPC (Anti-ghrelin antibody immunomarking,  $\times 40$ ). GPC: Ghrelin-producing cells.

Table 17: The number of GPC according to patients' gender and gastric region

Characteristics	Unit	Total	Women (16; 76.2%)	Men (5; 23.8%)	<i>p</i> *
GPC average no. in fundus	mean $\pm$	14.85 $\pm$	16.05 $\pm$	11.04 $\pm$	<0.001
	SD	7.02	7.49	3.47	
	min.; max.	4.4; 31.2	4.4; 31.2	5.6; 15.2	
GPC average no. in body	mean $\pm$	16.6 $\pm$	17.92 $\pm$	12.36 $\pm$	<0.001
	SD	7.2	7.2	5.9	
	min.; max.	3.6; 28.2	6; 28.2	3.6; 18.4	
GPC average no. in antrum region	mean $\pm$	13.75 $\pm$	13.83 $\pm$	13.48 $\pm$	<0.001
	SD	8.12	7.17	11.7	
	min.; max.	3.8; 33.6	3.8; 28.8	4.6; 33.6	
Total average GPC	mean $\pm$	15.06 $\pm$	15.93 $\pm$	12.29 $\pm$	<0.001
	SD	5.97	5.77	6.4	
	min.; max.	4.6; 23.26	6; 23.26	4.6; 21.93	

GPC: Ghrelin-producing cells; SD: Standard deviation; \*Comparison between regions.

In the study group the mean plasma acyl ghrelin level was 14.95 pg/mL [95% confidence interval (CI) 4.88– 25.02], a slightly lower level being found in women compared to men – 14.37 pg/mL (95% CI 2.77–25.96) and 16.82 pg/mL (95% CI 15.24–48.88), respectively, without significant correlation between gender ( $p > 0.05$ ). No significant correlations were registered between the acyl ghrelin level and anthropometric parameters, or GPC, except for patients' age ( $r^2 = -0.437$ ,  $p = 0.048$ ).

#### 4.2.5. Discussions

Clinicians need a rapid and cost-efficient algorithm for the detection of *H. pylori* infection. The histological diagnosis is used as the main diagnosis method in symptomatic

patients, but also as a screening method in areas with high prevalence of infection. The correct histological diagnosis is also very important in clinical practice to evaluate the efficiency of treatment.

There are several techniques for *H. pylori* infection detection, some of which are non-invasive [for instance the fecal antigen test, the serological diagnosis or the urea breath test (UBT)], other invasive (the histological examination, rapid urease test (RUT), microbiological culture and polymerase chain reaction (PCR)] due to the need of gastric mucosa biopsy taken during gastroscopy [Malfertheiner, 2015]. Numerous factors can influence the choice for the test used in the detection of infection, for example the sensibility and specificity of the test, the clinical circumstances (which could be extremely variable), or the cost efficiency of the test used. Furthermore, each of these tests has its own limitations.

The histological diagnosis is performed on gastric biopsy samples, allowing further for the description and classification of the inflammatory lesions of the gastric mucosa, which is frequently associated with *H. pylori* and will influence the risk of developing gastric cancer through their severity and extension. The endoscopic findings and the microscopic examination of the biopsy sample allow for a complete assessment of the gastric mucosa and also, if the case, for the diagnosis of asymptomatic premalignant gastric lesions. The contribution of an experienced pathologist and the quality of the gastric mucosa biopsy are two essential requirements for the correct histological examination. Incorrect or insufficient biopsies, sampled only from the corpus and not from the antrum, the reduced density of the *H. pylori* colonies, their distribution and type of staining used, previous treatment with proton pump inhibitors, could lead to false negative results. Despite these limitations, the histological examination is generally considered as the gold standard in the direct detection of *H. pylori* infection and it is also the oldest used method.

In our study, the histological examination for the detection of *H. pylori* was performed for all included patients, twice: first time preoperatively, in the biopsy taken by gastroscopy, and second time in the stomach fragment removed by surgery, therefore after the *H. pylori* eradication treatment, when needed. The results showed that, prior to surgery, 51.4% of patients had *H. pylori* infection and all were treated, and in the resection piece, only 11.4% of patients were positive for *H. pylori*. Among them, only one patient had undergone the eradication treatment. The others had not been previously been diagnosed with *H. pylori* infection, meaning that they were probably infected in the time between preoperative evaluation and surgery or they had paucibacillary forms before surgery and could not be diagnosed on the gastric biopsy. However, in all of these patients, the *H. pylori* colonies were rare or isolated.

In patients who are not subjected for gastroscopy, the most used and easy method for diagnosis is serological, assessing the level of anti-*H. pylori* IgG antibodies. There is currently a wide range of commercially available kits, and the tests are cheap and easy to use. However, this method cannot differentiate between active infection and asymptomatic colonization, or between current or previous infection. The level of antibodies could remain high even a few months after the eradication of infection, which makes this test unsuitable for assessing the efficiency of treatment. However, serological tests remain useful in identifying patients at high risk of developing gastric cancer, which depends on the degree of gastric atrophy and intestinal metaplasia and the majority of authors conclude that the serological diagnosis is still useful as screening in epidemiological studies.

In our study, the macroscopic aspect of the stomach during gastroscopy was normal in 50% of those without anti-*H. pylori* antibodies and in only 17.6% of those with anti-*H. pylori* antibodies; also, congestion was present in 33.3% of those without antibodies, and in 67.6% of those with antibodies, with a statistical significant difference ( $p=0.048$ ). We could, therefore, suggest that the presence of congestion at gastroscopy and anti-*H. pylori* antibodies in the same patient are sufficient argument to start eradication treatment, without the need of

biopsy, which could be a useful algorithm for those centers with no possibilities for pathological examinations.

Bacterial culture from the gastric biopsy is considered being the definitive proof of *H. pylori* infection, but, due to technical difficulties, the sensibility and specificity of the test could vary extremely, as greatly as to 42% and it is therefore not considered to be the gold standard. The method would allow for the in vitro assessment of sensibility/resistance of certain antibiotics, when it is necessary to use the second line of treatment after failure to eradicate the infection first time. However, in clinical practice, other easier and less invasive tests are used. UBT has a higher sensibility and specificity compared to other invasive test, but its specificity declines when other urease-producing bacteria are found in the intestine.

The interest for comparing different methods of diagnosis of *H. pylori* infection exists ever since the 1980s. A study published in 1997 compared the serological assessment of anti-*H. pylori* IgG antibodies (through ELISA – enzyme-linked immunosorbent assay) and the histological examination of the gastric biopsy (Giemsa staining) with the microbiological culture (as reference). The results showed that the serological diagnosis, as a non-invasive method, has a high agreement with the positive results from the invasive examinations. Another similar study compared the serological method for detection of *H. pylori* infection with the histological method, and found statistically significant differences ( $p < 0.001$ ) between the two tests, similar to ours: 63.3% of patients had high levels of antibodies, but only 47.9% had the histological diagnosis of *H. pylori* infection. The authors found that these differences were maintained after adjustment for age, race and gender, and the use of antibiotics was associated with a significant reduction in the prevalence of *H. pylori* infection. The results allowed the authors to conclude that the serological method reports a higher prevalence of *H. pylori* infection compared with the histological method, and suggested the efficiency of antibiotic treatment for the eradication.

In a more recent study, Shin [Shin et al., 2012] was the first to underline the association between metabolic syndrome and *H. pylori* infection, diagnosed through serology and histology. However, focusing on the means of detection of *H. pylori* infection, we noticed that their results were similar to ours: the authors found a kappa agreement coefficient of 0.69, whereas in our study found, it was equal to 0.686. Moreover, the limitations of this quoted study were that it was a retrospective study on a large group of patients, but with missing values in some patients (some did not perform gastroscopy, histological data were not available in all), whereas our study is prospective and has data in all patients for both methods for diagnosis.

A study from 2013 published the results from 91 patients referred for routine gastroscopy [Khalifehgholi et al., 2013], which showed that the prevalence of *H. pylori* infection was 50.5% in the histological examination, and the serological method showed the poorest specificity and accuracy compared to other tests. However, we should acknowledge the fact that symptomatic patients and those previously treated with antibiotics were excluded from the analysis. The results of this study allowed for a classification of the tests used to detect *H. pylori* infection, according to their accuracy, and considered that the histological method is more suitable than serology. The authors concluded that, although invasive, the biopsy is to be preferred to serology, but even proposed that the two methods be combined in confirming the diagnosis of *H. pylori* infection.

Regarding patients with morbid obesity referred to bariatric surgery, studies report very different prevalence of *H. pylori* infection, between 11% and 85%, but higher than in similar non-obese populations. The large differences between prevalence, found in literature, could be partially explained by the different methods used to detect the infection or by the study methodology (prospective versus retrospective studies). Our study showed a prevalence of 58.6% of *H. pylori* infection (using the serological method of diagnosis), and 51.4% (using the histological method), which are considered high prevalence for this type of population.

A retrospective study, which included 680 patients who underwent laparoscopic sleeve gastrectomy, reported a 7.8% prevalence of *H. pylori* in the resected stomach pieces [Almazeedi et al., 2014], lower than our results, where 11.4% of patients presented *H. pylori* in the resected stomach. Furthermore, the authors did not observe an increase in the risk of post-operative complications in patients which presented *H. pylori*, meaning that the presence of infection was not a post-operative risk factor. Similarly, to the conclusions of these authors, we did not observe early post-operative complications in our study group, neither in patients with *H. pylori* infection nor in those without.

Our results showed that patients with anti-*H. pylori* IgG antibodies had an odds ratio of 32.667 (95% CI 7.311– 145.956) of having *H. pylori* infection at the histological examination. Also, the serological diagnosis had a sensibility of 90.3% and specificity of 77.8%. Therefore, taking into consideration all above-mentioned data, we could suggest that a reasonable algorithm for assessing patients with morbid obesity prior to bariatric surgery is that the histological examination of the endobiopsy is to be performed only in those with positive *H. pylori* infection at serology. However, gastroscopy should be performed in all patients referred to bariatric surgery, in order to assess other possible gastric pathological findings.

To the best of our knowledge, this is the first study to evaluate the concordance of two diagnostic tests for *H. pylori* infection in asymptomatic morbidly obese patients referred to bariatric surgery in our country. Also, as an absolute novelty, we showed data not only on both methods of diagnosis (serological and histological), but also on the histological aspect of the resected stomach, as a measure of therapeutic efficiency. There are several strengths to our study. First of all, our study is prospective. Secondly, all subjects were asymptomatic, and they all underwent the same common algorithm of preoperative assessment, by the same examiners, including the fact that the two diagnosis tests for *H. pylori* infection were performed in all patients, by the same specialists. Thirdly, all patients who were *H. pylori* positive in the histological test followed the same eradication treatment regime (the triple therapy). This allowed for a thorough and correct interpretation of results.

The limitations of our study consist in the lack of adjustment of the results according to dietary factors, socio-economic status or previous treatment with proton pump inhibitors, which was not possible due to the relatively small number of subjects for this sort of statistical procedures. Also, for the histological diagnosis of *H. pylori* infection, only one method was used.

Published data on the distribution of ghrelin producing cells are not uniform. The highest number of GPC was reported in the upper part of the stomach, fundus, or gastric body [Kim et al., 2012; Takiguchi et al., 2012]. In our study on obese subjects, the main location of GPC was in the gastric body, with statistically significant differences between the number of the cells present in this site and fundus and antral region, respectively. Relatively few data are available in the literature on the number of GPC in the stomach of obese patients. A study on 18 morbidly obese patients who underwent metabolic surgery showed hypoactivity of gastric X/A-like cells in the obese group compared to controls [Dadan et al., 2009], the interpretation of these results suggesting the existence of an adaptive mechanism in obese people, which decreases ghrelin levels and thus food intake in order to restore the body's energy balance. In 2012, Goitein et al. published the results of a study on plasma ghrelin level, distribution of ghrelin messenger ribonucleic acid (mRNA) expression by reverse transcription polymerase chain reaction (RT-PCR) and distribution of GPC by immunohistochemistry in resected stomach specimens from 20 morbidly obese patients who underwent sleeve gastrectomy [Goitein et al., 2012]. The results showed that the expression of ghrelin mRNA decrease gradually from the fundus towards the preantral region.

The prevalence of GPC shared the same pattern, with the highest percentage of positive ghrelin cells in the fundus, intermediate in the body, and the lowest in the preantral

region ( $p=0.08$ ). Similar results were also obtained by Abdemur et al., who reported a higher number of GPC in the gastric fundus compared to the body and antral region in obese patients who underwent metabolic surgery [Abdemur et al., 2014]. Our results complete the ongoing profile of GPC in obesity, while we demonstrated an inverse correlation between their number and the anthropometric parameters (namely weight, BMI and WC).

Our results also show gender differences in the number of GPC, data in agreement with those obtained by a group of Turkish authors who showed that the number of ghrelin immunopositive cells was higher in women ( $p=0.007$ ) [Gündoğan et al., 2013]. The authors showed an increased number in the fundus proximal body vs. distal body ( $p=0.0001$ ), consistent with our findings. Surprisingly, the results of the plasma acyl ghrelin analysis were not concordant with those obtained through the immunohistochemical assessment of GPC; we cannot demonstrate correlations between the plasma acyl ghrelin level, the patients' gender or the specific parameters for obesity.

Data on the relationship between *H. pylori* infection and plasma ghrelin level are controversial. Thus, some authors reported that *H. pylori* infection is associated with a significant decline in plasma ghrelin level, and plasma ghrelin level increases after *H. pylori* eradication, while other studies show that plasma ghrelin level is higher in patients with *H. pylori* infection or ulcers and the eradication of *H. pylori* infection would be associated with reduced plasma ghrelin levels, or even that there is no relationship between *H. pylori* infection and ghrelin level. These contradicting results may be explained by the differences in study population cohorts, inclusion criteria, methods of *H. pylori* infection diagnosis, etc. as well as by the fact that most studies measured total ghrelin levels rather than active acyl ghrelin. The study by Campana et al., published in 2007, showed that plasma acyl ghrelin level is higher in patients with chronic atrophic gastritis [Campana et al., 2007]. This opposite dynamic of acyl ghrelin compared to plasma total ghrelin level could be a compensatory increase in plasma active ghrelin level in response to gastric atrophy. Moreover, a recent study showing that plasma acyl ghrelin levels have increased one year after *H. pylori* eradication and the expression of gastric pre-proghrelin mRNA was upregulated [Choi et al., 2016].

Moreover, the literature focusing on the relationship between *H. pylori* infection and the number of GPC in the stomach is rather scarce. Published studies suggest that *H. pylori* infection causes a decrease in the number of ghrelin-immunoreactive cells in the oxyntic mucosa both in normal weight and obese patients, and the number of GPC and plasma ghrelin levels increase significantly after *H. pylori* infection eradication, thus confirming the hypothesis according to which the reduced number of GPC in the gastric mucosa due to *H. pylori* infection causes a decrease in plasma ghrelin level [Paoluzi et al., 2013; Danciu et al., 2016].

Our results are consistent with the findings reported in the literature, and show that the number of GPC is lower in *H. pylori*-infected individuals and in those with gastritis lesions, the number of cells being lower the greater the depth of gastritis. Also, our results confirm that the density of ghrelin immunoreactive cells was higher in the oxyntic mucosa of *H. pylori*-negative compared with *H. pylori*-positive patients, those with morbid obesity included. The decrease in the number of GPC is more significant in patients with severe glandular atrophy and intestinal metaplasia of the gastric body mucosa.

There are many studies on *H. pylori* and bariatric surgery, that have been published after we communicated our results. For instance, a Turkish team investigated the incidence of *H. pylori* infection in patients undergoing endoscopy and in patients undergoing LSG surgery, in a retrospective study [Turan and Kocaöz S, 2019]. Starting from the idea that despite a high prevalence of *H. pylori* detected by immunohistochemistry in resected gastric specimens, the postoperative prevalence of *H. pylori* is lower when detected by urea breath

test. The prevalence found in their study was lower (50.1%) compared to our study, although the methods they used (Giemsa staining on gastric endoscopic biopsies) was the same as we used. On the other hand, *H. pylori*-associated chronic gastritis was diagnosed in 31.42% of the patients with laparoscopic sleeve gastrectomy (LSG). These rates are similar to those already published in literature (between 10 and 44%), although other researchers have found to be lower in patients undergoing LSG, but failed to find a significant correlation between obesity and *H. pylori* prevalence [Xu et al., 2017].

Interestingly, although in our daily practice and according to the European Association of Endoscopic Surgery (EAES) guidelines, the gastroenterologists perform preoperative gastro-endoscopy in order to identify an acute form of *H. pylori* gastritis and avoid surgery in this context, there are opinions, including the above-mentioned Turkish team that do not recommend to routinely perform EGD on patients preoperatively because it was not shown to be associated with symptoms in the postoperative period [Loewen et al., 2008]. They rely on their observation that there is no significant difference in the rate of *H. pylori* before and after LSG surgery and on the lack of significant correlation between *H. pylori* and excess weight or between *H. pylori* and symptoms in the postoperative period [Turan and Kocaöz S, 2019].

As a consequence of the obesity incidence increasing, also the obesity surgery increased as a treatment method, mostly in morbid obesity patients. LSG is the only technique which permits histopathological examination of the stomach, still, studies assessing the pathological changes in resected stomachs and correlations with other patients' characteristics are very few. A recent study realized in United States on 649 patients found that less than 10% of the patients associated chronic non-specific gastritis, while infection with *H. pylori* was identified in less than 5% [Ge et al., 2019]. In our patients, about half had chronic gastritis before surgery and the *H. pylori* infection was double (11.4%) than in the American study. The differences could be explained by the techniques used preoperatively to identify the infection with *H. pylori*. We used serology tests and Giemsa on gastric endobiospy, while the above-mentioned study used only serology, due to insurance reasons. It is very likely that using two methods, including the golden standard (histological examination) increases the sensibility and decreases the rate of false negative results.

Our results are similar to those published before or after us showing that the incidence of abnormal changes ranges between 20-50%. Most often, was identified non-specific gastritis (7.2–44%), followed by *H. pylori* associated chronic gastritis (2.7–18%) [Viscido et al., 2017; Kopach et al., 2017]. An interesting direction was to assess the outcome of patients in relation with their preexisting hyperlipidemia or systemic hypertension. Ge et al. found that patients with hyperlipidemia had higher odds of presenting with abnormal findings in their stomachs, while patients with hypertension presented lower odds of presenting with abnormal findings in their stomachs [Ge et al., 2019]. The authors could not find an explanation for these associations.

More recent studies sustain that *H. pylori* induces different biological effects on some hormones (e.g., ghrelin, leptin) resulting in the control of both appetite and growth [Aimasso et al., 2019]. The effect depends mostly on the duration of infection and on the treatment. It would be interesting to assess the nutritional effects of *H. pylori* infection in patients after LSG, correlated with ghrelin status.

## Final remarks

The discovery of *H. pylori* infection changed the view on chronic gastritis and other risk factors for cardiometabolic diseases and cancer. Obese patients, already at high cardio-metabolic risk, have higher prevalence of *H. pylori* infection. This is to be seriously

considered when referring patients for bariatric surgery. However, the lack of international agreement in regards to the algorithm for detection of *H. pylori* infection in bariatric patients creates difficulties for the multidisciplinary obesity surgery teams.

The results of our first study confirm the high prevalence of *H. pylori* infection in asymptomatic obese patients referred for laparoscopic sleeve gastrectomy. We found a high correlation between the serological and histological detection of *H. pylori* infection. However, as gastroscopy should be performed in all patients referred to surgery, our data favor the histological evaluation of all patients followed by the eradication treatment.

The second study assessed the ghrelin producing cells in obese subjects, showing a higher number in women than in men, a predominant distribution in the gastric corpus, being correlated with anthropometric parameters (such as, weight, BMI, WC), presence of *H. pylori* infection and gastritis. These results help a deeper understanding of the ghrelin involvement in the obesity pathogenic mechanism, associated or not with other gastric pathologic conditions.

### **4.3. The role of adipose-derived stem cells in an experimental rat model wound healing**

#### **4.3.1. Introduction**

Depending on the size and on the repairing process, burn lesions influence daily life quality. In the past two decades, new solutions such as mesenchymal cell based (adipose-derived stem cells [ADSCs]) tissue engineering substitutes or paracrine-fashioned therapies were applied extensively in laboratory or clinical trials [Klinger et al., 2008; Hu et al., 2013]. Adipose-derived stem cells and adipose tissue have an important role in the complex wound repair processes, which include inflammation, granulation tissue, and remodeling. It was demonstrated that adipocyte lineage cells or subcutaneous injections with adipocytes are activated in the early phases of wound healing and could promote the appearance of scar tissues [Klinger et al., 2008]. During healing of skin burns, the adipocytes interacts with fibroblast and extracellular matrix deposition leading to a normal regeneration. In the absence of adipocytes, these interactions are abrogated, and abnormal dermal remodeling during conjunctive repair of the lesion appear [Schmidt and Horsley, 2013]. Since fat grafting accelerates wound healing around the injection sites, their role is evident, but the exact mechanisms of action will have to be defined in the future. The main effectors from the injected fat (adipocytes and ADSC) stimulate the wound healing. ADSCs can differentiate in vitro into adipogenic cell-lines and, eventually, adipocytes. It is unclear if these mature adipocytes retain the wound healing abilities of their precursor ADSCs. Various in vitro adipogenic differentiation protocols are available at present, using maintenance medium recipe (Dulbecco's modified Eagle's medium [DMEM] plus 10% fetal bovine serum [FBS]), or other mixtures inducers for adipogenic differentiation [Scott et al., 2011]. At high concentration, dexamethasone (an anti-inflammatory steroid) enhances adipogenic differentiation. Also, insulin (a peptide hormone which controls the metabolism of carbohydrates and fats) and 3-isobutyl-1-methylxanthine (IBMX, a competitive, nonselective phosphodiesterase [PDE] inhibitor) are the main regulators of peroxisome proliferator-activated receptor- $\gamma$  (PPAR- $\gamma$ ) and/ or CCAAT/enhancer-binding protein- $\alpha$  activation, leading to adipogenic gene expression [Gabrielli et al., 2014]. Despite the continuous growing data in literature on adipogenic inducers functions and mechanisms, there is no unanimously accepted standardized protocol for selections of inducers and culture duration aiming the adipogenic differentiation. Adipocytes proliferation and maturation depends on

the type of adipogenic differentiation inducer, and this may indirectly influence the role of differentiated adipocytes during skin wound healing.

### 4.3.2 Aims

The purpose of this study was to investigate the effects of adipocytes originating from adipose-derived stem cells during healing of skin burn wounds in a rat model compared to ADSC and fat injection control groups. We also aimed to investigate whether different adipogenic induction protocols affect their capacities in wound healing, by analyzing the morphological changes and cell proliferation capabilities of differentiated adipocytes in mixed cultured with alternative adipogenic cocktail inducers (IBMX and/or insulin). In addition, the effects of differentiated adipocytes (cocultured under different adipogenic protocols) on wound healing were compared with ADSC and fat injection (prepared by Coleman technique) groups. Through this study, we targeted to standardize an in vitro adipogenic differentiation protocol for burn wound healing in a rat experimental model.

### 4.3.3. Materials and methods

#### *Animals*

Animal experiments were conducted in accordance with the Guide for the Care and Use of Laboratory Animals from the National Research Council (United States) and following the protocols approved by Grigore T. Popa University of Medicine and Pharmacy, Iasi, Romania.

#### *Isolation and Culture of Adipose-Derived Stem Cells*

The inguinal fat pads from male adult Wistar rats (procured from the animal farm of Grigore T. Popa University of Medicine and Pharmacy) were harvested in a sterile fashion and washed with sterilized phosphate-buffered saline (PBS) with 5% penicillin–streptomycin (500 UI/ml Penicillin, 500 mg/ml streptomycin). The protocols used for isolation and culture of ADSCs were as follows: the fat pads were minced and digested with 2 mg/ml of type IA collagenase (C9891, Sigma–Aldrich, St. Louis, MO, United States) for 30 to 45 minutes at 37°C. After centrifugation, the pelleted stromal vascular fraction containing ADSCs was resuspended, passed through a 70-µm cell strainer (#352350, Becton, Dickinson and Company, Franklin Lakes, NJ, United States), and incubated in stromal medium (low-glucose DMEM [D6046, Sigma–Aldrich] supplemented with 10% FBS and 1% penicillin–streptomycin) at 37°C in 5% CO<sub>2</sub> atmosphere. The medium was renewed every 2 to 3 days until the cells reached a confluence of 80 to 90%. Cells were then detached by the application of trypsin–EDTA for subculture.

#### *Induction of Adipogenesis*

In view of the existence of diverse protocols for adipogenic differentiation,<sup>11</sup> we established six separate conditions in order to observe the discrepancies of morphological changes, proliferation abilities, and the capacities in wound healing between different adipogenic inducers. Shortly, ADSCs (passage 2–3) were seeded at the density of 10,000 cells/cm<sup>2</sup> with the stromal medium in a six-well plate on day 0. After washing with PBS, basal differentiation medium (high-glucose DMEM [4500 mg/L glucose]+10% FBS + 1% P–S + 0.5 µM dexamethasone [H02AB02, Medochemie LTD., Limassol, Cyprus] + 50 µM diclofenac sodium [M01AB05, Salutas Pharma GMBH, Frankfurt am Main, Germany]) plus different adipogenic cocktail inducers were replenished starting from day 1: +IBMX–INSULIN, 0.5 mM IBMX (I5879, Sigma–Aldrich) only; +IBMX+INSULIN, 0.5 mM IBMX+200 mUI/ml insulin (Insulin Humulin R, A10AB01, Lilly France SAS, Neuilly-sur-

Seine Cedex, France); –IBMX+INSULIN, 200 mUI/ml insulin only; +IBMX(D1–5)+INSULIN, 0.5 mM IBMX + 200 mUI/ml insulin for 5 days and thereafter 200 mUI/ml insulin only for the rest of days 11; LOW DMEM, low-glucose DMEM (1000 mg/L glucose); HIGH DMEM, high-glucose DMEM (4500 mg/L glucose). The differentiation media were renewed once every 3 days until adipocytes were developed (day 11). On day 11, cells were fixed with 10% formalin solution and air dried for fat staining. A 2% of Sudan IV (S4261, Sigma–Aldrich) was applied for neutral lipid staining followed by a counter staining the nuclei with Mayer’s hematoxylin solution (MHS16, Sigma–Aldrich).

#### *In vitro Morphological and Proliferation Changes During Adipogenic Differentiation*

The photos of morphological changes in diverse adipogenic cocktails were taken sequentially on day 1, 3, 6, 9, and 11 by using a phase contrast microscope with a digital single-lens-reflex camera at 200 folds of magnification. Cell numbers between different adipogenic protocols were calculated by two investigators who were blind to group assignments.

#### *Skin Burn Model and Wound Healing Assessment in Rats*

Adult Wistar male rats weighing between 250 and 300 g were anesthetized using 3 to 4% isoflurane inhalation (N01AB06, Rompharm Company S.R.L., Otopeni, Romania) and the anesthesia was maintained with 1 to 2% isoflurane when performing burn infliction. The dorsum of the rat was shaved and a 3-cm-diameter burn wound was inflicted using hot steam for 2 seconds directed toward the skin through an electrovalve and a round-shaped rubber funnel. Immediately after skin burn infliction, 12 rats were randomly divided into 4 groups. To allow equal distribution, each rat received a total 1 ml of liquid divided in four cardinal points (ie, 0.25 ml/point) in the subcutaneous tissue under the burn wound. Group 1 (control) received PBS injection only; group 2 (+ADSCs) received a total of 1 million of ADSC injection; group 3 (–IBMX+INSULIN) received a total of 1 million ADSC-origin differentiated adipocytes pretreated with 200 mUI/ml insulin without IBMX for 11 days; and group 4 (+IBMX[D1–5]+INSULIN) were injected with ADSC-origin differentiated adipocytes ( $1 \times 10^6$  cells) cocultured with 0.5 mM IBMX and 200 mUI/ml insulin for 5 days and 200 mUI/ml insulin only thereafter for the next 6 days. Visual macroscopic changes were documented using photographs taken with a single-lens-reflex camera at day 0, 7, 12, 14, 16, 18, and 21 after burn infliction. Actual wound size (cm<sup>2</sup>) was calibrated and analyzed using Image J software in accordance with the scale in each image. Differences between the wound areas were measured by two investigators who were blind to group assignments. In addition, 4-mm-diameter punch biopsies were taken from the cardinal points of the burn wounds and fixed in 10% neutral formalin solution for further histological analyzes. After fixation for 12 hours, biopsies were routinely processed by paraffin embedding. Four-micrometer thickness hematoxylin and eosin stained sections were independently evaluated by two pathologists.

#### *Fat Injection (Coleman Technique) in Skin Burn Wound Healing Model*

In order to evaluate the effects of fat tissues on burn wound healing (as a comparative control to ADSCs or differentiated adipocytes), inguinal fat pads harvested from rats (n = 3) were washed with saline and minced using iris scissors until they became gel-like in appearance. Followed by suction through a 1-mm cannula into 10 ml syringes, the gel was centrifuged at 200 rpm for 2 minutes. The supernatant containing the fat was discarded, and then  $10^6$ /ml of the cell suspension aliquot was injected 0.25 ml at each cardinal point under the burn area in the subdermal plane. The follow-up procedures for rats were similar to cell-injected groups.

#### *Statistical Analysis*

The statistical software SPSS version 13.0 was used for data analysis. The results were expressed as mean  $\pm$  SD. A 6 (differentiation protocols)  $\times$  5 (time sample points) repeated measures analysis of variance and Bonferonni post hoc comparisons were used to analyze the ability of cell proliferation in different adipogenic differentiations. In addition, a

5 (differentiation protocols)  $\times$  7 (time sample points) repeated measures analysis of variance and Bonferonni post hoc comparisons were used to evaluate the effects of ADSCs, differentiated adipocytes (with or without IBMX), and fat injection on skin burn wound healing. The significance level was set as  $P < 0.05$ .

#### 4.3.4. Results

##### *Morphological Changes During Adipogenic Differentiation*

Under phase contrast microscopy, cultured rat ADSCs showed a spindle-shaped, fibroblastic morphology. In cytochemistry observation, the nuclei of ADSCs were stained with dark blue by hematoxylin, but negative for Sudan IV (scarlet; Figure 28, E5 and F5). No significant morphological differences were found between low-glucose (Figure 28E) and high-glucose DMEM (Figure 28F) groups. ADSCs treated with basal adipogenic medium (high-glucose DMEM + 10% FBS + 1% P-S + 0.5  $\mu$ M dexamethasone + 50  $\mu$ M diclofenac sodium) plus 200 mUI/ml insulin without IBMX (Figure 18C) showed a spindle-shaped morphology and developed significant lipid accumulation in cytoplasm starting from day 6 after the adipogenic induction (Figure 28, C3). However, ADSCs cocultured with adipogenic medium with IBMX but without insulin (Figure 28A) exhibited the least lipid accumulation (Figure 28, A4 and A5). By contrast, spherical-shaped changes were noticed in IBMX-positive groups (+IBMX+INSULIN, +IBMX-INSULIN, or +IBMX[D1-5] +INSULIN, Figure 28A, B, and D), and marked lipid accumulation appeared only after IBMX treatment was discontinued (Figure 28, D4 and D5). Interestingly, larger lipid droplet formation was observed in IBMX-negative group (Figure 28, C4 and C5) than in the IBMX-positive (for 5 days) group (Figure 28, D4 and D5). However, continuous IBMX treatment (for 11 days, Figure 28A, B) not only confined lipid droplet accumulation (Figure 28, A5 and B5), but also accelerated cell detachment (Figure 28, A4-A5 and B4-B5, respectively).

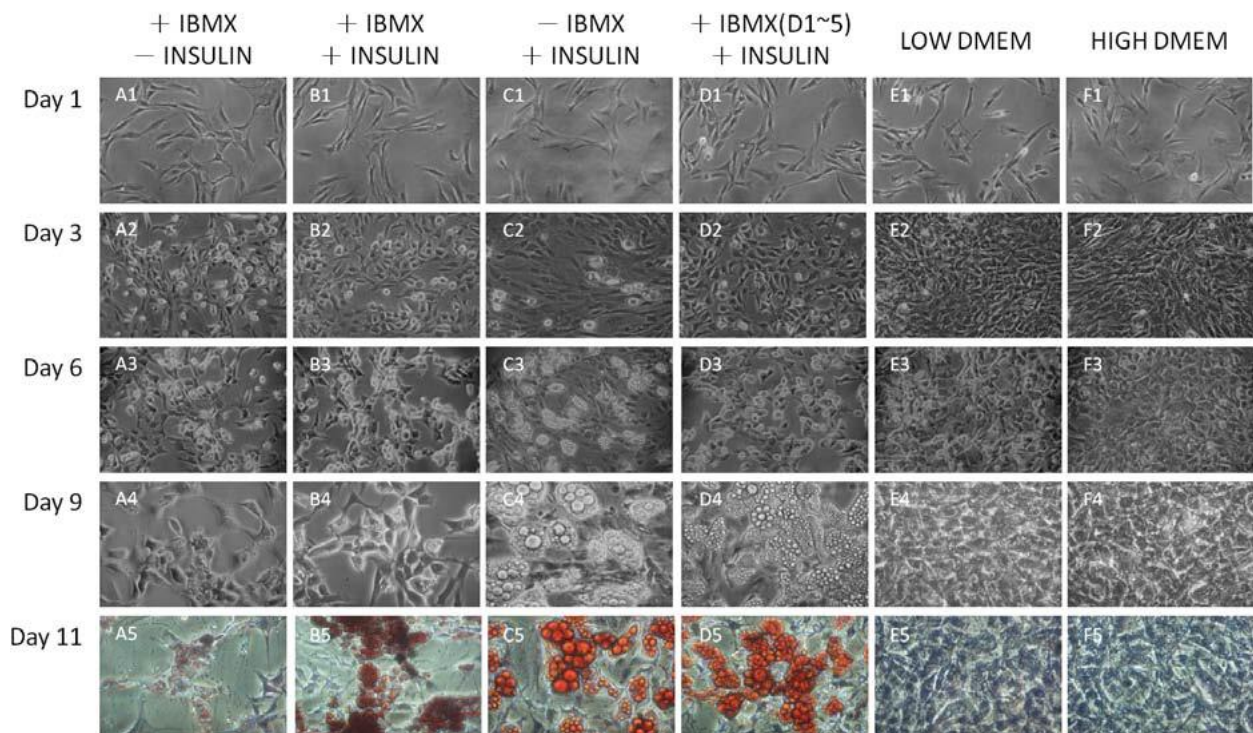


Figure 28: In vitro time course of morphological changes in adipogenesis. The photos of differentiated adipocytes were taken sequentially on day 1, 3, 6, 9, and 11 of adipogenic differentiation by using a microscope with a single-lens-reflex camera at 200 folds of magnification. Photos on day 9 and day 11 were locally magnified in proportion (400 folds) to exhibit comprehensive details of the cells.

### *Proliferation Abilities of Differentiated Adipocytes*

Cell numbers in all groups were significantly increased from day 0 to day 11 (\* $P < 0.001$ , day 1 vs day 3, 6, 9, and 11), but only cells cultured with stromal media (low and high DMEM) continued to proliferate until day 9. Cells cocultured with adipogenic media plus cocktail inducers did not show significant mitotic expansion after day 3 of differentiation (+ $P < .001$ , day 3 vs day 6, 9, and 11). In addition, there were no significant differences of cell proliferation between low- and high-glucose DMEM groups ( $P = 0.517$ ). However, in the group treated with IBMX for 5 days (+IBMX[D1–5]+INSULIN), not only lipid droplets started to accumulated significantly (Figure 28, D4–D5), but also the ability of cell proliferation resumed after discontinuing IBMX treatment on day 6 [ $\ddagger P < 0.001$ , LOW or HIGH DMEM or +IBMX(D1–5)+INSULIN vs +IBMX+INSULIN and +IBMX–INSULIN].

### *Skin Burn Wound Healing*

ADSCs, differentiated adipocytes, and fat tissues promoted skin burn wound healing in rats; differentiated adipocytes and fat grafting accelerated early healing relative to ADSCs. Three-centimeter-diameter dorsum skin burn inflictions were performed on 15 Wistar male rats, and then the rats were randomly assigned to five groups of different cell injections for wound healing assessments: control (PBS-injected), +ADSCs (ADSC-injected), –IBMX+INSULIN (adipocytes pretreated with differentiation cocktails without IBMX), +IBMX(D1–5)+INSULIN (adipocytes pretreated with differentiation cocktails with IBMX for only 5 days), and +fat injection (prepared by Coleman technique). Wound size was calibrated and analyzed by using Image J software in accordance with the scale attached in each photo on day 0, 7, 12, 14, 16, 18, and 21 after burn infliction (Figure 29A).

Overall, the wound healing process was observed early at day 7 after the burn infliction and continued for 3 weeks (day 0 vs day 12, 14, 16, 18, and 21 in all groups,  $P < 0.001$ ). However, ADSC-origin differentiated adipocytes cocultured with IBMX for 5 days (+IBMX[D1–5]+INSULIN) as well as the injected fat initiated wound healing process earlier than all other groups in the first week after burn infliction (day 7), and had achieved significant wound size reduction ( $P < 0.001$ , Figure 29B). Compared with the natural healing process (control group), all other groups exhibited accelerated wound healing on day 12, 14, 16, 18, and 21 after burn infliction ( $P < 0.001$ , Figure 29B). Although burn wounds injected with ADSCs, differentiated adipocytes, or fat tissues (prepared by Coleman technique) expedited wound healing, the changes of wound sizes in these groups did not reach significant differences on day 16 and thereafter ( $P > 0.05$ , day 16 vs day 18 and 21). On the contrary, wound healing process in control group continued markedly to the end of the third week (day 21). Furthermore, for the first 2 weeks, fat-injected group showed the most prominent wound healing capacity compared with ADSCs or ADSC-origin differentiated adipocyte- injected groups ( $P < 0.001$ , Figure 29B). Even though burn wounds injected with adipocytes pretreated with differentiation cocktail inducers without IBMX (–IBMX+INSULIN) demonstrated more potent wound healing capacity than control group (\* $P < 0.001$ ), this group exhibited minor wound healing capacity compared with ADSC-injected, adipocyte (+IBMX(D1–5)+INSULIN)-injected, and fat-injected groups ( $P < 0.001$ , Figure 29B). Histological Evaluation of Skin Burn Wound Healing Four-millimeter punch biopsies were performed from the wounds for all groups on day 12, 14, 16, 18, and 21. Microscopic evaluation revealed that epithelial regeneration was complete in +ADSC and +IBMX(D1–5) +INSULIN samples starting with day 12. In fat-injected rats, the epithelium was uniformly regenerated at day 14. In +IBMX(D1–5) +INSULIN group and in fat-injected group, we observed reduced fibrosis and mild lymphocytic inflammatory infiltration limited to the superficial dermis (maturation and remodeling phase) from day 12 to day 21 (Figure 30), while the fibrosis and the inflammatory infiltration was mild to moderate in +ADSC group (fibroplasia and granulation phase; Figure 30).

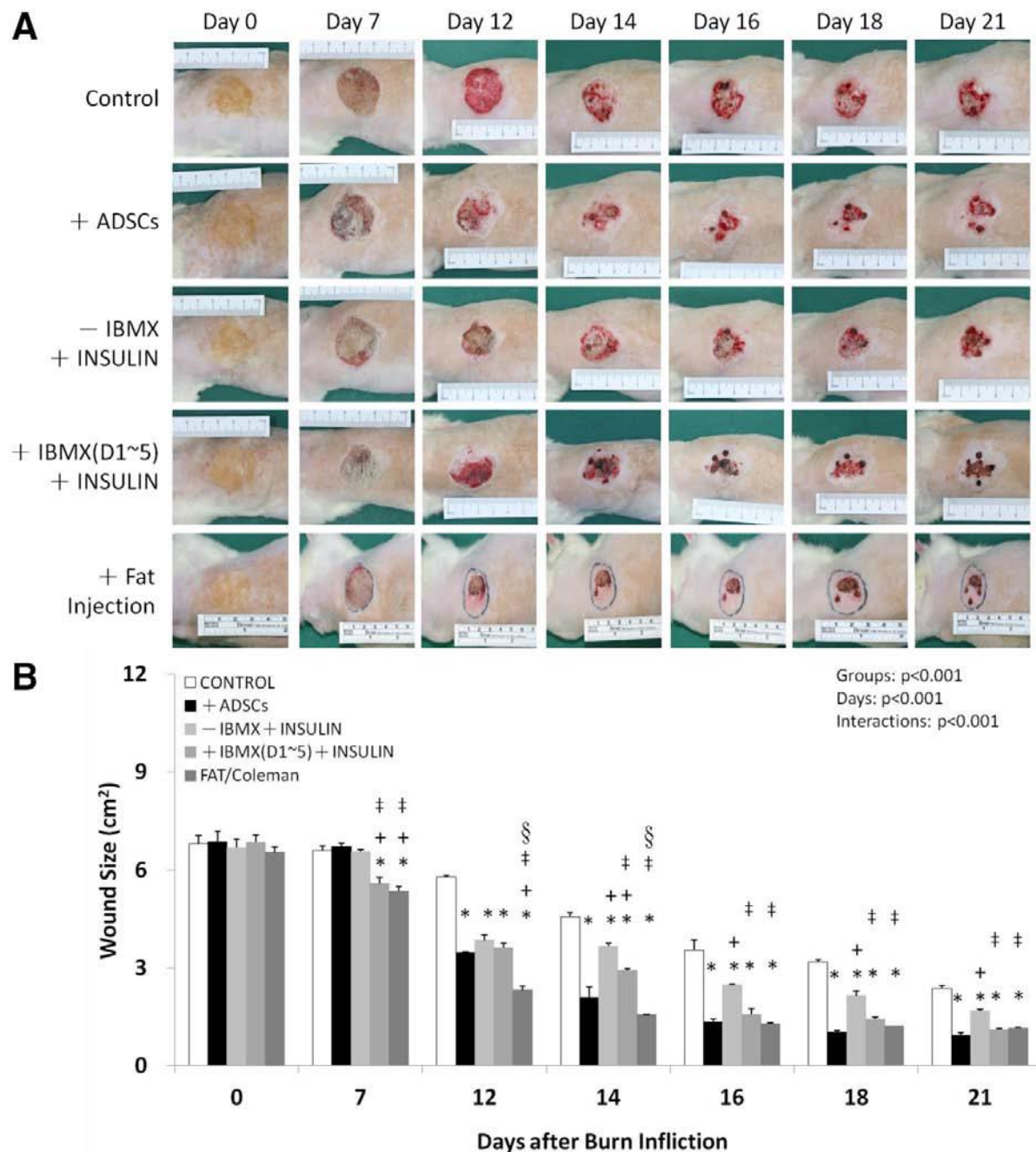


Figure 29: ADSCs, differentiated adipocytes, and fat tissues improved skin burn wound healing in rats, but differentiated adipocytes and fat grafting accelerated early healing process relative to ADSC. Rat skin burns were inflicted as indicated in methodology and then injected with ADSCs, adipocytes pretreated with different cocktail inducers, or fat tissues prepared by Coleman technique. Photos were taken sequentially on day 0, 7, 12, 14, 16, 18, and 21 after burn infliction. A. Representative images of wound healing on day 0, 7, 12, 14, 16, 18, and 21 after burn infliction. B. The unhealed wound sizes (cm<sup>2</sup>) of the control (PBS-injected, blank bar), ADSC-injected (filled bar), adipocyte-injected (without IBMX [light-gray bar] and with IBMX treatment for 5 days [medium-gray bar]), and fat-injected groups (dark-gray bar). Data were expressed as mean  $\pm$  SD (n = 3). \* $P < 0.001$ , control vs all groups; † $P < 0.001$ , ADSC-injected group vs adipocyte- and fat-injected groups; ‡ $P < 0.001$ , adipocytes pretreated without IBMX group vs adipocytes pretreated with IBMX and fat injection groups; § $P < 0.001$ , adipocytes pretreated with IBMX group vs fat injection group.

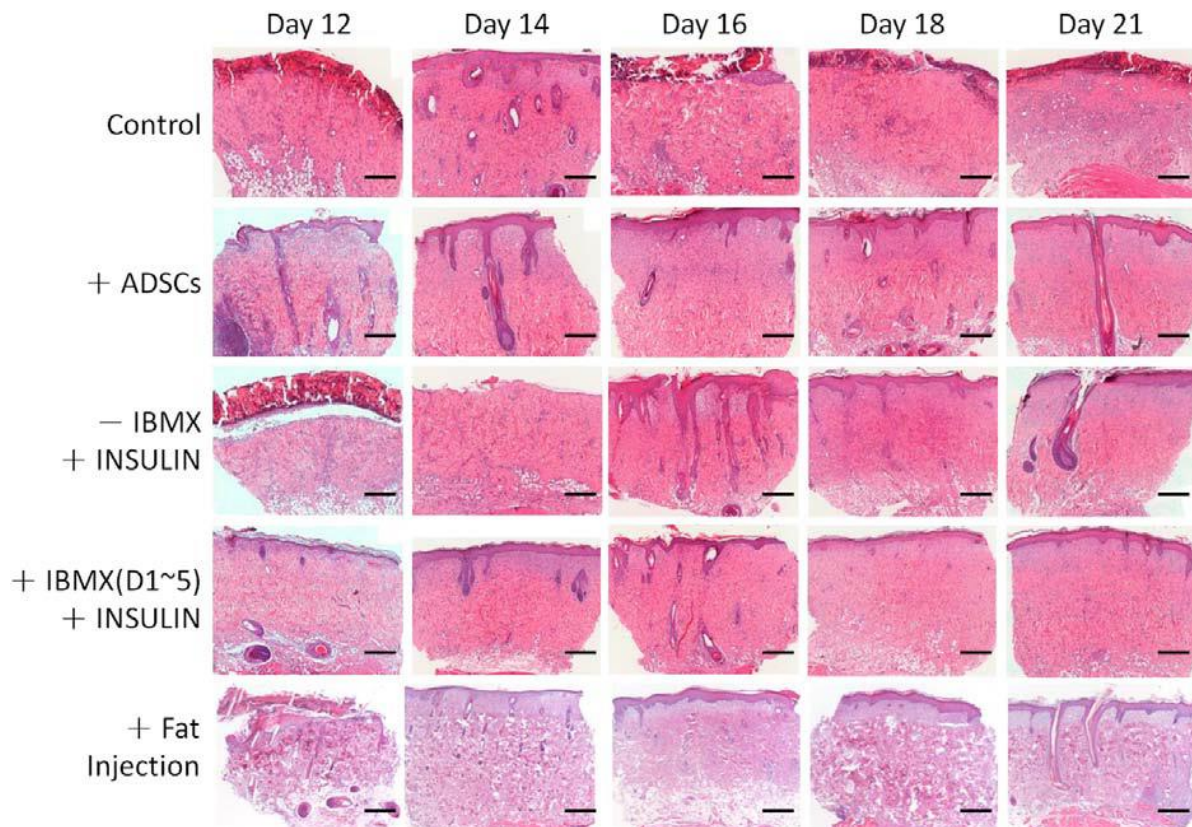


Figure 30: Microscopic evaluation of burn wound healing. Reduced fibrosis and mild lymphocytic inflammatory infiltration limited to the superficial dermis were observed in +IBMX(D1-5) +INSULIN and +Fat Injection groups, while the fibrosis and the inflammatory infiltration were mild to moderate in +ADSC group. In -IBMX +INSULIN group, the healing process was uneven due to delayed reepithelization, and moderate chronic inflammation with dermis and hypodermis infiltration was also noticed. In CONTROL group, large areas with no reepithelization and abundant chronic inflammation were observed. Bar: 500  $\mu$ m.

In -IBMX +INSULIN group, the healing process was uneven, areas with complete reepithelization alternating with areas with no epithelial buds, covered only by fibrino-leukocytic exudates. In addition, the fibrotic changes affected the upper reticular dermis and were accompanied by moderate chronic inflammatory infiltration in dermis and hypodermis (day 12 to day 20; Figure 30). The microscopic results also showed that the morphology in control group was similar to that observed in -IBMX +INSULIN group, except the fact that areas with no reepithelization were more extensive in the control group (Figure 30).

#### 4.3.5. Discussions

To our knowledge, this is the first study to compare the effects of various adipogenic cocktail inducers on the morphological changes, proliferation abilities, and wound healing capacities of adipocytes between different protocols. Our results indicated that among well-known adipogenic inducers (e.g., dexamethasone, insulin, and IBMX), a prolonged treatment of IBMX (with or without insulin for 11 days) resulted in cell deterioration (rounding-up and detachment of cells) and mitotic inhibition. However, a short-term treatment of IBMX (with insulin for 5 days) or a cocktail medium lack of IBMX led to successful adipogenesis. Although ADSCs, adipogenic differentiated cells, and processed fat injection groups achieved similar wound healing results, differentiated adipocytes (+IBMX[D1-5]+INSULIN) and fat injections showed early skin wound healing compared with ADSC injection groups only. Furthermore, ADSC-injected, adipocyte-injected (briefly cocultured with IBMX for 5

days), and fat injected groups exhibited better wound healing capacities than adipocytes treated without IBMX (–IBMX+INSULIN) group.

#### *Morphological Changes and Cell Proliferation*

In view of the existence of diverse protocols for mesenchymal cell–originated adipogenic differentiation, the uses of adipogenic cocktail inducers such as dexamethasone, insulin, and IBMX were mentioned repeatedly [Scott et al., 2011]. Among them, inducers such as insulin and IBMX that are involved in the master regulator of adipogenesis, PPAR- $\gamma$ , are of interest to disparate specialties of medicine [Kim et al., 2010; Gabrielli et al., 2014]. In our study, we used in vitro culture system to test the necessities of these two inducers for primary ADSC-origin adipogenic differentiation. The cytochemistry staining results showed that ADSCs cocultured with adipogenic medium (high-glucose DMEM + 10% FBS + 1% P–S + 0.5  $\mu$ M dexamethasone + 50  $\mu$ M diclofenac sodium) plus 200 mUI/ml insulin without IBMX (Figure 28C) displayed a spindle-shaped morphology and developed significant lipid accumulation in cytoplasm starting from day 6 after adipogenic induction (Figure 28, C3). However, ADSCs cocultured with adipogenic medium with IBMX but without insulin (Figure 18A) exhibited the least lipid accumulation (Figure 28, A4 and A5), implying that insulin played an important role in lipid accumulation. Our findings were consistent with data already published, concluding that insulin regulated the mRNA expression of PPAR- $\gamma$ . Moreover, under the condition supplemented with insulin, the addition of IBMX and the coculture duration with IBMX also affected adipogenesis. Marked lipid accumulation appeared only after IBMX treatment was discontinued on day 6 (Figure 28, D4–D5). When the ADSC-originated cells were cocultured with IBMX for longer period (11 days), signs of cell deterioration such as detachment of the cells from the culture surface were observed (Figure 28, B4–B5). The results indicated that with the existence of insulin, IBMX was also a potent inducer for adipogenesis, but only short-term treatment of IBMX (for 5 days) preserved successful adipogenic differentiation. IBMX is a competitive, nonselective PDE inhibitor, which raises intracellular cyclic AMP (cAMP) and thus activates protein kinase A. Protein kinase A signaling pathway is required for transcriptional activation of PPAR- $\gamma$  and the expression of adipogenic genes [Gabrielli et al., 2014]. Although we have found that either insulin itself or insulin combined with IBMX could regulate adipogenesis, the above-mentioned study found that insulin and IBMX were prerequisite inducers for adipogenic differentiation of 3T3-L1 fibroblasts. Unfortunately, their results were inconsistent with our findings. However, IBMX was not the mandatory component for murine ADSC-originated adipogenesis [Scott et al., 2011]. On the contrary, insulin was widely used to induce proliferation and differentiation of pre-adipocytes [Scott et al., 2011]. The discrepancies of the results between ours and other similar studies [Kim et al., 2010; Gabrielli et al., 2014] may be resulted from the cell types used for adipogenic differentiation. At least for primary ADSCs, a precise identity and heterogeneity are still under investigation. In our study, we discovered that primary ADSCs could be differentiated into adipocytes only by coculturing with insulin and dexamethasone except IBMX, which exhibited similar results to those already published. Besides morphological changes, the abilities of cell proliferation were also varied between different adipogenic inducers. In order to compare the effects of adipogenic inducers on mitotic expansions of differentiated adipocytes, we have calculated cell numbers following the time courses of adipogenic differentiation. Our results demonstrated that cells cocultured with stromal media (low- and high-glucose DMEM supplemented with 10% FBS + 1% P–S) continued to proliferate from day 0 to day 9, but cells cocultured with adipogenic cocktail inducers exhibited growth arrest since day 3 of differentiation (+P < 0.001, day 3 vs day 6, 9, and 11). However, cell growth resumed when IBMX was discontinued. Similarly, by day 2 of the differentiation course, CCAAT/enhancer-binding protein- $\alpha$  protein initiated to accumulate, and after it was phosphorylated by the cyclin D3, a proliferation inhibition effect was induced [Moreno-Navarrete and Fernández-Real, 2012]. Furthermore, a biphasic effect

of IBMX incorporation with insulin depended on the intracellular level of cAMP was noted. In the beginning, the IBMX-potentiated intracellular cAMP accumulation markedly elevated DNA synthesis; once cAMP exceeded a certain level, an inhibition of DNA synthesis was observed, suggesting that cAMP was equipped with both stimulatory and inhibitory effects on the regulation of mitosis. This also explains the abrogation of cell growth in long-term IBMX treatment groups in our study (Figures 28A and B). Nevertheless, the cell growth arrest was reversible upon removal of the PDE inhibitor. Therefore, when IBMX treatment was discontinued starting on day 6 in our study, the ability of cell proliferation of differentiated adipocytes returned, indicating that the inhibition of cell growth was IBMX-dependent.

#### *Wound Healing Capacities*

Due to their adipogenic and angiogenic properties, ADSCs have been widely used in clinical settings for cosmetic or reconstructive surgeries, including as an adjunct to wound healing therapies following thermal injuries [Naderi et al., 2014]. By contrast, intradermal adipocytes were considered harmful for wound healing because of its poor circulation and easy liquefaction, which offered bacteria an excellent environment to propagate and resulted in local and systemic infections. Nonetheless, these traditional concepts have been challenged by the novel discoveries of adipose tissue, including its secretion functions (e.g., cytokines, growth factors, eicosanoids, and more) and potential for skin wound healing [Schmidt and Horsley, 2013]. So far most of the tissue-engineered substitutes for clinical soft-tissue reconstruction involved a concomitant incorporation of ADSCs and adipocytes [Schmidt and Horsley, 2013], an independent functional examination of differentiated adipocytes on wound healing has been missing. Our study compared the effects of ADSCs and differentiated adipocytes on wound size reduction after skin burn infliction, respectively. The results showed that compared with the control group (injection of PBS), subcutaneous injections of ADSCs, differentiated adipocytes (-IBMX+INSULIN and +IBMX[D1-5]+INSULIN), or processed fat under the wound accelerated wound healing after the first week (day 7) of burn infliction and continued for 3 weeks (day 21;  $P < 0.001$  for day 0 vs day 12, 14, 16, 18, and 21 in all groups). Previous studies have proved that the wound healing process was promoted through either direct ADSCs or adipocytes and/or paracrine effects [Morissette Martin et al., 2015]. In the above-mentioned study, the levels of pro-proliferative and angiogenic factors such as vascular endothelial growth factor, hepatocyte growth factor, and leptin were significantly elevated in adipose dressing-containing in vitro culture system, so a paracrine-fashioned mechanism was suggested in skin wound healing. Besides the well-known role in satiety and weight control, leptin also possessed angiogenic activity [Morissette Martin et al., 2015]. In our case, although we did not investigate the hormone levels in burn models, significant weight reduction was observed in adipocyte-injected groups (data not shown), suggesting that adipocyte-secreted leptin (paracrine-fashioned) might be involved in wound healing. According to other published results [Schmidt and Horsley, 2013], adipocytes were also responsible for fibroblast (precursor) proliferation, repopulation, and dermal reconstruction following inflammation during acute skin wound healing, which suggested that mature adipocyte-released adipokines might be the key chemotactic agents for fibroblast recruitment. In the absence of adipocytes, fibroblast and extracellular matrix depositions were abrogated, leading to abnormal dermal remodeling/regeneration at lesion site [Schmidt and Horsley, 2013; Morissette Martin et al., 2015] and our results were consistent with these findings. In our study, ADSCs, differentiated adipocytes, and fat injection accelerated wound healing (\* $P < 0.001$ , control vs. all other groups; Figures 29B and 30), but differentiated adipocyte injection group (+IBMX[D1-5]+INSULIN) as well as fat injection group initiated wound healing process earlier than any of the other groups ( $P < 0.001$ , Figure 29B). Similarly, according to our hematoxylin and eosin observations, we found reduced fibrosis and mild lymphocytic inflammatory infiltration limited to the superficial dermis (maturation

and remodeling phase) from day 12 to day 21 in +IBMX(D1–5)+INSULIN and fat-injected groups, while the fibrosis and the inflammatory infiltration was mild to moderate (fibroplasias and granulation phase) in +ADSC group (Figure 20), pointing out that mature adipocytes, not mesenchymal stem cells (ADSCs), might expedite acute wound healing (at day 7) by promoting fibroblast recruitment [Schmidt and Horsley, 2013]. ADSC-promoted wound healing may be initiated through intercellular and/or paracrine mechanisms as previously mentioned and thus was slightly slower than adipocyte-injected group at the beginning of wound healing. Adipocyte-injected group without coculturing with IBMX (–IBMX+INSULIN) exhibited the least wound healing capacity compared with ADSC-injected and adipocyte-injected groups (+IBMX[D1–5] +INSULIN; ‡P < 0.001; Figures 29B and 30). Short-course IBMX (+IBMX[D1– 5] +INSULIN) have more potent wound healing abilities than IBMX-free differentiated adipocytes (–IBMX +INSULIN). Further research is needed in order to identify the favorable conditioning agent responsible for the increased wound healing ability.

#### *Study Limitations*

This study examined morphological changes, cell growth, and wound healing capacities of ADSCs and ADSC-origin differentiated adipocytes. The results were mainly based on macroscopic and microscopic observations. To obtain a better knowledge in the progress/quality of wound healing, associated mechanisms and the fate of implanted cells, the use of traceable fluorescence-labeled ADSCs and adipocytes as well as corresponding adipokines' measurements or specific fibroblast staining are suggested. Adipocytes cocultured with continuous IBMX (for 11 days) were missing in skin wound healing groups due to their cell deterioration phenomenon during in vitro cell culture. We have excluded the cell toxicity effects of the solvent (DMSO) by coculturing ADSCs with adipogenic cocktail inducers plus DMSO (data not shown). Moreover, ADSCs-plus-adipocytes injection group in wound healing model was lacking. We only replaced such group with fat injection prepared by Coleman technique. Whether ADSCs-plus-adipocytes therapy has synergistic effects in wound repair will be added in future studies.

Similar studies confirmed our results. For instance, the ADSC role in improving the healing process was demonstrated for wounds induced by ischemia, such as: burn wounds [Loder et al., 2015], radiation ulcers [Huang et al., 2013], diabetic wounds or surgical experimental wounds with exposed bone [Hamada et al., 2019]. Blood flow is essential in tissue regeneration because it provides the nutrients and the oxygen, but also the removal of necrotic wastes. Therefore, their presence is mandatory inside the wounds. Concerning the wounds with exposed bone, the blood flow is reduced, yet addition of ADSC increased the number of blood capillaries in the wound, and the wound area decreased faster by healing [Hamada et al., 2019].

The intense reduction of inflammation and fibrosis observed in our study after ADSCs were transplanted into the burn wounds, was confirmed in another study, by seeding of Wharton's jelly stem cells (which is a Wharton's jelly-like matrix of the umbilical cord, a rich source of mesenchymal stem cells) onto the acellular dermal matrix scaffold. The result was an improved angiogenesis with granulation tissue formation, and later on the decrease of inflammation, necrosis and fibrosis after 21 days [Nazempour et al., 2020].

Regarding the reduction of the wound area, similar to our results, a significant reduction in size of the burn wound was observed after transplantation of ADSCs (40.44-84.9%) in comparison with the control group (32.26-69.7%) was observed in other studies published after ours [Motamed et al., 2017; Franck et al., 2019]. Also, after transplantation of mesenchymal stem cells the surface of the necrosis reduced by 20% compared to control groups in acute burn injuries [Imam and Rizk, 2019].

All these studies aim to finding new solutions for wound healing when the lost tissue and the damage are extensive (usually, burn-induced), but also for those lesions in organs and

tissues with limited capacities of regeneration, such are the human teeth and periodontium. Mesenchymal stem cells were the first to be considered a promise for regenerative medicine because they can be easily identified as fibroblast-like cells in the bone marrow [Ghieh et al., 2015]. Also, they have the capacity to differentiate into other mesenchymal cells, generating bone, cartilage, and/or fat tissue. As we proved in our study, many others suggested alternative mesenchymal stem cells sources (e.g., bone marrow, adipose tissue, synovium fluid, skeletal muscle). A promising source of mesenchymal stem cells is the dental pulp, because being inside the dental cavity surrounded by mineralized dentin, it is kind of sealed niche that preserves it from environmental differentiation stimuli and maintains stem cells properties in the adult tissue. Dental pulp mesenchymal stem cells derive during tooth development from ectodermal cells that migrate from the neural tube to the oral/maxillo-facial region and finally they differentiate into mesenchymal cells [Aurrekoetxea et al., 2015]. Many intra-oral tissues (deciduous teeth, wisdom teeth, the gingiva) are very easy to access and obtain by dental professionals. Therefore, they should recognize the promise of the emerging field of regenerative dentistry and the possibility of obtaining stem cells during conventional dental treatments that can be banked for autologous therapeutic use in the future (bone and nerve regeneration, neurological disorders or organ transplantation) [Mendi et al., 2019].

### **Final remarks**

Evidence reported in this study suggests that differentiated adipocytes achieve similar wound healing results as ADSC and fat injection, but differentiated adipocytes (+IBMX[D1–5]+INSULIN) as well as fat grafting (prepared by Coleman technique) accelerate early healing process relative to ADSC. Our study provides an alternative option (adipogenic differentiated cells vs fat prepared by Coleman technique—the mixture of stem cells, mediators, and cytokines) for future researchers who may be interested in elaborating on the single-lineage effects and underlying mechanisms of adipocytes in skin burn wound healing. However, further research is needed in order to explore the conditioning that would enhance differentiated adipocytes' abilities for wound healing.

## **4.4. Different effects of fish oil on serum lipids and hepatic morphology show that a balanced diet is preferable to dietary supplements**

### **4.4.1. Introduction**

Dietary supplements with polyunsaturated fatty acids (PUFAs), mainly used in the form of fish-oil (FO) are known to have a protective and alleviating role in cardiovascular diseases (CVD) and hepatic steatosis; improvement of serum lipid profile and the prevention atherosclerosis development are considered essential for such a role. High-fat intake and lipid metabolism disorders, such as elevated serum total cholesterol (TC), low-density lipoprotein cholesterol (LDL), and triglycerides (TG), as well as decreased high-density lipoprotein cholesterol (HDL) are just some of the most frequent and important CVD-associated risk-factors. High-fat intake also relates to hepatic lipids accumulation, increased TG storage, which further leads to steatosis, triggering metabolic dysfunctions such as insulin resistance and dyslipidemia [Nassir et al., 2015]. Nowadays, there is increased awareness, not only among scientists, but also in the general population, regarding the negative effects of a fat-rich diet and on its propensity to cause atherosclerosis, CVD, fatty liver disease, and stroke [Yang et al., 2017; Banefelt et al., 2016].

Despite their negative role in the pathogenesis of many diseases, fats are essential for living organisms. PUFAs represent a category of essential fats, classified according to the position of the first double bond relative to the end-methyl group. N-3 and n-6 fatty acids (FA) are the most biologically significant PUFA classes, synthesized from the essential FAs alpha-linolenic and linoleic acid, respectively. N-3 PUFA intake is associated with a protective effect against CVD. N-6 vs. n-3 ratio is very important for human health, as N-3 and n-6 PUFAs compete with one another for the active site of the enzyme responsible for their metabolism (an overabundance of one class will limit the metabolic production of the longer chain products of the other; lowering the n-6 vs. n-3 ratio would facilitate the metabolism of alpha-linolenic acid). The typical Western diet provides n-6 and n-3 PUFAs in a ratio ranging from 8:1 to 25:1 [Ander et al., 2003], values in severe contrast with the health agencies' recommendations (approximately 4:1) [Holub, 2002]. Several animal studies evidenced n3-PUFAs inhibitory effect on the development and destabilization of atherosclerotic plaques [Takashima et al., 2016]; some randomized human trials showed that they reduce CVD-mortality endpoints, such as sudden death and fatal myocardial infarction. N-3 PUFA protection against hepatic steatosis has also been proven [Yang et al., 2019]. Fish-products are considered the most common dietary source of n-3 PUFA, containing large amounts of the  $\omega$ -3 FA such as eicosapentaenoic acid (EPA) and docosahexaenoic acid (DHA) [Ochi and Tsuchiya, 2018].

Since the 1970s, an increased adherence to the Western diet, rich in hydrogenated FAs was observed, mostly among young individuals. In the United States of America, over the past decades there has been a considerable transition of habitual dietary patterns high in complex carbohydrates and fibers towards a diet rich in sugars, fats, and animal products. However, more recently, an increased awareness in the Western population regarding the role a healthy diet in preventing metabolic diseases and a tendency to reduce saturated FAs intake was observed. Eighty-three percent of EU citizens consider they have healthy diets, with a peak in the Netherlands (95%), and with 22% of the-responders declaring they have changed their eating habits over the past year (consuming more vegetables, less fats and sugars, fewer calories, and drinking more water). Even in the US, for the last 12 years, national estimates report that obesity has leveled-off at an about 35%-prevalence. Mediterranean diets, based on PUFAs, such as  $\omega$ -3 and  $\omega$ -6, have become ever more popular [Granado-Casas et al., 2019], as well as the use of  $\omega$ -3 FA supplements, such as FO. The global  $\omega$ -3 market was estimated at 2.29 billion USD in 2018 and it is expected to expand, North America being the most important consumer of such products [Grand View Research, 2019]. Numerous studies prove the  $\omega$ 3-FAs benefits, but data are somehow contradictory; molecular mechanisms involved in atherosclerosis and liver steatosis prevention are poorly understood. For the  $\omega$ 3-presumed anti-atherogenic action, conclusive evidence has yet to be provided. There might be significant differences in the impact of PUFAs on the mentioned processes related to individual's dietary particularities. A large segment of population is not confined exclusively to only one type of diet. The n-3 PUFA action can be influenced by the association with other substances or individual metabolic profile. PUFA-sources and EPA vs. DHA ratio are extremely variable and they generate a high rate of doubt. Therefore, designing a study in order to analyze, compare and quantify the  $\omega$ 3-efficacy in conditions of Western, Mediterranean, and heterogeneous diet or simulation of different metabolic profiles would bring new insights on this matter.

#### **4.4.2. Aim**

The aim was to evaluate n-3 PUFA effects on body weight (BW) and on the main parameters of lipid metabolism (cholesterol, TG), in an experimental rat-model with different

diets, combining proven atherogenic factors (cholesterol, cholic acid and 2-thiouracil) and potential anti-atherogenic factors (FO), administered successively or simultaneously. Also, the study aimed to quantify both the early and the late/persistent biological response to n-3 PUFA during induced-hyperlipidemia and to correlate it to aortic and hepatic histological hypothetical modifications (atherogenesis, steatosis), before or after changing the dietary habits.

#### 4.4.3. Materials and methods

##### Laboratory animals

The experiment was carried out on an initial number of 60 five-week old male albino Wistar rats (non con-sanguine), weighing  $150 \pm 10$  g, purchased from “I. C. Cantacuzino” National Institute of Research and Development for Microbiology and Immunology, Bucharest, Romania. The animals were individually housed in polypropylene cages, according to European standards in the Laboratory for Pharmacology Research, in a controlled environment (temperature:  $23 \pm 2^\circ\text{C}$ , with 50–60% relative humidity interval, central ventilation and artificial light-dark cycles – 12/12 h per day). The animals had free access to water and standard food, provided ad-libitum. Before the enrolment of the animals into the experimental study, the rats were acclimatized for 7 days.

##### Substances

Cholesterol (95%) was purchased from Alfa Aesar, Heysham, England, cholic acid from Merck, Darmstadt, Germany, 2-Tiouracil and concentrated n-3 fatty acids (DHA/EPA, 200/250 mg) from Sigma-Aldrich Co, Deisenhofen, Germany; all other chemicals and reagents (analytical grade) were purchased from Alfa Aesar, Heysham, England.

##### Diets

For the standard diet (SD), regular food consisted in pellets, manufactured by “I. C. Cantacuzino” National Institute of Research and Development for Microbiology and Immunology, Bucharest, Romania. Its composition is summarized as follows: crude proteins – 18.55%; crude fats – 2.65%; crude fibers – 6.8%; salts – 0.48% and water – 10.65%. The standard diet was intentionally free of EPA and DHA.

The hypercholesterolemia diet (high fat diet – HFD) consisted in supplementation of drinking water with standardized suspension (CCT suspension) containing cholesterol 4%, cholic acid 1% and 2-thiouracil 0.5%. The diet was designed to induce atherogenic and hepatic steatosis changes, as well as metabolic lipid disturbances (hyperlipidemia).

The n-3 PUFA treatment consisted in the oral gavage of a suspension containing fish-oil from capsules (50 mg/kg b.w. daily).

##### Experimental design and diet administration method

Sixty rats were randomly divided into 6 groups of 10 and the experiment carried out for 42 days 6 weeks.

The first group (SD, standard diet) was used as control. Food was provided as standard diet with no supplementation, for 42 days.

The second group (n3) received standard food and FO by oral gavage (50mg/kg/day), for 42 days. It was designed to assess the hypothetical benefits of  $\omega$ -3 FA in regular-diet conditions.

The third group (HFD) received standard food plus the corresponding suspension described in the “Diets” section in the drinking water, for for 42 days. It served as a model of HFD-triggered disease.

The fourth group (HFD+n3) received the described HFD suspension and FO 50mg/kg/day, for 42 days. It served to assess the hypothetical benefits of  $\omega$ -3 FA in HFD conditions.

The fifth group (CA1: combined alternative 1) received both n-3 PUFA and HFD diet for 14 days, followed by HFD diet only during days 15-28, and n-3 PUFA 50mg/kg/day associated to SD, for the last 2 weeks (days 29-42).

The sixth group (CA2: combined alternative 2) received HFD with no FO for the first 14 days, both n-3 PUFA and HFD diet from day 15 to 28, and n-3 PUFA 25mg/kg/day associated to SD, for the last 2 weeks (days 29-42).

CA1 and CA2 groups served as models of different transition from HFD to a regular diet, which has an increased similarity with the Mediterranean diet, using n-3 PUFA for cardiovascular protection.

To reproduce identical stress conditions induced by oral gavage to all subjects, distilled water was administrated by gavage once per day to those subjects that did not receive FO-gavage that day.

Standard food and water were provided *ad libitum*. During the experiment, the individual BW and the quantity of the consumed food and water, as well as urine and faeces amounts were measured daily.

After each 14 days feeding cycle of, two rats from each group were euthanized with an intra-peritoneal injection of sodium pentobarbital (45mg/kg) for minimizing the tissue alterations for better histological examinations. At the end of the 42 diet days, all rats were euthanized under same conditions for histological assessment of liver and aorta samples.

#### Biochemical determination

Total cholesterol (TC), low-density lipoprotein cholesterol (LDL) and high-density lipoprotein cholesterol (HDL) levels were determined using kits supplied by BD Biosciences Co., Heidelberg, Germany and a biochemistry analyser type VITROS® 350 Chemistry System (Johnson & Johnson Ortho-Clinical Diagnostics) (colorimetric methods). Blood samples were collected from the orbital sinus stored in standard biochemistry vacutainers, on days 14th, 28th and 42th. Values are expressed in mg/dL.

#### Histopathological examination

After the rats were euthanized, the entire aorta and the liver from each rat were removed, rinsed with cold saline solution, dried with filter paper, grossly examined under a magnifying glass (5x) and routinely processed. Six to eight 4 mm samples were taken from different levels of each aorta, in transverse and longitudinal sections. Fixation was performed using 10% neutral buffered formalin at room temperature, for at least 24h. Then, the specimens were dehydrated with ethanol in ascending grades from 75% to 99.6%, immersed in xylene and paraffin embedded. Sections of 4-5µm thickness were stained with hematoxylin and eosin (HE) and van Gieson trichrome for evaluation in light microscopy. Examination of aortic samples was performed in longitudinal and transversal sections and consisted of counting the collagen layers. Regarding the liver samples, the study focused on the semi-quantitative evaluation of fatty change.

#### Ethical policies

The study on rats was conducted in compliance with the European Guidelines for Human and Animal Rights Directive 2010/63/EU for animal experiments and was approved by the Research Ethics Committee of the “Grigore T. Popa” University of Medicine and Pharmacy from Iași, Romania (registration: no. 25812/11.XI.2014).

#### Statistical data analysis.

Statistics was performed using SPSS-software version 20 for Windows (IBM, Chicago, Illinois, United State of America). The normal distribution of each group and for each test was assessed using the Shapiro-Wilk test. When the test showed normal distribution, the results were expressed in graphs and tables as average  $\pm$  standard deviation (such as quantitative data values for body weight, TC, LDL and HDL cholesterol, TG). In such cases, one-way ANOVA was used to test for differences among groups; paired samples T-Test for same-group comparison at different moments were used. When the same test

revealed abnormal distribution, the Kruskal-Wallis test was used for between-groups comparison, and data are presented in tables as median and quartiles (q1 – q3). A value of  $P < 0.05$  was considered significant.

#### 4.4.4. Results

##### *Body weight, growth, food and water intake (sintetic data)*

During the accommodation period and in the following 42 days, the rats' BW increased constantly in all 6 groups, independently of the diets. After the accommodation period, the percentage increase in the BW was  $25.69 \pm 4.75\%$  vs. 7 days before in the SD-group, similar to the other 5 groups. Day 0 was considered the last of the 7 accommodation days.

By the end of 6-weeks of different diets application after acclimatization, the most evident BW-increase was in HFD-rats (from  $187.1 \pm 5.86\text{g}$  – day 0 to  $292.33 \pm 3.26\text{g}$  – day 42) and the least evident in n3-group (from  $186.1 \pm 5.86\text{g}$  – day 0 to  $248.17 \pm 2.85\text{g}$  – day 42). For the SD-group, the increase was from  $186.1 \pm 4.25\text{g}$  – day 0 to  $260.67 \pm 4.58\text{g}$  – day 42. In the HFD+n3 group, the increase was from  $185.1 \pm 4.15\text{g}$  – day 0 to  $268.33 \pm 11.15\text{g}$  – day 42, marking significant protection of n3-PUFA over excessive weight gain (WG) in HFD conditions ( $P < 0.001$ , HFD vs. HFD+n3 groups). In CA1 group, BW increase was higher ( $P < 0.01$ ) vs. n3 and lower ( $P < 0.001$ ) vs. HFD; for CA2 group it was higher ( $P < 0.01$ ) vs. n3 and lower ( $P < 0.01$ ) vs. HFD. The intermediate WG in CA1 and CA2 groups (between HFD and n3-groups) can be explained by the adding of n3-PUFA during half of the HFD-period and mainly during the last 14 days, under SD-conditions.

In order to evaluate BW-increase at different stages of the experiment, a BW-increase was calculated in a certain moment vs. 7 days before (i.e.: day 28 vs. 21), considering the first day after the acclimatization as day 1.

There were no significant differences between groups after the first 7 days.

During days 7 to 14, a slight difference could already be observed: WG was more evident ( $P < 0.05$ ) in HFD vs. SD-group, and less evident in n3-group vs. SD ( $P < 0.05$ ); n3-PUFA added to HFD did not induce significant protection against increased WG in HFD+n3 and CA1 groups.

The HFD-group tendency to gain more weight, as well as the tendency of n3-group to gain less weight vs. SD-group was also evident in the following four weeks. FO adding to HFD offered a relative protective effect against excessive WG in HFD+n3 vs. HFD group, during weeks 3, 4 and 5 of different diets application, but not during the last week.

Between days 14-21, CA2 group, on a HFD with n3-PUFA supplementation during that period, had a relative protection against excessive WG ( $P < 0.05$  vs. HFD), and so it was during the days 21 to 28 ( $P < 0.01$ , CA2 vs. HFD).

Between days 28-35 or 35-42, PUFA addition to SD in groups CA1 and CA2, previously exposed to high-fat intake, did not cause a less evident BW increase vs. SD. From days 35-42, however, FO offered relative protection against excessive WG in CA1 and in CA2 groups vs. HFD groups.

No significant changes in the amounts of consumed food, water or excreted urine and feces could be detected between groups at any of the considered moments, so no correlations could be established to the BW. No relevant changes in the feeding-pattern upon switching of the diets were seen in CA1 or CA2 groups.

##### *Biochemical determinations*

Total serum cholesterol was initially similar in the studied groups, with values ranging from 78 to 103mg/dL.

After the first 2 weeks, in n3-rats, TC was lower vs. initially ( $P < 0.05$ ) and vs. SD-rats ( $P < 0.05$ ). In the HFD- and CA2-groups, TC was higher vs. initially and vs. SD-rats ( $P < 0.001$ ). For CA1 and HFD+n3-rats, PUFA offered a relative protection against TC-increase ( $P < 0.001$  vs. HFD and CA2-groups), but TC was higher vs. initially ( $P < 0.05$ ) or n3 and SD-group ( $P < 0.001$ ,  $0.01 < P < 0.05$ ) respectively.

After 4 weeks of different diet application, HFD-rats continued to have increasing TC ( $P < 0.001$  vs. 14 days before). In the n3-group, TC was unchanged vs. 14 days before, but significantly lower vs. SD-rats ( $P < 0.01$ ). In the HFD+n3 group, TC was insignificantly higher vs. 2 weeks before, but lower ( $P < 0.001$ ) vs. HFD-group. In HFD+n3 group, TC was lower vs. HFD-group ( $P < 0.001$ ), but higher vs. initially and SD-group ( $P < 0.05$ ) and vs. n3-group ( $P < 0.001$ ). For CA1 and CA2 groups, TC-concentrations higher ( $P < 0.05$ ) vs. HFD+n3 group, yet much lower ( $P < 0.001$ ) vs. HFD group.

After 6 weeks, there was a confirmation of the ascending TC-tendency in HFD group ( $P < 0.01$  vs. 14 days before). In the n3-group, TC was insignificantly changed vs. 14 and 28 days before. In the HFD+n3 group, TC was lower vs. HFD-group ( $P < 0.001$ ) and higher vs. 2 weeks before ( $P < 0.05$ ). In CA1 and CA2-groups, TC was insignificantly lower vs. to 14 days before, indicating that reversal to standard diet after 4 weeks of HFD-exposure, needs more than 2 weeks-period for a significant TC-lowering effect, even under PUFA-protection conditions.

Serum HDL-cholesterol was initially similar in the studied groups, with values ranging from 41 to 64mg/dL.

After 14 days, HDL-changes in SD, HFD, HFD+n3, CA1, and CA2 groups were insignificant. For the n3 group, HDL was higher vs. initially and vs. SD-, HFD- and CA2-groups ( $P < 0.05$ ), but insignificantly different vs. HFD+n3 or CA1 groups.

After 4 weeks, in n3-rats HDL was higher vs. SD-group and vs. 2 weeks before ( $P < 0.05$ ), and vs. initially ( $P < 0.01$ ). In HFD-rats, HDL was lower vs. SD or vs. 14 days ( $P < 0.05$ ), and vs. initially ( $P < 0.01$ ). At that moment of the experiment, the protective role of a normal diet, combined with FO vs. HFD with no PUFA protection became more evident than 14 days before (n3 vs. HFD:  $P < 0.001$ ) in terms of HDL-increase. In HFD+n3-rats, HDL was insignificantly modified vs. 14 and 28 days before, but higher vs. HFD-group ( $P < 0.05$ ) and lower vs. n3 group ( $P < 0.001$ ). For CA1-rats, HDL was insignificantly lower vs. HFD+n3 group and vs. 2 weeks before, but lower vs. initially ( $P < 0.01$ ). For CA2 group, serum HDL was insignificantly changed vs. initially, HFD, HFD+n3, and CA1 groups, but significantly lower vs. n3 group ( $P < 0.001$ ).

On day 42, in n3-group, HDL was higher in SD group vs. initially, and vs. 4 weeks before ( $P < 0.01$ ), but not vs. 2 weeks before. In the HFD group, HDL-value confirmed the decreasing tendency of this parameter, which is lower vs. SD-group ( $P < 0.05$ ), vs. initially and vs. 28 days before ( $P < 0.01$ ), but not vs. 14 days before. In the HFD+n3 group, HDL was insignificantly modified vs. 14 and 28 days before, significantly higher vs. HFD-group ( $P < 0.05$ ) and lower vs. n3 group ( $P < 0.001$ ) and vs. initially ( $P < 0.05$ ). In CA1 group, HDL was higher vs. HFD+n3 group ( $P < 0.01$ ) and vs. HFD rats ( $P < 0.001$ ), vs. 2 and 4 weeks before ( $P < 0.05$ ), and insignificantly modified vs. initially. In CA2 group, HDL was insignificantly changed vs. initially, 2 and 4 weeks before, and vs. CA1 group, but lower vs. n3 group ( $P < 0.01$ ) and higher vs. HFD group ( $P < 0.01$ ).

Serum LDL-cholesterol was initially similar in the studied groups, with values ranging from 15 to 39mg/dL.

After the first 2 weeks, n3-rats had lower LDL vs. initially and SD-rats ( $P < 0.05$ ). In the HFD- and CA2-groups, LDL was higher vs. initially and vs. SD rats ( $P < 0.001$ ). For the CA1 and HFD+n3-groups, n3-PUFA induced a relative protection against LDL increase: LDL was lower ( $P < 0.05$ ) vs. HFD and CA2-group, yet evidently higher vs. initially and SD groups ( $P < 0.05$ ) or n3- ( $P < 0.001$ ).

After 2 more weeks, HFD-rats continued to have ever increasing LDL ( $P < 0.01$  vs. the 14 days before). In n3-rats, LDL was lower vs. 14 days before ( $P < 0.01$ ) and vs. SD rats ( $P < 0.001$ ). In HFD+n3 group, LDL was higher vs. 2 weeks before ( $P < 0.001$ ), vs. initially ( $P < 0.01$ ), and vs. SD- and n3-groups ( $P < 0.001$ ), but lower vs. HFD group ( $P < 0.01$ ). So, compared to 14 days before, in the HFD+n3 group the increase in LDL was even more evident as for the HFD group. For CA1 and CA2 groups, LDL was insignificantly higher vs. HFD+n3-group and insignificantly lower vs. HFD-group.

After 6 weeks from the study's beginning, there was a slight, yet significant LDL-increase vs. initially in the SD-group ( $P < 0.05$ ). For the HFD group, there was a confirmation of the ascending LDL-concentration tendency ( $P < 0.01$  vs. 14 days before). In the n3-rats, LDL was insignificantly changed compared to 14 days before, yet significantly higher vs. initially ( $P < 0.01$ ) and vs. 28 days before ( $P < 0.05$ ) and vs. control group ( $P < 0.001$ ). In the HFD+n3 group, LDL was lower vs. HFD-group ( $P < 0.05$ ) and higher vs. 2 weeks before ( $P < 0.05$ ). For CA1 and CA2 groups, LDL was insignificantly lower vs. to 14 days before, but lower vs. HFD+n3 ( $P < 0.01$ ) and vs. HFD-group ( $P < 0.001$ ).

Serum triglycerides were initially similar in the studied groups, with values ranging from 51 to 76mg/dL.

After the first 2 weeks, in n3 group, TG concentration was lower vs. initially and SD rats ( $P < 0.05$ ). In the HFD and CA2 groups, TG were higher vs. initially and SD rats ( $P < 0.01$ ) and n3-rats ( $P < 0.001$ ). For the HFD+n3 and CA1 groups, n3-PUFA did not offer significant protection against TG-increase.

After 4 weeks, HFD group continued to have increasing TG ( $P < 0.001$  vs. 14 days before). In n3-group, TG concentration was unchanged vs. 14 days before, but lower vs. SD-rats ( $P < 0.05$ ). In HFD+n3 group, TG concentration was higher vs. 2 weeks before ( $P < 0.001$ ), but lower ( $P < 0.05$ ) vs. HFD group, suggesting that n3-PUFA protection against increased TG under HFD-conditions is evident after a longer period compared to SD-conditions. For CA1 and CA2 groups, TG were insignificantly different vs. HFD and HFD+n3 groups, and higher vs. 14 days before ( $P < 0.01$ ).

After 6 weeks, for the HFD group there was a confirmation of the ascending TG-tendency ( $P < 0.01$  vs. 14 days before). In the n3-group, TG were insignificantly lower vs. 14 days before, yet significantly lower vs. SD-group, vs. initially ( $P < 0.01$ ) and vs. 28 days before ( $P < 0.05$ ). Such results suggest that n3 PUFA decreasing-TG effect in regularly-fed individuals is dependent on the supplementation-time. In the HFD+n3 group, TG were lower vs. HFD-group ( $P < 0.05$ ) and insignificantly higher vs. 2 weeks before. For CA1 group, TG were lower vs. HFD-rats ( $P < 0.001$ ) and HFD+n3-groups ( $P < 0.01$ ) and vs. 2 weeks before ( $P < 0.05$ ). In CA2-group, TG were lower vs. HFD ( $P < 0.001$ ) and vs. CA1-group ( $P < 0.05$ ), but insignificantly lower vs. HFD+n3 group and vs. 2 weeks before, suggesting that reverting to normal diet and adding PUFA as a dietary supplement after 4 weeks of exposure to HFD induces a dose-dependent TG-lowering effect.

## **Morphological analysis**

### *Aorta samples*

On gross examination under the magnifying glass, no changes of the wall thickness were observed. No adherent recent or organized thrombi were observed in the lumen of the aortic samples.

After the first 14 days of exposure to different diets, the evaluation revealed non-significant changes in all 6 groups. Thoracic aorta samples from all groups revealed a thickness of 6-8 layers of collagen in the media (Fig 31a). The number of layers remained constant during the three stages of the experiment for SD and n-3 groups.

After 28 days of exposure to different diets, for the rest of the study groups the aortic wall thickness was increased, due to the increased number of collagen layers (8-12 layers)

and hydropic changes of smooth muscle fibers in HFD+n3, CA1 and CA2 groups – Fig 31b; 12-13 layers in HFD-group – Fig 31c.

At the end of the experiment (day 42), although the smooth muscle fibers continued to present hypertrophy or hydropic vacuolization, the number of collagen layers decreased for HFD+n3 and CA1 groups to 8-10 layers, to 8-11 layers for CA2, and to 10-12 layers for HFD (Fig 31d). None of the classical atherosclerotic lesions (plaques) were observed in the examined aortic samples.

For all study groups samples, the intimal layer was continuous, although the endothelial lining was focally interrupted, but without fibrin network adherent to the basal membrane. Also, no inflammatory infiltrate (neutrophils or lymphocytes) and no foamy cells (macrophages) were observed in the examined sections.

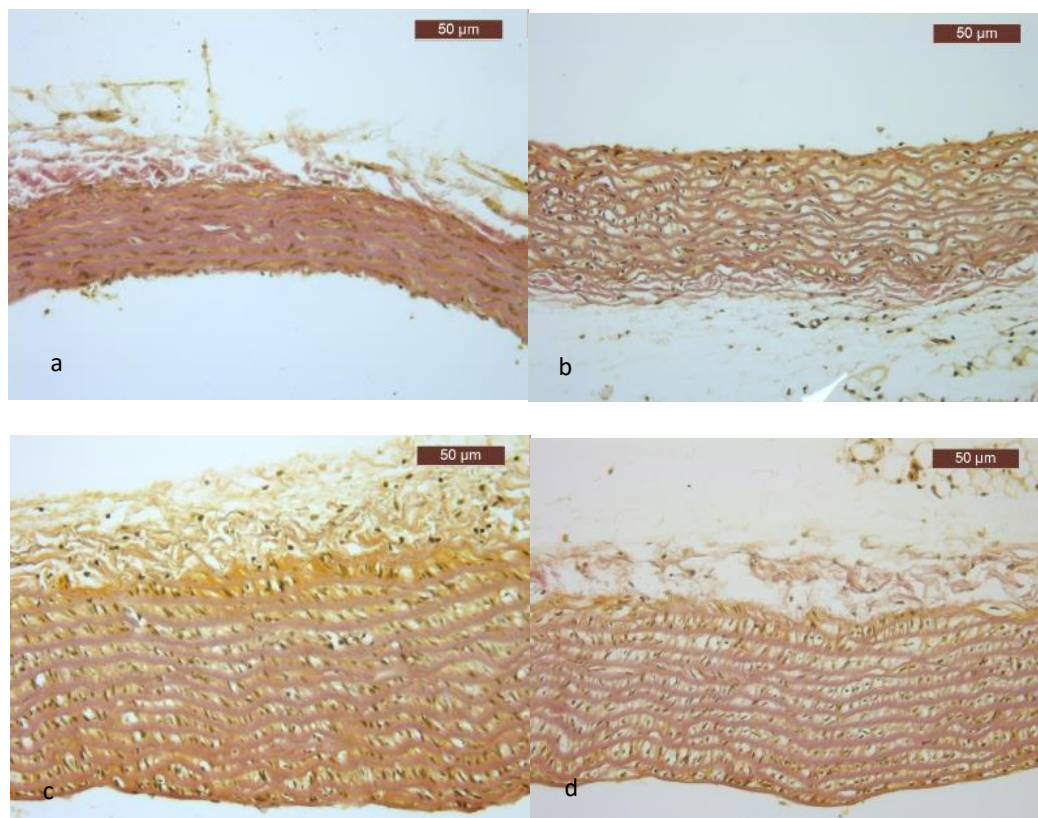


Fig 31. Histopathological aspects of aortic changes (van Gieson trichrome staining): (a) normal aorta after the first 14 days, all groups; (b) thickened aorta (12 collagen layers and vacuolated smooth muscle fibers) from HFD group after the 28 days; (c) thickened aorta from HFD+n3 group after the 28 days; (d) thickened aorta from CA2 group, at the end of the experiment.

#### *Liver samples*

Regarding the liver samples, no morphological changes were observed for SD and n3 groups during the experiment (Fig 32a). After the second phase, hydropic change in the hepatocytes was observed in HFD and CA2 groups (Fig 32b), while in the HFD-n3 and CA1 group focal microvesicular fatty changes were observed in the hepatocytes surrounding the central vein – grade I fatty change (< 33% of hepatocytes) (Fig 32c). After 42 days, grade III microvesicular fatty change aspects were observed in the liver from HFD+n3 and CA2 groups and grade III macrovesicular fatty change (diffuse, > 80% of hepatocytes) in HFD group (Fig 32d). Normal architecture without any fatty change in the liver hepatocytes was observed in the CA1 group, by the end of the experiment.

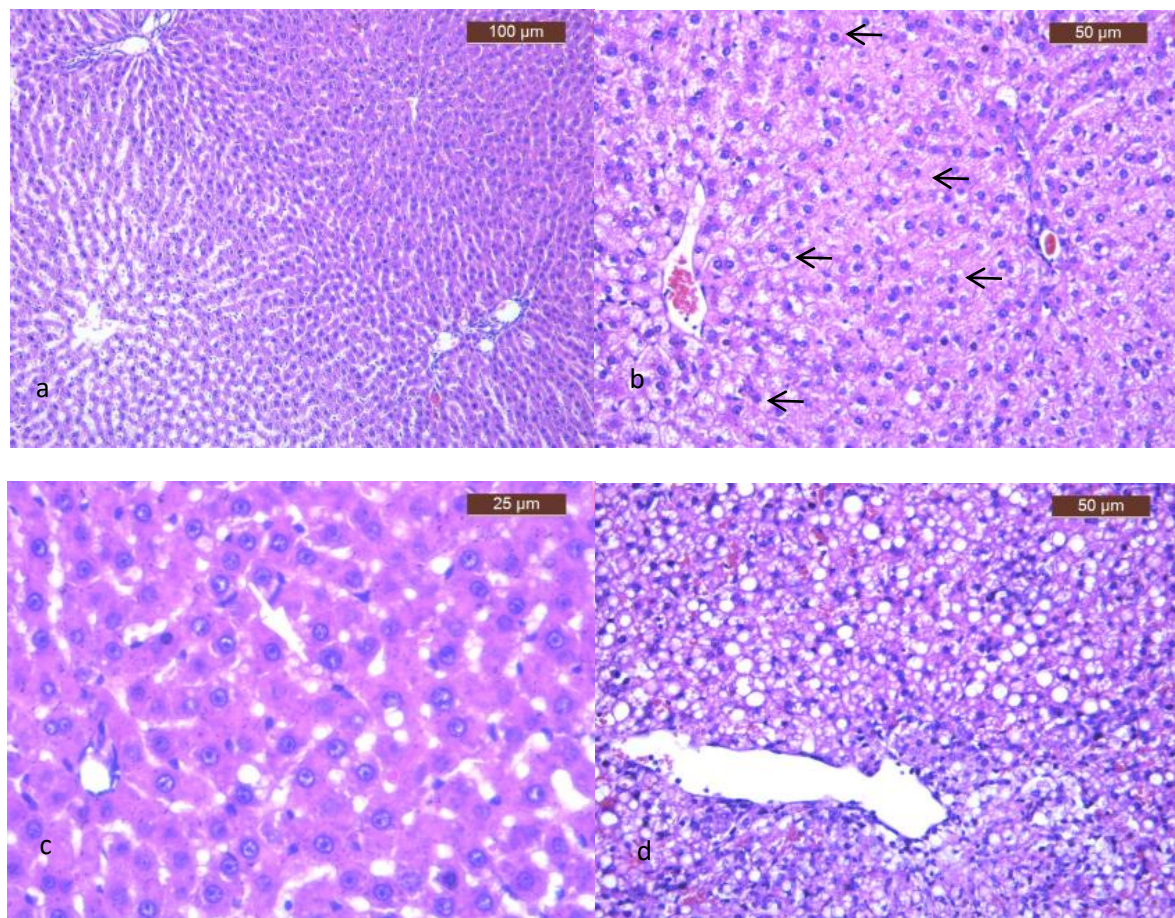


Fig 32. Histopathological aspects of liver changes (hematoxylin and eosin staining): (a) normal liver from SD and n-3 groups; (b) important diffuse hydropic change (arrows) after 28 days, in HFD+n3 and CA1 groups; (c) microvesicular fatty change grade I after the second stage, in HFD group, after 28 days; (d) diffuse macrovesicular fatty change stage III after 42 days, in HFD-group.

#### 4.4.5. Discussion

This study reveals a dose and time-dependent positive FO-effect against WG, increased serum TG, TC, LDL and decreased HDL, incipient atheromatosis and fatty change in rats, under both normal and HFD conditions. Nevertheless, in HFD-rats, while evident, FO-protection has far from counteracted the HFD-induced consequences. We have proved the beneficial effect of FO, more evident at 50mg/kg/day vs. 25mg/kg/day, added as a supplement to SD, for 2 weeks, after 28 days of HFD-period.

Weight-gain was observed, as expected, in all groups during the 42 days of different diet application, as the animals were 6 weeks-old when diets application started, but it was not equal: it was more evident in HFD-rats with no PUFA-supplementation, while n3-PUFA added to HFD offered a relative protection against excessive WG. Reduced WG due to n3-PUFA administration was also seen in regular-diet conditions.

There are many experimental studies stating the protective effect of n3-PUFA against WG, under both regular and hyperlipidic diet conditions [Yang et al., 2016]. However, partial results sometimes disagree: FO adding to HFD for 13 weeks induces a slight (yet insignificant) WG-increase. A diet with 7% FO, rich in n-3  $\alpha$ -linolenic acid, induced more

WG than standard chow food. In SD-conditions, insignificant BW lowering-effect for FO was reported, but the dose they used was approximately 30 times higher than in the current experiment (1.5g/kg/dose), so supplementary energetic intake could be significant [Wu et al., 2016]. Addition of 2%-cholesterol to chow food induced a decrease in food consumption after 4 to 8 weeks [Khan et al., 2017], while in this experiment HFD induced more WG than regular food from weeks 1 to 6, but without influencing food consumption.

In human studies, the FO-effectiveness of in boosting weight-loss has mainly been documented under balanced-diet conditions, but results are somehow controversial. There are studies reporting small changes in BW due to FO, especially the reduction of abdominal fat, which is more evident when FO is combined with life-style changes [Du et al., 2015].

Reduction of serum TG by FO is mainly attributed to the n3-PUFA content. There are several hypothetical biochemical mechanisms, such as decreased very low-density lipoprotein-cholesterol (VLDL)-secretion in humans, while some animal researches suggested three general processes: reduced availability of FAs or other substrates (probably due to elevated beta-oxidation), reduced hepatic delivery of free FAs, reduced liver FAs synthesis; increased phospholipid synthesis; decreased activity of TG-synthesizing enzymes (diacylglycerol acyltransferase or phosphatidic acid phosphohydrolase). Yet, it is difficult to ascertain if such an effect is mainly manifest in subjects with initial high TG levels and / or high-fat diets or in individuals with normal lipidic profile. This study evidenced a slight TG decrease ( $P < 0.05$ ) due to n3-PUFA supplementation after 2 or 4 weeks, and a more evident one ( $P < 0.01$ ) after 6 weeks in SD-rats; however, for the HFD groups, n3-PUFA TG-lowering effect was insignificant at 14 days, and became evident ( $P < 0.05$ ) at 4 and 6 weeks. In the CA1 group, the last 14 days of FO administration associated with a normal diet were enough to lower TG to a level just slightly above controls; such an effect could not be seen in the CA2 group, which received just half of CA1 FO-dose. One might infer that FO is less efficient in lowering serum TG under HFD conditions vs. regular lipid content diets conditions.

When evaluating serum cholesterol, a more evident  $\omega$ 3-FA-induced decrease for LDL was observed as compared to TC levels in SD rats. In rats on HFD, n3-PUFA determined a less evident LDL-lowering effect, while TC is more evidently decreased. As FO generally increases HDL, it would be reasonable to assume that  $\omega$ 3-FA, under HFD-conditions also decreases other cholesterol fractions, such as VLDL, IDL (intermediate density lipoprotein), and chylomicrons (fractions with high TG content), findings which were not determined by the current research. The HDL-increasing effect of FO-adding to low, moderated, or high cholesterol diets was proven [Surette et al., 1992], in Syrian hamsters; on the other hand, another study [Naik et al., 2018] claimed a lack of effect regarding flaxseeds oil (rich in  $\omega$ -3 FA) administration on HDL and LDL in normal-fed rats, while in HFD-rats it decreased serum VLDL, LDL and TG; the doses they used were difficult to be compared to the ones used in the current study, but the administration period was double. For a 0.5% cholesterol-supplemented diet, the TC-lowering effect of dietary n-3 PUFA was not seen. It was reported that n6-PUFA lowers TC more than n3-PUFA in hamsters on a 5% cholesterol-supplemented diet.

An interesting situation could be observed in mixed diets groups, where, after 4 weeks of hyperlipidic diet, neither dose of FO associated to regular diet could revert cholesterol-changes, except for a slight HDL-increase ( $P < 0.05$ ) in the CA1 group vs. 14 days before.

**The histological study** revealed that aortic thickness slightly decreased or remained unchanged in those groups receiving n-3 PUFA diets (n3, HFD+n3, CA1 and CA2). Structural changes, especially in the aorta, develop slower than the biochemical ones. Generally, it is known that a  $\omega$ 3-rich diet has a protective role against atherogenesis. The mechanisms involved are related to improved serum lipid profiles and antioxidant activity, as shown by various epidemiological, clinical, and experimental studies [Torres et al., 2015;

Sokoła-Wysoczańska et al., 2018]. Shen et al., 2018 used a HFD 6 weeks-model to induce atherogenic lipid modifications (increased TC, LDL, TG, and reduced HDL), supplemented with a nitric oxide synthase inhibitor, to facilitate the development of intracranial atherosclerotic stenosis in rats; they noticed that under such conditions,  $\omega$ 3-FA 5 mg/kg/day supplementation induced an improvement of blood lipid profile, with an absence of morphological changes; some of the FA-associated benefits included reduced reactive-oxygen species production and nicotinamide adenine dinucleotide phosphate oxidase brain-activity. In a previous similar experiment, the same authors [Shen et al., 2016] showed that the middle cerebral artery lumen stenosis and intimal thickening induced by HFD is attenuated by the  $\omega$ 3-FA, and the morphological improvement is accompanied by biochemical changes, such as reduced level of inflammatory markers [interleukin 6 (IL-6) and tumor necrosis factor  $\alpha$  (TNF- $\alpha$ )], CD68, monocyte chemoattractant protein (MCP-1), interferon- $\gamma$ , brain expression of inducible nitric oxide synthase, and vascular cell adhesion molecule-1 (VCAM-1). Intake of PUFA was linked to increased expression of adiponectin, a cytokine which reduces inflammation and the risk of atherosclerosis [Silva Figueiredo et al., 2017].

Naik et al., 2018 proved that grain flaxseeds (*Linum usitatissimum*; one of the richest plant-based  $\alpha$ -linolenic acid ester of plant sterols sources) administration in Wistar albino rats on a HFD improved not only lipid profile, but also the majority of the histological incipient atherosclerotic changes in the aorta. It determined a proliferation of endothelial cells with new vascular channel formation in the liver and in between cardiac muscle fibers. A study evaluating the effects of flaxseed oil demonstrated its efficacy in ameliorating atherosclerosis, optimizing overall lipid levels, lowering oxidative stress and inflammation [Han et al., 2015]. A study on mice showed that fresh flaxseed can suppress hypercholesterolemic atherosclerosis in a rabbit model. However, when the same oil was administered after being heated, it increased hepatic and plasma malondialdehyde (a potentially pro-atherogenic factor), and enlarged the aortic wall thickness, lumen and diameter in mice on a regular diet [Nogueira et al., 2016].

It was also proven here that FO provides a relative protection against hepatic steatosis, in a time- and dose-dependent fashion, probably in relation with the improvement in serum lipid profiles. This effect has been intensively studied and current findings are in agreement with the medical literature. For instance, in animal studies, it was reported a protective effect induced by EPA against increased cholesterol and altered liver changes histology and that grain flaxseeds also improves liver fatty changes in HFD-rats [Naik et al., 2018]. Several human studies also proved the alleviation of liver morphology and lipids accumulation by  $\omega$ 3-FAs-administration [Nogueira et al., 2016]; one study even reported a reduction in liver fibrosis [Li et al., 2015;], but there are also research papers proving their limited effectiveness of in non-alcoholic steatohepatitis [Sanyal et al., 2014].

Some data on the pathophysiology of hepatic lipids storage and the associated morphological changes are mentioned below, in order to discuss the possible molecular mechanisms involved in n3-PUFA protective effect in the light of molecular pathogeny data. Lipids accumulation involves, in a first stage, insulin resistance and visceral obesity, which promotes the FAs synthesis from glucose and inhibit their  $\beta$ -oxidation. The FA excess leads to TG synthesis, which are stored in the liver, inducing high rates of mitochondrial  $\beta$ -oxidation and consequent production of reactive oxygen species, such as superoxide radical ( $O_2^{\bullet-}$ ) and hydrogen peroxide ( $H_2O_2$ ). High levels of such molecules, generated as a consequence of lipids peroxidation, inactivate the apoptotic caspase system and induce necrotic cell death. In a further stage, the progression to steatosis involves the activation of different transcription factors, such as sterol regulatory element binding protein 1c (SREBP-1c), peroxisome proliferator-activated receptor  $\gamma$  (PPAR $\gamma$ ) and carbohydrate responsive element-binding protein (ChREBP), which activate the expression of a series of genes

essential for lipogenesis [Jump et al., 2018]. Other mechanisms include increased secretion by the adipose tissue of pro-inflammatory, fibrogenic and prothrombotic adipocytokines (IL-6, TNF- $\alpha$ ) and the reduced production of adiponectin, a potent anti-inflammatory, insulin-sensitizing adipocytokine. Inflammation is a component of the wound healing process leading to the deposition of extracellular matrix and fibrosis.

N-3 PUFAs, especially EPA and DHA, regulate gene transcription factors and therefore can act on control key pathways of hepatic lipid metabolism. They potently activate PPAR $\alpha$ , which, in turn, up-regulates several genes involved in the stimulation of FA oxidation and down-regulates pro-inflammatory cytokines (TNF- $\alpha$ , IL-6) genes. They also activate PPAR $\gamma$ , resulting in increased fat oxidation and improved insulin sensitivity. N-3 PUFAs decrease endogenous lipid production by inhibiting the expression and processing of SREBP-1 (a stimulator of the transcription of several lipogenic and glycolytic genes, in response to increased glucose and insulin levels). N-3 PUFAs inhibit hepatic glycolysis and lipogenesis and suppress the activity of ChREBP (another regulator of glycolytic, and lipogenic genes, such as L-pyruvate kinase and fatty acid synthase) [Marchisello et al., 2019] and increase the expression of adiponectin, a promotor of hepatic metabolic enhancement [Nogueira et al., 2016].

Certain aspects observed throughout the present study may be considered indicators of the limited FO-effectiveness in the case of high-fat intake vs. a balanced-dietary pattern. FO did not fully counteract the damaging effects of a cholesterol-rich diet and their effects appeared scarce even when reverting to a balanced diet. For instance, when considering WG in developing animals, n3 group exhibited lower weekly WG vs. controls between weeks 2 to 6 (SD-conditions), but in HFD-rats, the protection against excessive WG was restricted to weeks 3 to 5. FO supplementation for 14 days (25 or 50mg/kg/day), associated with a SD, but applied after 28 days of high-fat intake, did not lower the weight-gaining trend (in weeks 5 and 6, for CA1 and CA2 groups, there was no significant difference vs. to SD-rats in weekly WG-percentage).

When considering the lipid profile, it could be seen that, after the first 2 weeks of FO administration, TG were decreased only in SD-conditions ( $P < 0.05$ , SD vs. n3 group) and insignificantly lowered in HFD rats. The TG-decreasing n3-PUFA effect was less evident under HFD vs. SD conditions at 42 days (n3 vs. SD:  $0.001 < P < 0.01$ ; HFD vs. HFD+n3:  $0.1 < P < 0.05$ ). LDL-decrease induced by n3-PUFA was less evident under HFD vs. SD conditions at 28 and 42 days. In HFD-rats, FO mainly decreases TC, while the decrease of the atherogenic LDL-fraction, even though significant, was not as evident. HDL-increase has only been evident after 28 days of FO-supplementation in HFD-rats, while in SD rats it could be seen after only 14 days.

FO, 50mg/kg/day, for 14 days, associated to a SD, after 28 days of HFD (CA1 group), just slightly decreased TG and increases HDL-cholesterol vs. 14 days before, but with no effect on LDL or TC; half of the mentioned dose failed to induce any biochemical improvement in the CA2 group.

Diets lacking n-3 PUFA (HFD group) induced progression of fatty changes from stage I to stage III in the liver. High-extent alterations of liver morphology may represent a limiting factor for the possible benefit of n-3 PUFA supplementation, especially in the CA2 group.

The findings of the current study claiming the superior efficacy of n-3 PUFAs under SD vs. HFD-conditions are in agreement with some of the above-cited research papers. In animals  $\omega$ 3-FAs evidently lower plasma TC and TG in SD-conditions, but not when diets are supplemented with 0.5% cholesterol; a 5%-cholesterol supplemented diet increased TC more when combined with n3-PUFA vs. n6-PUFA; in humans, n3-PUFA is more effective in promoting weight-loss when associated to a balanced diet.

In the past decades, there is an increased tendency to consume foods rich in carbohydrates and fat, but also an ascending trend in using dietary supplements such as vitamins and minerals (especially calcium, magnesium, zinc, iron, and selenium compounds – recommended for various reasons, including anti-oxidant defence, immune system stimulation, antianxiety etc.). Most of the available  $\omega$ -3 supplements are FO products, accounting for more than 75% of the total, followed by krill-oil. However, it is important to use supplements wisely and increased awareness on their negative effects or limited effectiveness under certain conditions is advised.

#### Study strengths and limitations

One of the main purposes of the present study was to evidence possible differences in the presumptive n3-PUFA beneficial effect under standard, mixed, and high-fat diet conditions. The animal model in our study involved HFD-exposure, either continuous or intermittent. The current study's design was centred around two mixed diet models in animals, in an attempt to simulate the diversity of human feeding patterns and to provide information on the presumed protective role of PUFAs on several relevant parameters under different conditions. The data related to n3-PUFA-effect under mixed diet conditions, similar to the day-to-day human-feeding patterns, represent an element of novelty in medical literature. There is still no standardized approach in PUFAs' effects-testing and there are significantly different baselines in respect to nutritional and other lifestyle habits of different populations. It is important, but difficult as well, to establish the different extent of FO protective role against cardiovascular and liver diseases and dyslipidemia development. The results evidenced that  $\omega$ -3 have reduced effectiveness when their administration is associated to or follow a period of high-lipids intake.

The study rather reproduced the situation where n3-PUFAs are administered as a dietary supplement and not as a component of a so-called "healthy" diet.

The experimental research performed is helpful for a better understanding of certain mechanisms and to predict the  $\omega$ 3-PUFAs possible benefits. However, the experiment does not completely mirror the complexity of pathological factors. Aggravating or protecting factors such as smoking, lifestyle, physical exercise, genetics, age etc. and their influence on the biochemical parameters lipid metabolism or other aspects related to atherosclerosis and non-alcoholic liver disease were not taken into account. Certain aspects influencing feeding-behaviour (such as the impact of high amount of fat corresponding to the HFD on taste perception and satiety) were not considered. HFD was administered as a suspension added to the drinking water, whereas in humans, high amount of fat are regularly found in food and the greasy sensation is more likely to be tempered by different other tastes. PUFAs were administered by oral gavage, a manoeuvre which is unpleasant for the animal-subject, and might influence the amount of consumed food and liquid for a period of time. Indeed, in order to reproduce same stress conditions, placebo was administrated by the same procedure once daily to the subjects which did not receive FO.

Other indirect effects of applied treatment on feeding-behaviour (such as through influences on the mood) or locomotor activity (indeed, very limited to the subjects of the experiment, maintained in individual cages) and BW-evolution could not be realized.

Some possibly relevant biochemical parameters, such as VLDL, IDL, chylomicrons, fasting glycaemia, insulin, glycated haemoglobin, circulating n3-PUFA levels were not assessed. VLDL assessment could have been specifically relevant, especially as in HFD-rats, PUFAs lower more evidently TC than LDL and increase HDL, while in SD-rats mainly LDL and not TC was lowered.

While atherosclerosis and liver steatosis are mainly described for the case of adult patients, our study was based on determinations using a rat-model during the development period. In humans, atherosclerotic and liver modifications associated to HFD develop slowly,

in a chronic fashion, over a long time period (years), whereas the study period was limited to six weeks.

One more shortcoming is that only two animals were sacrificed in each after each two-week period for histopathological examination. Even so, the modifications were evident and characteristic, as to allow pertinent conclusions.

### **Final remarks**

Our study proves that the metabolic, hepatic and cardiovascular benefits of  $\omega$ 3-rich fish-oil are more evident under balanced-diet conditions. Fish-oil cannot fully counteract the impairment induced by high-fat intake, even when reverting to a standard diet after a fat-excess period. These findings argue that more awareness should be promoted, in the general population, on the benefits of adopting a responsible attitude over a healthy diet and on the relative lack of effectiveness of fish-oil in preventing dyslipidemia and cardiovascular diseases, if associated to high-fat intake. It is necessary to make proper difference between n3-PUFA administered as dietary supplements and a diet rich in  $\omega$ 3-FA natural sources. From the clinical perspective, it is necessary to design experimental models that take into consideration combined feeding-patterns applied for a longer period of time, which are capable to better reproduce the human feeding habits.

## **Section II – Future projects in professional, academic and scientific fields**

### **II.1. Projects regarding the professional and academic activity**

First of all, I am a Pathologist and all my achievements were founded and rely on this. Therefore, the level of my professional expertise dictates the performances in both academic and scientific fields, as they are all intermingled. So, it is difficult to speak about professional improvement and dissociating it from my teaching activities and research. Although, in biology, evolution is not necessarily dependent on long-term plans and goals, and doesn't have an innate tendency for progress, in medicine, having purposes is the only way to get higher. Regarding my activities as pathologist, I will continue to learn based on individual study and by attending professional national and international conferences (organized by European Society of Pathology and/or International Academy of Pathology), as medical knowledge continuously increases. Individual study, attending professional national and international scientific meetings. Regarding novelties, I will make efforts to stay informed with the latest discoveries in pathology in order to update the diagnostic protocols I use, according to global trends, both for routine techniques as for immunohistochemistry. I will also focus my training on those fields that I consider soft spots, trying to enlarge my horizons.

Beside adaptation, other outcomes of evolution are cooperation and coevolution. It is mandatory to cooperate with colleagues and sustain them, pathologists or from other specialties (mainly, oncology, surgery, gastro-enterology, radiology, dermatology, etc.), for both beneficial and development. So far, as a pathologist, interaction with clinicians brought a fruitful relation, based on trust and professional excellence, serving the patients best interests.

At national and international level, as member of the Society for Clinical Cytology, or founder of the Association for Digestive Pathology offered me the position and the instruments for knowledge dissemination and collaboration with peers worldwide.

Teaching for the residents in Pathology represents an important part of my daily activity as they are the next generations of pathologists. Improving my professionalism, providing them detailed explanations, encouraging them to individual study, to attend as much as possible scientific meetings, lectures and courses, stimulating them to publish scientific papers and including them in research projects are some of the directions I follow. I applied and obtained funds under an institutional grant for infrastructural development, which allowed me to purchase a multihead microscope for simultaneous examination (one examiner and 4 observers). More than this, a digital camera can acquire microscopical images; my intentions are to create a teaching database including images from basic lesions to rarest diseases. With time I will digitalize the whole slide collection which now includes over 1000 slides.

### **II.2. Projects regarding scientific activity**

For the future, I intend to continue and expand some of the research themes that I have developed after I finished the PhD thesis as part of international multicenter teams but, also, to start new, promising ones, as follows:

- The predictive role of correlation between serology and histopathological stage in celiac disease;
- PD-1 and PDL-1 expression in colorectal cancer and in head and neck cancers.

### **II.2.1. The predictive role of correlation between serology and histopathological stage in celiac disease**

Coeliac disease is an autoimmune disease affecting mainly the small intestine characterized by increased immunological sensitivity to gluten from food, resulting in chronic inflammation and tissue damage of the mucosa, especially in genetically susceptible individuals [Rostamy et al., 2017; Lebwohl et al., 2018]. The prevalence is about 1-2% of the global population, mostly in the Western countries, and is increasing. Still, the real prevalence is higher, because CD is largely underdiagnosed in asymptomatic individuals [Rostamy et al., 2017; Singh et al., 2018]. In the routine practice, gastroenterologists use serological screening for most patients suspected for CD aiming to detect antibody positivity, such as immunoglobulin A (IgA) antibodies to tissue transglutaminase 2 (tTG) and anti-endomysial IgA antibodies (EMA) [Lebwohl et al., 2018]. Because these serological markers are not 100% sensitive for detecting celiac disease, it should be confirmed by histopathological examination of a duodenal biopsy to identify the specific mucosal. Still, there are histological changes in the duodenal mucosa that can mimic CD, hence the need for a non-invasive method to diagnose the CD [Tierney et al., 2015].

Although for long time, CD was considered to be a disease associated with childhood, it is now regarded as occurring at any age. The disease onset has 2 peaks: in the first 2 decades and around the 5<sup>th</sup> decade of life [Husby et al., 2012; Werkstetter et al., 2017]. Scientists and, most important, gastroenterologists with practice in adult clinics are now questioning if biopsies are mandatory in all adult patients with symptomatic CD, as well, calling the lack of international consensus guidance [Previtali et al., 2018].

In this general context, the directions for my future research projects regarding the celiac disease will be:

1. In collaboration with gastroenterologists, I intend to design a study that investigates adult patients with high serum levels of tTG and to find correlations with the microscopical changes found in duodenal biopsies. The study groups should include cohorts of symptomatic and asymptomatic patients with diagnosed CD in different Marsh stages and with different levels of serum markers, ranging from normal to borderline and high (x10, x20 times higher than normal) and patients with non-specific gastrointestinal symptoms, but negative for serological markers.

The endoscopical biopsy from patients suspected for CD will be correlated with the level of the titer of IgA tTG antibodies, the EMA antibodies and the HLA compatibility group of the patients. Depending on these correlations, the results could lead to a diagnostic protocol standardization which recommends biopsy avoidance in a clearly defined subgroup of CD patients for clinical practice.

2. Another important issue in diagnosing gluten sensitivity is the non-classical clinical presentation (extra-intestinal features: ataxia, anemia, or osteoporosis) and the asymptomatic one, with patients who do not report any obvious symptoms at presentation. In the past years, a broader group of disorders that falls under the spectrum of CD have been recognized, including “potential” and “seronegative” coeliac disease, but also the non-celiac gluten sensitivity (NCGS). Despite the increasing interest from the medical community, the etiology and mechanism of the associated symptoms are largely unknown and no biomarkers have been identified.

My future project will aim to morphologically characterize these subgroups of gluten sensitivity conditions in correlation with clinical manifestation and/or serological tests.

For instance, beside the architectural changes of the villi, the increasing number and the type of intraepithelial lymphocytes (as local immune response), the project will investigate the systemic immune activation, by assessing the levels of soluble CD14 and lipopolysaccharide-binding protein, as well as antibody reactivity to microbial antigens.

I intend to design a study group to compare the expression of innate immune markers in different Marsh stages, including the influx of basophils (CD203c), expression of IL18 and IL15, as well as expression of heat shock protein (HSPA1A), expression of IFNG and CD19 (B-cells).

Also, I intend to investigate the levels of fatty acid-binding protein 2 and whether it correlates with the markers of systemic immune activation, thus, suggesting a compromised intestinal epithelial barrier integrity.

The study can demonstrate the presence of objective markers of systemic immune activation and gut epithelial cell damage in individuals who report sensitivity to wheat in the absence of coeliac disease.

### **II.2.2. PD-1 and PDL-1 expression in colorectal cancer and in head and neck cancers**

Generally speaking, the innate immune system is the first who starts fighting against an aggression, trying to isolate or eliminate the pathogen agent (microbial or not microbial). Although mechanisms are not clear, more and more data sustain the role played by inflammation in development and progression of cancer [Lasry et al., 2016].

In digestive tract, the innate immune system is represented by the innate lymphoid cells (ILC), located at the mucosal surface. Innate lymphoid cells are innate lymphocytes with no other lineage markers, involved in the early antigen defense, allergy, inflammation and tumorigenesis [Artis and Spits, 2015; Serafini et al., 2015].

After being recognized in the early stages, the tumor cells are attacked by the immune system through the tumor infiltrating lymphocytes (TIL) [Schreiber et al., 2011]. TIL produce IFN- $\gamma$  (such as NK, NKT, and  $\gamma\delta$ T cells) or kill and eliminate the tumor cells directly (NK and cytotoxic T lymphocytes - CTL) [Sun et al., 2011]. If the TIL are not specifically selected and stimulated against tumor cells or if some mutations appear, the tumor cells escape the immune attack.

In this general context, my future research projects will aim to:

1. Evaluate if and how the chronic inflammation from the microenvironment changes the lymphocytes action mechanisms and promotes the tumor cells development. Considering that tumor cells start producing immunosuppressive cytokines (vascular endothelial growth factor - VEGF, transforming growth factor- $\beta$  - TGF- $\beta$ ) converting effector T lymphocytes into regulatory T lymphocytes, the study will investigate the secretion of IL-10 and PD-L1, who are supposed to suppress CTL.

Tumor antigen stimulation maintains the expression of inhibitory receptors on T lymphocytes (Programmed death-1 /PD-1 and CTLA-4), inhibiting the effector T lymphocytes and stimulating the tumor development and progression [Wang et al., 2020]. Programmed cell death protein 1 (PD-1) or CD279 (cluster of differentiation 279), is a cell surface receptor protein located on pro-B cells and germinal center associated helper T cells with role in regulating the immune system's response by down-regulating the immune system and promoting self-tolerance by suppressing T cell inflammatory activity. This prevents the immune system from killing cancer cells [Syn et al., 2017]. It is an immune checkpoint that guards against autoimmunity by promoting apoptosis of antigen-specific T-cells in lymph

nodes or by reducing apoptosis in regulatory suppressive T cells. PD-1 binds two ligands, PD-L1 and PD-L2 [Wang et al., 2020].

The study will aim to describe and evaluate the intratumoral heterogeneity of ILC and their role in tumor progression/development or suppression. For instance, the expression of activating receptors in the early stages of tumorigenesis and/or inhibitory receptors in the late stages, the expression of Heparan sulphate 3-O-sulfotransferase 1 (HS3ST1) and PD1 in tumor infiltrating ILC. Targeting HS3ST1 and PD1 might lead to a potential immunotherapy for CRC patient treatment [Okazaki et al., 2013; Wang et al., 2020]. Therefore, new antitumor therapeutic solutions might be revealed by a better characterization and understanding of these immune changes. For instance, PD-1 inhibitors can block PD-1 and activate the immune system to attack tumor cells.

2. Another research direction will target the Programmed death-ligand 1 (PD-L1), also known as CD274, or B7 homolog 1 (B7-H1), which is a type 1 transmembrane protein that plays a major role in suppressing the adaptive arm of immune system during pregnancy, tissue allografts, autoimmune disease and inflammations (hepatitis). The immune system reacts to antigens that are associated with immune system activation by exogenous or endogenous danger signals. In turn, clonal expansion of antigen-specific CD8+ T cells and/or CD4+ helper cells is propagated. The binding of PD-L1 to the inhibitory checkpoint molecule PD-1 transmits an inhibitory signal, which reduces the proliferation of antigen-specific T-cells in lymph nodes, while simultaneously reducing apoptosis in regulatory T cells (anti-inflammatory, suppressive T cells) - further mediated by a lower regulation of the gene Bcl-2 [Chemnitz et al., 2004]. As a consequence, the upregulation of PD-L1 may allow cancers to evade the host immune system.

3. Similar to other carcinomas (pulmonary, eso-gastric junction, breast, kidney), the interest for assessing the expression of PD-L1 on the surface of the tumor cells in HNSCC or macrophages and its interaction with PD1 from the surface of cytotoxic T lymphocytes increased. The difference between carcinomas in the head and neck area and those from other organs is the HPV etiology, a viral one, stimulating the inner immune system. PD-L1 overexpressed tumors may have a poorer outcome due to the suppressed antitumor activity of their cytotoxic T lymphocytes, but, at the same time, might be more responsive to treatment with PD-L1 inhibitors [Patel and Kurzrock, 2015; Wu et al., 2015].

The main purpose of my future research project will be the assessing PD1 and PD-L1 expression in HPV-positive and HPV-negative carcinomas developed in different location of the head and neck region, with a special focus on the tumors of the salivary glands. Also, I will look for correlations between the PD1/PD-L1 status and the tobacco smoking.

Study groups will be represented by patients with primary carcinomas in the head and neck region, with and without lymph node metastasis, grouped on the histological type, presence of HPV infection, tobacco smoking history, neoadjuvant therapy and survival.

PD1 and PD-L1 expression will be investigated on formalin-fixed, paraffin-embedded tumor blocks, using immunohistochemical testing. Assessing the PD-L1 and PD1 immunohistochemical expression will be done after obtaining a certification for PD-L1 and PD1 evaluation.

For both PD1 and PD-L1, the first phase of the study will be the standardization of the evaluation, by adopting a scoring system. To date, different research teams use different combinations between the intensity score and the proportion of the positive cells. For instance, evaluating the PD-L1 expression results in calculating the Combined Positive Score and the Tumor Proportion Score. PDL1 expression can be considered positive when the Combined Positive Score  $\geq 1$ , which is the number of PD-L1 staining cells (tumor cells, lymphocytes, macrophages) divided by total number of viable tumor cells, multiplied by 100. The Tumor Proportion Score is defined as the percentage of PD-L1-positive tumor cells.

### **II. 3. Final remarks**

This habilitation thesis presents my professional, academic and scientific achievements during the postdoctoral period (2006-2020). The opportunity of selecting the candidates and coordinating the PhD students would greatly motivate me to continue my development as an academic professor and pathologist.

Last but not least, one of the most important duty for me will be to proudly promote the home University. I consider that establishing new contacts and improving the existing ones are the best ways, for me and my PhD students, to get involved in national and international projects, to access funds, develop and obtain recognition.

### Section III – References

- \*\*\* WHO report on the global tobacco epidemic Romania 2017. Available from: [http://www.who.int/tobacco/surveillance/policy/country\\_profile/rou.pdf?ua=1](http://www.who.int/tobacco/surveillance/policy/country_profile/rou.pdf?ua=1) accessed: July 21, 2020
- \*\*\* WHO. Global Status Report on noncommunicable diseases 2014. WHO Press, Geneva, Switzerland, 2014, [http://apps.who.int/iris/bitstream/10665/148114/1/9789241564854\\_eng.pdf?ua=1](http://apps.who.int/iris/bitstream/10665/148114/1/9789241564854_eng.pdf?ua=1), accessed: July 21, 2020
- Abdemur A, Slone J, Berho M, Gianos M, Szomstein S, Rosenthal RJ. Morphology, localization, and patterns of ghrelin-producing cells in stomachs of a morbidly obese population. *Surg Laparosc Endosc Percutan Tech* 2014; 24(2):122–126
- Abu-Zekry M, Diab M, Catassi C, Catassi C, Fasano A. Prevalence of celiac disease in Egyptian children disputes the East-West agriculture-dependent spread of the disease. *J Pediatr Gastroenterol Nutr* 2008; 47:136-140
- Adilbay D, Adilbayev G, Kidirbayeva G, et al. HPV infection and P16 expression in oral and oropharyngeal cancer in Kazakhstan. *Infect Agent Cancer* 2018; 13:2
- Ahi, K. A method and system for enhancing the resolution of terahertz imaging. *Measurement* 2019; 138:614–619
- Aimasso U, D'onofrio V, D'eusebio C, et al. Helicobacter pylori and nutrition: a bidirectional communication. *Minerva Gastroenterol Dietol* 2019; 65(2):116-129
- Almazeedi S, Al-Sabah S, Alshammari D, et al. The impact of *Helicobacter pylori* on the complications of laparoscopic sleeve gastrectomy. *Obes Surg* 2014; 24(3):412–415
- Ander BP, Dupasquier CM, Prociuk MA, Pierce GN. Polyunsaturated fatty acids and their effects on cardiovascular disease. *Exp Clin Cardiol* 2003; 8(4):164–172
- Angell H.K., Bruni D., Barrett J.C., Herbst R., Galon J. The Immunoscore: Colon Cancer and Beyond. *Clin Cancer Res* 2020; 26:332–339
- Aoki K, Taketo MM. Adenomatous polyposis coli (APC): a multi-functional tumor suppressor gene. *J Cell Sci* 2007; 120:3327–3335
- Artis D, Spits H. The biology of innate lymphoid cells. *Nature* 2015; 517:293–301
- Aurrekoetxea M, Garcia-Gallastegui P, Irastorza I, et al. Dental pulp stem cells as a multifaceted tool for bioengineering and the regeneration of craniomaxillofacial tissues. *Front Physiol* 2015; 6:289–299
- Aziz I, Evans KE, Hopper AD, Smillie DM, Sanders DS. A prospective study into the aetiology of lymphocytic duodenitis. *Aliment Pharmacol Ther* 2010; 32:1392-1397
- Baboci L, Holzinger D, Boscolo-Rizzo P, et al. Low prevalence of HPV driven head and neck squamous cell carcinoma in North-East Italy. *Papillomavirus research (Amsterdam, Netherlands)* 2016; 2:133-140
- Banefelt J, Hallberg S, Fox KM, et al. Work productivity loss and indirect costs associated with new cardiovascular events in high-risk patients with hyperlipidemia: estimates from population-based register data in Sweden. *Eur J Health Econ* 2016; 17(9):1117–1124
- Batterham RL, Cummings DE. Mechanisms of diabetes improvement following bariatric/metabolic surgery. *Diabetes Care* 2016; 39(6):893–901
- Bizzaro N, Tozzoli R, Tonutti E, Fabris M, Tonutti E. Cutting-edge issues in celiac disease and in gluten intolerance. *Clin Rev Allergy Immunol* 2012; 42:279-287
- Bosch FX, Broker TR. Comprehensive control of human papillomavirus infections and related diseases. ICO Monograph 'Comprehensive Control of HPV Infections and Related Diseases'. *Vaccine* 2013; 30; 31(Suppl 6):G1-31
- Boscolo-Rizzo P, Pawlita M, Holzinger D. From HPV-positive towards HPV-driven oropharyngeal squamous cell carcinomas. *Cancer treatment reviews* 2016; 42:24-29
- Braakhuis BJ, Brakenhoff RH, Meijer CJ, Snijders PJ, Leemans CR., Human papilloma virus in head and neck cancer: the need for a standardised assay to assess the full clinical importance. *Eur J Cancer* 2009; 45(17):2935-2939
- Bratman SV, Bruce JP, O'Sullivan B, et al. Human papillomavirus genotype association with survival in head and neck squamous cell carcinoma. *JAMA Oncology* 2016; 2(6):823-826

- Brownlee AB, Bromberg E, Roslin MS. Outcomes in patients with *Helicobacter pylori* undergoing laparoscopic sleeve gastrectomy. *Obes Surg* 2015; 25(12):2276–2279
- Brun MA, Formanek F, Yasuda A, Sekine M, Ando N, Eishii Y. Terahertz imaging applied to cancer diagnosis. *Phys Med Biol* 2010; 55:4615–4623
- Burum-Auensen E, DeAngelis PM, Schjølberg AR, et al. Reduced level of the spindle checkpoint protein BUB1B is associated with aneuploidy in colorectal cancers. *Cell Prolif* 2008; 41:645–659
- Cammarota G, Cuoco L, Cesaro P, et al. A highly accurate method for monitoring histological recovery in patients with celiac disease on a gluten-free diet using an endoscopic approach that avoids the need for biopsy: a double-center study. *Endoscopy* 2007; 39:46-51
- Campana D, Nori F, Pagotto U, et al. Plasma acylated ghrelin levels are higher in patients with chronic atrophic gastritis. *Clin Endocrinol (Oxf)* 2007; 67(5):761–766
- Camps J, Armengol G, Del Rey J, et al. Genome-wide differences between microsatellite stable and unstable colorectal tumors. *Carcinogenesis* 2006; 27:419–428
- Casorzo L, Dell’Aglío C, Sarotto I, Risio M. Aurora kinase A gene copy number is associated with the malignant transformation of colorectal adenomas but not with the serrated neoplasia progression. *Hum Pathol* 2015; 46:411–418
- Castellsague X, Alemany L, Quer M, et al. HPV involvement in head and neck cancers: comprehensive assessment of biomarkers in 3680 patients. *J Natl Cancer Inst* 2016; 108(6):djv403
- Catanzaro R, Occhipinti S, Calabrese F, et al. Irritable bowel syndrome: new findings in pathophysiological and therapeutic field. *Minerva Gastroenterol Dietol* 2014; 60:151-163
- Catassi C, Bai JC, Bonaz B, et al. Non-Celiac Gluten sensitivity: the new frontier of gluten related disorders. *Nutrients* 2013; 5:3839-3853
- Cedar H, Bergman Y. Linking DNA methylation and histone modification: patterns and paradigms. *Nat Rev Genet* 2009; 10:295-304
- Cervantes A, Elez E, Roda D, et al. Phase I pharmacokinetic/pharmacodynamic study of MLN8237, an investigational, oral, selective aurora a kinase inhibitor, in patients with advanced solid tumors. *Clin Cancer Res* 2012; 18:4764–4774
- Charlesworth RPG, Andronicos NM, Scott DR, et al. Can the sensitivity of the histopathological diagnosis of coeliac disease be increased and can treatment progression be monitored using mathematical modelling of histological sections? – A pilot study. *Adv Med Sci* 2017; 62:136–142
- Charlesworth RPG, Agnew LL, Scott DR, Andronicos NM. Equations defined using gene expression and histological data resolve coeliac disease biopsies within the Marsh score continuum. *Comput Biol Med* 2019; 104:183-196
- Charlesworth RP, Marsh MN. From 2-dimensional to 3-dimensional: Overcoming dilemmas in intestinal mucosal interpretation. *World J Gastroenterol* 2019; 25(20):2402-2415
- Chemnitz JM, Parry RV, Nichols KE, June CH, Riley JL. SHP-1 and SHP-2 associate with immunoreceptor tyrosine-based switch motif of programmed death 1 upon primary human T cell stimulation, but only receptor ligation prevents T cell activation. *J Immunol* 2004; 173(2):945–954
- Chen H, Xu H, Dong J, et al. Tumor necrosis factor-alpha impairs intestinal phosphate absorption in colitis. *Am J Physiol Gastrointest Liver Physiol* 2009; 296:G775–G778
- Chen H, Ma SH, Yan WX, Wu XM, Wang XZ. The diagnosis of human liver cancer by using THz fiber-scanning near-field imaging. *Chin Phys Lett* 2013; 30:030702
- Chernock RD, Wang X, Gao G, et al. Detection and significance of human papillomavirus, CDKN2A(p16) and CDKN1A(p21) expression in squamous cell carcinoma of the larynx. *Mod Pathol* 2013; 26(2):223-231
- Chiu ST, Chang KJ, Ting CH, Shen HC, Li H, Hsieh FJ. Overexpression of EphB3 enhances cell-cell contacts and suppresses tumor growth in HT-29 human colon cancer cells. *Carcinogenesis* 2009; 30:1475-1486
- Cho I, Blaser MJ, Francois F, Mathew JP, Ye XY, Goldberg JD, Bini EJ. *Am J Epidemiol* 2005; 162:579-585

- Choe YH, Song SY, Paik KH, et al. Increased density of ghrelin-expressing cells in the gastric fundus and body in Prader–Willi syndrome. *J Clin Endocrinol Metab* 2005; 90(9):5441–5445
- Choi YJ, Kim N, Yoon H, et al. Increase in plasma acyl ghrelin levels is associated with abatement of dyspepsia following *Helicobacter pylori* eradication. *J Gastroenterol* 2016; 51(6):548–559
- Chou R, Bougatsos C, Blazina I, Mackey K, Grusing S, Selph S. Screening for celiac disease: evidence report and systematic review for the US Preventive Services Task Force. *JAMA* 2017; 317(12):1258–1268
- Chung CH, Zhang Q, Kong CS, et al. p16 protein expression and human papillomavirus status as prognostic biomarkers of nonoropharyngeal head and neck squamous cell carcinoma. *J Clin Oncol* 2014; 32(35):3930–3938
- Ciclitira PJ. Does clinical presentation correlate with degree of villous atrophy in patients with celiac disease? *Nat Clin Pract Gastroenterol Hepatol* 2007; 4:482–483
- Ciobanu RC, Schreiner O, Lucanu N, et al. Advanced image processing in support of THz imaging for early detection of gastric cancer. In Proceedings of the 2018 International Conference and Exposition on Electrical and Power Engineering (EPE), Iasi, Romania, 18–19 October 2018
- Clevers H. Wnt/beta-catenin signaling in development and disease. *Cell* 2006; 127:469–480
- Corazza GR, Villanacci V, Zambelli C, et al. Comparison of the interobserver reproducibility with different histologic criteria used in celiac disease. *Clin Gastroenterol Hepatol* 2007; 5:838–843
- Crissey MA, Guo RJ, Fogt F, et al. The homeodomain transcription factor CDX1 does not behave as an oncogene in normal mouse intestine. *Neoplasia* 2008; 10:8–19
- Dadan J, Hady HR, Zbucki RL, Iwacewicz P, Bossowski A, Kasacka I. The activity of gastric ghrelin positive cells in obese patients treated surgically. *Folia Histochem Cytobiol* 2009; 47(2):307–313
- Danciu M, Simion L, Poroach V, et al. The role of histological evaluation of *Helicobacter pylori* infection in obese patients referred to laparoscopic sleeve gastrectomy. *Rom J Morphol Embryol* 2016; 57(4):1303–1311
- D’Assoro AB, Haddad T, Galanis E. Aurora-A kinase as a promising therapeutic target in cancer. *Front Oncol* 2015; 5:295
- Davalos V, Dopeso H, Castano J, et al. EPHB4 and survival of colorectal cancer patients. *Cancer Res* 2006; 66:8943–8948;
- De Andrés A, Camarero C, Roy G. Distal duodenum versus duodenal bulb: intraepithelial lymphocytes have something to say in celiac disease diagnosis. *Dig Dis Sci* 2015; 60:1004–1009
- De Gregorio V, Imparato G, Urciuolo F, Netti PA. Micro-patterned endogenous stroma equivalent induces polarized crypt-villus architecture of human small intestinal epithelium. *Acta Biomater* 2018; 81:43–59
- de Onis M, Blossner M. The World Health Organization Global Database on Child Growth and Malnutrition: methodology and applications. *Int J Epidemiol* 2003; 32:518–526
- De Palma GD, Forestieri P. Role of endoscopy in the bariatric surgery of patients. *World J Gastroenterol* 2014; 20(24):7777–7784
- Dickson BC, Streutker CJ, Chetty R. Coeliac disease: an update for pathologists. *J Clin Pathol* 2006; 59:1008–1016
- Diep CB, Kleivi K, Ribeiro FR, Teixeira MR, Lindgjaerde OC, Lothe RA. The order of genetic events associated with colorectal cancer progression inferred from meta-analysis of copy number changes. *Genes Chromosomes Cancer* 2006; 45:31–41
- Doradla P, Alavi K, Joseph C, Giles R. Single-channel prototype terahertz endoscopic system. *J Biomed Opt* 2014; 19:080501
- Du S, Jin J, Fang W, Su Q. Does fish oil have an anti-obesity effect in overweight/obese adults? A meta-analysis of randomized controlled trials. *PLoS One* 2015; 10(11):e0142652
- Economopoulou P, Kotsantis I, Psyrris A. Special Issue about Head and Neck Cancers: HPV Positive Cancers. *Int J Mol Sci* 2020; 21(9):3388
- Fearon ER, Vogelstein B. A genetic model for colorectal tumorigenesis. *Cell* 1990; 61:759–767
- Ferguson A, Murray D. Quantitation of intraepithelial lymphocytes in human jejunum. *Gut* 1971; 12:988–994

- Ferlay J, Soerjomataram I, Dikshit R, et al. Cancer incidence and mortality worldwide: sources, methods and major patterns in GLOBOCAN 2012. *Int J Cancer* 2015; 136(5):E359-386.
- Fiorucci G, Puxeddu E, Colella R, Paolo Reboldi G, Villanacci V, Bassotti G. Severe spruelike enteropathy due to olmesartan. *Rev Esp Enferm Dig* 2014; 106:142-144
- Franck CL, Senegaglia AC, Leite L, de Moura S, Francisco NF, Ribas Filho JM. Influence of adipose tissue-derived stem cells on the burn wound healing process. *Stem Cells Int* 2019; 2019:2340725
- Freeman HJ, Gujral N, Thomson ABR. Celiac Disease assays in A. B. R. Thomson and E. A. Shaffer, Editors. *First Principles of Gastroenterology and Hepatology*. Canada: Canadian Academic Publishers Ltd, Chapter 8: Celiac Disease, pg. 229-256, 2012.
- Fridman WH, Pages F, Sautes-Fridman C, Galon J. The immune contexture in human tumors: impact on clinical outcome. *Nat Rev Cancer* 2012; 12:298–306
- Fritscher-Ravens A, Schuppan D, Ellrichmann M, et al. Confocal endomicroscopy shows food-associated changes in the intestinal mucosa of patients with irritable bowel syndrome. *Gastroenterology* 2014; 147:1012-1020
- Fu T, Li P, Wang H, et al. c-Rel is a transcriptional repressor of EPHB2 in colorectal cancer. *J Pathol* 2009; 219:103-113
- Fukasawa K. Oncogenes and tumor suppressors take on centrosomes. *Nat Rev Cancer* 2007; 7:911–924
- Gabrielli M, Martini CN, Brandani JN, Iustman LJ, Romero DG, del C Vila M. Exchange protein activated by cyclic AMP is involved in the regulation of adipogenic genes during 3T3-L1 fibroblasts differentiation. *Dev Growth Differ* 2014; 56:143–151
- Galon J, Costes A, Sanchez-Cabo F, et al. Type, density, and location of immune cells within human colorectal tumors predict clinical outcome. *Science* 2006; 313:1960–1964
- Galon J, Pages F, Marincola FM, et al. Cancer classification using the immunoscore: a worldwide task force. *J Transl Med* 2012; 10:205
- Galon J, Bruni D. Approaches to treat immune hot, altered and cold tumors with combination immunotherapies. *Nat Rev Drug Discov* 2019; 18:197–218
- Granier C, Dariane C, Combe P, Verkarre V, Urien S, Badoual C, et al. Tim-3 Expression on tumor-infiltrating PD-1(+) CD8(+) T cells correlates with poor clinical outcome in renal cell carcinoma. *Cancer Res* 2017; 77:1075–1082
- Garnier-Lengliné H, Cerf-Bensusan N, Ruemmele FM Celiac disease in children. *Clin Res Hepatol Gastroenterol* 2015; 39(5):544-551
- Gautschi O, Heighway J, Mack PC, et al. Aurora kinases as anticancer drug targets. *Clin Cancer Res* 2008; 14:1639–1648
- Ge L, Moon RC, Nguyen H, de Quadros LG, Teixeira AF, Jawad MA. Pathologic findings of the removed stomach during sleeve gastrectomy. *Surg Endosc* 2019; 33(12):4003-4007
- Gentile NM, Murray JA, Pardi DS. Autoimmune enteropathy: a review and update of clinical management. *Curr Gastroenterol Rep* 2012; 14:380-385
- Gerlach U, Kayser G, Walch A, et al. Centrosome-, chromosomal-passenger- and cell-cycle-associated mRNAs are differentially regulated in the development of sporadic colorectal cancer. *J Pathol* 2006; 208: 462–472
- Gheit T, Abedi-Ardekani B, Carreira C, Missad CG, Tommasino M, Torrente MC. Comprehensive analysis of HPV expression in laryngeal squamous cell carcinoma. *J Med Virol* 2014; 86(4):642-646
- Gheit T, Anantharaman D, Holzinger D, et al. Role of mucosal high-risk human papillomavirus types in head and neck cancers in central India. *Int J Cancer* 2017; 141(1):143-151
- Ghieh F, Jurjus R, Ibrahim A, et al. The use of stem cells in burn wound healing: a review. *Biomed Res Int* 2015; 2015:ID 684084
- Giet R, Petretti C, Prigent C. Aurora kinases, aneuploidy and cancer, a coincidence or a real link? *Trends Cell Biol* 2005; 15:241–250
- Gillison ML, Chaturvedi AK, Anderson WF, et al. Epidemiology of human papillomavirus-positive head and neck squamous cell carcinoma. *J Clin Oncol* 2015; 33:3235–3242

- Goitein D, Lederfein D, Tzioni R, Berkenstadt H, Venturero M, Rubin M. Mapping of ghrelin gene expression and cell distribution in the stomach of morbidly obese patients – a possible guide for efficient sleeve gastrectomy construction. *Obes Surg* 2012; 22(4):617–622
- Goktas S, Yildirim M, Suren D, et al. Prognostic role of Aurora-A expression in metastatic colorectal cancer patients. *J BUON* 2014; 19:686–691
- Goos JA, Coupe VM, Diosdado B, et al. Aurora kinase A (AURKA) expression in colorectal cancer liver metastasis is associated with poor prognosis. *Br J Cancer* 2013; 109:2445–2452
- Goryachuk A, Simonova A, Khodzitsky M, Borovkova M, Khamid A. Gastrointestinal cancer diagnostics by terahertz time domain spectroscopy. In Proceedings of the 2017 IEEE International Symposium on Medical Measurements and Applications (MeMeA), Rochester, MN, USA, 7–10 May 2017; pp. 134–137
- Granado-Casas M, Alcubierre N, Martín M, et al. Improved adherence to Mediterranean Diet in adults with type 1 diabetes mellitus. *Eur J Nutr* 2019; 58(6):2271–2279
- Grand View Research. Omega 3 Market Size, Trends, Industry Report: <https://www.grandviewresearch.com/industry-analysis/omega-3-market> (2019) Accessed 21 July 2020
- Green PH, Lebwohl B, Greywoode R. Celiac disease. *J Allergy Clin Immunol* 2015; 135(5):1099–1106
- Guan Z, Wang XR, Zhu XF, et al. Aurora A, a negative prognostic marker, increases migration and decreases radiosensitivity in cancer cells. *Cancer Res* 2007; 67:10436–10444
- Guandalini S. A biopsy-avoiding approach to the diagnosis of celiac disease – how accurate is the immersion technique? *Nat Clin Pract Gastroenterol Hepatol* 2006; 3:542–543
- Guillet JP, Recur B, Frederique L, et al. Review of terahertz tomography techniques. *J Infrared Millim Terahertz Waves* 2014; 35:382–411
- Gujral N, Freeman HJ, Thomson AB. Celiac disease: prevalence, diagnosis, pathogenesis and treatment. *World J Gastroenterol* 2012; 18:6036–6059
- Gündoğan M, Çalli Demirkan N, Tekin K, Aybek H. Gastric histopathological findings and ghrelin expression in morbid obesity. *Turk Patoloji Derg* 2013; 29(1):19–26
- Hamada T, Matsubara H, Yoshida Y, Ugaji S, Nomura I, Tsuchiya H. Autologous adipose-derived stem cell transplantation enhances healing of wound with exposed bone in a rat model. *PLoS ONE* 2019; 14(5):e0214106
- Han A, Newell EW, Glanville J, et al. Dietary gluten triggers concomitant activation of CD4+ and CD8+  $\alpha\beta$  T cells and  $\gamma\delta$  T cells in celiac disease. *Proc Natl Acad Sci USA* 2013; 110:13073–13078
- Han H, Yan P, Chen L, et al. Flaxseed oil containing  $\alpha$ -linolenic acid ester of plant sterol improved atherosclerosis in apoE deficient mice. *Oxid Med Cell Longev* 2015; 2015:958217
- Hanahan D, Weinberg RA. Hallmarks of cancer: the next generation. *Cell* 2011; 144:646–674
- Harper JW, Holleran SF, Ramakrishnan R, Bhagat G, Green PH. Anemia in celiac disease is multifactorial in etiology. *Am J Hematol* 2007; 82:996–1000
- Hasson RM, Briggs A, Carothers AM, et al. Estrogen receptor  $\alpha$  or  $\beta$  loss in the colon of Min/+ mice promotes crypt expansion and impairs TGF $\beta$  and HNF3 $\beta$  signaling. *Carcinogenesis* 2014; 35(1):96–102
- Hayat M, Cairns A, Dixon MF, et al. Quantitation of intraepithelial lymphocytes in human duodenum: what is normal? *J Clin Pathol* 2002; 55:393–394
- He X, Zhang Q, Lu G, Ying G, Wu F, Jiang J. Tunable ultrasensitive terahertz sensor based on complementary graphene metamaterials. *RSC Adv* 2016; 6:52212–52218
- Holub BJ. Clinical nutrition: 4. Omega-3 fatty acids in cardiovascular care. *CMAJ* 2002; 166(5):608–615
- Hopper AD, Cross SS, Sanders DS. Patchy villous atrophy in adult patients with suspected gluten-sensitive enteropathy: is a multiple duodenal biopsy strategy appropriate? *Endoscopy* 2008; 40:219–224
- Hou D, Li X, Cai J, et al. Terahertz spectroscopic investigation of human gastric normal and tumor tissues. *Phys Me. Biol* 2014; 59:5423–5440
- Hryniuk A, Grainger S, Savory JG, Lohnes D. Cdx function is required for maintenance of intestinal identity in the adult. *Dev Biol* 2012; 363:426–437

- Hryniuk A, Grainger S, Savory JG, Lohnes D. CDX1 and CDX2 function as tumor suppressors. *J Biol Chem* 2014; 289(48):33343-33354
- Hu L, Zhao J, Liu J, Gong N, Chen L. Effects of adipose stem cell-conditioned medium on the migration of vascular endothelial cells, fibroblasts and keratinocytes. *Exp Ther Med* 2013; 5:701-706
- Huang SP, Huang CH, Shyu JF, et al. Promotion of wound healing using adipose-derived stem cells in radiation ulcer of a rat model. *J Biomed Sci* 2013; 20:51
- Husby S, Koletzko S, Korponay-Szabo IR, et al. European society for pediatric gastroenterology, hepatology, and nutrition guidelines for the diagnosis of coeliac disease. *J Pediatr Gastroenterol Nutr* 2012; 54:136-160
- Imam RA, Rizk AA. Efficacy of erythropoietin pretreated mesenchymal stem cells in murine burn wound healing: possible in vivo transdifferentiation into keratinocytes. *Folia Morphol (Warsz)* 2019; 78(4):798-808
- Jass JR, Whitehall VL, Young J, Leggett BA. Emerging concepts in colorectal neoplasia. *Gastroenterology* 2002; 123:862-876
- Ji YB, Kim SH, Jeong K, et al. Terahertz spectroscopic imaging and properties of gastrointestinal tract in a rat model. *Biomed Opt Express* 2014; 5:4162
- Ji YB, Lee ES, Kim SH, Son JH, Jeon TI. A miniaturized fiber-coupled terahertz endoscope system. *Opt Express* 2009; 17:17082-17087
- Ji YB, Park CH, Kim H, et al. Feasibility of terahertz reflectometry for discrimination of human early gastric cancers. *Biomed Opt Express* 2015; 6:1398.
- Jones AM, Douglas EJ, Halford SE, et al. Array-CGH analysis of microsatellite-stable, near-diploid bowel cancers and comparison with other types of colorectal carcinoma. *Oncogene* 2005; 24:118-129
- Joseph CS, Patel R, Neel VA, Giles RH, Yaroslavsky AN. Imaging of ex vivo nonmelanoma skin cancers in the optical and terahertz spectral regions. *J Biophotonics* 2014; 7:295-303
- Jump DB, Lytle KA, Depner CM, Tripathy S. Omega-3 polyunsaturated fatty acids as a treatment strategy for nonalcoholic fatty liver disease. *Pharmacol Ther* 2018; 181:108-125
- Kashanian HA, Ghaffary HB, Bagherzadeh NC. Gastric cancer diagnosis using terahertz imaging. *Majlesi J Multimed Process* 2015; 4:1-7
- Khalifehgholi M, Shamsipour F, Ajhdarkosh H, et al. Comparison of five diagnostic methods for Helicobacter pylori. *Iranian J Microbiol* 2013; 5(4):396-401
- Khan SA, Makki A. Dietary changes with omega-3 fatty acids improves the blood lipid profile of wistar albino rats with hypercholesterolaemia. *Int J Med ResHealth Sci* 2017; 6(3):34-40
- Kim HH, Jeon TY, Park DY, et al. Differential expression of ghrelin mRNA according to anatomical portions of human stomach. *Hepatogastroenterology* 2012; 59(119):2217-2221
- Kim SP, Ha JM, Yun SJ, et al. Transcriptional activation of peroxisome proliferator-activated receptor-gamma requires activation of both protein kinase A and Akt during adipocyte differentiation. *Biochem Biophys Res Commun* 2010; 399:55-59
- Klein A, Zang KD, Steudel WI, et al. Different mechanisms of mitotic instability in cancer cell lines. *Int J Oncol* 2006; 29:1389-1396
- Klinger M, Marazzi M, Vigo D, Torre M. Fat injection for cases of severe burn outcomes: a new perspective of scar remodeling and reduction. *Aesthetic Plast Surg* 2008; 32:465-469
- Koh HM, Jang BG, Hyun CL, et al. Aurora Kinase A Is a Prognostic Marker in Colorectal Adenocarcinoma. *J Pathol Transl Med* 2017; 51(1):32-39
- Kojima M, Hosoda H, Date Y, Nakazato M, Matsuo H, Kangawa K. Ghrelin is a growth-hormone-releasing acylated peptide from stomach. *Nature* 1999; 402(6762):656-660
- Kopach P, Genega EM, Shah SN, Kim JJ3, Suarez Y. The significance of histologic examination of gastrectomy specimens: a clinicopathologic study of 511 cases. *Surg Obes Relat Dis* 2017; 13:463-467
- Koskinen O, Collin P, Korponay-Szabo I, et al. Gluten-dependent small bowel mucosal transglutaminase 2-specific IgA deposits in overt and mild enteropathy coeliac disease. *J Pediatr Gastroenterol Nutr* 2008; 47:436-442

- Krysiak R, Szkróbka W, Okopień B. The Effect of Gluten-Free Diet on Thyroid Autoimmunity in Drug-Naïve Women with Hashimoto's Thyroiditis: A Pilot Study. *Exp Clin Endocrinol Diabetes* 2019; 127(7):417-422
- Kumar SR, Scheinet JS, Ley EJ, et al. Preferential induction of EphB4 over EphB2 and its implication in colorectal cancer progression. *Cancer Res* 2009; 69:3736-3745
- Kurppa K, Collin P, Viljamaa M, et al. Diagnosing mild enteropathy celiac disease: a randomized, controlled clinical study. *Gastroenterology* 2009; 136:816-823
- Lam AK, Ong K, Ho YH. Aurora kinase expression in colorectal adenocarcinoma: correlations with clinicopathological features, p16 expression, and telomerase activity. *Hum Pathol* 2008; 39:599–604
- Lasry A, Zinger A, Ben-Neriah Y. Inflammatory networks underlying colorectal cancer. *Nat Immunol* 2016; 17:230–240
- Lassen P, Lacas B, Pignon J, MARCH Collaborative Group, et al. Prognostic impact of HPV-associated p16-expression and smoking status on outcomes following radiotherapy for oropharyngeal cancer: the MARCH-HPV project. *Radiother Oncol* 2018; 126:107–115
- Lassmann S, Danciu M, Muller M, et al. Aurora A is differentially expressed and regulated in chromosomal and microsatellite instable sporadic colorectal cancers. *Mod Pathol* 2009; 22:1385-1397
- Lassmann S, Kreutz C, Schoepflin A, et al. A novel approach for reliable microarray analysis of microdissected tumor cells from formalin-fixed and paraffin-embedded colorectal cancer resection specimens. *J Mol Med* 2009; 87:211–224
- Lassmann S, Weis R, Makowiec F, et al. Array CGH identifies distinct DNA copy number profiles of oncogenes and tumor suppressor genes in chromosomal- and microsatellite-unstable sporadic colorectal carcinomas. *J Mol Med* 2007; 85:289–300
- Lebwohl B, Blaser MJ, Ludvigsson JF, et al. Decreased risk of celiac disease in patients with *Helicobacter pylori* colonization. *Am J Epidemiol* 2013; 178:1721-1730
- Lebwohl B, Kapel RC, Neugut AI, Green PH, Genta RM. Adherence to biopsy guidelines increases celiac disease diagnosis. *Gastrointest Endosc* 2011; 74:103-109
- Lebwohl B, Sanders DSS, Green PH. Coeliac Disease. *Lancet* 2018; 391(10115):70-81
- Lender N, Talley NJ, Enck P, et al. Review article: associations between *Helicobacter pylori* and obesity - an ecological study *Aliment Pharmacol Ther* 2014; 40(1):24
- Lentini L, Amato A, Schillaci T, et al. Simultaneous Aurora A/STK15 overexpression and centrosome amplification induce chromosomal instability in tumor cells with a MIN phenotype. *BMC Cancer* 2007; 7:212
- Lewis JS Jr, Beadle B, Bishop JA, et al. Human papillomavirus testing in head and neck carcinomas: Guideline from the College of American Pathologists. *Arch Pathol Lab Med* 2018; 142(5):559–97
- Li YH, Yang LH, Sha KH, Liu TG, Zhang LG, Liu XX. Efficacy of poly-unsaturated fatty acid therapy on patients with nonalcoholic steatohepatitis. *World J Gastroenterol* 2015; 21(22):7008-7013
- Lilja-Fischer JK, Eriksen JG, Georgsen JB, et al. Prognostic impact of PD-L1 in oropharyngeal cancer after primary curative radiotherapy and relation to HPV and tobacco smoking. *Acta Oncologica* 2020; 59(6):666-672
- Lim SK, Gopalan G. Aurora A kinase interacting protein 1 (AURORA AIP1) promotes Aurora A degradation through an alternative ubiquitin-independent pathway. *Biochem J* 2007; 403:119–127
- Liu C, Mann D, Sinha UK, Kokot NC. The molecular mechanisms of increased radiosensitivity of HPV-positive oropharyngeal squamous cell carcinoma (OPSCC): an extensive review. *J Otolaryngol Head Neck Surg* 2018; 47(1):59
- Loder S, Peterson JR, Agarwal S, et al. Wound healing after thermal injury is improved by fat and adipose-derived stem cell isografts. *J Burn Care Res* 2015; 36(1):70–76
- Loewen M, Giovanni J, Barba C. Screening endoscopy before bariatric surgery: a series of 448 patients. *Surg Obes Relat Dis* 2008; 4(6):709–712
- Losurdo G, Principi M, Iannone A, et al. Predictivity of Autoimmune Stigmata for Gluten Sensitivity in Subjects with Microscopic Enteritis: A Retrospective Study. *Nutrients* 2018; 10(12):2001

- Malfertheiner P. Diagnostic methods for *H. pylori* infection: choices, opportunities and pitfalls. *United European Gastroenterol J* 2015; 3(5):429–431
- Manfredi MG, Ecsedy JA, Meetze KA, et al. Antitumor activity of MLN8054, an orally active small-molecule inhibitor of Aurora A kinase. *Proc Natl Acad Sci USA* 2007; 104:4106–4111
- Mantsch HH, Naumann D. Terahertz spectroscopy: The renaissance of far infrared spectroscopy. *J Mol Struct* 2010; 964:1–4.
- Many N, Biedermann L. Adult Celiac Disease. *Praxis (Bern)* 2016; 105(14):803-810
- Marchisello S, Di Pino A, Scicali R, et al. Pathophysiological, molecular and therapeutic issues of nonalcoholic fatty liver disease: an overview. *Int J Mol Sci* 2019; 20(8):1948
- Marsh MN, Heal CJ. Evolutionary developments in interpreting the gluten-induced mucosal celiac lesion: an archimedean heuristic. *Nutrients* 2017; 9:213
- Marsh MN, Rostami K. What is a normal intestinal mucosa? *Gastroenterology* 2016; 151:784–788
- Marur S, D'Souza G, Westra WH, Forastiere AA. HPV-associated head and neck cancer: a virus-related cancer epidemic. *Lancet Oncol* 2010; 11(8):781-789
- Masterson L, Moualed D, et al. De-escalation treatment protocols for human papillomavirus-associated oropharyngeal squamous cell carcinoma: a systematic review and meta-analysis of current clinical trials. *Eur J Cancer* 2014; 50(15):2636-2648
- Mechanick JI, Youdim A, Jones DB, et al. Clinical practice guidelines for the perioperative nutritional, metabolic, and nonsurgical support of the bariatric surgery patient – 2013 update: cosponsored by American Association of Clinical Endocrinologists, The Obesity Society, and American Society for Metabolic & Bariatric Surgery. *Obesity (Silver Spring)* 2013; 21(Suppl 1):S1–S27
- Mena M, Lloveras B, Tous S, et al. Development and validation of a protocol for optimizing the use of paraffin blocks in molecular epidemiological studies: The example from the HPV-AHEAD study. *PLoS One* 2017; 12(10):e0184520
- Mendi A., Ulutürk H., Ataç M.S., Yılmaz D. Stem Cells for the Oromaxillofacial Area: Could they be a promising source for regeneration in dentistry?. In: Turksen K. (eds) *Cell Biology and Translational Medicine, Volume 5. Advances in Experimental Medicine and Biology*, 2019, vol 1144. Springer
- Merlos-Suarez A, Batlle E. Eph-ephrin signaling in adult tissues and cancer. *Curr Op Cell Biol* 2008; 20:194-200
- Michaud DS, Langevin SM, Eliot M, et al. High-risk HPV types and head and neck cancer. *Int J Cancer* 2014; 135(7):1653-1661.
- Mihai CT, Luca A, Danciu M, et al. In vitro evaluation of novel functionalized nanoparticles for terahertz imaging. *Med Surg J* 2019; 123:139–146
- Milano AF, Singer RB. The Cancer Mortality Risk Project—cancer mortality risks by anatomic site: Part I—Introductory Overview; Part II—Carcinoma of the Colon: 20-Year Mortality Follow-up Derived from 1973-2013 (NCI) SEER\*Stat Survival Database. *J Insur Med* 2017; 47:65–94
- Mirghani H, Amen F, Moreau F, et al. Human papilloma virus testing in oropharyngeal squamous cell carcinoma: what the clinician should know. *Oral Oncol* 2014; 50(1):1-9
- Mirghani H, Bellera C, Delaye J, et al. Prevalence and characteristics of HPV-driven oropharyngeal cancer in France. *Cancer Epidemiology* 2019; 61:89-94
- Mlecnik B, Tosolini M, Kirilovsky A, et al. Histopathologic-based prognostic factors of colorectal cancers are associated with the state of the local immune reaction. *J Clin Oncol* 2011; 29:610–618
- Mooney PD, Wong SH, Johnston AJ, et al. Increased detection of celiac disease with measurement of deamidated gliadin peptide antibody before endoscopy. *Clin Gastroenterol Hepatol* 2015; 13:1278–1284
- Moreno-Navarrete JM, Fernández-Real JM. Adipocyte differentiation. In: Symonds ME, editor. *Adipose tissue biology*. 1<sup>st</sup> ed. New York: Springer-Verlag; 2012. p. 17–38
- Morissette Martin P, Maux A, Laterreur V, et al. Enhancing repair of full-thickness excisional wounds in a murine model: Impact of tissue-engineered biological dressings featuring human differentiated adipocytes. *Acta Biomater* 2015; 22:39–49

- Motamed S, Taghiabadi E, Molaie H, et al. Cell-based skin substitutes accelerate regeneration of extensive burn wounds in rats. *Am J Surg* 2017; 214:762-769
- Murray JA, Rubio-Tapia A, Van Dyke CT, et al. Mucosal atrophy in celiac disease: extent of involvement, correlation with clinical presentation, and response to treatment. *Clin Gastroenterol Hepatol* 2008; 6:186-193
- Naderi N, Wilde C, Haque T, et al. Adipogenic differentiation of adipose-derived stem cells in 3-dimensional spheroid cultures (microtissue): implications for the reconstructive surgeon. *J Plast Reconstr Aesthet Surg* 2014; 67:1726–1734
- Nagtegaal ID, Glynne-Jones R. How to measure tumor response in rectal cancer? An explanation of discrepancies and suggestions for improvement. *Cancer Treat Rev* 2020; 84:101964
- Naik HS, Srilatha C, Sujatha K, Sreedevi B, Prasad TNVKV. Supplementation of whole grain flaxseeds (*Linum usitatissimum*) along with high cholesterol diet and its effect on hyperlipidemia and initiated atherosclerosis in Wistar albino male rats. *Vet World* 2018; 11(10):1433-1439
- Nakao K, Mehta KR, Fridlyand J, et al. High resolution analysis of DNA copy number alterations in colorectal cancer by array-based comparative genomic hybridization. *Carcinogenesis* 2004; 25:1345–1357
- Nassir F, Rector RS, Hammoud GM, Ibdah JA. Pathogenesis and prevention of hepatic steatosis. *Gastroenterol Hepatol (NY)* 2015; 11:167–175
- Nazempour, M, Mehrabani, D, Mehdinavaz-Aghdam, R, et al. The effect of allogenic human Wharton's jelly stem cells seeded onto acellular dermal matrix in healing of rat burn wounds. *J Cosmet Dermatol* 2020; 19:995–1001
- Nishida N, Nagasaka T, Kashiwagi K, et al. High copy amplification of the Aurora A gene is associated with chromosomal instability phenotype in human colorectal cancers. *Cancer Biol Ther* 2007; 6:525–533
- Nogueira MA, Oliveira CP, Ferreira Alves VA, et al. Omega-3 polyunsaturated fatty acids in treating non-alcoholic steatohepatitis: A randomized, double-blind, placebo-controlled trial. *Clin Nutr* 2016; 35(3):578-586
- Nogueira MS, Kessuane MC, Lobo Ladd AA, Lobo Ladd FV, Cogliati B, Castro IA. Effect of long-term ingestion of weakly oxidised flaxseed oil on biomarkers of oxidative stress in LDL-receptor knockout mice. *Br J Nutr* 2016; 116(2):258–269
- Nosho K, Baba Y, Tanaka N, et al. Tumor-infiltrating T-cell subsets, molecular changes in colorectal cancer, and prognosis: cohort study and literature review. *J Pathol* 2010; 222:350–366
- Ochi E, Tsuchiya Y. Eicosapentaenoic acid (EPA) and docosahexaenoic acid (DHA) in muscle damage and function. *Nutrients* 2018; 10(5):552
- Okazaki T, Chikuma S, Iwai Y, Fagarasan S, Honjo T. A rheostat for immune responses: the unique properties of PD-1 and their advantages for clinical application. *Nat Immunol* 2013; 14:1212–1218
- Oweida A, Bhatia S, Hirsch K. et al. Ephrin-B2 overexpression predicts for poor prognosis and response to therapy in solid tumors. *Mol Carcinog* 2017; 56(3):1189–1196
- Paoluzi OA, Del Vecchio Blanco G, Caruso R, et al. Helicobacter pylori infection associates with a mucosal downregulation of ghrelin, negative regulator of Th1-cell responses. *Helicobacter* 2013; 18(6):406–412
- Pagès F, Mlecnik B, Marliot F, et al. International validation of the consensus Immunoscore for the classification of colon cancer: a prognostic and accuracy study. *Lancet* 2018; 391(10135):2128–39
- Patel SP, Kurzrock R. PD-L1 expression as a predictive biomarker in cancer immunotherapy. *Mol Cancer Ther* 2015; 14:847–856
- Peña AS. Immunogenetics of non celiac gluten sensitivity. *Gastroenterol Hepatol Bed Bench* 2014; 7:1-5
- Popp A, Mäki M. Gluten-Induced Extra-Intestinal Manifestations in Potential Celiac Disease-Celiac Trait. *Nutrients* 2019; 11(2):320
- Previtali G, Licini L, D'Antiga L, et al. Celiac disease diagnosis without biopsy: Is a 10 ULN anti-transglutaminase result suitable for a chemiluminescence method? *J Pediatr Gastroenterol Nutr* 2018; 66:645–650

- Psyrri A, DiMaio D. Human papillomavirus in cervical and head and-neck cancer. *Nat Clin Pract Oncol* 2008; 5(1):24–31
- Qu XH, Huang XL, Xiong P, et al. Does Helicobacter pylori infection play a role in iron deficiency anemia? A meta-analysis. *World J Gastroenterol* 2010; 16:886-896
- Ranganathan S, Schmitt LA, Sindhi R. Tufting enteropathy revisited: the utility of MOC31 (EpCAM) immunohistochemistry in diagnosis. *Am J Surg Pathol* 2014; 38:265-272
- Reid CB, Fitzgerald A, Reese G, et al. Terahertz pulsed imaging of freshly excised human colonic tissues. *Phys Med Biol* 2011; 56:4333–4353
- Ren A, Zahid A, Fan D, et al. State-of-the-art in terahertz sensing for food and water security—A comprehensive review. *Trends Food Sci Technol* 2019; 85:241–251
- Rietbergen MM, Leemans CR, Bloemena E, et al. Increasing prevalence rates of HPV attributable oropharyngeal squamous cell carcinomas in the Netherlands as assessed by a validated test algorithm. *Int J Cancer* 2013; 132(7):1565-1571
- Roman A, Munger K. The papillomavirus E7 proteins. *Virology* 2013; 445(1–2):138–168
- Romero A, Kirchner H, Heppner K, Pfluger PT, Tschöp MH, Nogueiras R. GOAT: the master switch for the ghrelin system? *Eur J Endocrinol* 2010; 163(1):1–8
- Ropero S, Esteller M. The role of histone deacetylases in human cancer. *Mol Oncol* 2007; 1:19-25
- Rosinach M, Esteve M, González C, et al. Lymphocytic duodenosis: aetiology and longterm response to specific treatment. *Dig Liver Dis* 2012; 44:643-648
- Rostami K, Aldulaimi D, Holmes G, et al. Microscopic enteritis: Bucharest consensus. *World J Gastroenterol* 2015; 21:2593–2604
- Rostami K, Rostami Nejad M, Villanacci V, Danciu M. Microscopic enteritis and pathomechanism of malabsorption. *Autoimmun Highlights* 2010; 1:37-38
- Rostami K, Marsh MN, Johnson MW, et al. ROC-king onwards: intraepithelial lymphocyte counts, distribution & role in coeliac disease mucosal interpretation. *Gut* 2017; 66:2080–2086.
- Rostami K, Malekzadeh R, Catassi C, Akbari MR, Catassi C. Coeliac disease in Middle Eastern countries: a challenge for the evolutionary history of this complex disorder? *Dig Liver Dis* 2004; 36:694-697.
- Rostami K, Villanacci V. Microscopic enteritis: novel prospect in coeliac disease clinical and immunohistogenesis. Evolution in diagnostic and treatment strategies. *Dig Liver Dis* 2009; 41:245-252
- Rubino F, Nathan DM, Eckel RH, et al. Metabolic surgery in the treatment algorithm for type 2 diabetes: a Joint Statement by International Diabetes Organizations. *Diabetes Care* 2016; 39(6):861–877
- Ruchaud S, Carmena M, Earnshaw WC. Chromosomal passengers: conducting cell division. *Nat Rev Mol Cell Biol* 2007; 8:798–812.
- Santolaria S, Dominguez M, Alcedo J, et al. Lymphocytic duodenosis: etiological study and clinical presentations. *Gastroenterol Hepatol* 2013; 36:565-573
- Sanyal AJ, Abdelmalek MF, Suzuki A, Cummings OW, Chojkier M, EPE-A Study Group. No significant effects of ethyl-eicosapentanoic acid on histologic features of nonalcoholic steatohepatitis in a phase 2 trial. *Gastroenterology* 2014; 147(2):377-384
- Sapone A, Bai JC, Ciacci C, et al. Spectrum of gluten-related disorders: consensus on new nomenclature and classification. *BMC Med* 2012; 10:13
- Sathyamurthy A, Koushik AS, Gowri M, et al. Impact of molecular predictors on the response rates in head and neck cancer patients – an observational study. *Indian J Surg Oncol* 2016; 7(4):380–385
- Sauerland S, Angrisani L, Belachew M, et al. Obesity surgery: evidence-based guidelines of the European Association for Endoscopic Surgery (EAES). *Surg Endosc* 2005; 19(2):200–221
- Sbarbati A, Valletta E, Bertini M, et al. Gluten sensitivity and ‘normal’ histology: is the intestinal mucosa really normal? *Dig Liver Dis* 2003; 35:768-773
- Schache AG, Liloglou T, Risk JM, et al. Evaluation of human papilloma virus diagnostic testing in oropharyngeal squamous cell carcinoma: sensitivity, specificity, and prognostic discrimination. *Clin Cancer Res* 2011; 17(19):6262–6271
- Schimanski CC, Schmitz G, Kashyap A, et al. Reduced expression of HUGL-1, the human homologue of Drosophila tumour suppressor gene lgl, contributes to progression of colorectal cancer. *Oncogene* 2005; 24:3100–3109

- Schmidt BA, Horsley V. Intradermal adipocytes mediate fibroblast recruitment during skin wound healing. *Development* 2013; 140:1517–1527
- Schreiber RD, Old LJ, Smyth MJ. Cancer immunoediting: integrating immunity's roles in cancer suppression and promotion. *Science* 2011; 331:1565–1570
- Scott MA, Nguyen VT, Levi B, James AW. Current methods of adipogenic differentiation of mesenchymal stem cells. *Stem Cells Dev* 2011; 20:1793–1804
- Semrin G, Fishman DS, Bousvaros A, et al. Impaired intestinal iron absorption in Crohn's disease correlates with disease activity and markers of inflammation. *Inflamm Bowel Dis* 2006; 12:1101-1106
- Serafini N, Vosshenrich CA, Di Santo JP. Transcriptional regulation of innate lymphoid cell fate. *Nat Rev Immunol* 2015; 15:415–428
- Shen J, Hafeez A, Stevenson J, et al. Omega-3 fatty acid supplement prevents development of intracranial atherosclerosis. *Neuroscience* 2016; 334:226-235
- Shen J, Rastogi R, Guan L, et al. Omega-3 fatty acid supplement reduces activation of NADPH oxidase in intracranial atherosclerosis stenosis. *Neurol Res* 2018; 40(5):499-507
- Shin DW, Kwon HT, Kang JM, et al. Association between metabolic syndrome and Helicobacter pylori infection diagnosed by histologic status and serological status. *J Clin Gastroenterol* 2012; 46(10):840–845
- Siegel RL, Miller KD, Goding Sauer A, et al. Colorectal cancer statistics. *CA A Cancer J Clin* 2020
- Siegel RL, Miller KD, Jemal A. Cancer statistics, 2016. *CA A Cancer J Clin* 2016; 66:7–30
- Siegel RL, Miller KD, Jemal A. Cancer statistics, 2019. *CA A Cancer J Clin* 2019, 69, 7–34
- Silva Figueiredo P, Carla Inada A, Marcelino G, et al. Fatty acids consumption: the role metabolic aspects involved in obesity and its associated disorders. *Nutrients* 2017; 9(10):1158
- Sim YC, Park JY, Ahn KM, Park C, Son JH. Terahertz imaging of excised oral cancer at frozen temperature. *Biomed Opt Express* 2013; 4:1413–1421
- Singh P, Arora A, Strand TA, et al. Global prevalence of celiac disease: systematic review and meta-analysis. *Clin Gastroenterol Hepatol* 2018; 16(6):823-836
- Sokoła-Wysoczańska E, Wysoczański T, Wagner J, et al. Polyunsaturated fatty acids and their potential therapeutic role in cardiovascular system disorders-a review. *Nutrients* 2018; 10(10):1561
- Stjernstrøm KD, Jensen JS, Jakobsen KK, Grønhøj C, von Buchwald C. Current status of human papillomavirus positivity in oropharyngeal squamous cell carcinoma in Europe: a systematic review. *Acta Otolaryngol* 2019; 139(12):1112-1116
- Sugai T, Takahashi H, Habano W, et al. Analysis of genetic alterations, classified according to their DNA ploidy pattern, in the progression of colorectal adenomas and early colorectal carcinomas. *J Pathol* 2003; 200:168–176
- Sugano K, Tack J, Kuipers EJ, et al. Kyoto global consensus report on Helicobacter pylori gastritis. *Gut* 2015, 64(9):1353–1367
- Sun JC, Lanier LL. NK cell development, homeostasis and function: parallels with CD8(+) T cells. *Nat Rev Immunol* 2011; 11:645–657
- Surette ME, Whelan J, Lu GP, Broughton KS, Kinsella JE. Dependence on dietary cholesterol for n-3 polyunsaturated fatty acid-induced changes in plasma cholesterol in the Syrian hamster. *J Lipid Res* 1992; 33:263-271
- Syn NL, Teng MWL, Mok TSK, Soo RA. De-novo and acquired resistance to immune checkpoint targeting. *Lancet Oncol* 2017; 18(12):e731–e741
- Takashima A, Fukuda D, Tanaka K, et al. Combination of n-3 polyunsaturated fatty acids reduces atherogenesis in apolipoprotein E-deficient mice by inhibiting macrophage activation. *Atherosclerosis* 2016; 254:142-150
- Takiguchi S, Adachi S, Yamamoto K, et al. Mapping analysis of ghrelin producing cells in the human stomach associated with chronic gastritis and early cancers. *Dig Dis Sci* 2012; 57(5):1238–1246
- Tang KD, Menezes L, Baeten K, et al. Oral HPV16 Prevalence in Oral Potentially Malignant Disorders and Oral Cavity Cancers. *Biomolecules* 2020; 10(2):223
- Thoeni CE, Vogel GF, Tancevski I, et al. Microvillus inclusion disease: loss of Myosin vb disrupts intracellular traffic and cell polarity. *Traffic* 2014; 15:22-42

- Thorsson V, Gibbs DL, Brown SD, et al. The immune landscape of cancer. *Immunity* 2018; 48:812–830
- Tierney M, Bevan R, Rees CJ, et al. What do patients want from their endoscopy experience? The importance of measuring and understanding patient attitudes to their care. *Frontline Gastroenterol* 2015; 7:191–198
- Torres N, Guevara-Cruz M, Velazquez-Villegas LA, Tovar AR. Nutrition and atherosclerosis. *Arch Med Res* 2015; 46(5):408–426
- Turan G, Kocaöz S. Helicobacter Pylori Infection Prevalence and Histopathologic Findings in Laparoscopic Sleeve Gastrectomy. *Obes Surg* 2019; 29(11):3674-3679
- United European Gastroenterology. When is a coeliac a coeliac? Report of a working group of the United European Gastroenterology Week in Amsterdam, 2001. *Eur J Gastroenterol Hepatol* 2001; 13:1123-1128
- Ursu RG, Danciu M, et al. The burden of head & neck cancers in Iași, România, EUROGIN 2015, Seville, Spain
- Ursu RG, Danciu M, Spiridon IA, et al. Role of mucosal high-risk human papillomavirus types in head and neck cancers in Romania. *PLoS One* 2018; 13(6):e0199663
- US Preventive Services Task Force, Bibbins-Domingo K, Grossman DC, et al. Screening for Celiac Disease: US Preventive Services Task Force Recommendation Statement. *JAMA* 2017; 317(12):1252-1257.
- Vader G, Maia AF, Lens SM. The chromosomal passenger complex and the spindle assembly checkpoint: kinetochore-microtubule error correction and beyond. *Cell Div* 2008; 3:10.
- van Houten VM, Snijders PJ, et al. Biological evidence that human papillomaviruses are etiologically in-volved in a subgroup of head and neck squamous cell carcinomas. *Int J Cancer* 2001; 93(2):232-235
- Venuti A, Paolini F. HPV detection methods in head and neck cancer. *Head Neck Pathol* 2012; 6(Suppl 1):S63-74
- Viscido G, Signorini F, Navarro L, et al. Incidental finding of gastrointestinal stromal tumors during laparoscopic sleeve gastrectomy in obese patients. *Obes Surg* 2017; 27:2022–2025
- Wahaia F, Kasalynas I, Seliuta D, et al. Terahertz spectroscopy for the study of paraffn-embedded gastric cancer samples. *J Mol Struct* 2015; 1079:391–395
- Wahaia F, Kasalynas I, Venckevicius R, et al. Terahertz absorption and reflection imaging of carcinoma-affected colon tissues embedded in paraffn. *J Mol Struct* 2016; 1107:214–219
- Wahaia F, Valusis G, Bernardo LM, et al. Detection of colon cancer by terahertz techniques. *J Mol Struct* 2011; 1006:77–82
- Waluga M, Kukla M, Żorniak M, Bacik A, Kotulski R. From the stomach to other organs: Helicobacter pylori and the liver. *World J Hepatol* 2015; 7(18):2136–2146
- Wang Z, Zang C, Cui K, et al. Genome-wide mapping of HATs and HDACs reveals distinct functions in active and inactive genes. *Cell* 2009; 138:1019-1031
- Wang S, Qu Y, Xia P, et al. Transdifferentiation of tumor infiltrating innate lymphoid cells during progression of colorectal cancer. *Cell Res* 2020; 30:610–622
- Wang L, Peng Q, Sai B, et al. Ligand-independent EphB1 signaling mediates TGF- $\beta$ -activated CDH2 and promotes lung cancer cell invasion and migration. *J Cancer* 2020; 11(14):4123-4131
- Werkstetter KJ, Korponay-Szabó IR, Popp A, et al. Accuracy of tests for antibodies against tissue-transglutaminase in diagnosis of celiac disease, without biopsy. *Gastroenterology* 2017; 153(4):924-935
- Westra WH. Detection of human papillomavirus (HPV) in clinical samples: evolving methods and strategies for the accurate determination of HPV status of head and neck carcinomas. *Oral Oncol* 2014; 50(9):771-779
- Wirtz-Peitz F, Nishimura T, Knoblich JA. Linking cell cycle to asymmetric division: Aurora A phosphorylates the Par complex to regulate Numb localization. *Cell* 2008; 135:161–173
- Wohrle S, Wallmen B, Hecht A. Differential control of Wnt target genes involves epigenetic mechanisms and selective promoter occupancy by T-cell factors. *Mol Cell Biol* 2007; 27:8164-8177

- Wong NA, Britton MP, Choi GS, et al. Loss of CDX1 expression in colorectal carcinoma: promoter methylation, mutation and loss of heterozygosity analyses of 37 cell lines. *Proc Natl Acad Sci USA* 2004; 101:574-579
- Wu P, Wu D, Li L, et al. PD-L1 and survival in solid tumors: a meta-analysis. *PLoS One* 2015; 10:1–15
- Wu YQ, Dang RL, Tang MM, et al. Long chain omega-3 polyunsaturated fatty acid supplementation alleviates doxorubicin-induced depressive-like behaviors and neurotoxicity in rats: involvement of oxidative stress and neuroinflammation. *Nutrients* 2016; 8(4):243
- Xu MY, Liu L, Yuan BS, et al. Association of obesity with Helicobacter pylori infection: a retrospective study. *World J Gastroenterol* 2017; 23(15):2750–2756
- Yang G, Lee J, Lee S, et al. Krill oil supplementation improves dyslipidemia and lowers body weight in mice fed a high-fat diet through activation of AMP-activated protein kinase. *J Med Food* 2016; 19(12):1120-1129
- Yang J, Fernández-Galilea M, Martínez-Fernández L, Oxidative stress and non-alcoholic fatty liver disease: effects of omega-3 fatty acid supplementation. *Nutrients* 2019; 11(4):872
- Yang W, Shi H, Zhang J, Shen Z, Zhou G, Hu M. Effects of the duration of hyperlipidemia on cerebral lipids, vessels and neurons in rats. *Lipids Health Dis* 2017; 16(1):26
- Yasuda K, Nirei T, Sunami E, Nagawa H, Kitayama J. Density of CD4(+) and CD8(+) T lymphocytes in biopsy samples can be a predictor of pathological response to chemoradiotherapy (CRT) for rectal cancer. *Radiat Oncol* 2011; 6:49
- Zamani F, Mohamadnejad M, Shakeri R, et al. Gluten sensitive enteropathy in patients with iron deficiency anemia of unknown origin. *World J Gastroenterol* 2008; 14:7381-7385
- Zanini B, Lanzarotto F, Villanacci V, Carabellese N, Ricci C, Lanzini A. Clinical expression of lymphocytic duodenosis in “mild enteropathy” celiac disease and in functional gastrointestinal syndromes. *Scand J Gastroenterol* 2014; 49:794-800
- zur Hausen H. Papillomaviruses in the causation of human cancers – a brief historical account. *Virology* 2009; 384(2):260–265